

Supplementary Information

Electrochemical and mechanochemical synthesis of dihydrofuro[3,2-*c*]chromenones *via* intramolecular C_{sp}3-H cross-dehydrogenative oxygenation within warfarin framework: an efficient and straightforward dual approach

Indrajit Karmakar and Goutam Brahmachari*

Laboratory of Natural Products & Organic Synthesis, Department of Chemistry,
Visva-Bharati (a Central University), Santiniketan-731 235, West Bengal, India.

*Corresponding author: Prof. Dr. Goutam Brahmachari

(<http://orcid.org/0000-0001-9925-6281>)

E-mail: brahmg2001@yahoo.co.in; goutam.brahmachari@visva-bharati.ac.in

Table of Contents

1.	General information.....	S1
2.	General procedure for the synthesis of functionalized dihydrofuro[3,2- <i>c</i>]chromenones 2	S2
3.	Scanned copies of ^1H -NMR, ^{13}C -NMR, DEPT-135 NMR, and HRMS spectra for functionalized dihydrofuro[3,2- <i>c</i>]chromenones 2 (2-1–2-29) along with 2D-NMR (^1H - ^1H COSY, ^1H - ^{13}C HMQC and ^1H - ^{13}C HMBC) analysis of one representative compound 2-(2-hydroxybenzoyl)-3-(3-nitrophenyl)-2 <i>H</i> -furo[3,2- <i>c</i>]chromen-4(3 <i>H</i>)-one 2-6	S3–S138
4.	Single-crystal X-ray analysis of 2-(2-hydroxybenzoyl)-3-phenyl-2,3-dihydro-4 <i>H</i> -furo[3,2- <i>c</i>]chromen-4-one (2-1).....	S139–S140
5.	References.....	S141

1. General.

All chemicals (analytical grade) except starting warfarin analogues were purchased from reputed companies and used without further purification. All the starting warfarin derivatives used in this present study were synthesized as per the previous reported method.¹ ¹H, ¹³C and ¹⁹F NMR spectra were collected at 400, 100 and 376 MHz, respectively, on a Bruker DRX spectrometer using CDCl₃ as solvent. Chemical shifts were reported in δ (ppm), relative to the internal standard, TMS. The signals observed are described as s (singlet), d (doublet), t (triplet), and m (multiplet). Coupling constants are reported as J value in Hz. Structural assignments were made with additional information from gCOSY, gHSQC, and gHMBC experiments. Mass spectrometry was obtained using a Bruker maXis Impact (Q-TOF) high-resolution mass spectrometer. X-ray single crystallographic data were collected on X'Calibur CCD area-detector diffractometer. The melting points were recorded on a Chemilene CL-725 melting point apparatus and are uncorrected. Thin Layer Chromatography (TLC) was performed using silica gel 60 F₂₅₄ (Merck) plates. The ‘DC Variable Power Supply Unit’ has been designed and assembled with standard individual electrical parts purchased from reputed companies at the end of the present investigators. Graphite, Pt, Ag, Zn, and Cu plate-electrodes have been used for performing electrochemical cell reactions. A pictorial view (Figure S1) of the designed electrochemical set-up is shown below. A PM 100, Retsch GmbH, Germany, ball-milling apparatus was used for all reactions.

A pictorial view of the electrochemical experimental set-up



Figure S1a: Pictorial view (Front-View) of the experimental set-up for the model reaction showing the designed ‘DC Variable Power Supply’ unit tagged with Voltmeter and Ammeter, and an undivided electrochemical cell containing a pair of graphite plates (cathode and anode) and the reaction mixture within a glass vessel placed on a magnetic stirrer with constant stirring at ambient conditions.

A pictorial view of the mechanochemical experimental set-up



Figure S1b: Pictorial view PM 100, Retsch GmbH, Germany, ball-milling apparatus

2. General procedure for the synthesis of functionalized dihydrofuro[3,2-*c*]chromenones (2)

2.1 In Electrochemical cell

An oven-dried glass vessel was charged with warfarin analogues (**1**; 0.1 mmol), 4.5 mL of 0.07 M KI electrolyte solution in DMSO, and a magnetic stir bar in a sequential manner. The reaction vessel was then capped with a pair of graphite plate electrodes (both the cathode and anode are of the size in a dimension of 0.7 cm × 0.7 cm × 0.2 cm) placed at a 0.5 cm distance constructing an undivided electrochemical cell. Now, an uninterrupted flow of DC current (in mA) was maintained with a constant voltage of 7.0 V through the reaction mixture with stirring at ambient temperature for a stipulated time frame of 20-40 min. The progress of the reaction was monitored by TLC. On completion of the reaction, 20 mL of a mixture of ethyl acetate and saturated aqueous sodium thiosulfate solution in a proportion of 3:1 (v/v) was added to the resulting mixture and shaken well in a separating funnel. The organic layer was separated and dried over anhydrous sodium sulphate. The solvent was then removed under reduced pressure to obtain a white crude mass, which was then subjected to column chromatographic purification using EtOAc-hexane mixtures as eluents, to have pure products of dihydrofuro[3,2-*c*]chromenones **2** (**2a – 2t**). The structure of each compound was confirmed by spectral studies including $^1\text{H-NMR}$, $^{13}\text{C-NMR}$, DEPT-135, $^{19}\text{F NMR}$, 2D-NMR and HRMS. Further structural confirmation was done by single X-ray crystallographic studies with a representative entry, 2-(2-hydroxybenzoyl)-3-phenyl-2,3-dihydro-4*H*-furo[3,2-*c*]chromen-4-one (**2-1**).

2.2 In Ball-milling

A starting warfarin analogue (**1**; 0.2 mmol) mixed with I₂-DMSO (1:1 molar ratio) (1.0 equiv) and neutral alumina (1.5 g) used as the surface was subjected to ball-milling at 550 rpm using a 25 mL stainless steel jar with seven balls (10 mm in diameter) of the same material for 25-55 min. The ball-milling operation was performed using inverted rotation direction, with an interval of 5 min and taking a break of 10 sec. On completion of the reaction (monitored by TLC), 20 mL of ethyl acetate and saturated aqueous sodium thiosulfate solution in a proportion of 3:1 (v/v) was added to the resulting mixture and shaken well in a separating funnel. The organic layer was separated and dried over anhydrous sodium sulphate. The solvent was then removed under reduced pressure to obtain a white crude mass, which was then subjected to column chromatographic purification using EtOAc-hexane mixtures as eluents, to have pure products of dihydrofuro[3,2-*c*]chromenones **2** (**2-1 – 2-29**).

3. Scanned copies of ^1H NMR, ^{13}C NMR, DEPT-135, ^{19}F NMR, 2D-NMR (for model compound 2-6, along with showing the corresponding homo- and hetero-nuclear interactions in Table S1) and HRMS spectra for all the synthesized dihydrofuro[3,2-*c*]chromenones 2 (2-1–2-29) (Figure S2 – S130)

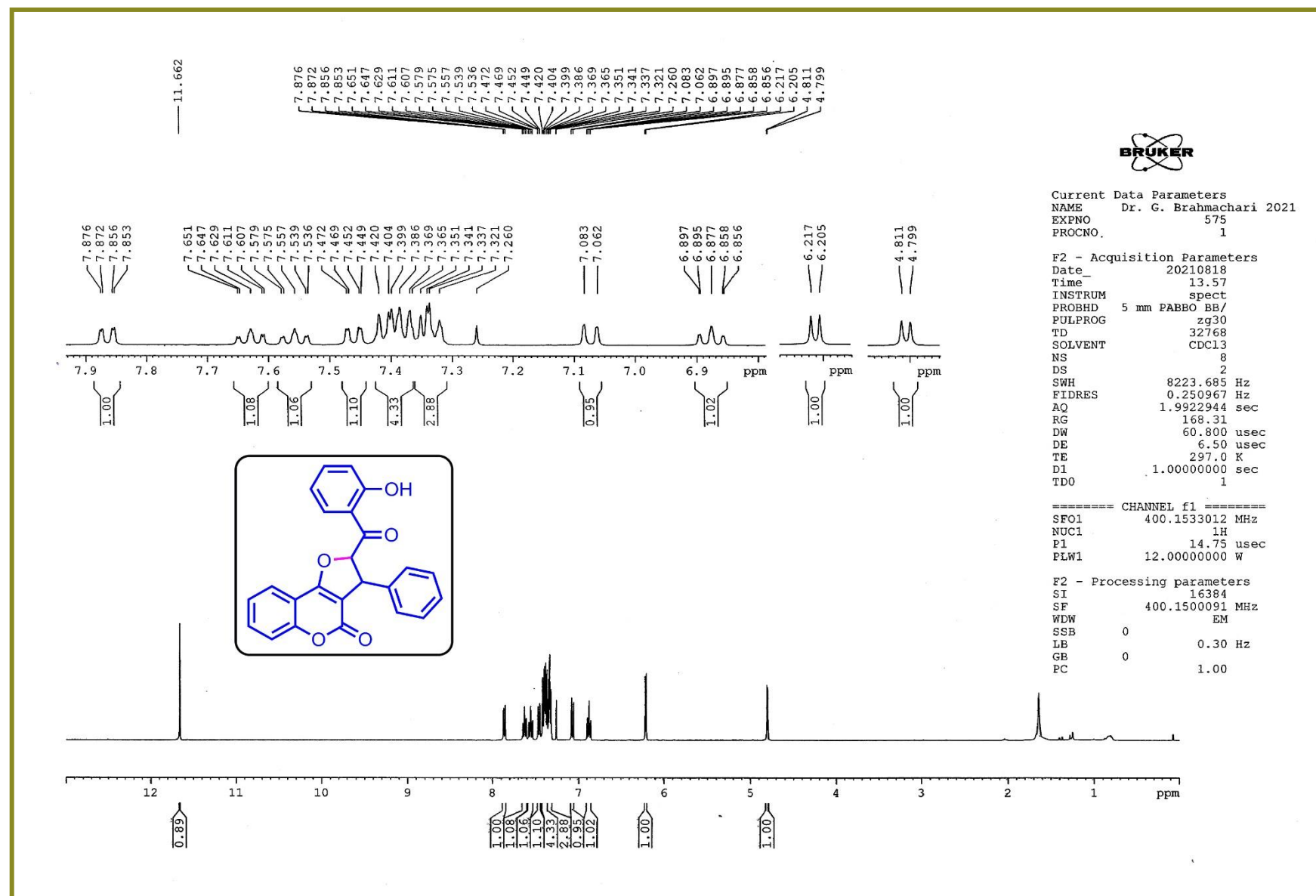


Figure S2. $^1\text{H-NMR}$ spectrum of 2-(2-hydroxybenzoyl)-3-phenyl-2,3-dihydro-4*H*-furo[3,2-*c*]chromen-4-one (**2-1**)

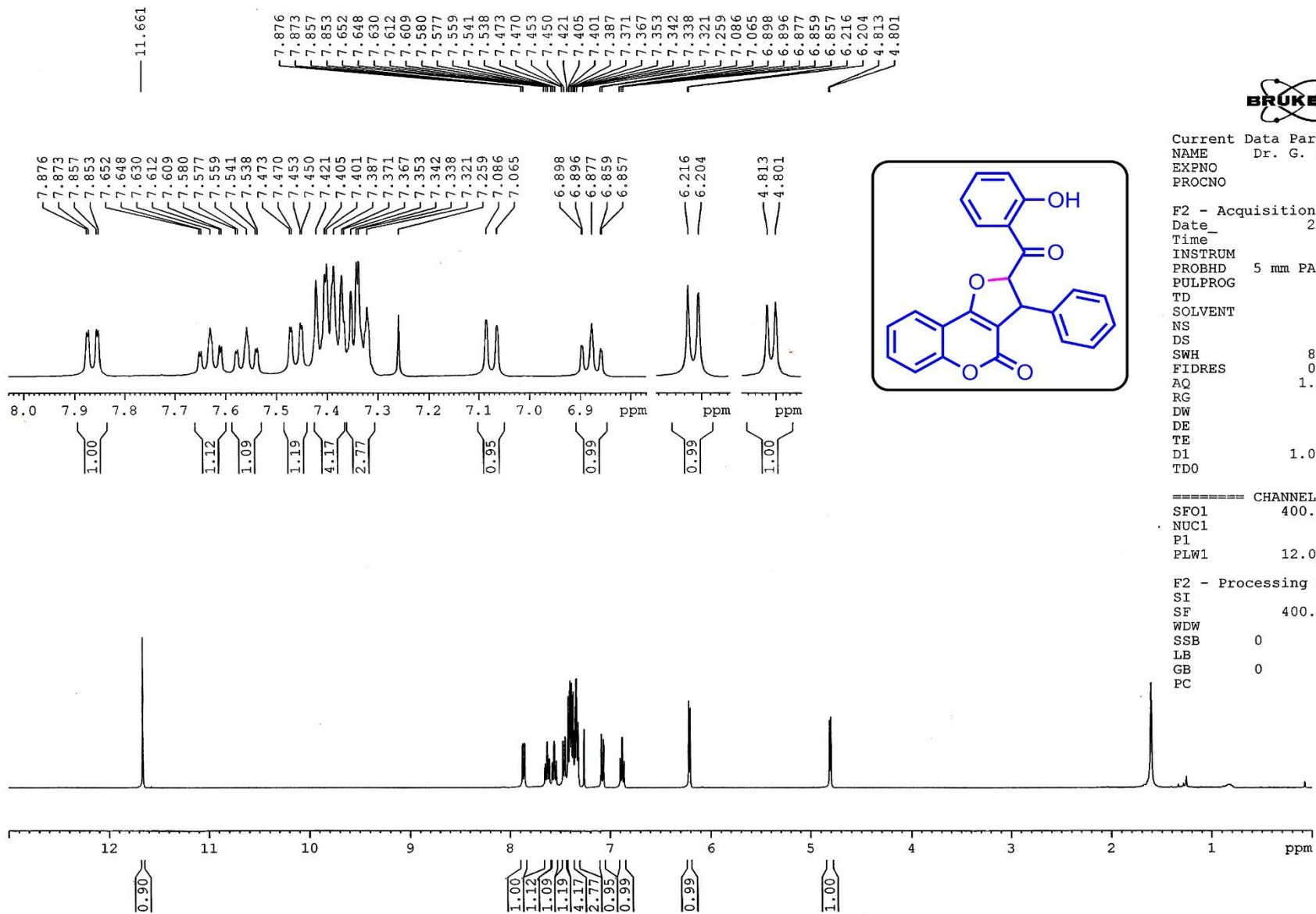


Figure S3. ¹H-NMR spectrum of 2-(2-hydroxybenzoyl)-3-phenyl-2,3-dihydro-4*H*-furo[3,2-*c*]chromen-4-one (**2-1**) [Larger Scale]

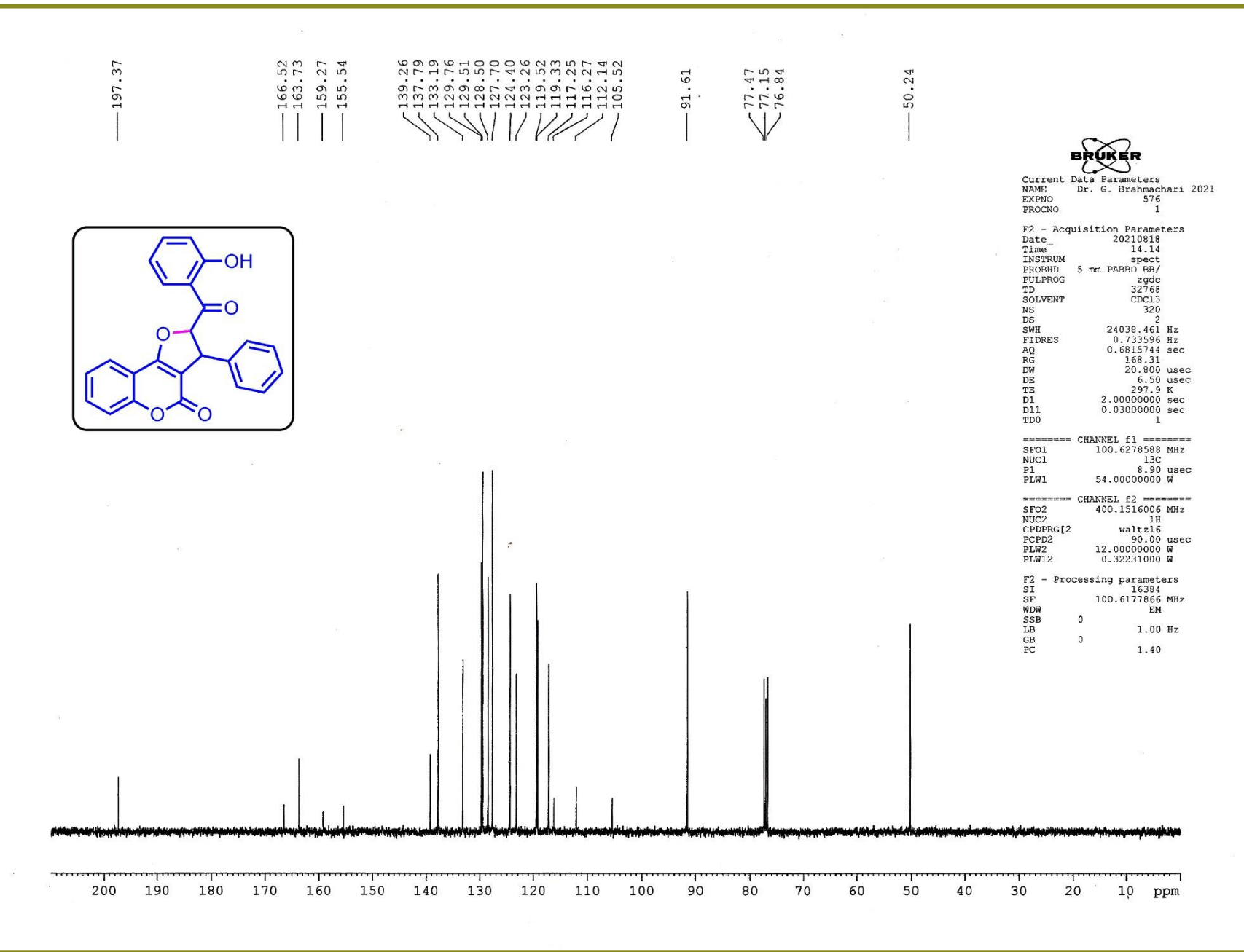


Figure S4. ^{13}C -NMR spectrum of 2-(2-hydroxybenzoyl)-3-phenyl-2,3-dihydro-4*H*-furo[3,2-*c*]chromen-4-one (**2-1**)

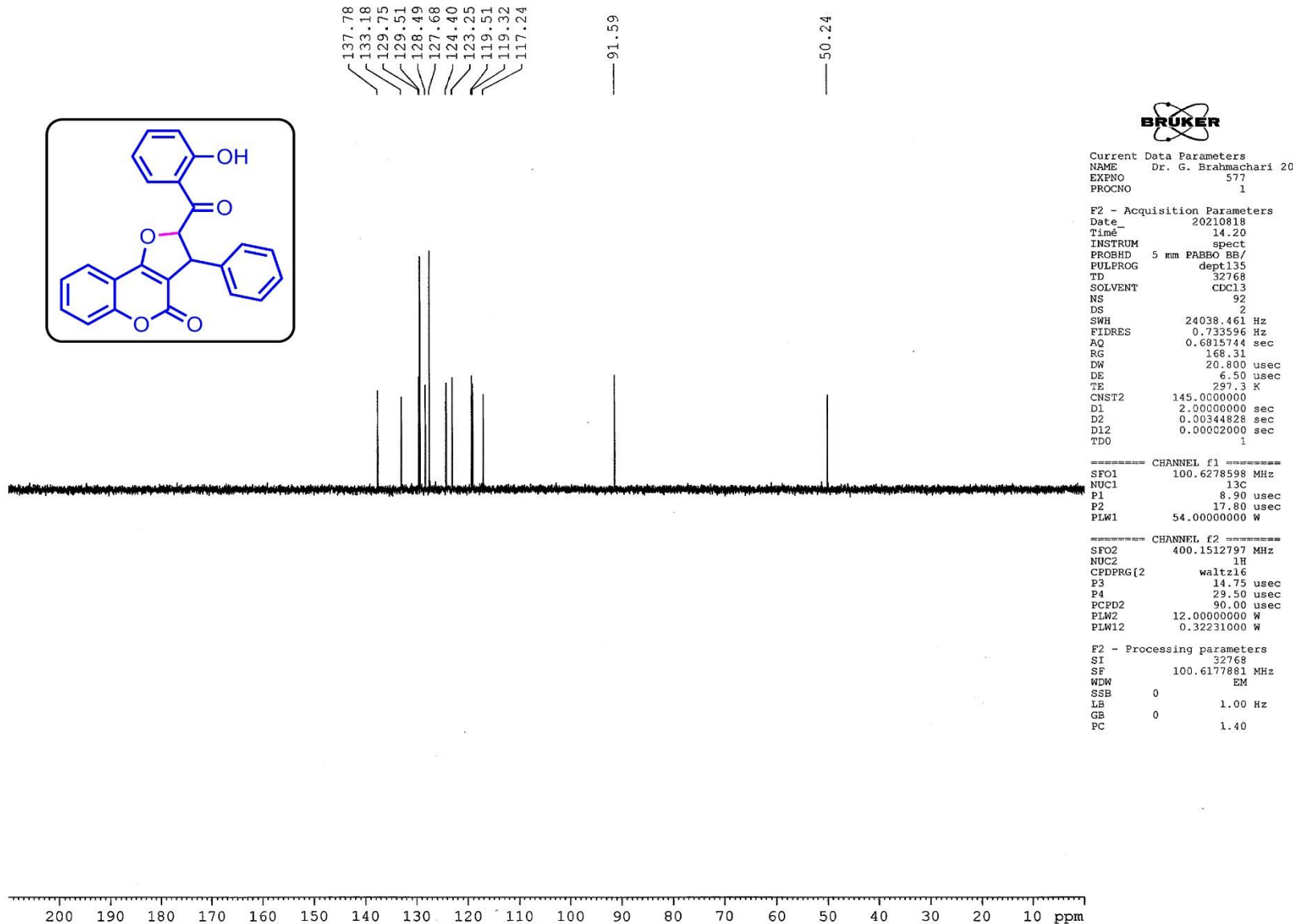


Figure S5. DEPT-135 NMR spectrum of 2-(2-hydroxybenzoyl)-3-phenyl-2,3-dihydro-4*H*-furo[3,2-*c*]chromen-4-one (**2-1**)

Acquisition Parameter

Source Type	ESI	Ion Polarity	Positive	Set Nebulizer	0.4 Bar
Focus	Active	Set Capillary	3400 V	Set Dry Heater	200 °C
Scan Begin	50 m/z	Set End Plate Offset	-500 V	Set Dry Gas	4.0 l/min
Scan End	3000 m/z	Set Charging Voltage	2000 V	Set Divert Valve	Source
		Set Corona	0 nA	Set APCI Heater	0 °C

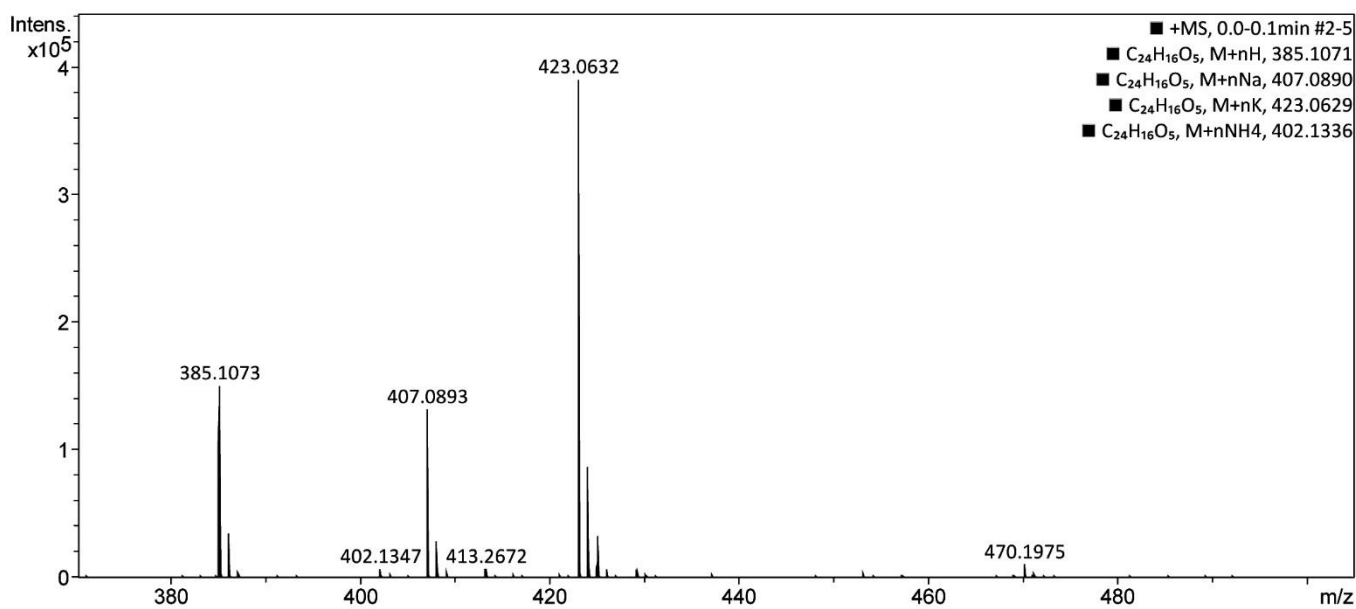
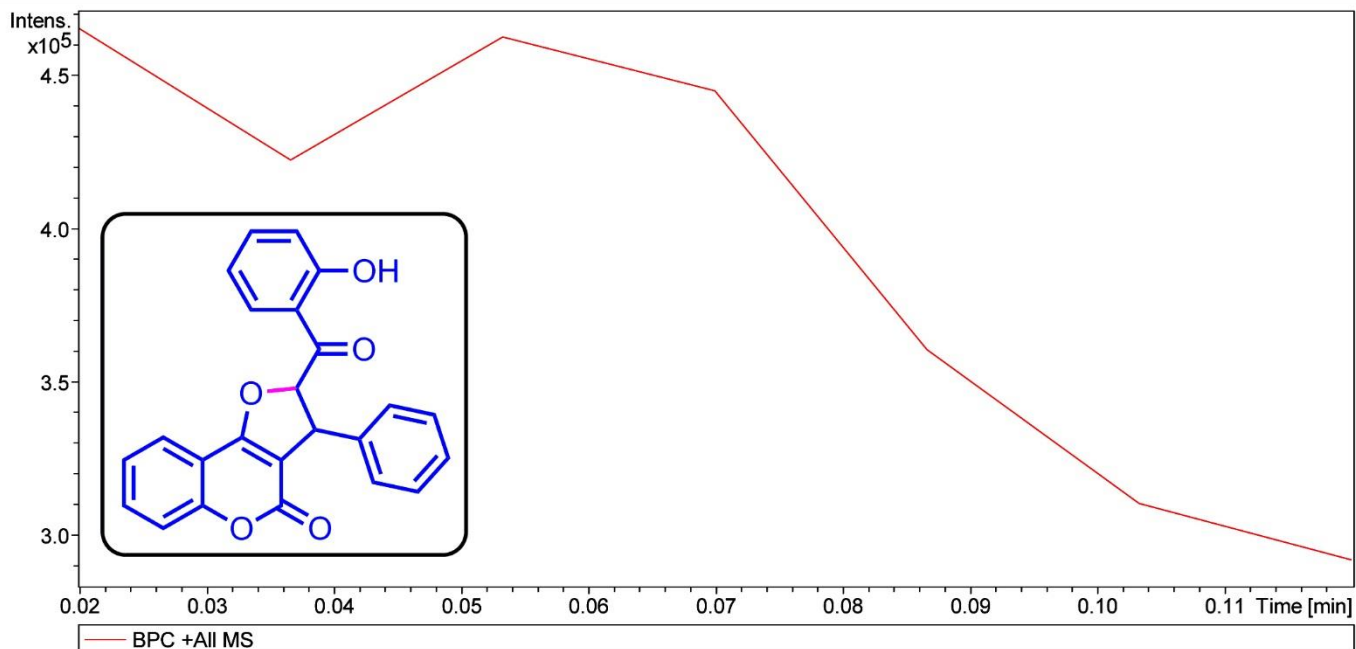


Figure S6. High-resolution Mass spectra of 2-(2-hydroxybenzoyl)-3-phenyl-2,3-dihydro-4H-furo[3,2-c]chromen-4-one (2-1)

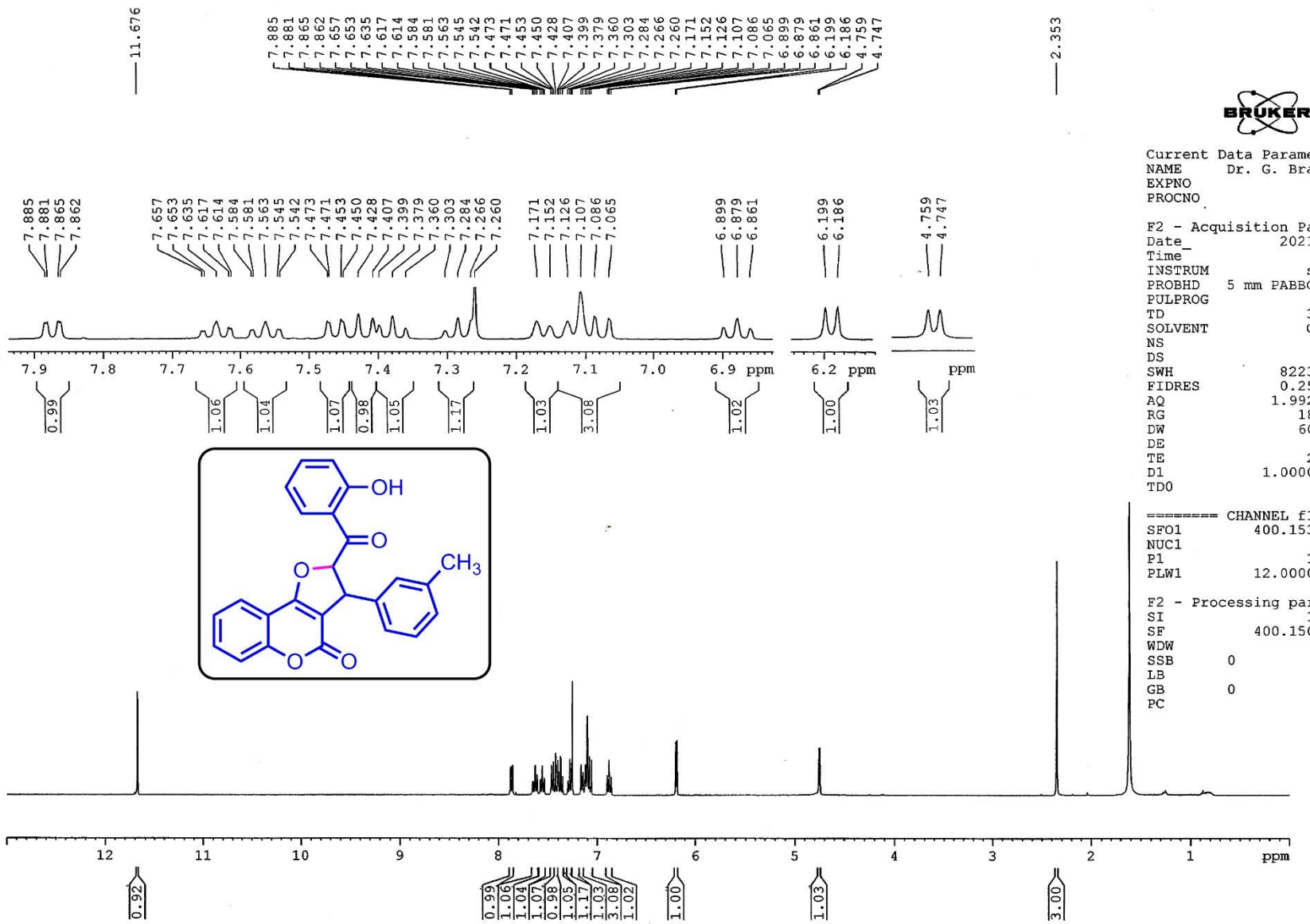


Figure S7. ^1H -NMR spectrum of 2-(2-hydroxybenzoyl)-3-(*m*-tolyl)-2,3-dihydro-4*H*-furo[3,2-*c*]chromen-4-one (**2-2**)

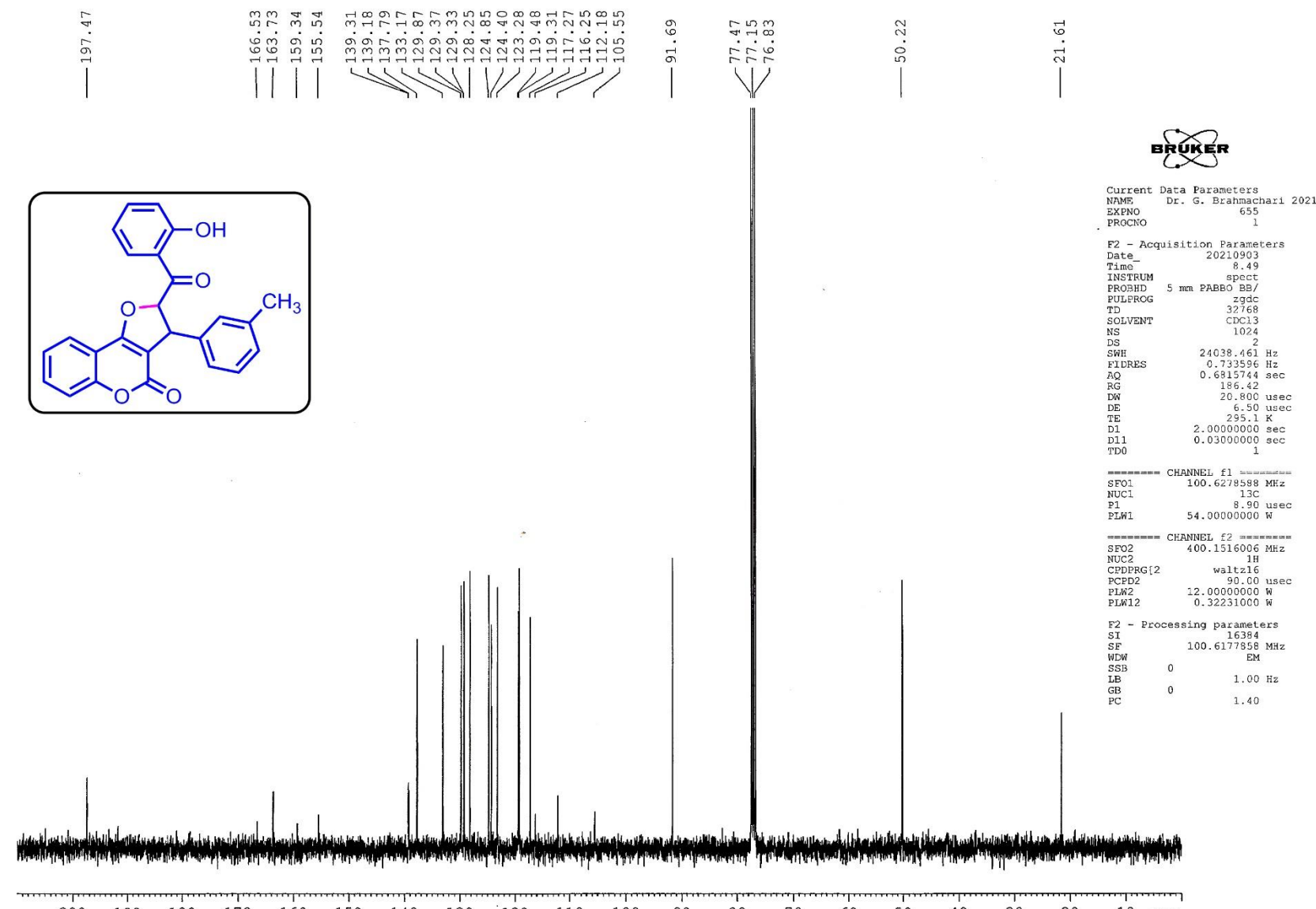


Figure S8. ^{13}C -NMR spectrum of 2-(2-hydroxybenzoyl)-3-(*m*-tolyl)-2,3-dihydro-4*H*-furo[3,2-*c*]chromen-4-one (**2-2**)

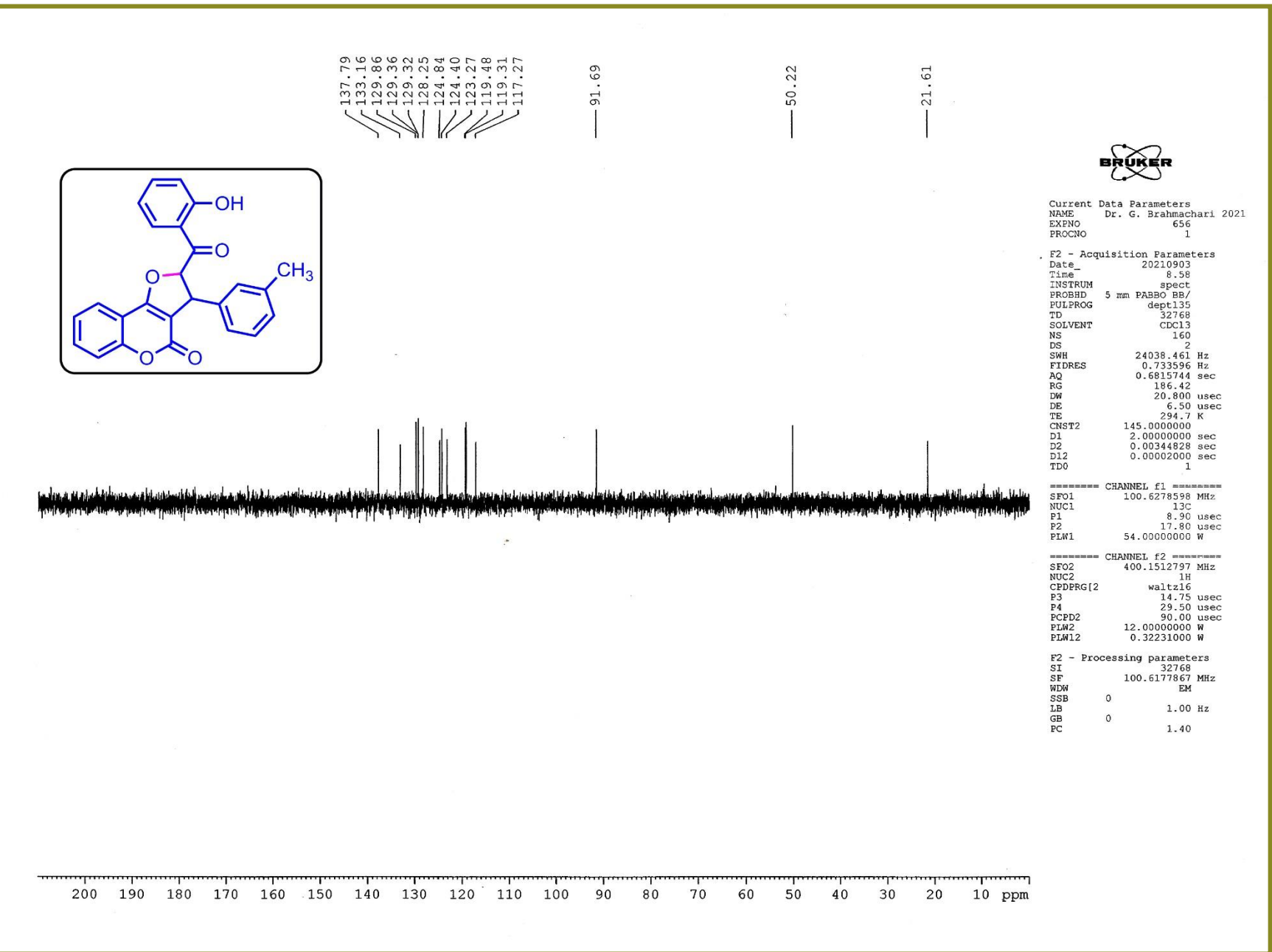


Figure S9. DEPT-135 NMR spectrum of 2-(2-hydroxybenzoyl)-3-(*m*-tolyl)-2,3-dihydro-4*H*-furo[3,2-*c*]chromen-4-one (**2-2**)

Acquisition Parameter

Source Type	ESI	Ion Polarity	Positive	Set Nebulizer	0.4 Bar
Focus	Active	Set Capillary	3400 V	Set Dry Heater	200 °C
Scan Begin	50 m/z	Set End Plate Offset	-500 V	Set Dry Gas	4.0 l/min
Scan End	3000 m/z	Set Charging Voltage	2000 V	Set Divert Valve	Source
		Set Corona	0 nA	Set APCI Heater	0 °C

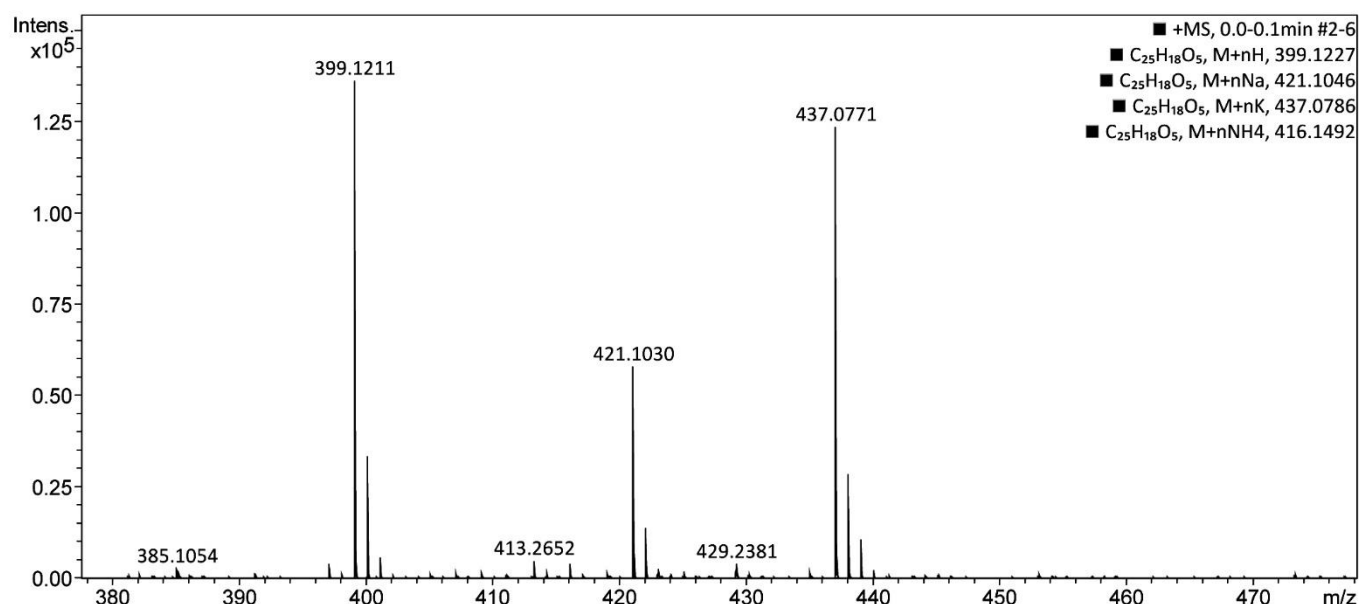
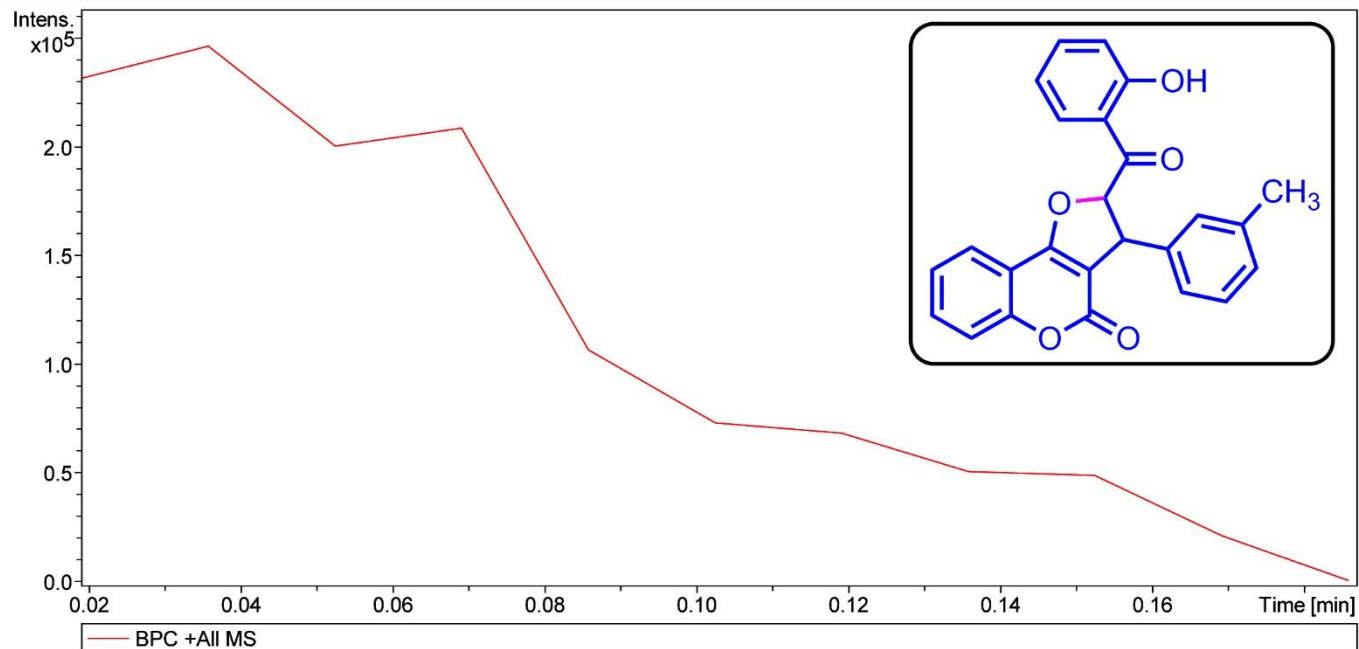


Figure S10. High-resolution Mass spectra of 2-(2-hydroxybenzoyl)-3-(*m*-tolyl)-2,3-dihydro-4*H*-furo[3,2-*c*]chromen-4-one (**2-2**)

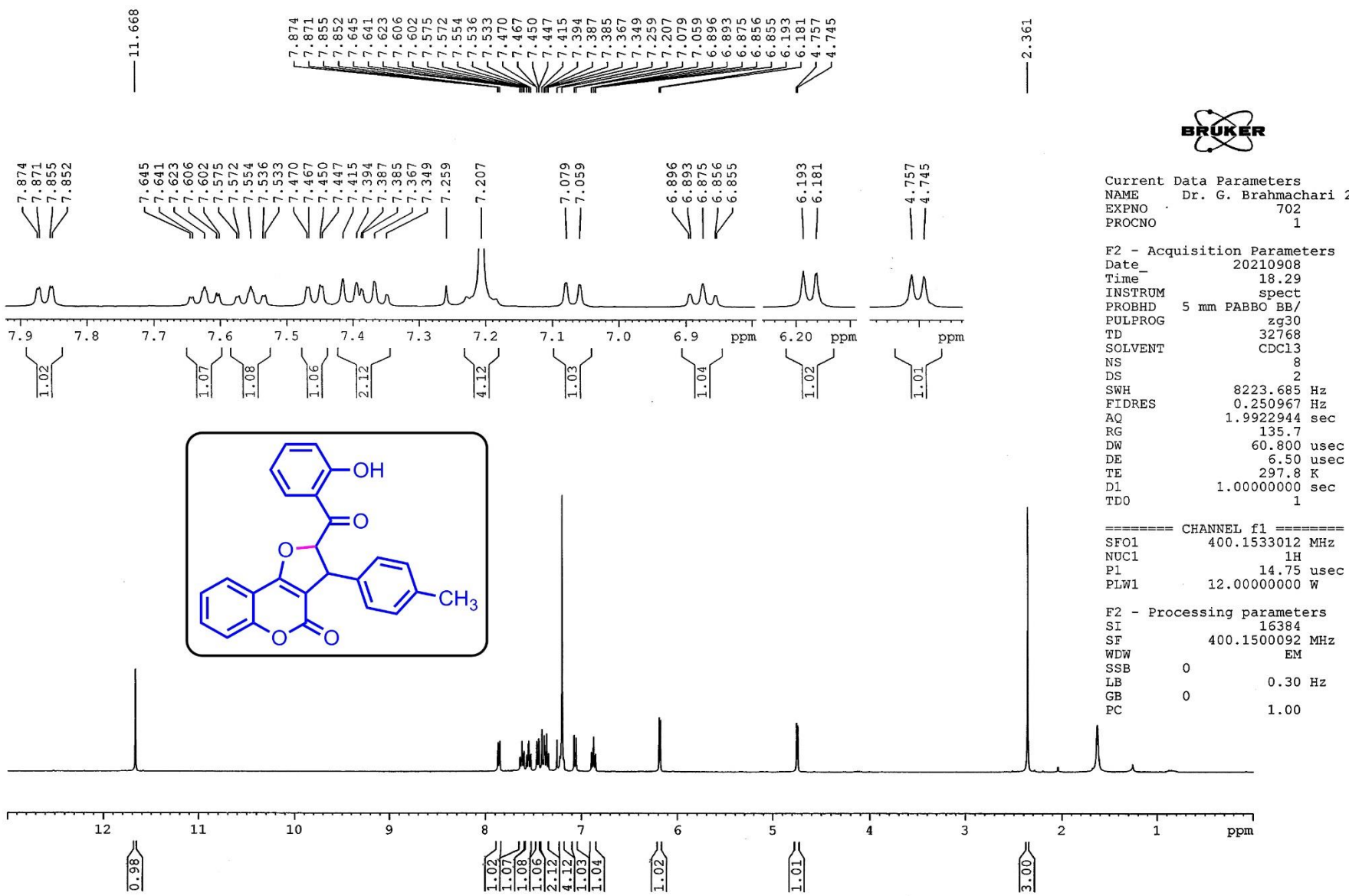


Figure S11. $^1\text{H-NMR}$ spectrum of 2-(2-hydroxybenzoyl)-3-(*p*-tolyl)-2,3-dihydro-4*H*-furo[3,2-*c*]chromen-4-one (2-3)

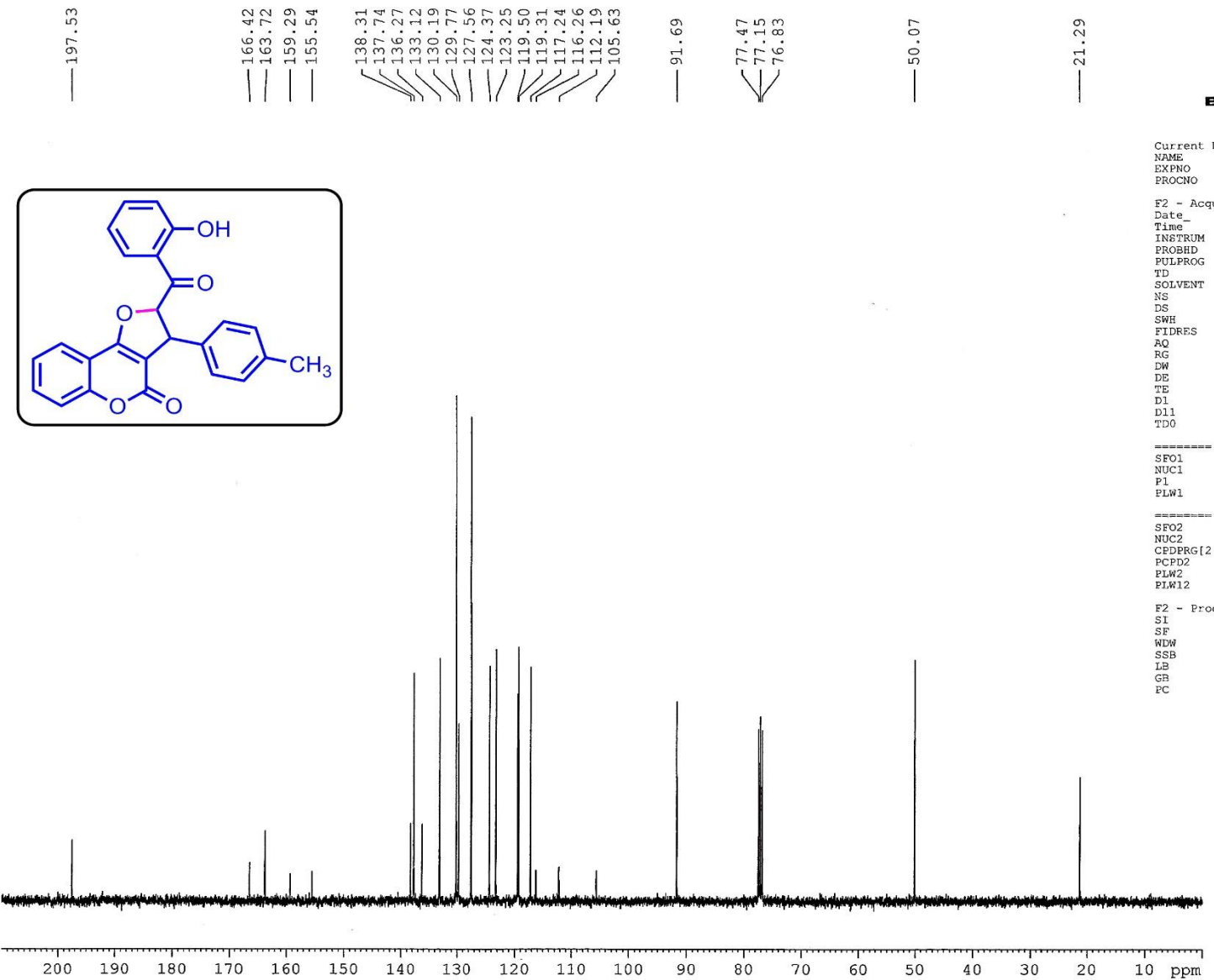


Figure S12. ¹³C-NMR spectrum of 2-(2-hydroxybenzoyl)-3-(*p*-tolyl)-2,3-dihydro-4*H*-furo[3,2-*c*]chromen-4-one (**2-3**)

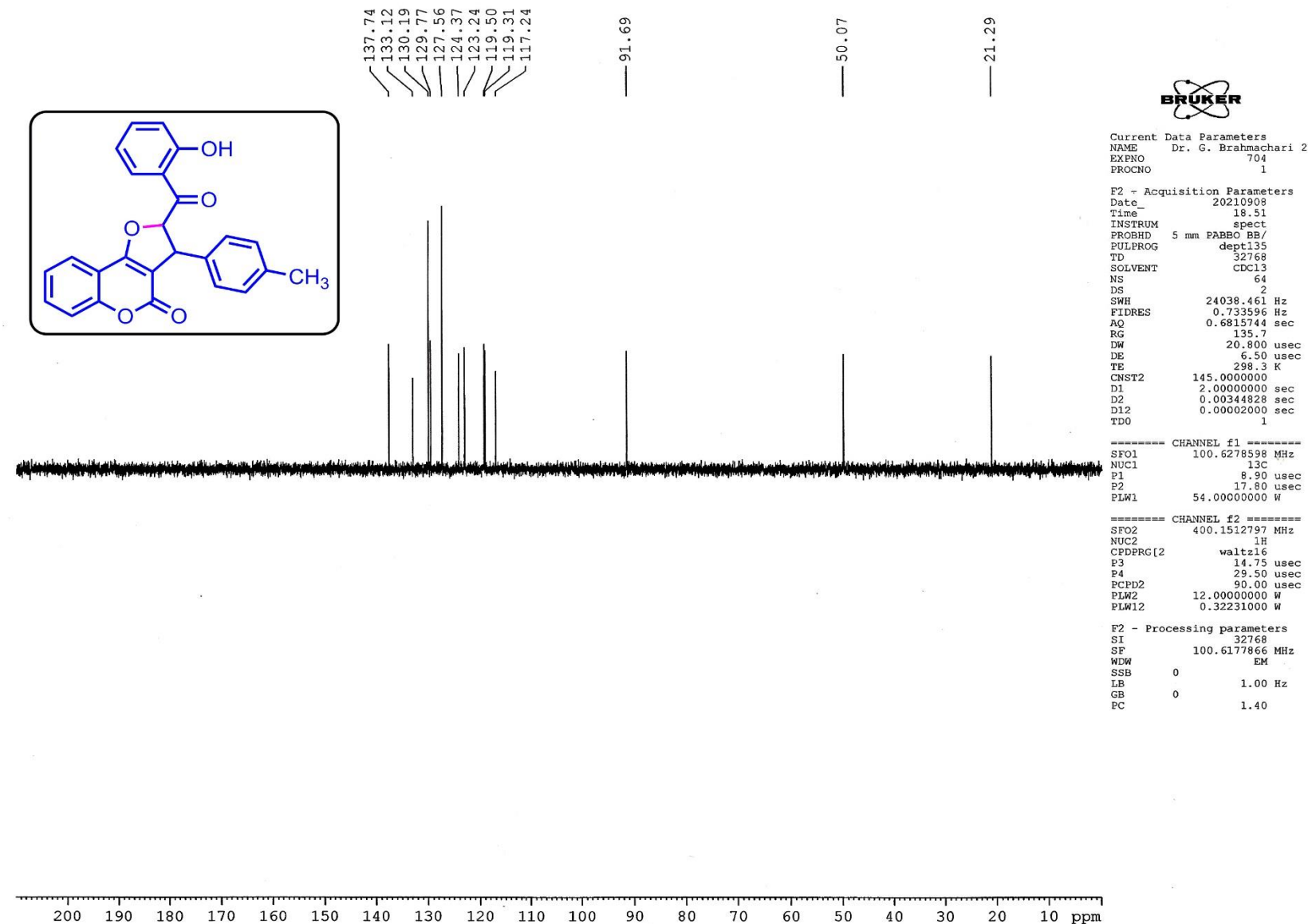


Figure S13. DEPT-135 NMR spectrum of 2-(2-hydroxybenzoyl)-3-(p-tolyl)-2,3-dihydro-4*H*-furo[3,2-*c*]chromen-4-one (**2-3**)

Acquisition Parameter

Source Type	ESI	Ion Polarity	Positive	Set Nebulizer	0.4 Bar
Focus	Active	Set Capillary	3400 V	Set Dry Heater	200 °C
Scan Begin	50 m/z	Set End Plate Offset	-500 V	Set Dry Gas	4.0 l/min
Scan End	3000 m/z	Set Charging Voltage	2000 V	Set Divert Valve	Source
		Set Corona	0 nA	Set APCI Heater	0 °C

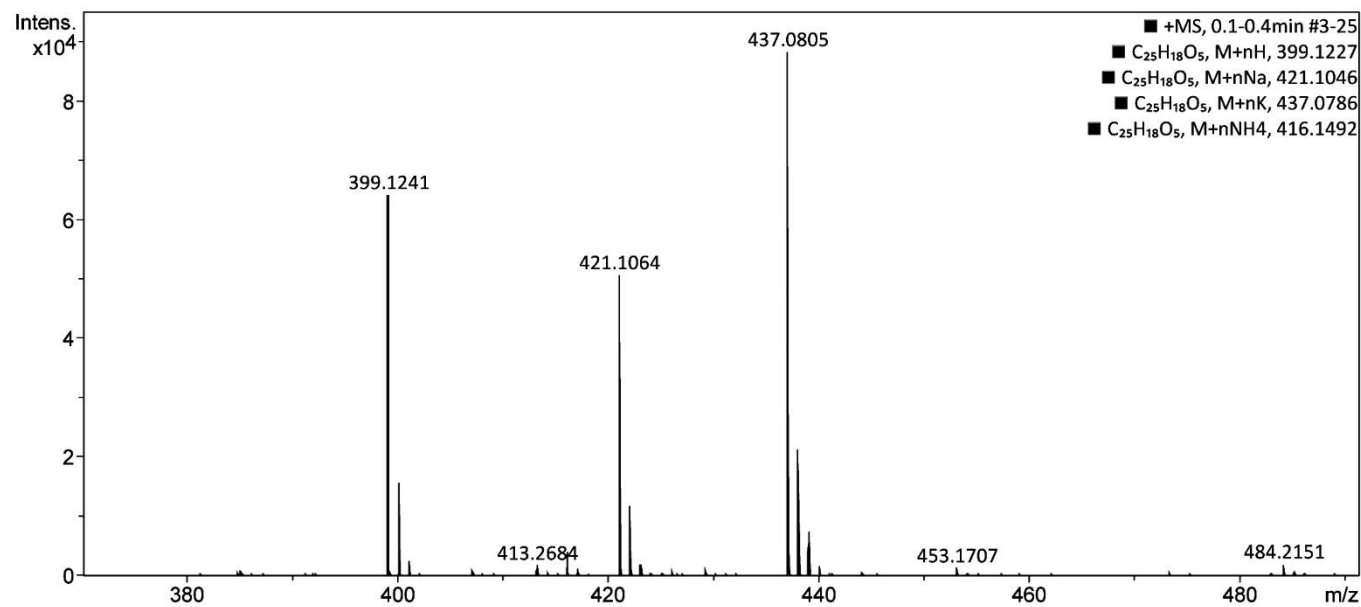
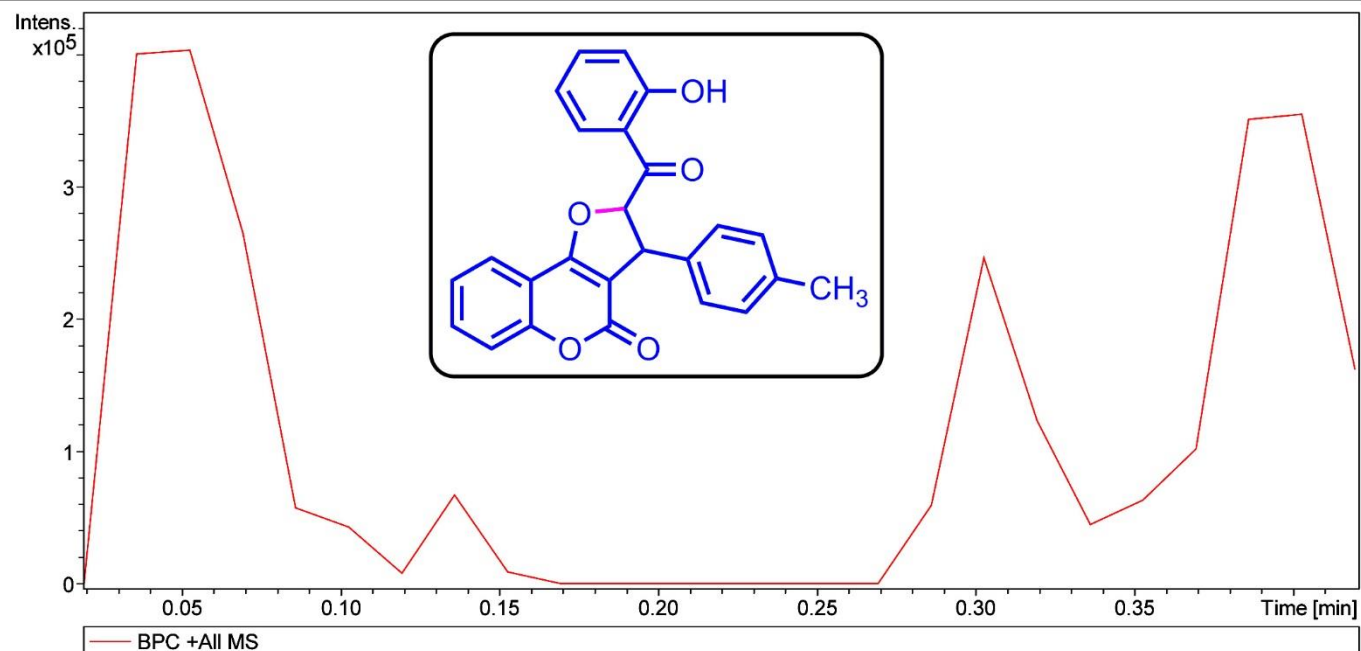


Figure S14. High-resolution Mass spectra of 2-(2-hydroxybenzoyl)-3-(*p*-tolyl)-2,3-dihydro-4*H*-furo[3,2-*c*]chromen-4-one (**2-3**)

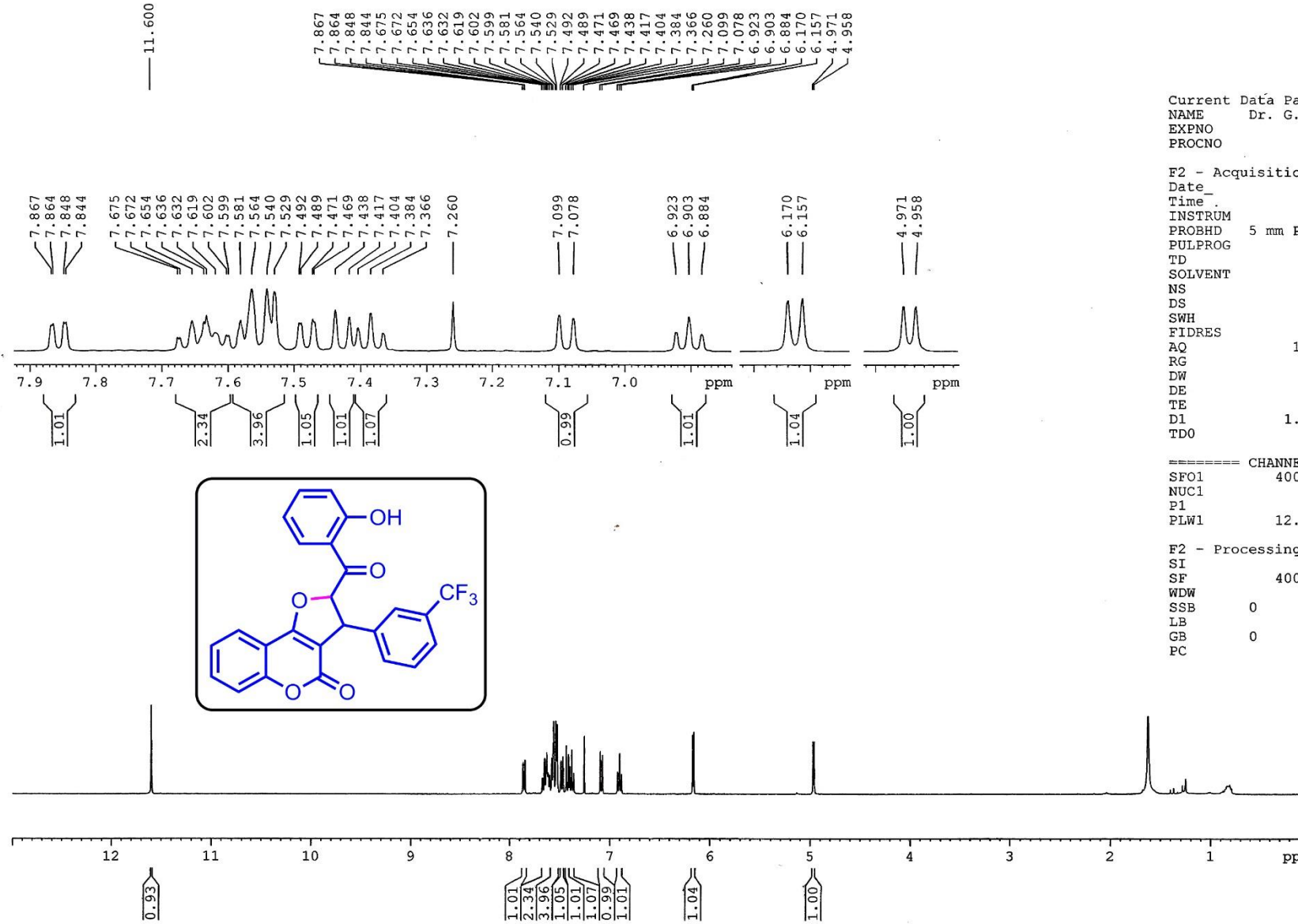


Figure S15. ¹H-NMR spectrum of 2-(2-hydroxybenzoyl)-3-(3-(trifluoromethyl)phenyl)-2,3-dihydro-4*H*-furo[3,2-*c*]chromen-4-one (**2-4**)

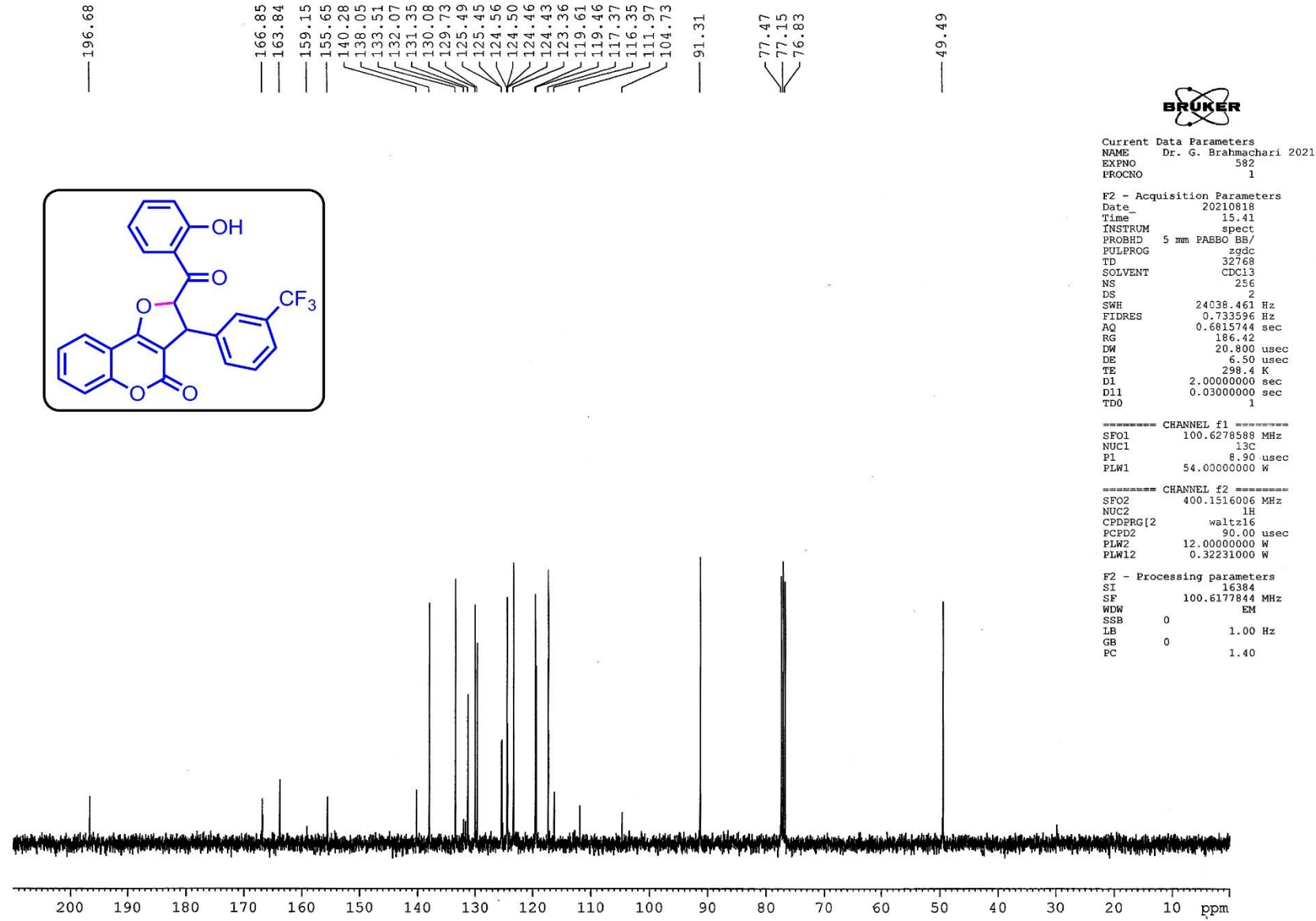


Figure S16. ^{13}C -NMR spectrum of 2-(2-hydroxybenzoyl)-3-(3-(trifluoromethyl)phenyl)-2,3-dihydro-4*H*-furo[3,2-*c*]chromen-4-one (2-4)

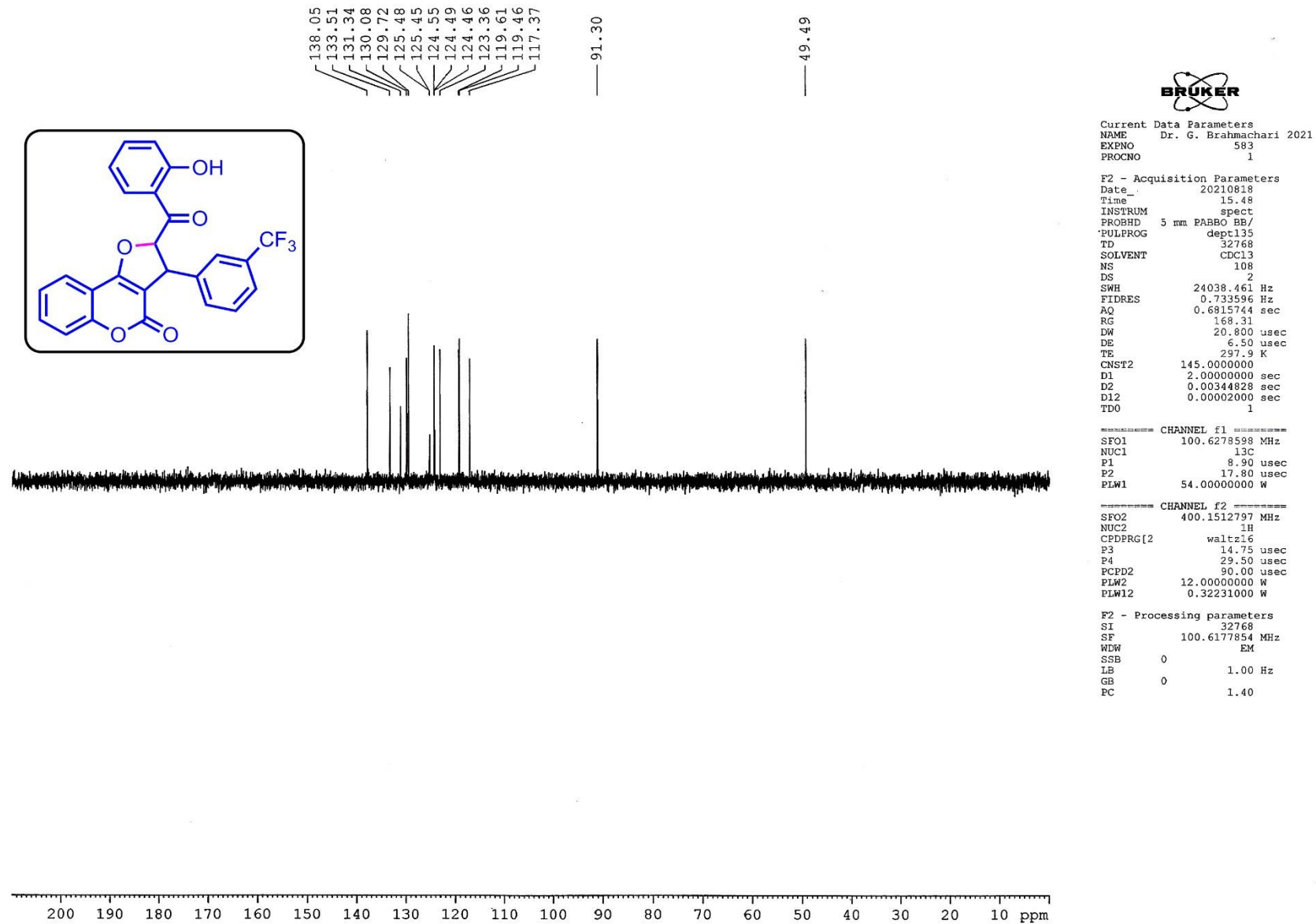


Figure S17. DEPT-135 NMR spectrum of 2-(2-hydroxybenzoyl)-3-(3-(trifluoromethyl)phenyl)-2,3-dihydro-4*H*-furo[3,2-*c*]chromen-4-one (**2-4**)

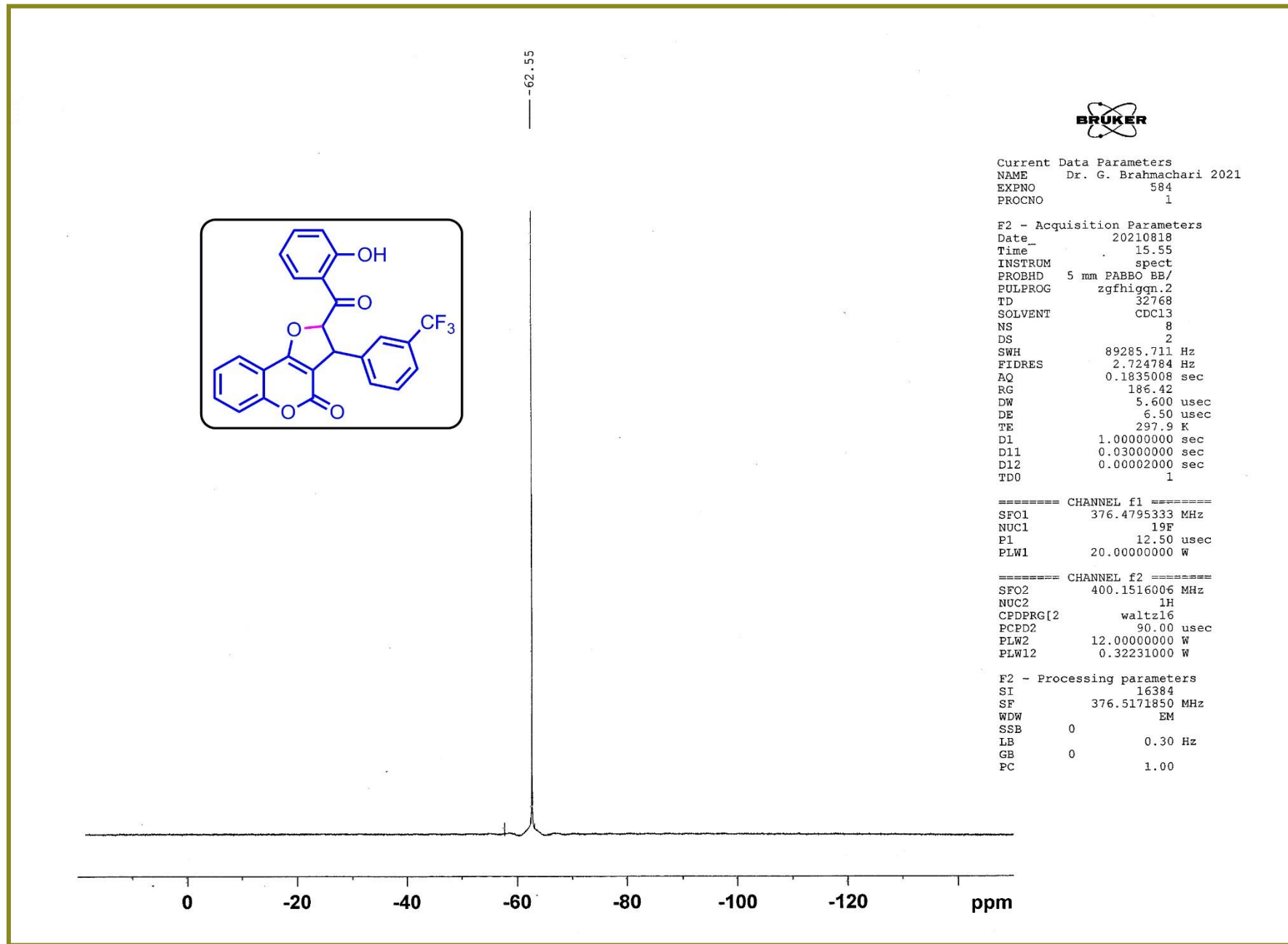


Figure S18. ^{19}F NMR spectrum of 2-(2-hydroxybenzoyl)-3-(3-(trifluoromethyl)phenyl)-2,3-dihydro-4*H*-furo[3,2-*c*]chromen-4-one (**2-4**)

Acquisition Parameter					
Source Type	ESI	Ion Polarity	Positive	Set Nebulizer	0.4 Bar
Focus	Active	Set Capillary	3400 V	Set Dry Heater	200 °C
Scan Begin	50 m/z	Set End Plate Offset	-500 V	Set Dry Gas	4.0 l/min
Scan End	3000 m/z	Set Charging Voltage	2000 V	Set Divert Valve	Source
		Set Corona	0 nA	Set APCI Heater	0 °C

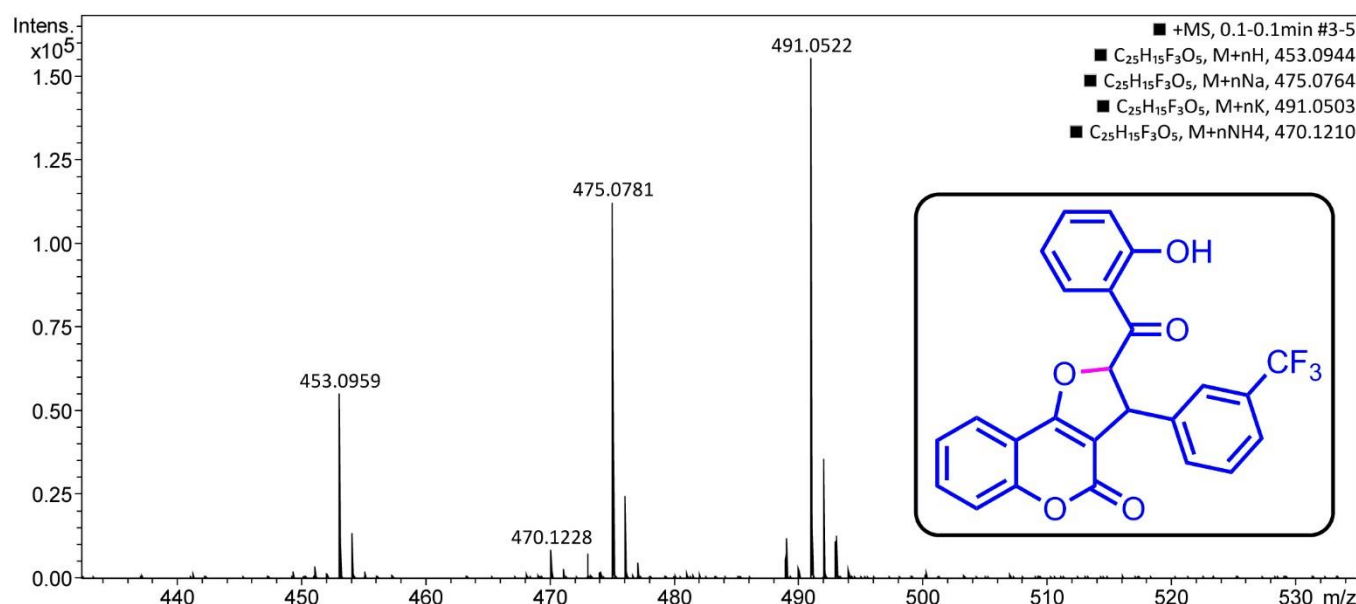
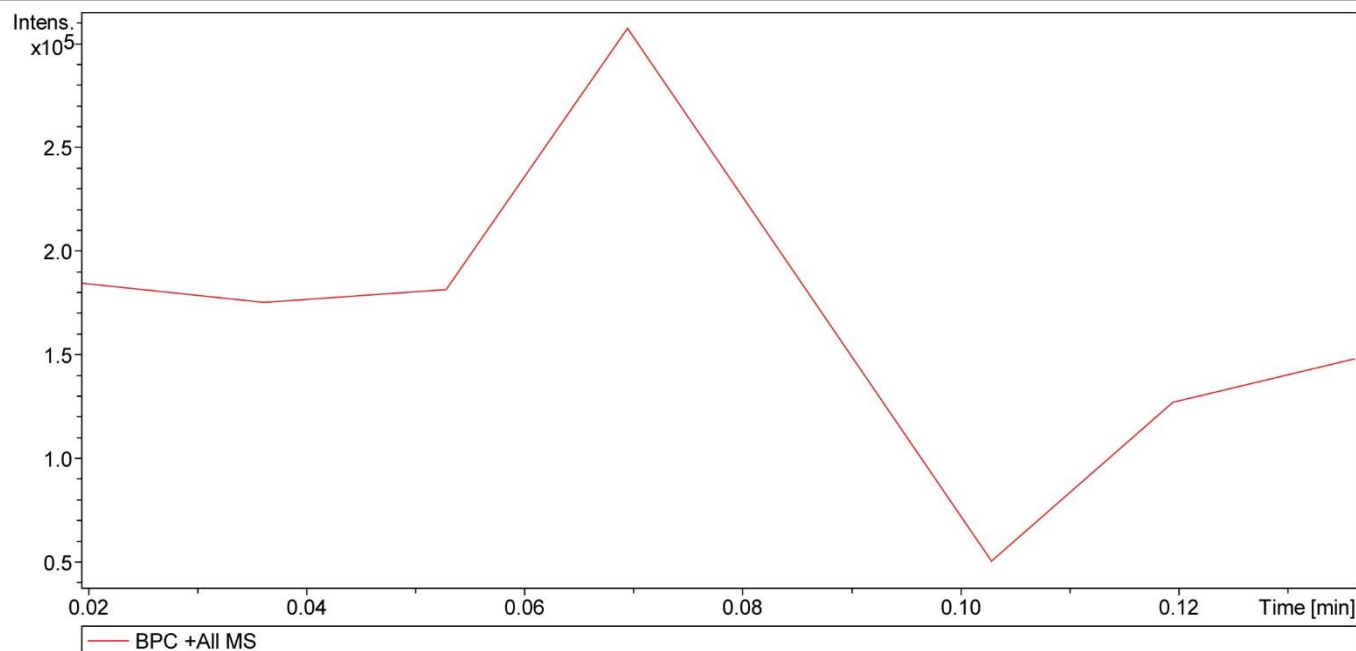


Figure S19. High-resolution Mass spectra of 2-(2-hydroxybenzoyl)-3-(3-(trifluoromethyl)phenyl)-2,3-dihydro-4H-furo[3,2-*c*]chromen-4-one (**2-4**)

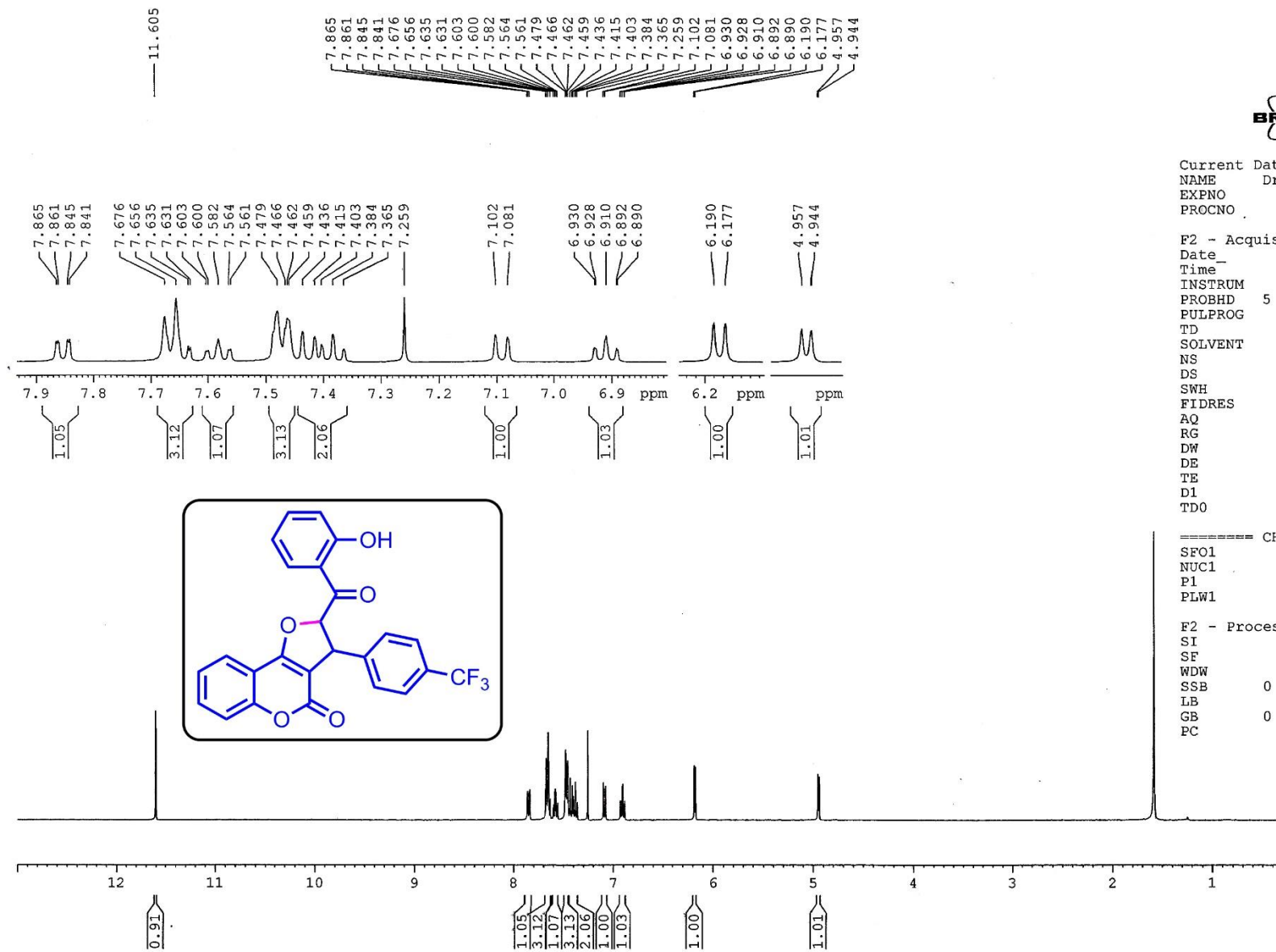


Figure S20. ^1H -NMR spectrum of 2-(2-hydroxybenzoyl)-3-(4-(trifluoromethyl)phenyl)-2,3-dihydro-4*H*-furo[3,2-*c*]chromen-4-one (**2-5**)

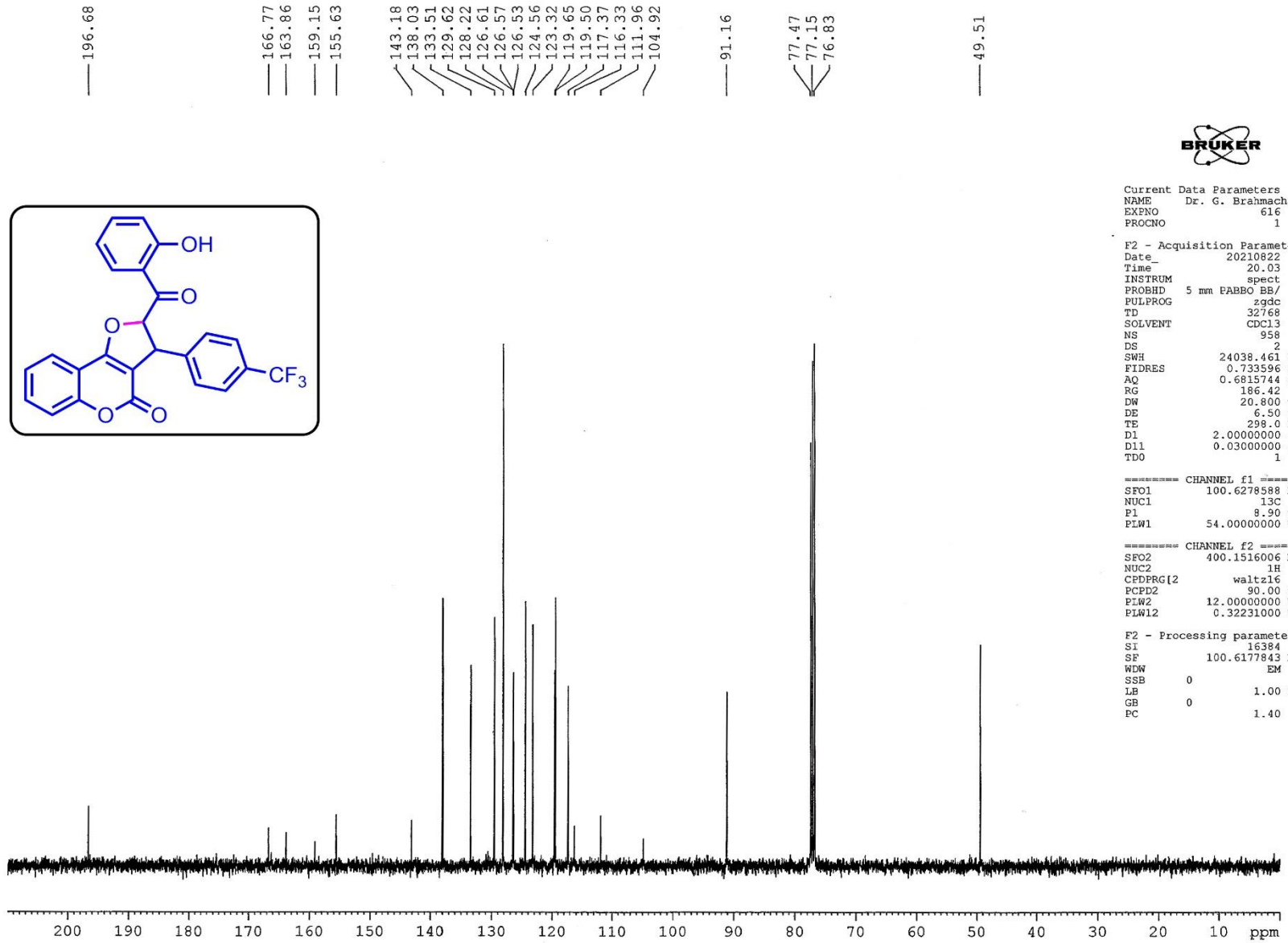


Figure S21. ^{13}C -NMR spectrum of 2-(2-hydroxybenzoyl)-3-(4-(trifluoromethyl)phenyl)-2,3-dihydro-4*H*-furo[3,2-*c*]chromen-4-one (**2-5**)

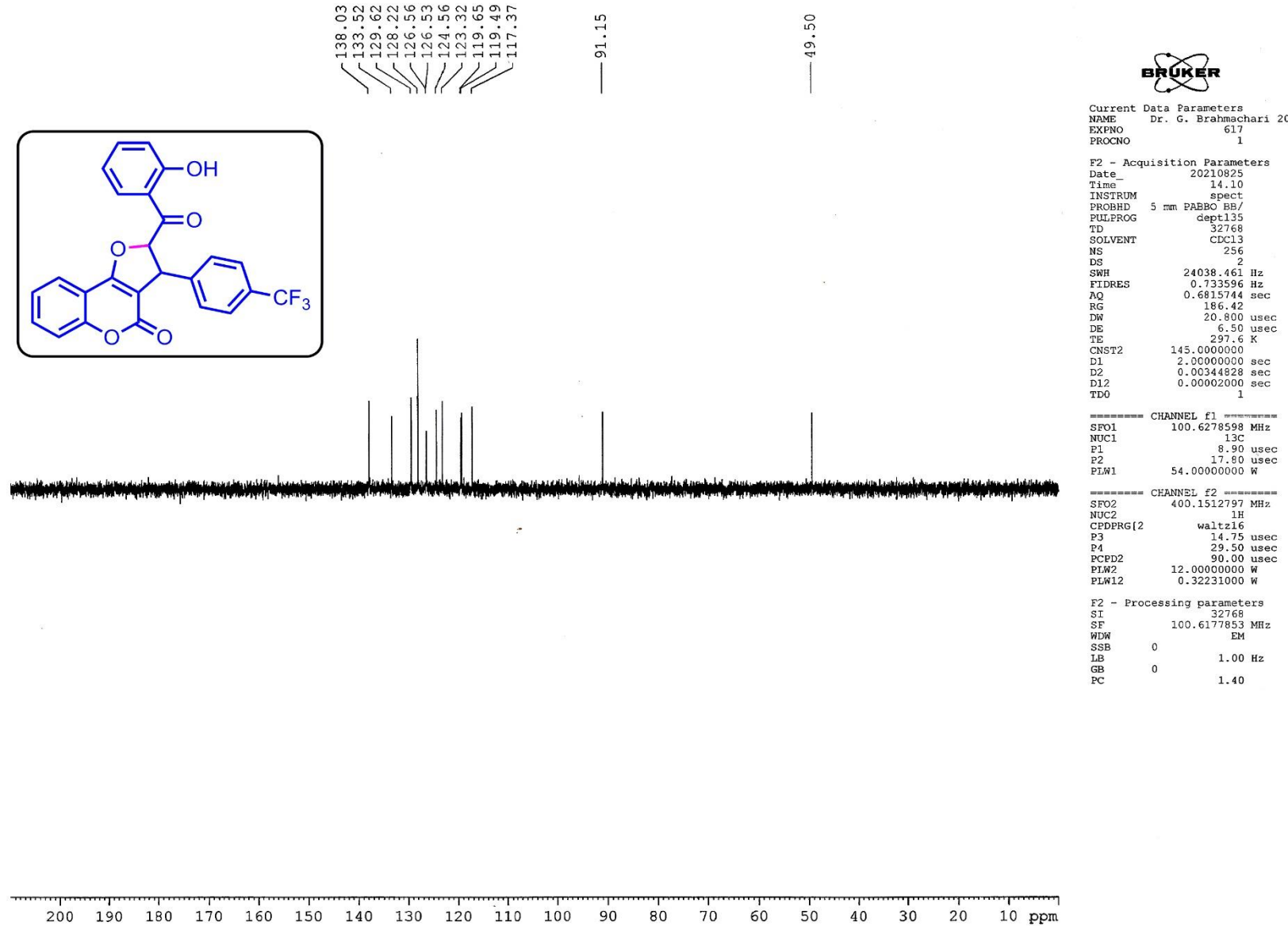


Figure S22. DEPT-135 NMR spectrum of 2-(2-hydroxybenzoyl)-3-(4-(trifluoromethyl)phenyl)-2,3-dihydro-4*H*-furo[3,2-*c*]chromen-4-one (**2-5**)

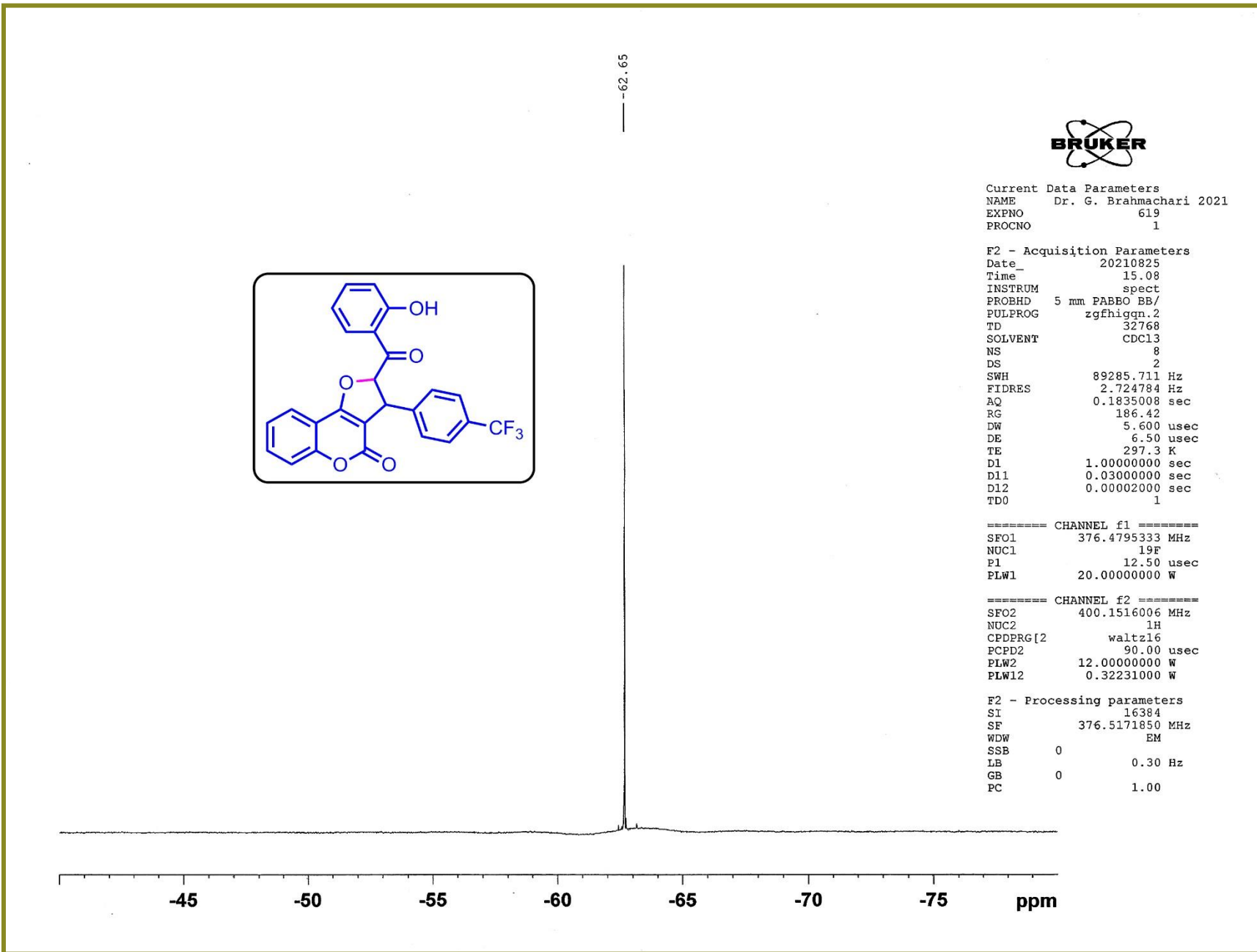


Figure S23. ¹⁹F NMR spectrum of 2-(2-hydroxybenzoyl)-3-(4-(trifluoromethyl)phenyl)-2,3-dihydro-4H-furo[3,2-c]chromen-4-one (**2-5**)

Acquisition Parameter

Source Type	ESI	Ion Polarity	Positive	Set Nebulizer	0.4 Bar
Focus	Active	Set Capillary	3400 V	Set Dry Heater	200 °C
Scan Begin	50 m/z	Set End Plate Offset	-500 V	Set Dry Gas	4.0 l/min
Scan End	3000 m/z	Set Charging Voltage	2000 V	Set Divert Valve	Source
		Set Corona	0 nA	Set APCI Heater	0 °C

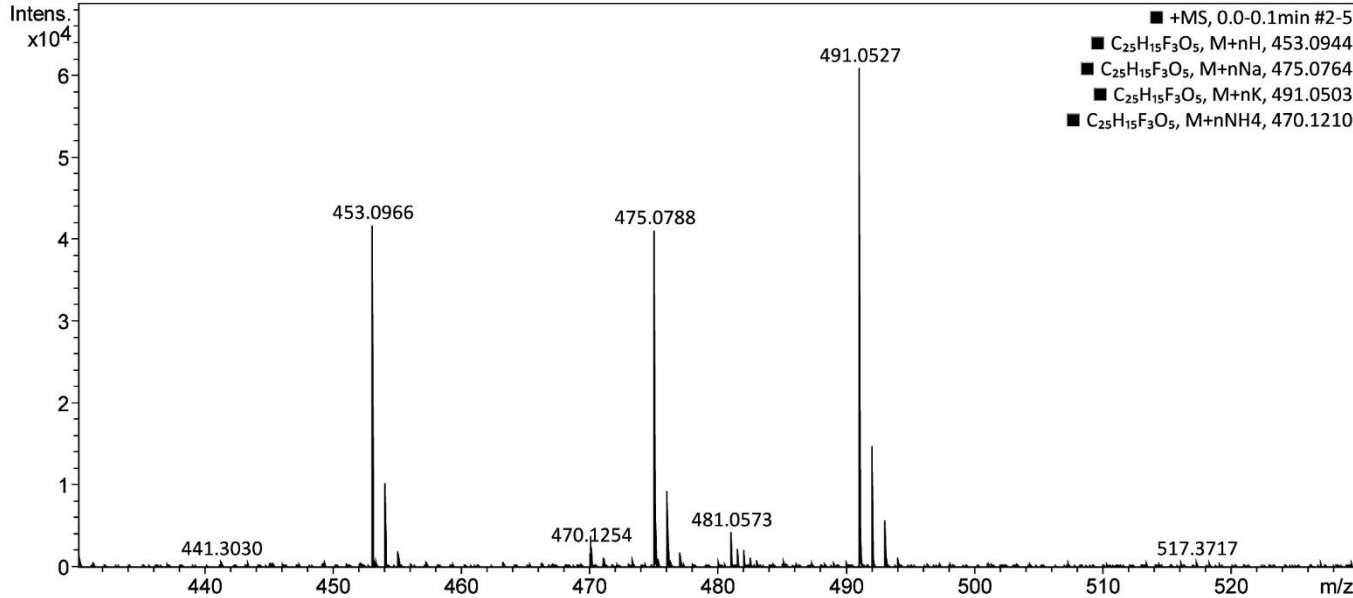
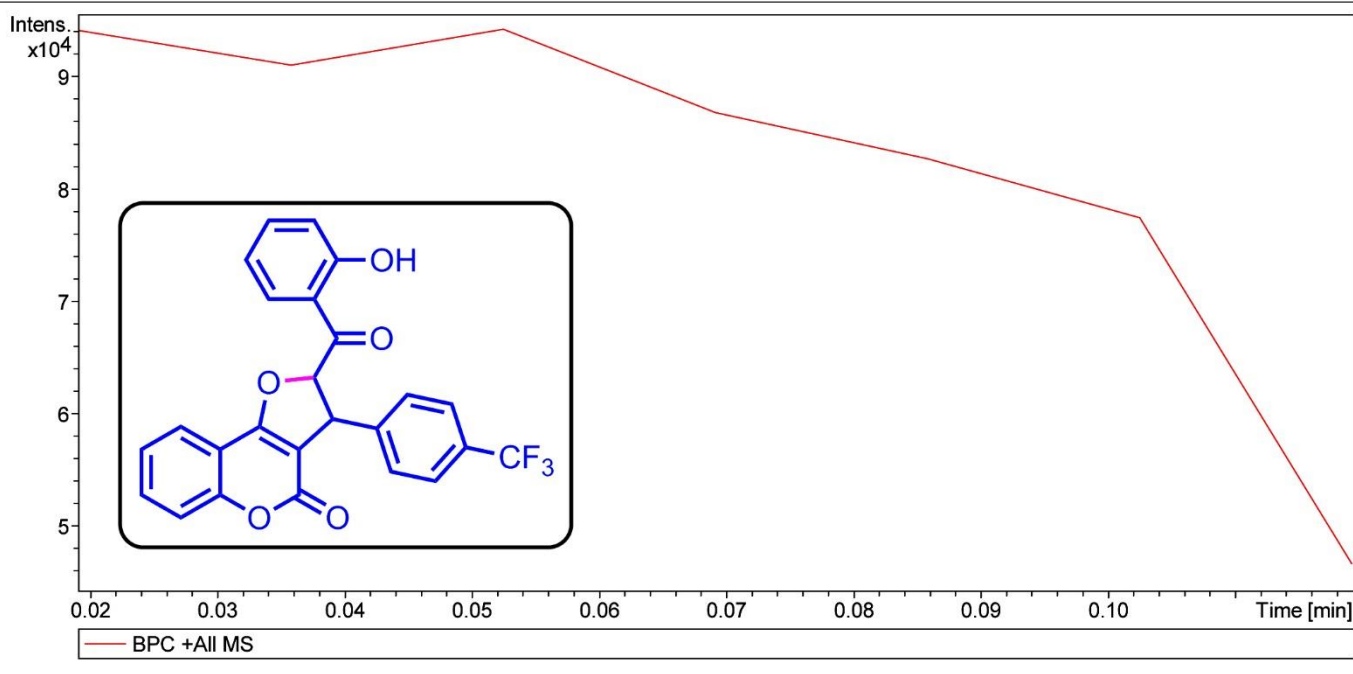


Figure S24. High-resolution Mass spectra of 22-(2-hydroxybenzoyl)-3-(4-(trifluoromethyl)phenyl)-2,3-dihydro-4H-furo[3,2-c]chromen-4-one (**2-5**)

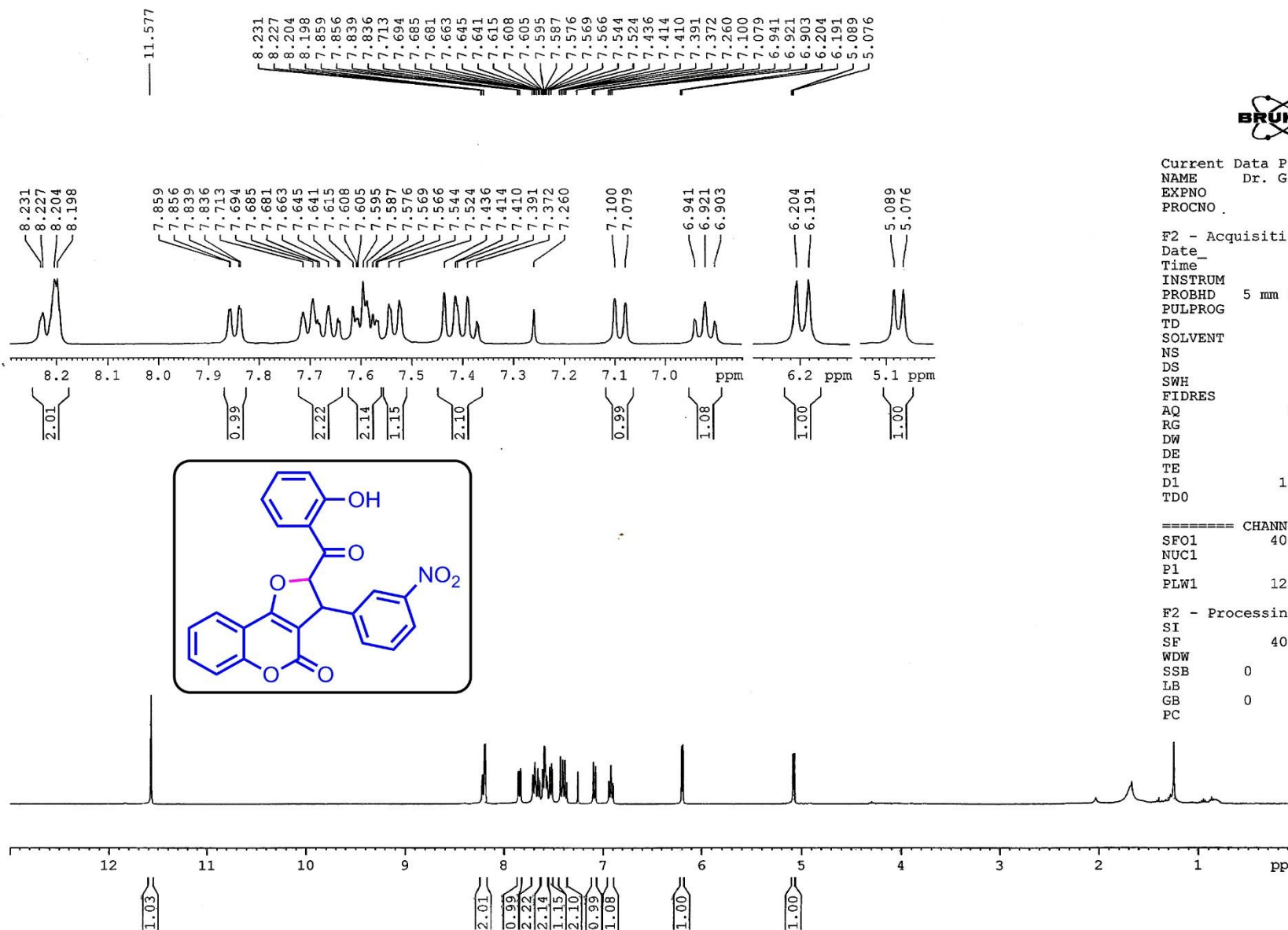


Figure S25. ¹H-NMR spectrum of 2-(2-hydroxybenzoyl)-3-(3-nitrophenyl)-2,3-dihydro-4*H*-furo[3,2-*c*]chromen-4-one (**2-6**)

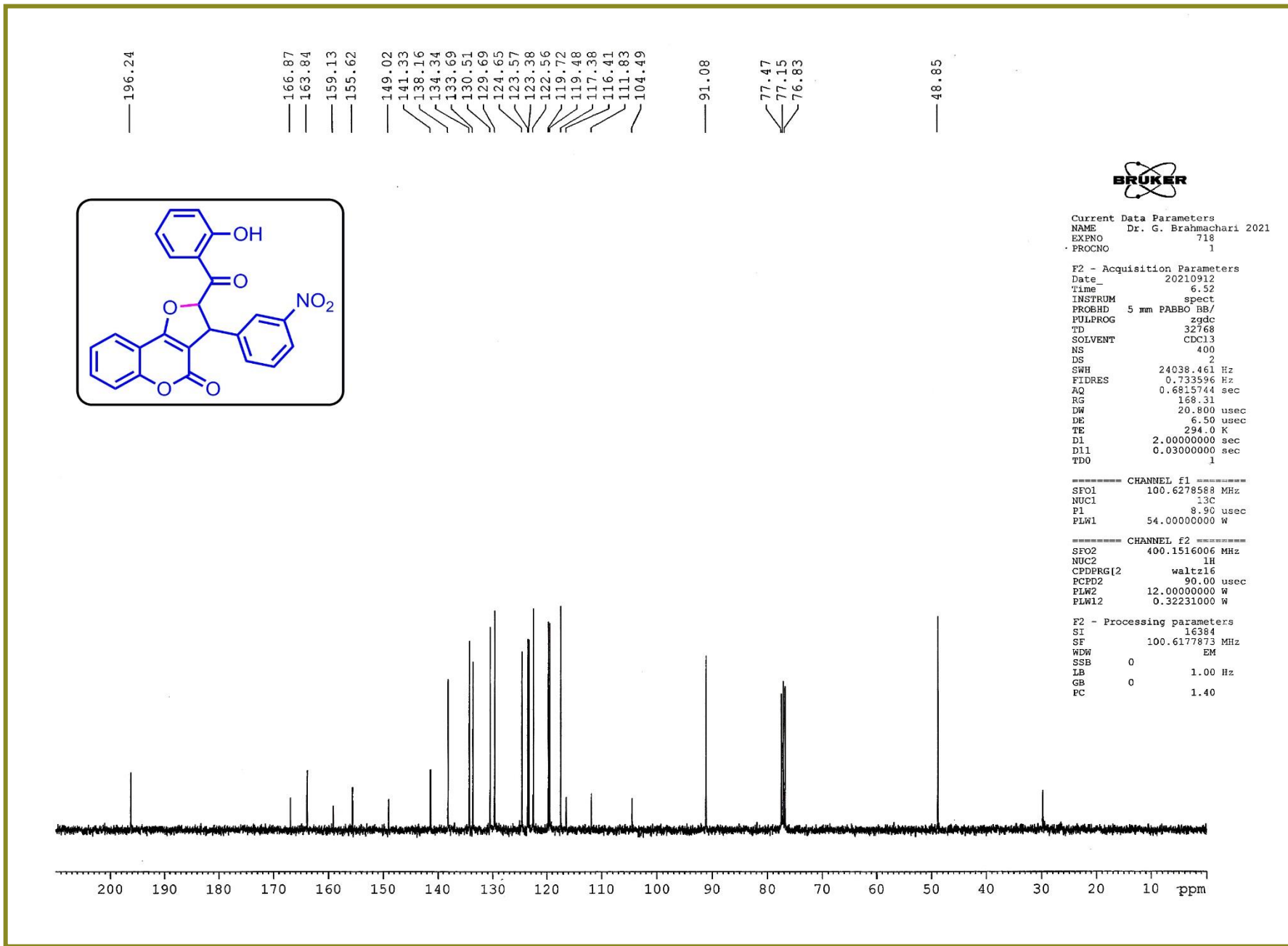


Figure S26. ^{13}C -NMR spectrum of 2-(2-hydroxybenzoyl)-3-(3-nitrophenyl)-2,3-dihydro-4*H*-furo[3,2-*c*]chromen-4-one (**2-6**)

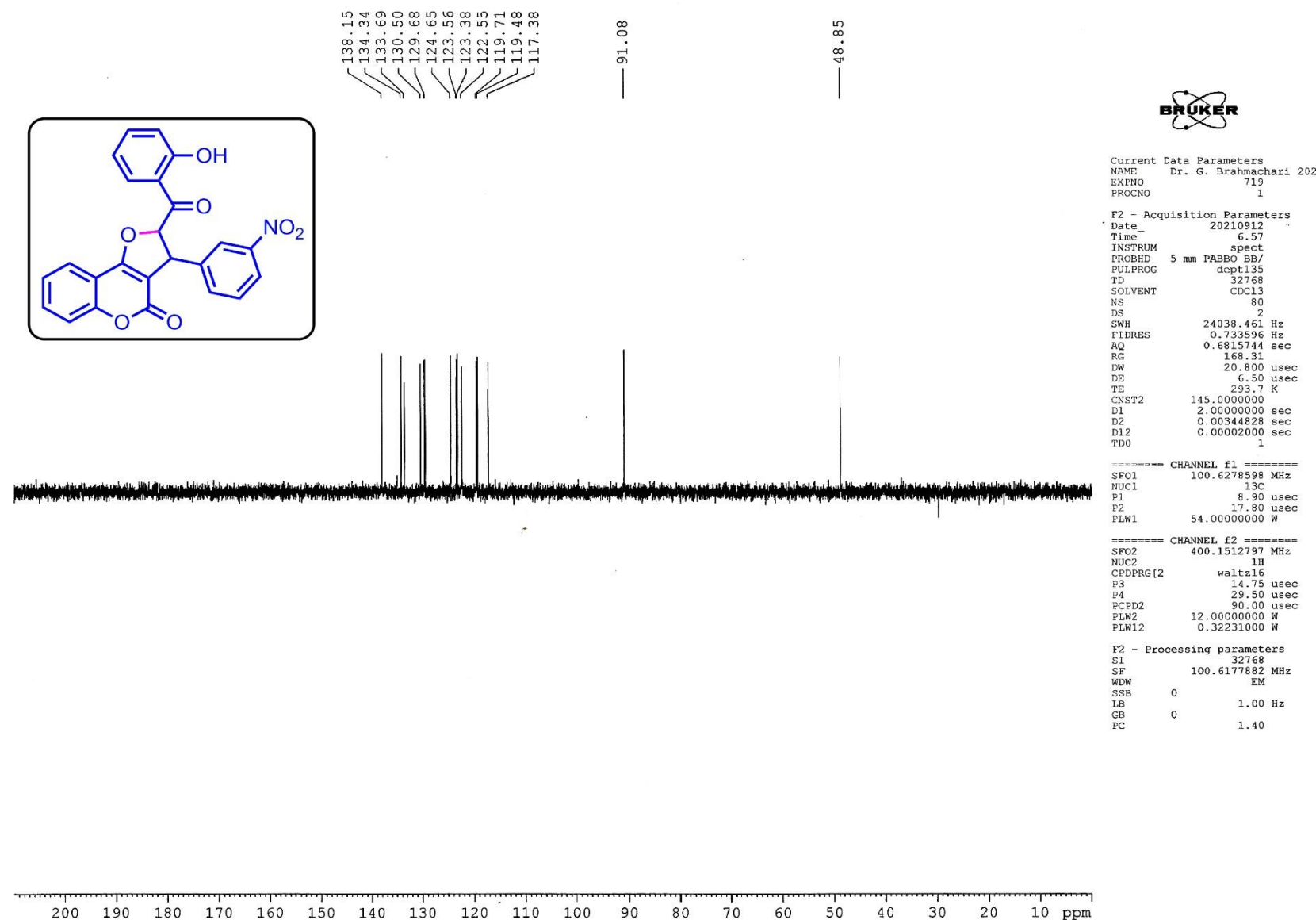


Figure S27. DEPT-135 NMR spectrum of 2-(2-hydroxybenzoyl)-3-(3-nitrophenyl)-2,3-dihydro-4*H*-furo[3,2-*c*]chromen-4-one (**2-6**)

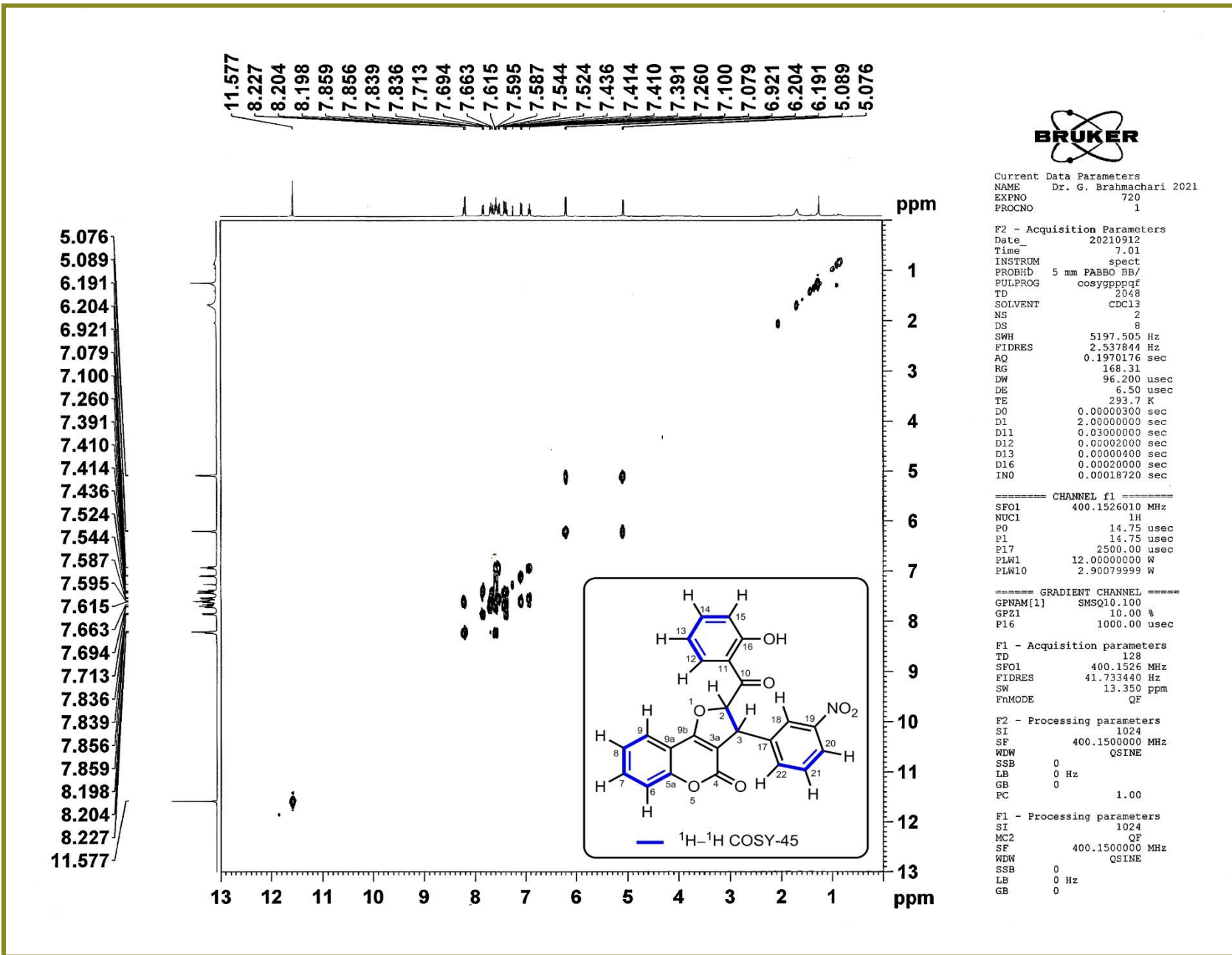


Figure S28. ¹H-¹H COSY-45 NMR spectrum of 2-(2-hydroxybenzoyl)-3-(3-nitrophenyl)-2,3-dihydro-4*H*-furo[3,2-*c*]chromen-4-one (**2-6**)

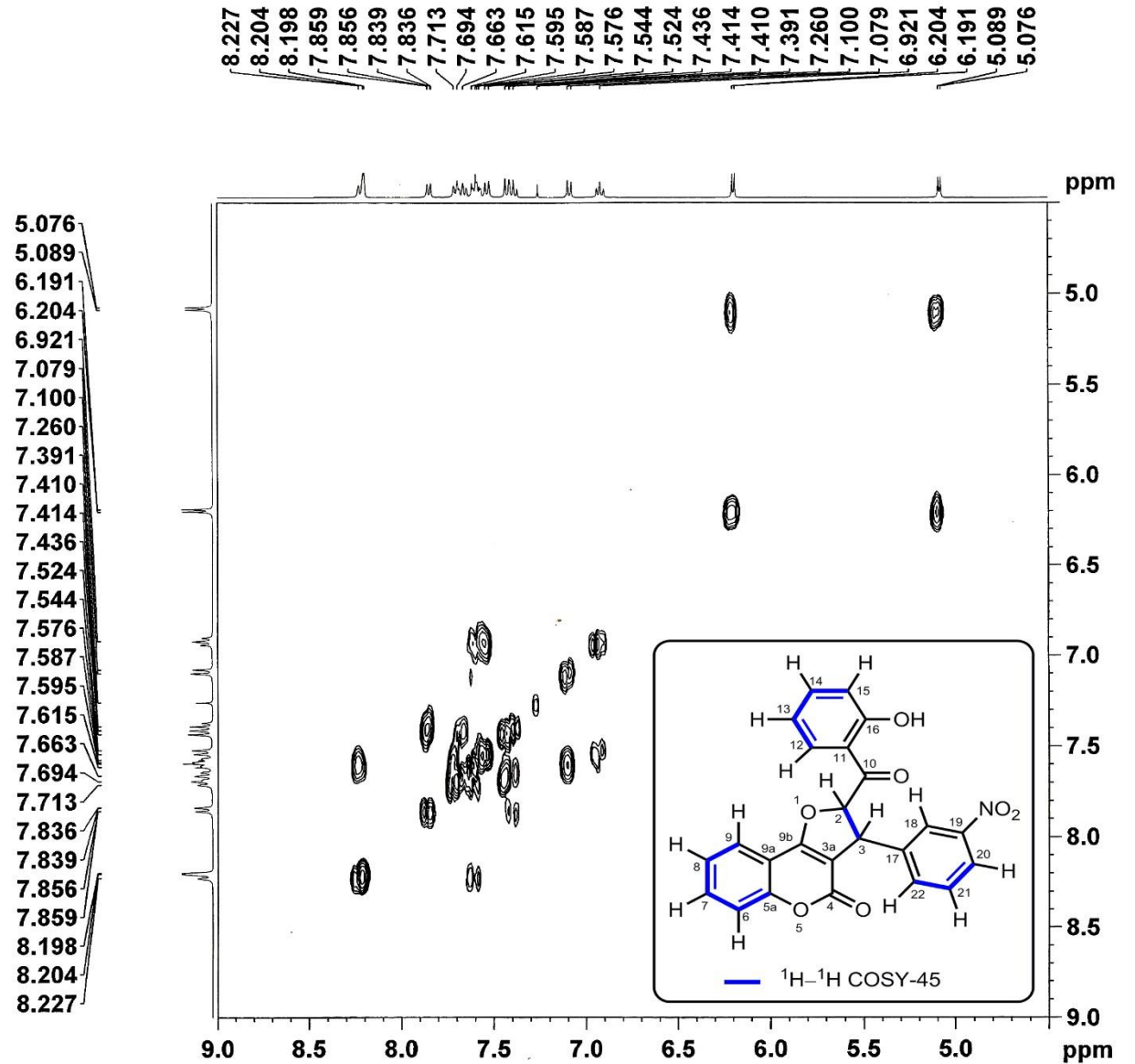


Figure S28a. ¹H-¹H COSY 45 NMR spectrum of 2-(2-hydroxybenzoyl)-3-(3-nitrophenyl)-2,3-dihydro-4*H*-furo[3,2-*c*]chromen-4-one (**2-6**) [Extended-1]

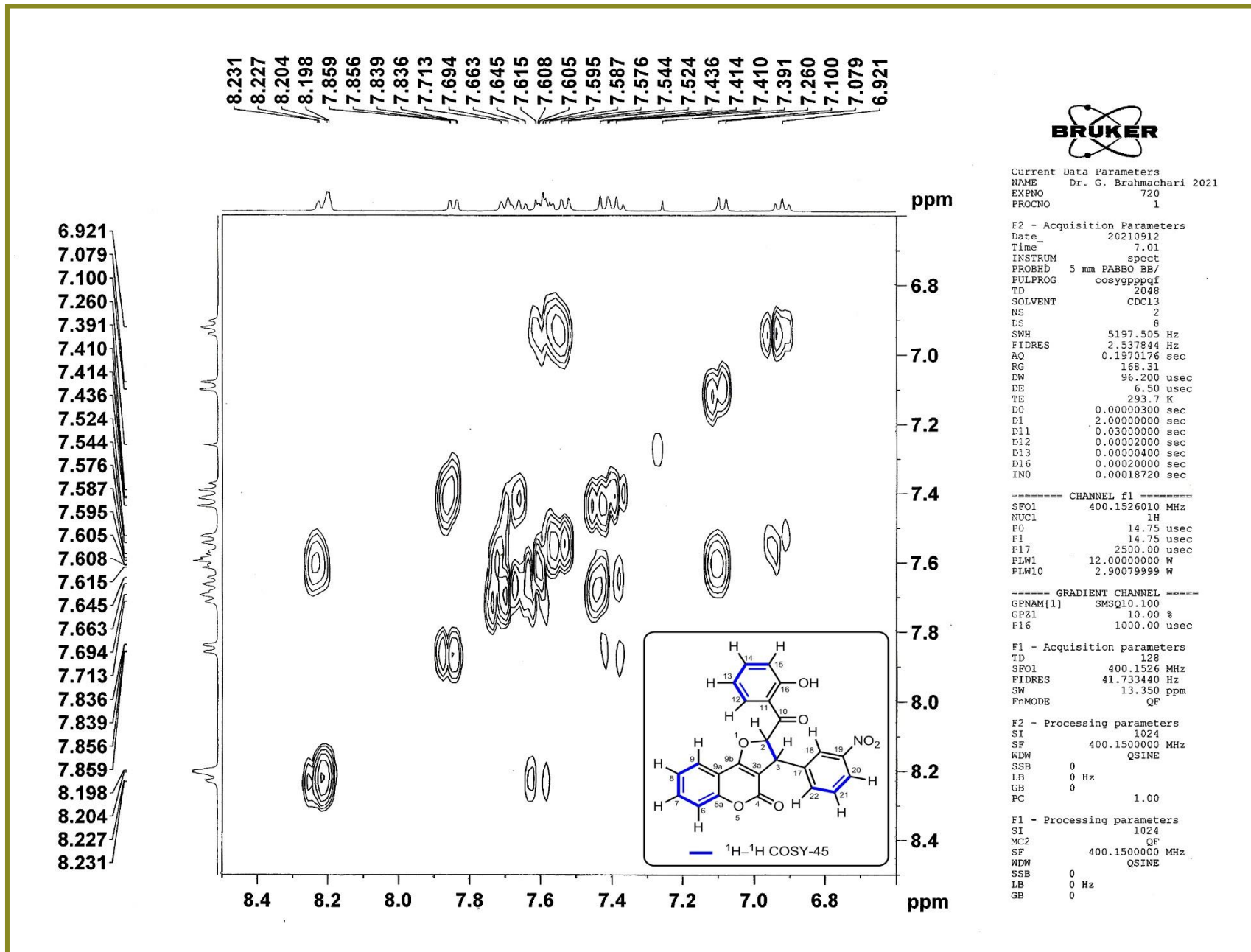


Figure S28b. ¹H-¹H COSY 45 NMR spectrum of 2-(2-hydroxybenzoyl)-3-(3-nitrophenyl)-2,3-dihydro-4*H*-furo[3,2-*c*]chromen-4-one (**2-6**) [Extended-2]

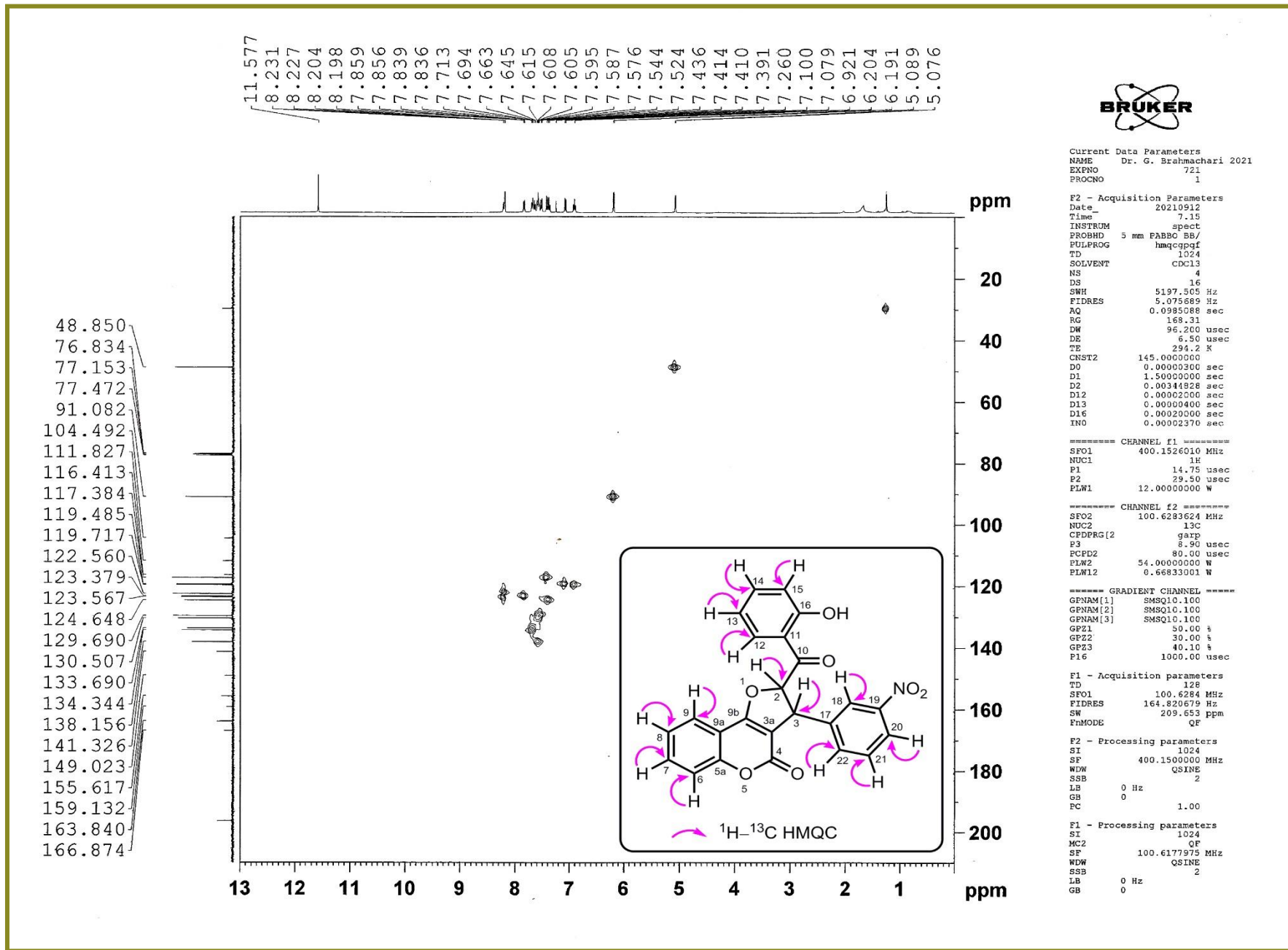


Figure S29. ¹H-¹³C HMQC NMR spectrum of 2-(2-hydroxybenzoyl)-3-(3-nitrophenyl)-2,3-dihydro-4*H*-furo[3,2-*c*]chromen-4-one (**2-6**)

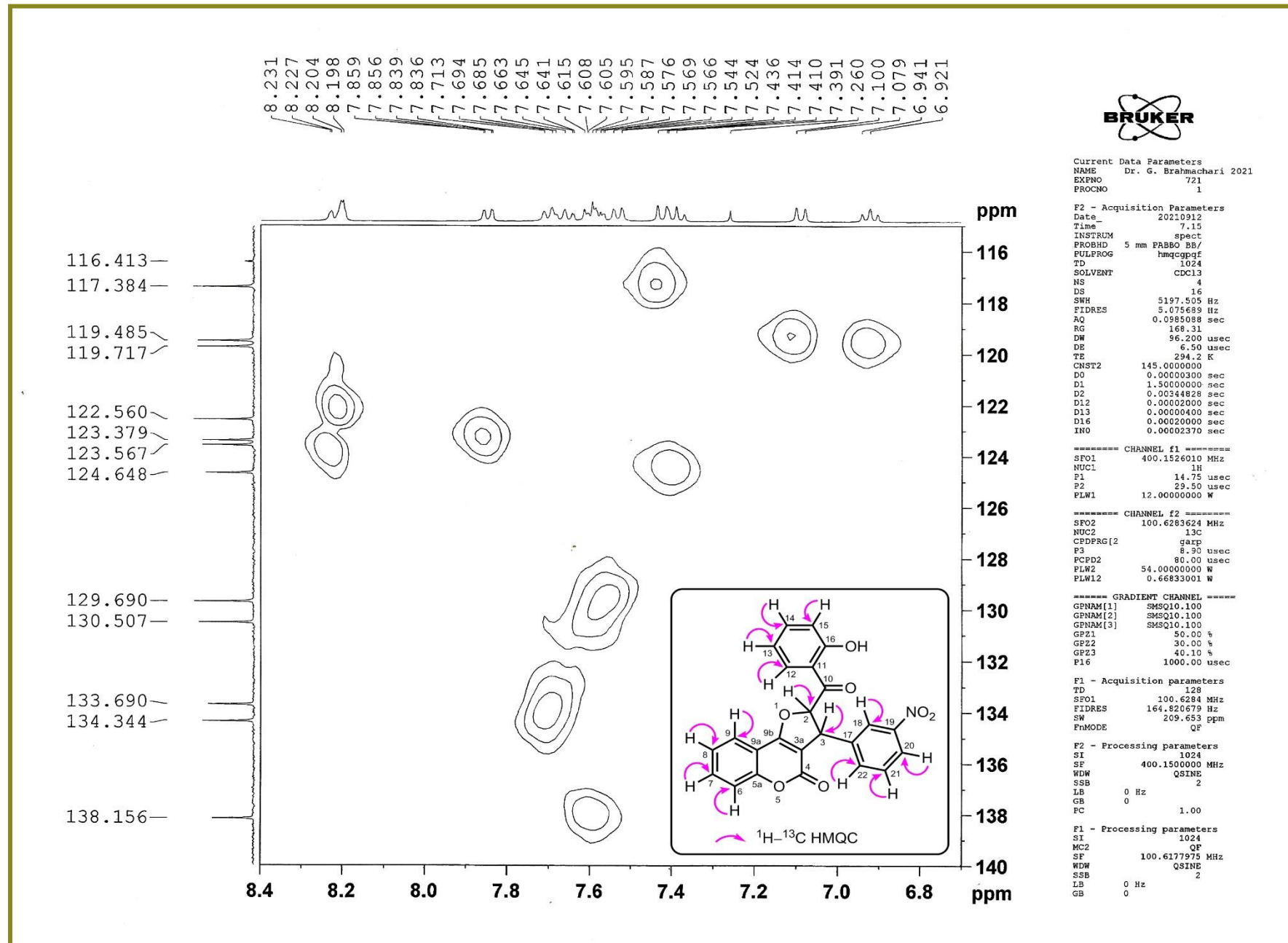


Figure S29a. ^1H - ^{13}C HMQC NMR spectrum of 2-(2-hydroxybenzoyl)-3-(3-nitrophenyl)-2,3-dihydro-4*H*-furo[3,2-*c*]chromen-4-one (**2-6**) [Extended-1]
S33

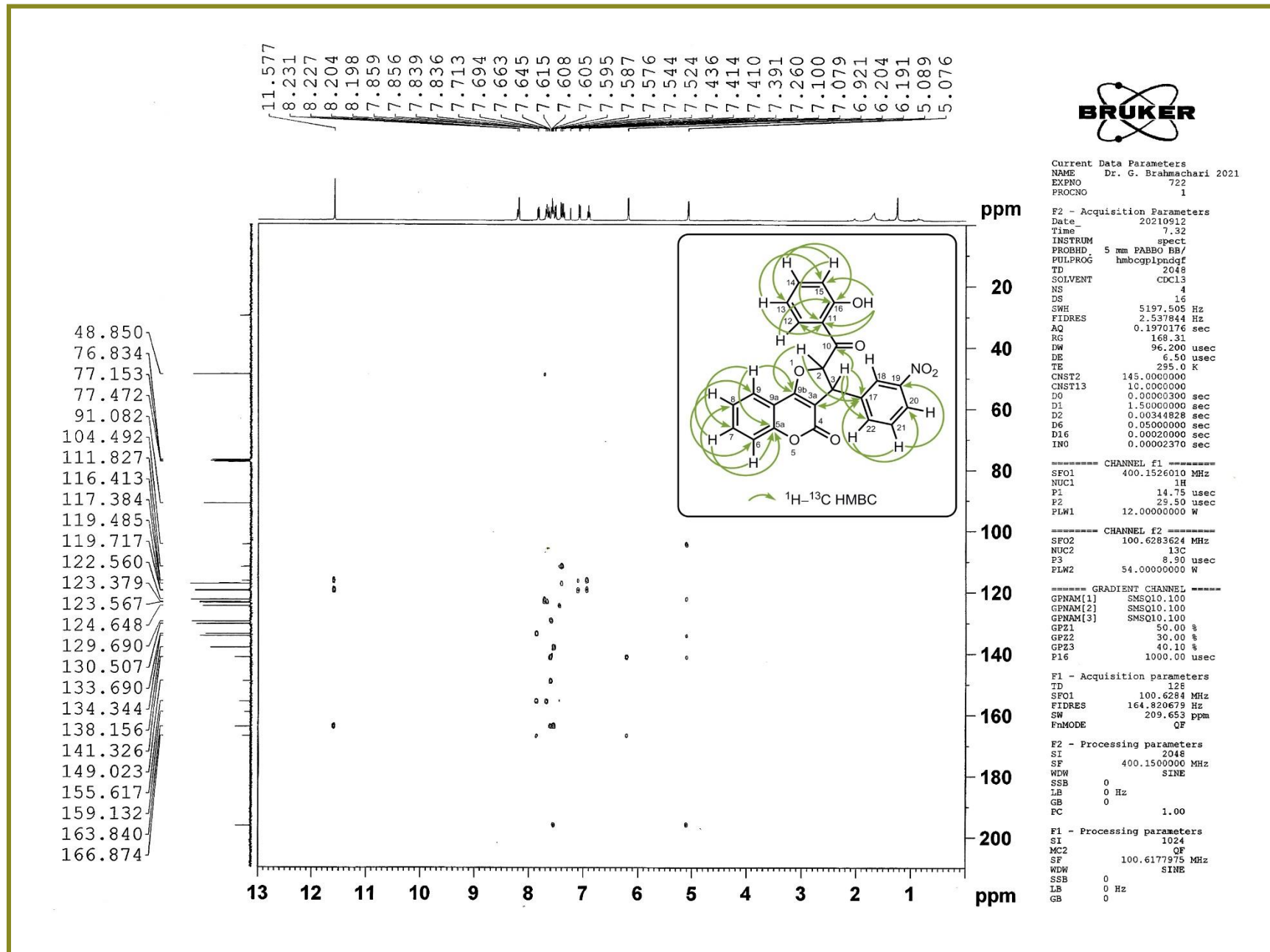


Figure S30. ¹H-¹³C HMBC NMR spectrum of 2-(2-hydroxybenzoyl)-3-(3-nitrophenyl)-2,3-dihydro-4*H*-furo[3,2-*c*]chromen-4-one (**2-6**)

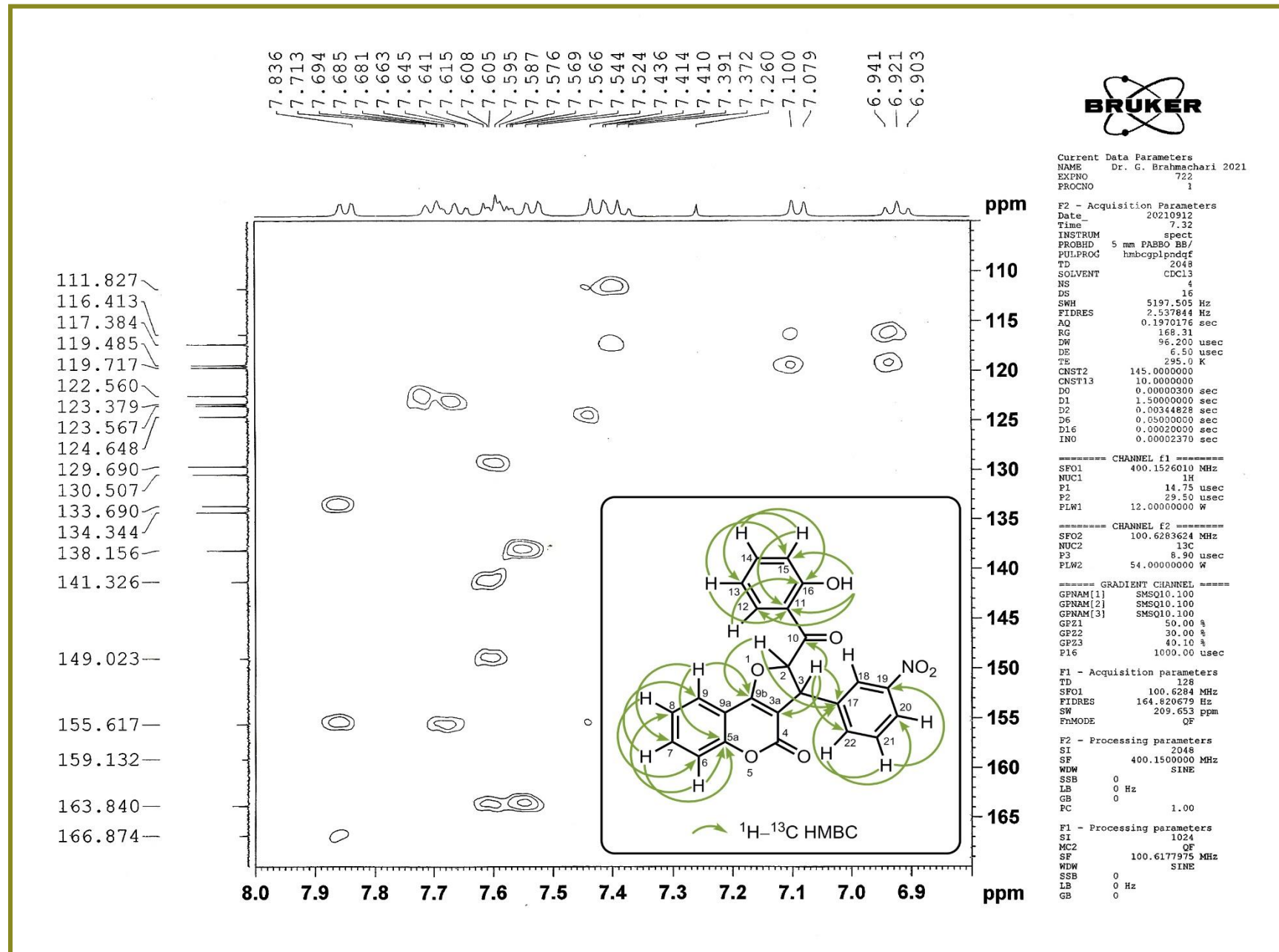


Figure S30a. ^1H - ^{13}C HMBC NMR spectrum of 2-(2-hydroxybenzoyl)-3-(3-nitrophenyl)-2,3-dihydro-4*H*-furo[3,2-*c*]chromen-4-one (**2-6**) [Extended-1]

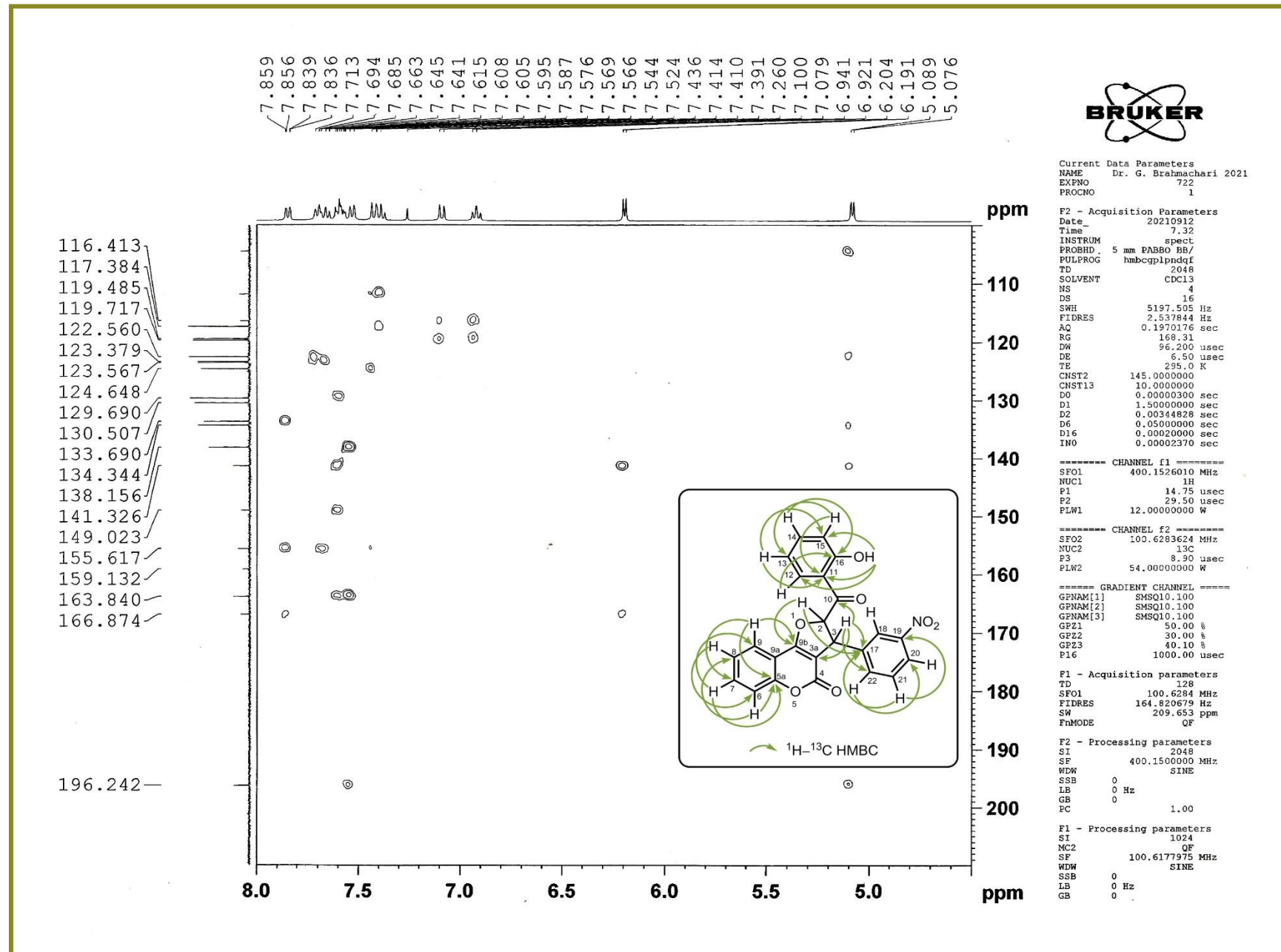
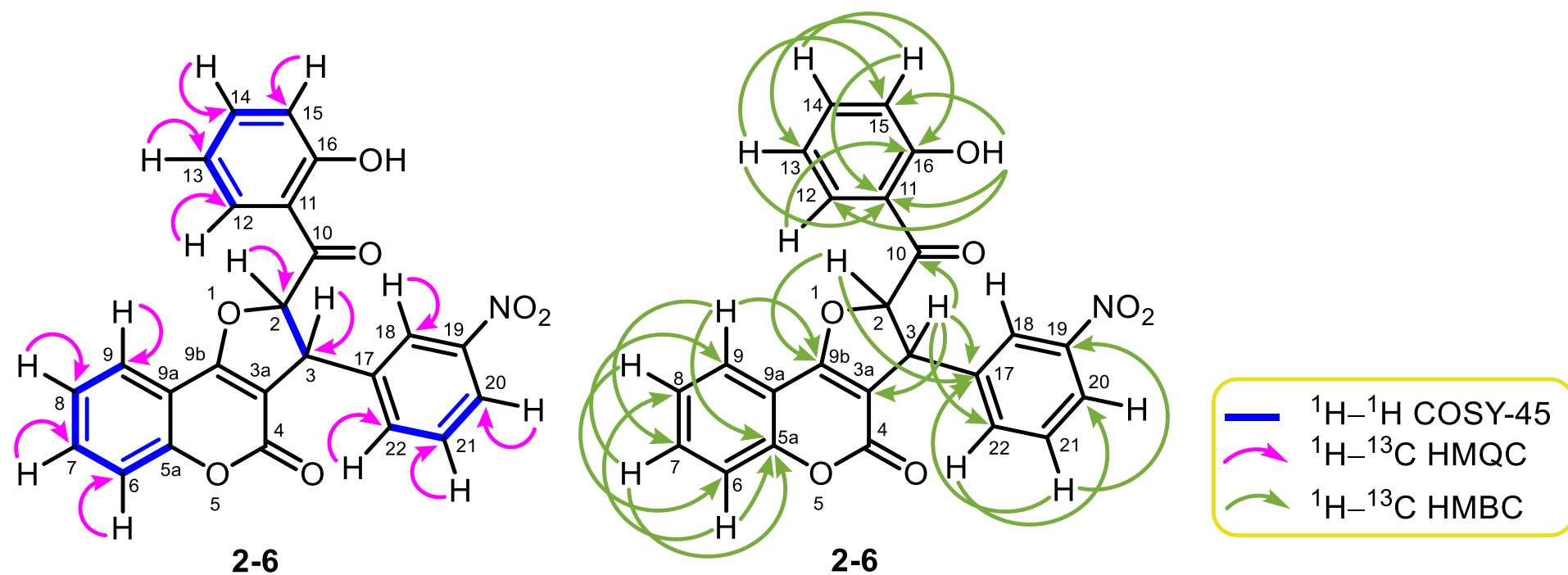


Figure S30b. ^1H - ^{13}C HMBC NMR spectrum of 2-(2-hydroxybenzoyl)-3-(3-nitrophenyl)-2,3-dihydro-4*H*-furo[3,2-*c*]chromen-4-one (**2-6**) [Extended-2]

Table S1. 2D-NMR properties of the representative compound, 2-(2-hydroxybenzoyl)-3-(3-nitrophenyl)-2,3-dihydro-4*H*-furo[3,2-*c*]chromen-4-one (**2-6**) showing the corresponding homo- and hetero-nuclear interactions



Carbon	¹ H (ppm/δ)	¹³ C (ppm/δ)	DEPT-135	¹ H- ¹ H COSY-45	¹ H- ¹³ C HMQC	¹ H- ¹³ C HMBC
C-2	6.19 (d, 1H, <i>J</i> = 5.2 Hz, ArCOCH<)	91.08	CH	δ 6.19 (H-2) vs δ 5.08 (H-3)	δ 6.19 (H-2) vs δ 91.08 (C-2)	δ 6.19 (H-2) vs δ 141.33 (C-17) and 166.87 (C-9b)
C-3	5.08 (d, 1H, <i>J</i> = 5.2 Hz, ArCH<)	48.85	CH	δ 5.08 (H-3) vs δ 6.19 (H-2)	δ 5.08 (H-3) vs δ 48.85 (C-3)	δ 5.08 (H-3) vs δ 104.49 (C-3a), 134.34 (C-22), 141.33 (C-17) and 196.24 (C-10)
C-3a	–	104.49	C	–	–	–
C-4	–	159.62	C	–	–	–

C-5a	–	155.62	C	–	–	–
C-6	7.44-7.37 (m, 2H, Ar-H)	117.38	CH	δ 7.44-7.37 (H-6) vs δ 7.71-7.64 (H-7)	δ 7.44-7.37 (H-6) vs δ 117.38 (C-6)	δ 7.44-7.37 (H-6) vs δ 124.65 (C-8) and 155.62 (C-5a)
C-7	7.71-7.64 (m, 2H, Ar-H)	133.69	CH	δ 7.71-7.64 (H-7) vs δ 7.44-7.37 (H-6 and H-8)	δ 7.71-7.64 (H-7) vs δ 133.69 (C-7)	δ 7.71-7.64 (H-7) vs δ 123.38 (C-9) and 155.62 (C-5a)
C-8	7.44-7.37 (m, 2H, Ar-H)	124.65	CH	δ 7.44-7.37 (H-8) vs δ 7.71-7.64 (H-7) and δ 7.85 (H-9)	δ 7.44-7.37 (H-8) vs δ 124.65 (C-8)	δ 7.44-7.37 (H-8) vs δ 111.83 (C-9a) and 117.38 (C-6)
C-9	7.85 (dd, 1H, <i>J</i> = 8.0 & 1.2 Hz, Ar-H)	123.38	CH	δ 7.85 (H-9) vs δ 7.44-7.37 (H-8)	δ 7.85 (H-9) vs δ 123.38 (C-9)	δ 7.85 (H-9) vs δ 133.69 (C-7), 155.62 (C-5a) and 166.87 (C-9b)
C-9a	–	111.83	C	–	–	–
C-9b	–	166.87	C	–	–	–
C-10	–	196.24	C	–	–	–
C-11	–	116.15	C	–	–	–
C-12	7.62-7.57 (m, 2H, Ar-H)	129.69	CH	δ 7.62-7.57 (H-12) vs δ 7.09 (H-13)	δ 7.62-7.57 (H-12) vs δ 129.69 (C-12)	δ 7.62-7.57 (H-12) vs δ 163.84 (C-16)
C-13	7.09 (d, 1H, <i>J</i> = 8.4 Hz, Ar-H)	119.49	CH	δ 7.09 (H-13) vs δ 7.62-7.57 (H-12) and 7.53 (H-14)	δ 7.09 (H-13) vs δ 119.49 (C-13)	δ 7.09 (H-13) vs δ 116.15 (C-11) and 119.72 (C-15)
C-14	7.53 (d, 1H, <i>J</i> = 8.0 Hz, Ar-H)	138.16	CH	δ 7.53 (H-14) vs δ 7.09 (H-13) and 6.94-6.90 (H-15)	δ 7.53 (H-14) vs δ 138.16 (C-14)	δ 7.53 (H-14) vs δ 163.84 (C-16)
C-15	6.94-6.90 (m, 1H, Ar-H)	119.72	CH	δ 6.94-6.90 (H-15) vs δ 7.53 (H-14)	δ 6.94-6.90 (H-15) vs δ 119.72 (C-15)	δ 6.94-6.90 (H-15) vs δ 116.15 (C-11) and 119.49 (C-13)
C-16	–	163.84	C	–	–	–
C-17	–	141.33	C	–	–	–
C-18	8.23-8.19 (m, 2H, Ar-H)	123.57	CH	–	δ 8.23-8.19 (H-18) vs δ 124.65 (C-8)	–
C-19	–	149.02	C	–	–	–

C-20	8.23-8.19 (m, 2H, Ar-H)	122.56	CH	δ 8.23-8.19 (H-20) vs δ 7.62-7.57 (H-21)	δ 8.23-8.19 (H-20) vs δ 122.56 (C-20)	–
C-21	7.62-7.57 (m, 2H, Ar-H)	130.51	CH	δ 7.62-7.57 (H-21) vs δ 8.23-8.19 (H-20) and 7.71-7.64 (H-22)	δ 7.62-7.57 (H-21) vs δ 130.51 (C-21)	δ 7.62-7.57 (H-21) vs δ 141.33 (C-17) and 149.02 (C-19)
C-22	7.71-7.64 (m, 2H, Ar-H)	134.34	CH	δ 7.71-7.64 (H-22) vs δ 7.62-7.57 (H-21)	δ 7.71-7.64 (H-22) vs δ 134.34 (C-22)	δ 7.71-7.64 (H-22) vs δ 122.56 (C-20)
Ar-OH	11.58 (s, 1H, Ar-OH)	–	–	–	–	δ 11.58 (Ar-OH) vs δ 116.15 (C-11), 119.72 (C-15) and 163.84 (C-16)

Acquisition Parameter

Source Type	ESI	Ion Polarity	Positive	Set Nebulizer	0.4 Bar
Focus	Active	Set Capillary	3400 V	Set Dry Heater	200 °C
Scan Begin	50 m/z	Set End Plate Offset	-500 V	Set Dry Gas	4.0 l/min
Scan End	3000 m/z	Set Charging Voltage	2000 V	Set Divert Valve	Source
		Set Corona	0 nA	Set APCI Heater	0 °C

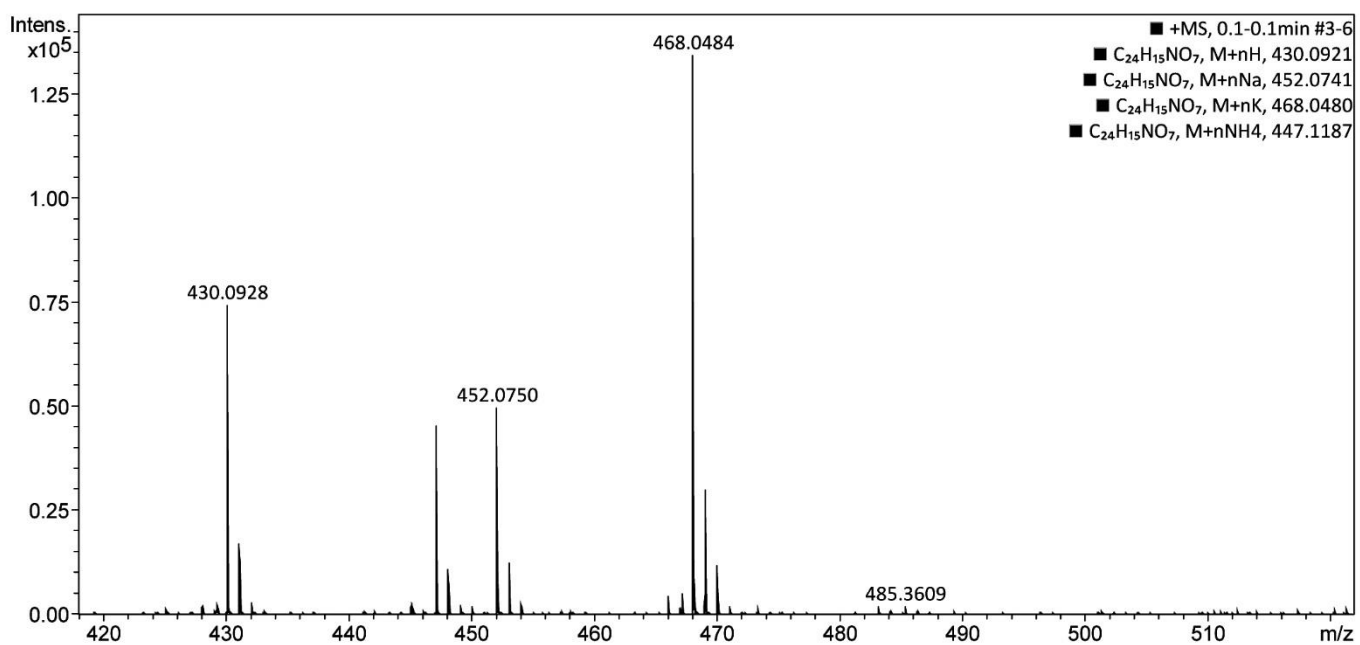
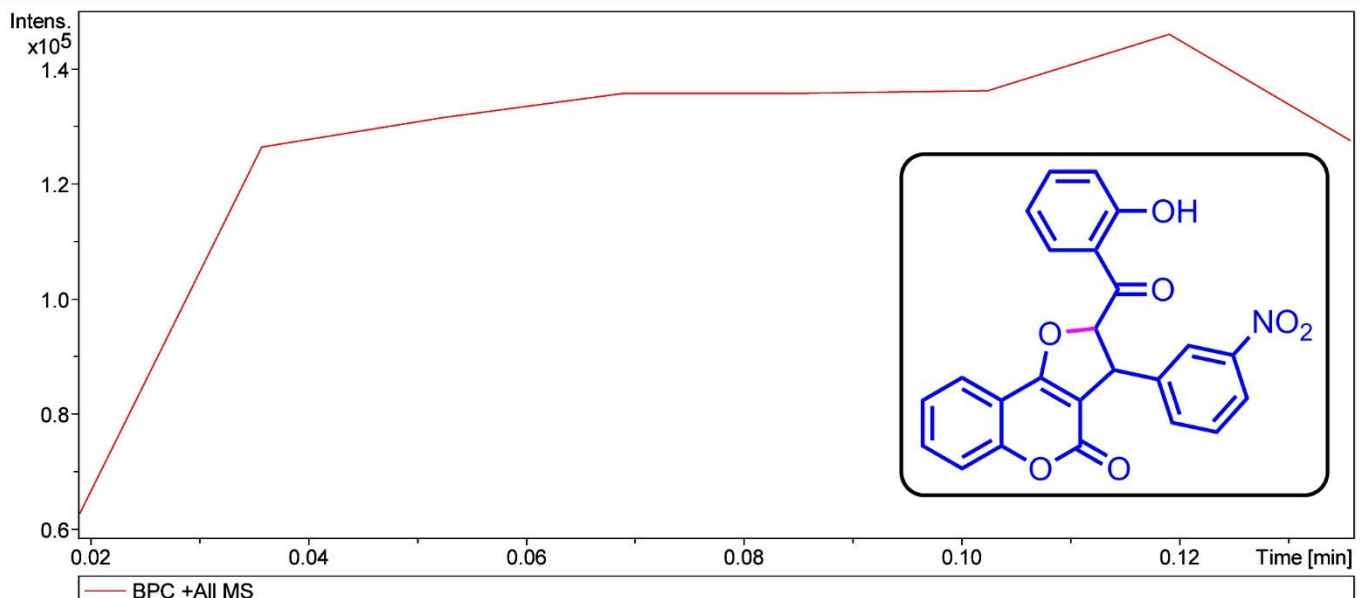
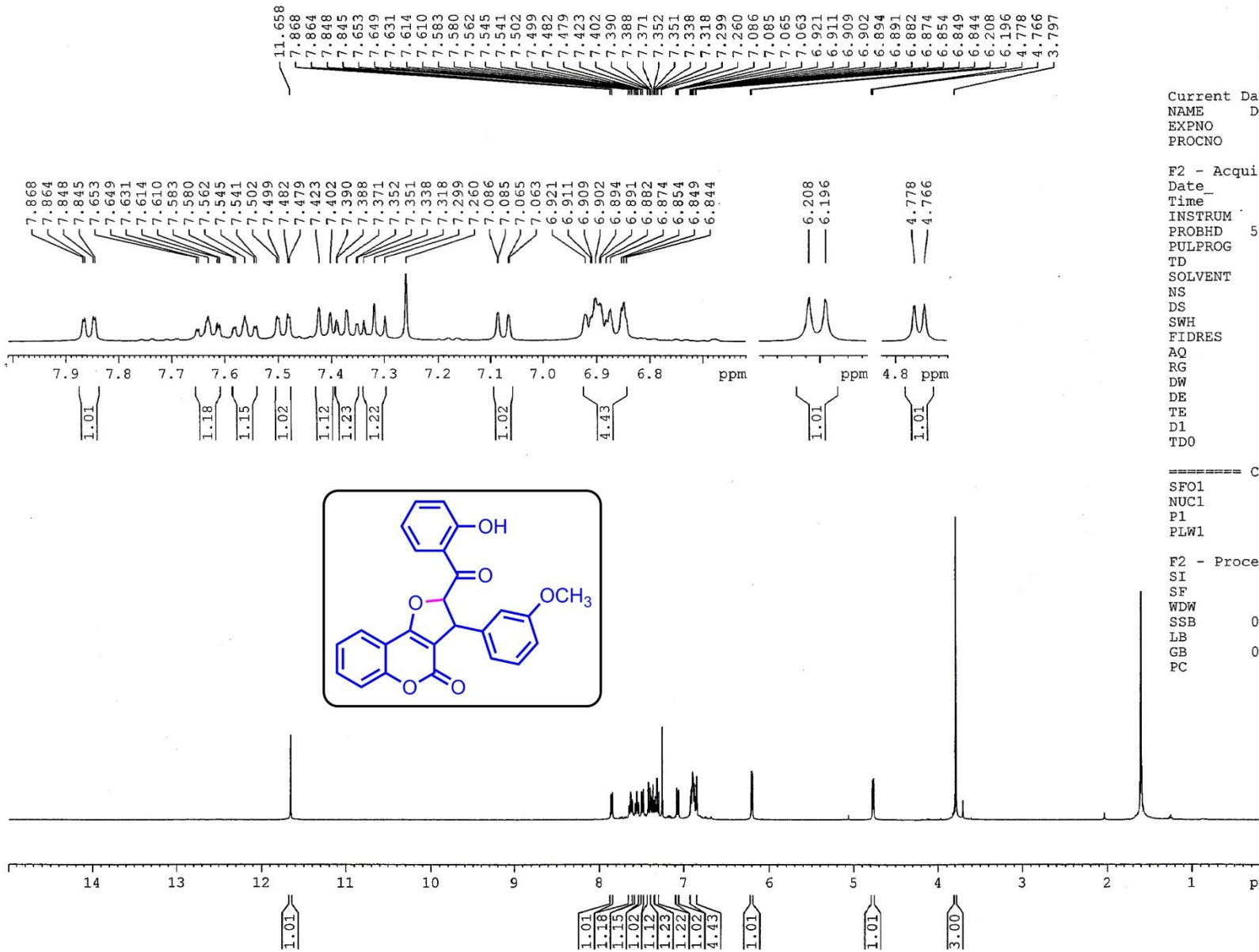


Figure S31. High-resolution Mass spectra of 2-(2-hydroxybenzoyl)-3-(3-nitrophenyl)-2,3-dihydro-4*H*-furo[3,2-*c*]chromen-4-one (**2-6**)



BRUKER

Current Data Parameters
NAME Dr. G. Brahmachari 2022
EXPNO 48
PROCNO 1

F2 - Acquisition Parameters
Date 20220216
Time 9.21
INSTRUM spect
PROBHD 5 mm PABBO BB/
PULPROG zg30
TD 32768
SOLVENT CDCl3
NS 16
DS 2
SWH 8223.685 Hz
FIDRES 0.250967 Hz
AQ 1.9922944 sec
RG 101.91
DW 60.800 usec
DE 6.50 usec
TE 296.3 K
D1 1.0000000 sec
TDO 1

===== CHANNEL f1 =====
SFO1 400.1533012 MHz
NUC1 1H
P1 14.75 usec
PLW1 12.0000000 W

F2 - Processing parameters
SI 16384
SF 400.1500094 MHz
WDW EM
SSB 0 0.30 Hz
LB 0
GB 0
PC 1.00

Figure S32. ¹H-NMR spectrum of 2-(2-hydroxybenzoyl)-3-(3-methoxyphenyl)-2,3-dihydro-4*H*-furo[3,2-*c*]chromen-4-one (**2-7**)

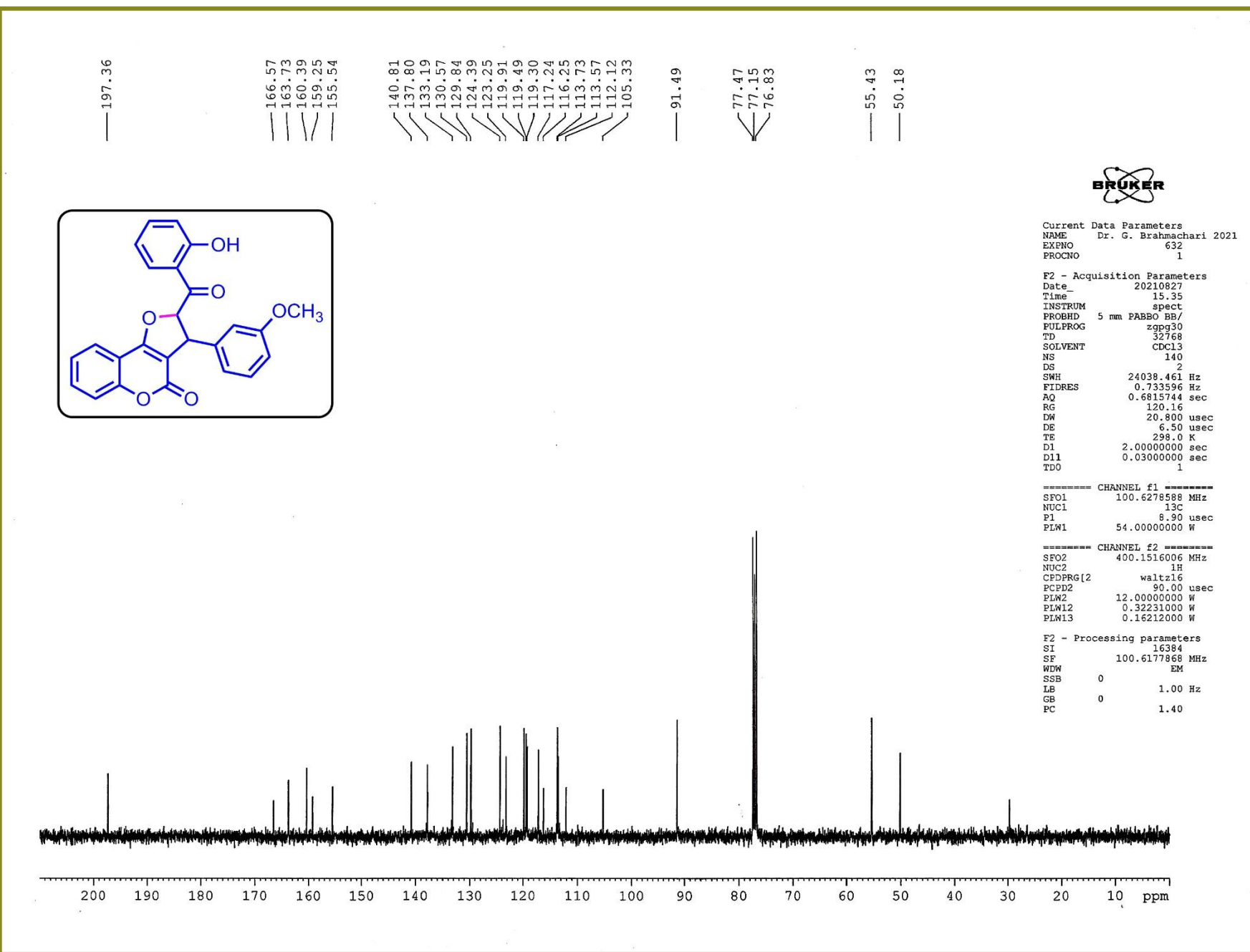


Figure S33. ¹³C-NMR spectrum of 2-(2-hydroxybenzoyl)-3-(3-methoxyphenyl)-2,3-dihydro-4H-furo[3,2-c]chromen-4-one (**2-7**)

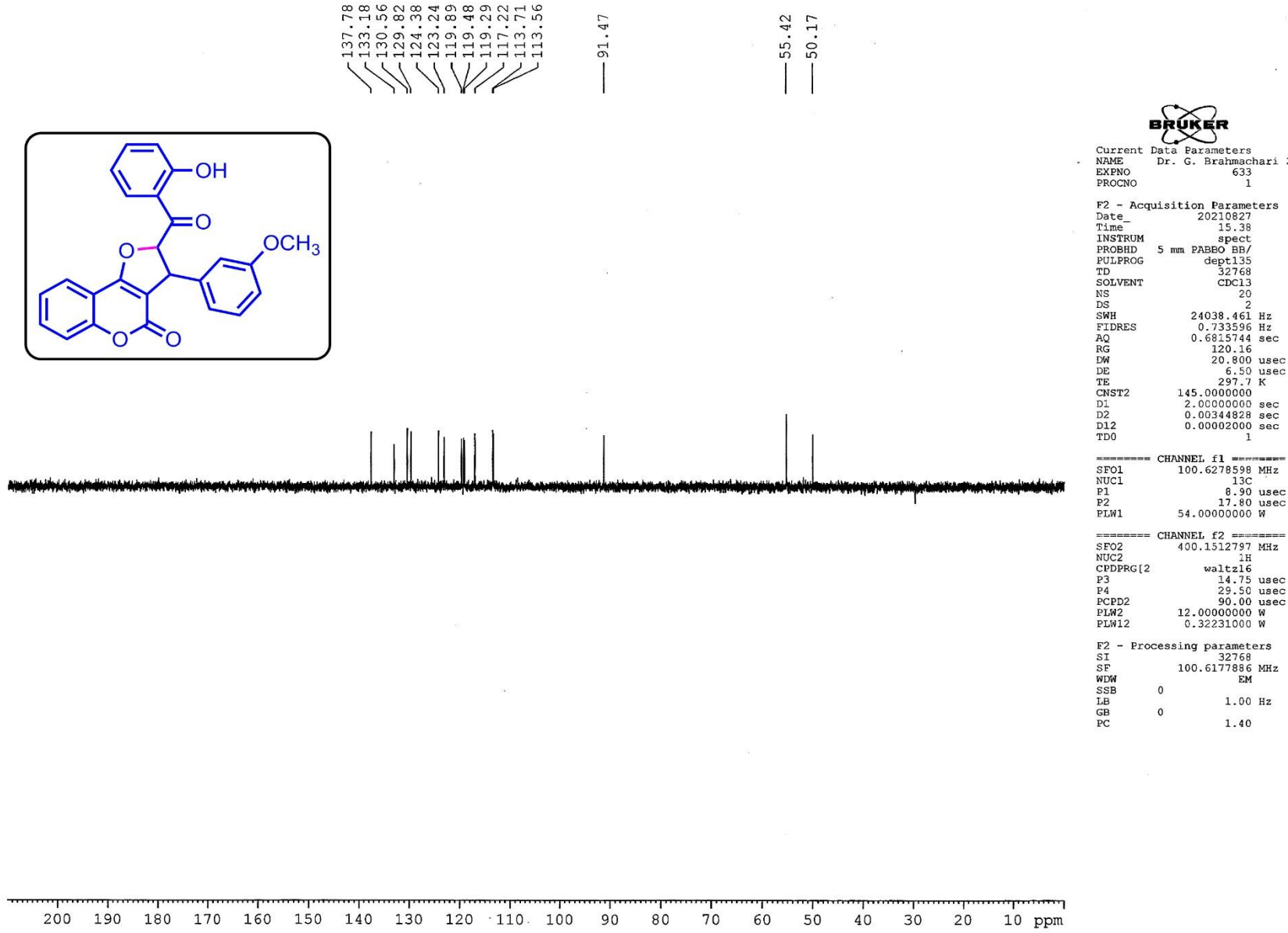


Figure S34. DEPT-135 NMR spectrum of 2-(2-hydroxybenzoyl)-3-(3-methoxyphenyl)-2,3-dihydro-4*H*-furo[3,2-*c*]chromen-4-one (**2-7**)

Acquisition Parameter

Source Type	ESI	Ion Polarity	Positive	Set Nebulizer	0.4 Bar
Focus	Active	Set Capillary	3400 V	Set Dry Heater	200 °C
Scan Begin	50 m/z	Set End Plate Offset	-500 V	Set Dry Gas	4.0 l/min
Scan End	3000 m/z	Set Charging Voltage	2000 V	Set Divert Valve	Source
		Set Corona	0 nA	Set APCI Heater	0 °C

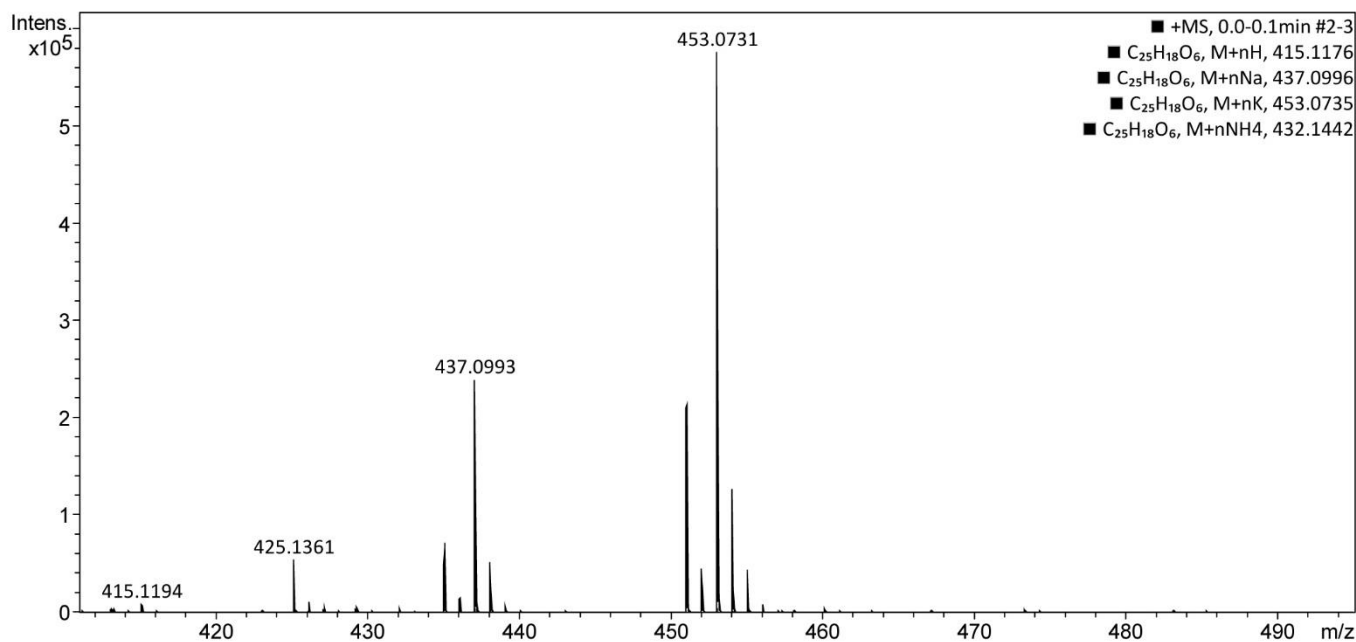
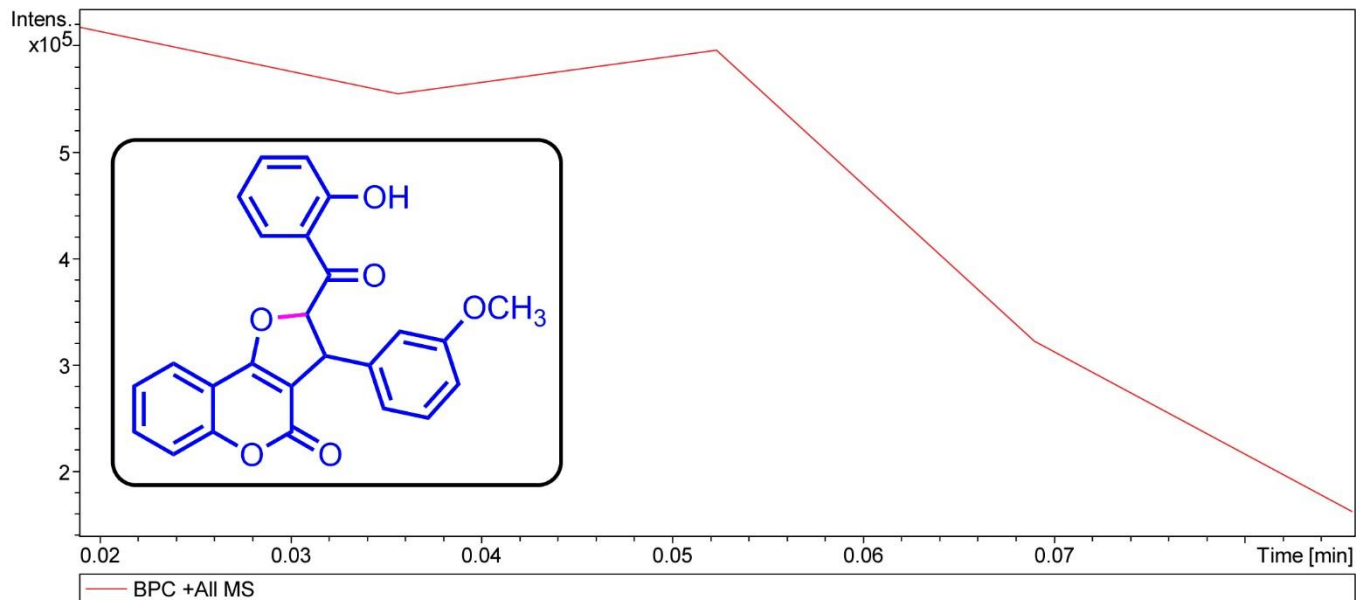


Figure S35. High-resolution Mass spectra of 2-(2-hydroxybenzoyl)-3-(3-methoxyphenyl)-2,3-dihydro-4H-furo[3,2-c]chromen-4-one (**2-7**)

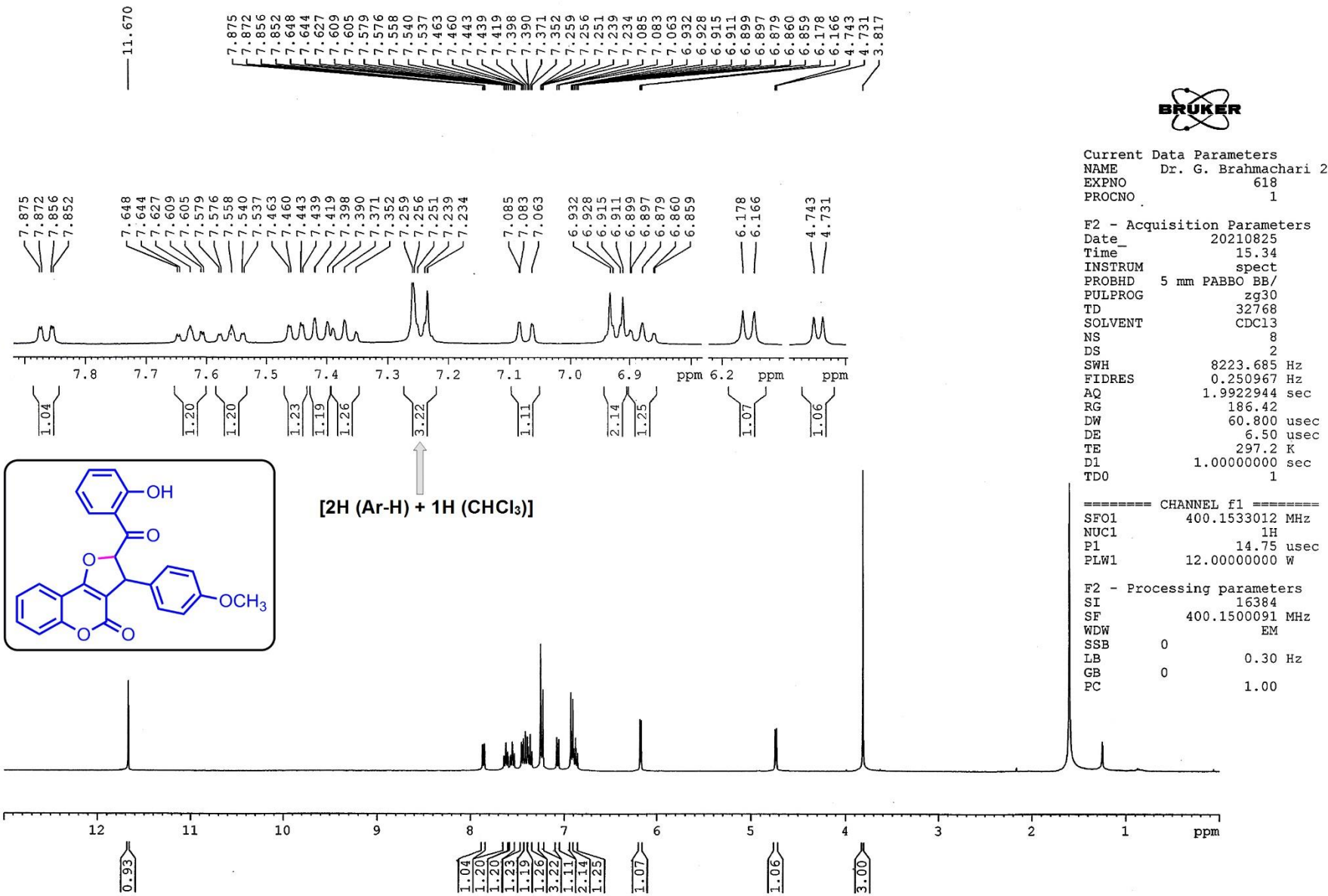


Figure S36. $^1\text{H-NMR}$ spectrum of 2-(2-hydroxybenzoyl)-3-(4-methoxyphenyl)-2,3-dihydro-4*H*-furo[3,2-*c*]chromen-4-one (2-8)

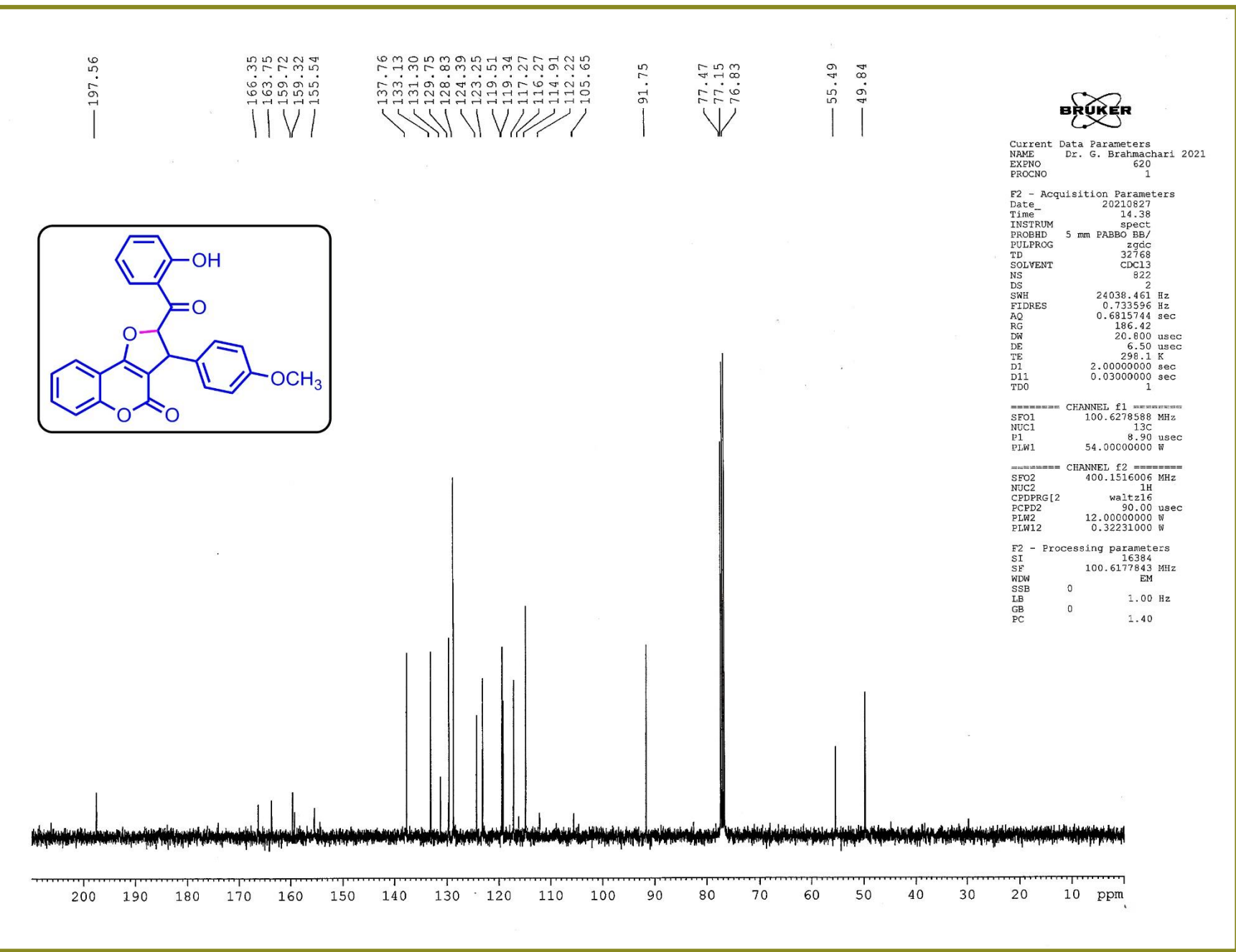


Figure S37. ^{13}C -NMR spectrum of 2-(2-hydroxybenzoyl)-3-(4-methoxyphenyl)-2,3-dihydro-4*H*-furo[3,2-*c*]chromen-4-one (**2-8**)

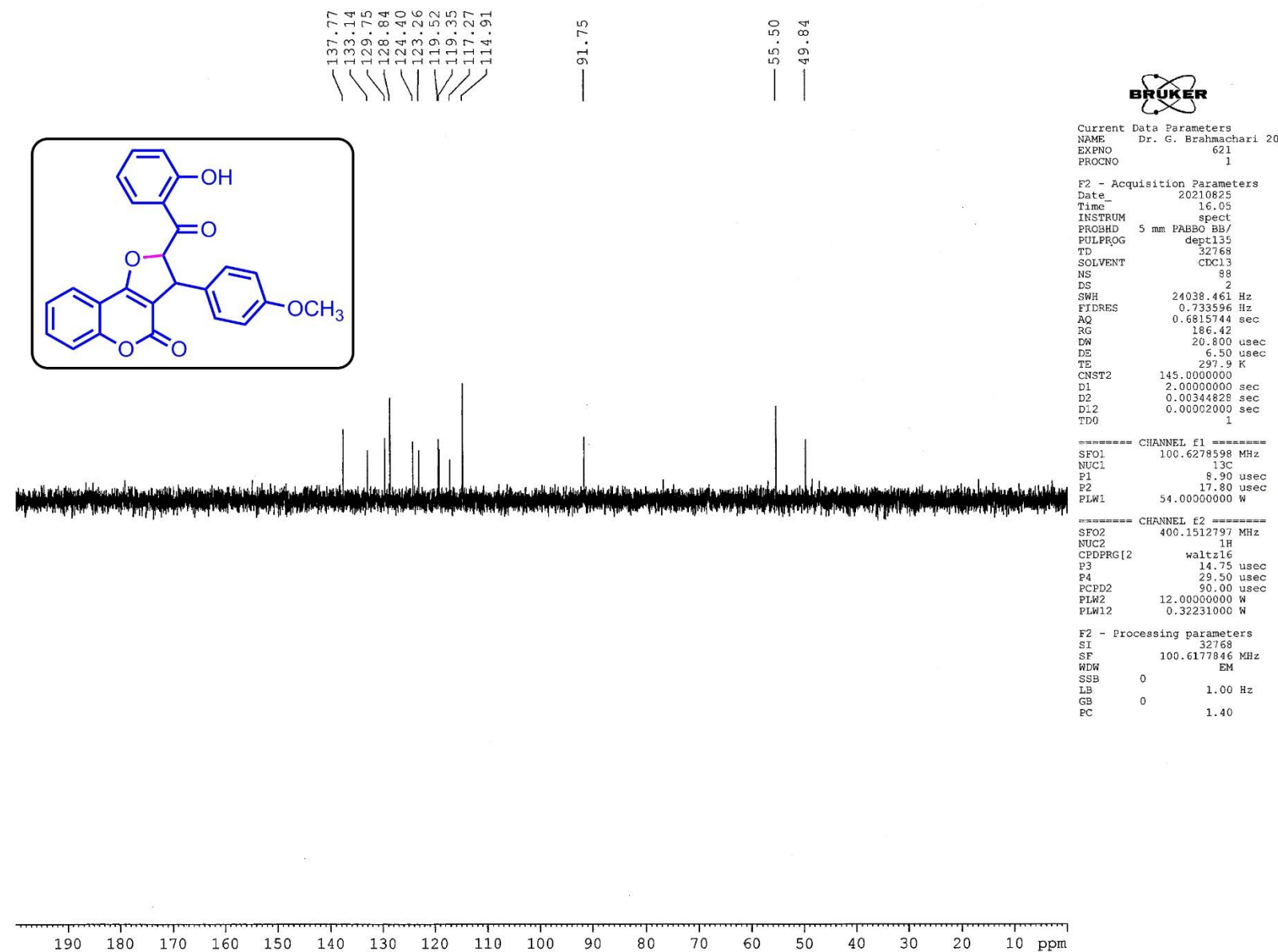


Figure S38. DEPT-135 NMR spectrum of 2-(2-hydroxybenzoyl)-3-(4-methoxyphenyl)-2,3-dihydro-4*H*-furo[3,2-*c*]chromen-4-one (**2-8**)

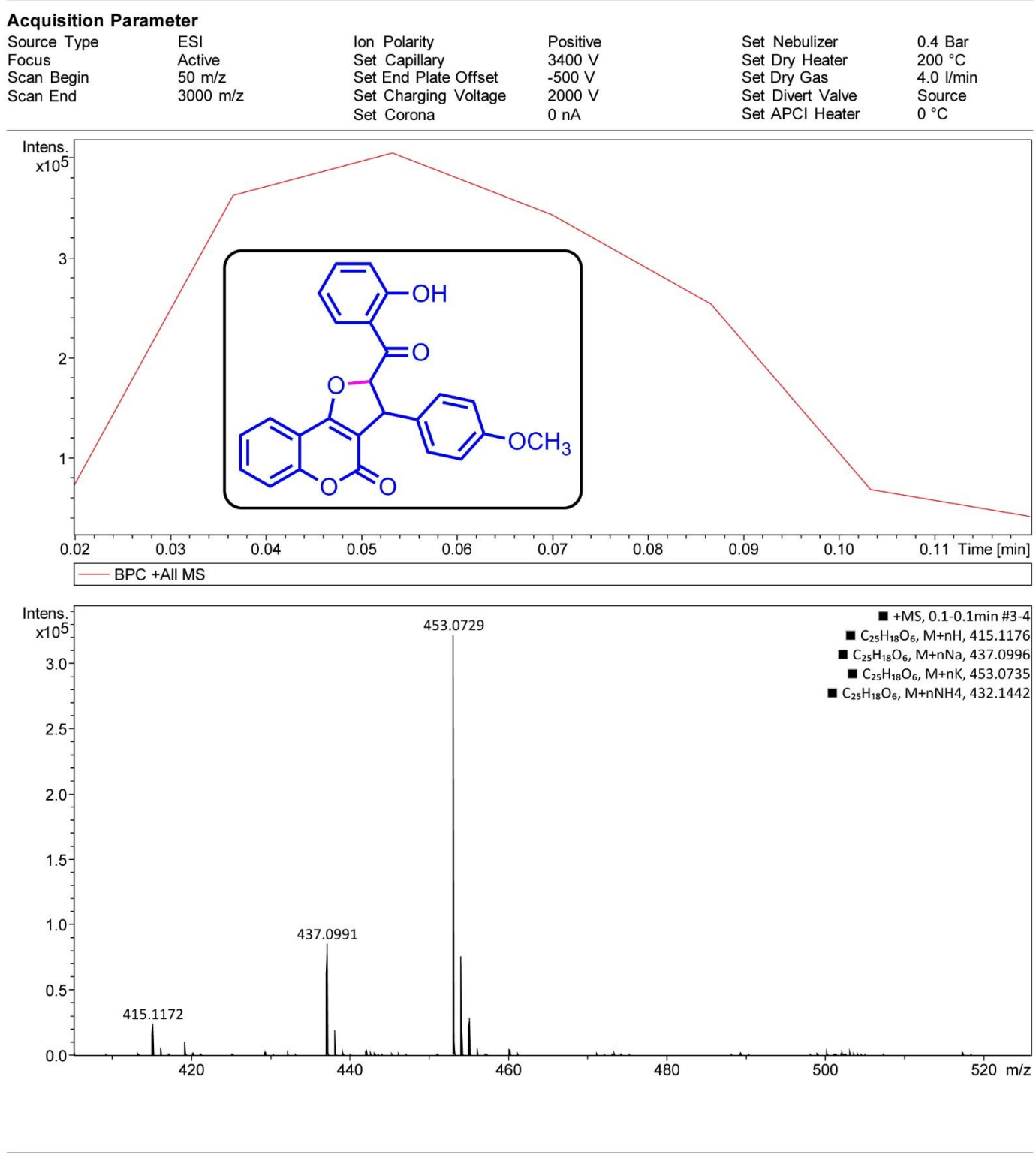


Figure S39. High-resolution Mass spectra of 2-(2-hydroxybenzoyl)-3-(4-methoxyphenyl)-2,3-dihydro-4*H*-furo[3,2-*c*]chromen-4-one (**2-8**)

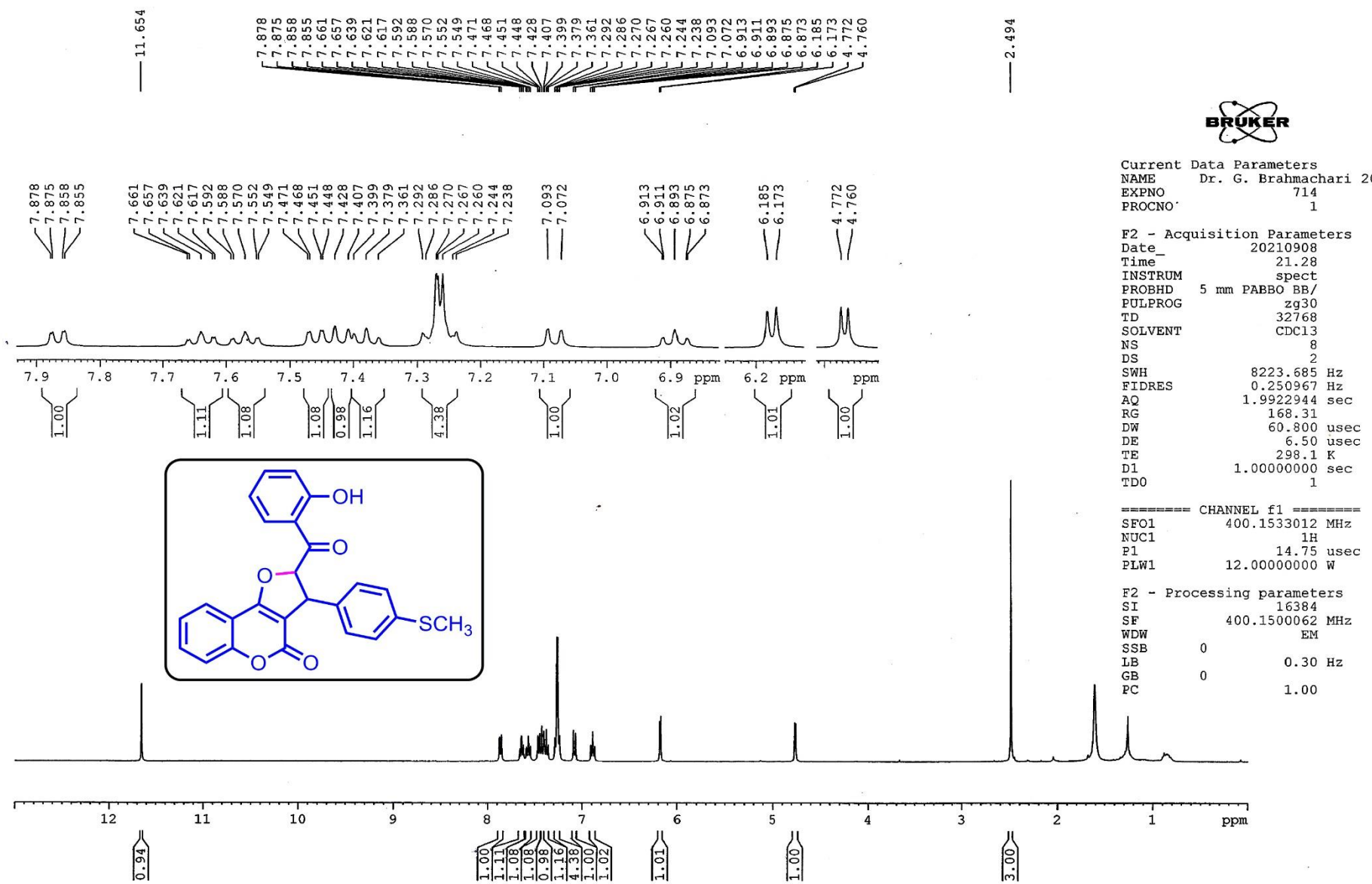


Figure S40. ¹H-NMR spectrum of 2-(2-hydroxybenzoyl)-3-(4-(methylthio)phenyl)-2,3-dihydro-4*H*-furo[3,2-*c*]chromen-4-one (**2-9**)

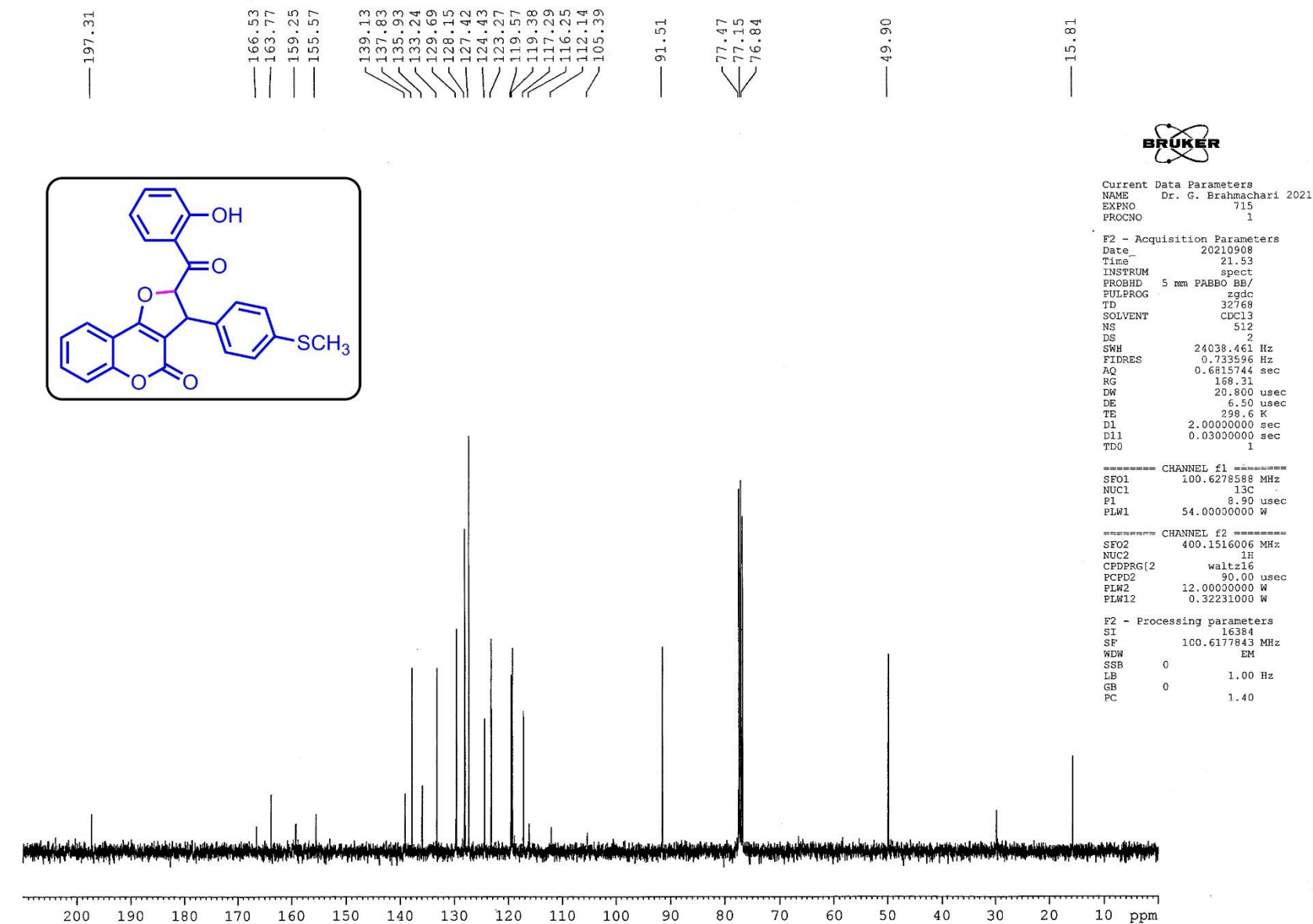


Figure S41. ^{13}C -NMR spectrum of 2-(2-hydroxybenzoyl)-3-(4-(methylthio)phenyl)-2,3-dihydro-4*H*-furo[3,2-*c*]chromen-4-one (**2-9**)

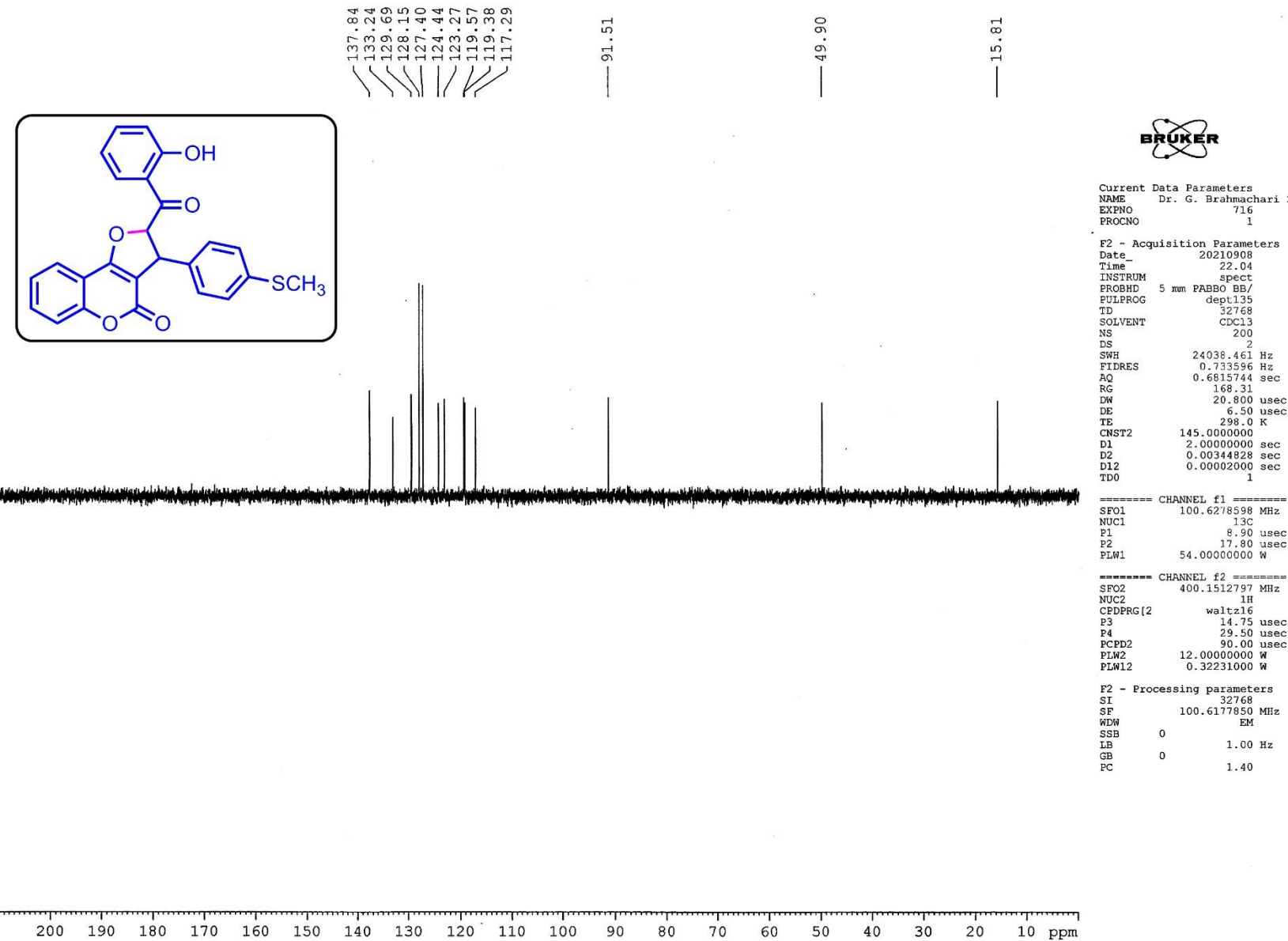


Figure S42. DEPT-135 NMR spectrum of 2-(2-hydroxybenzoyl)-3-(4-(methylthio)phenyl)-2,3-dihydro-4*H*-furo[3,2-*c*]chromen-4-one (**2-9**)

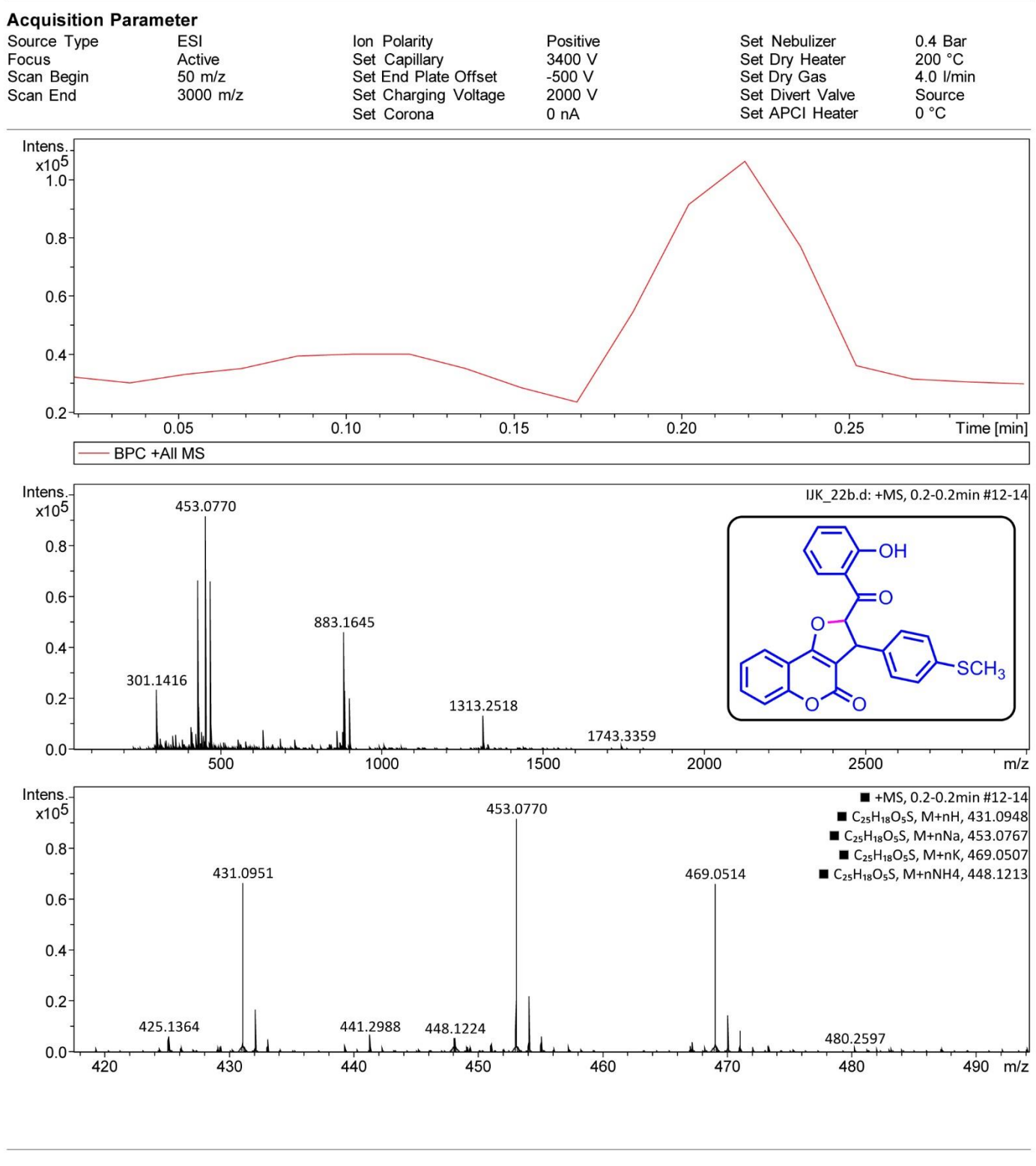


Figure S43. High-resolution Mass spectra 2-(2-hydroxybenzoyl)-3-(4-(methylthio)phenyl)-2,3-dihydro-4*H*-furo[3,2-*c*]chromen-4-one (**2-9**)

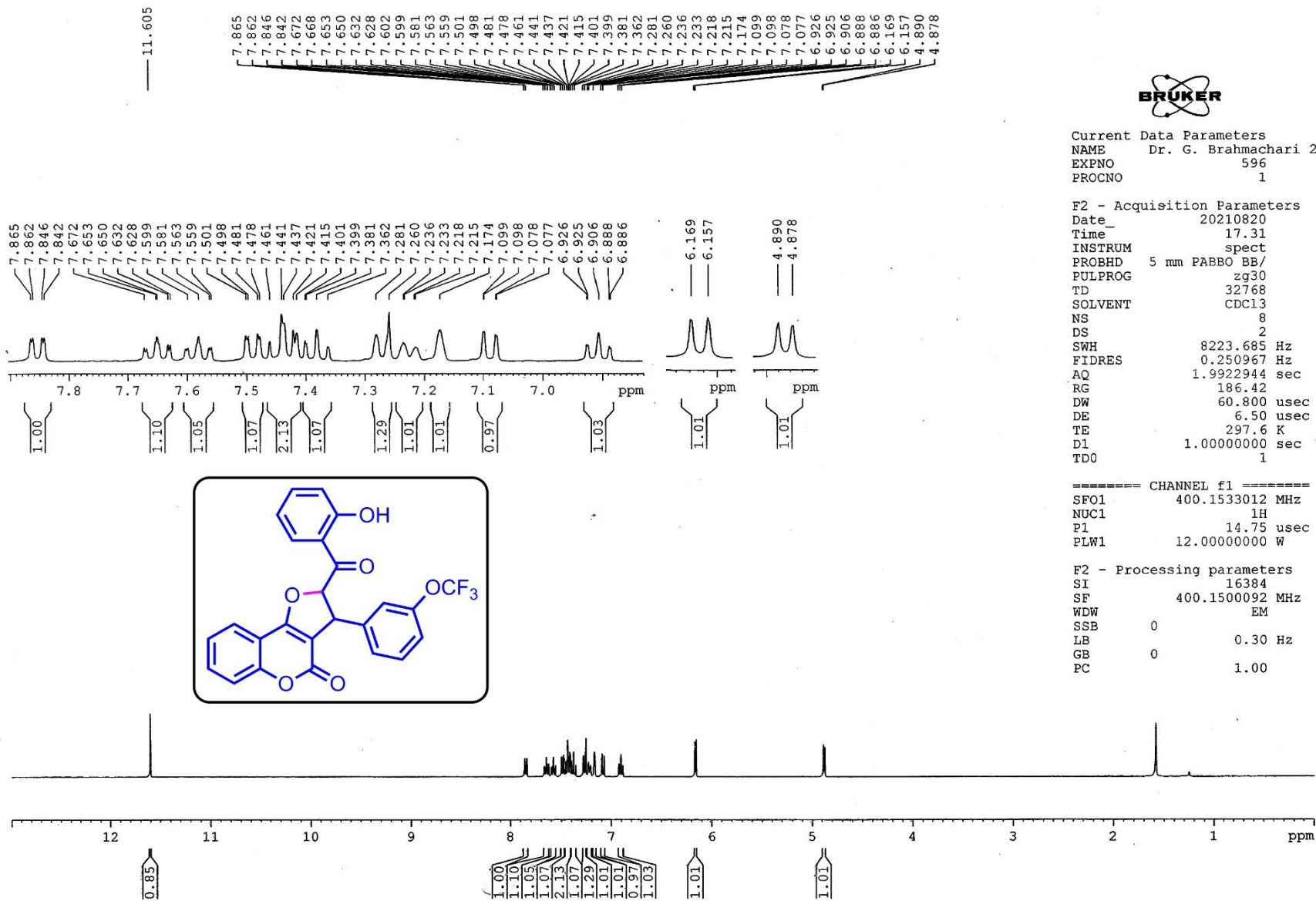


Figure S44. ¹H-NMR spectrum of 2-(2-hydroxybenzoyl)-3-(3-(trifluoromethoxy)phenyl)-2,3-dihydro-4H-furo[3,2-c]chromen-4-one (**2-10**)

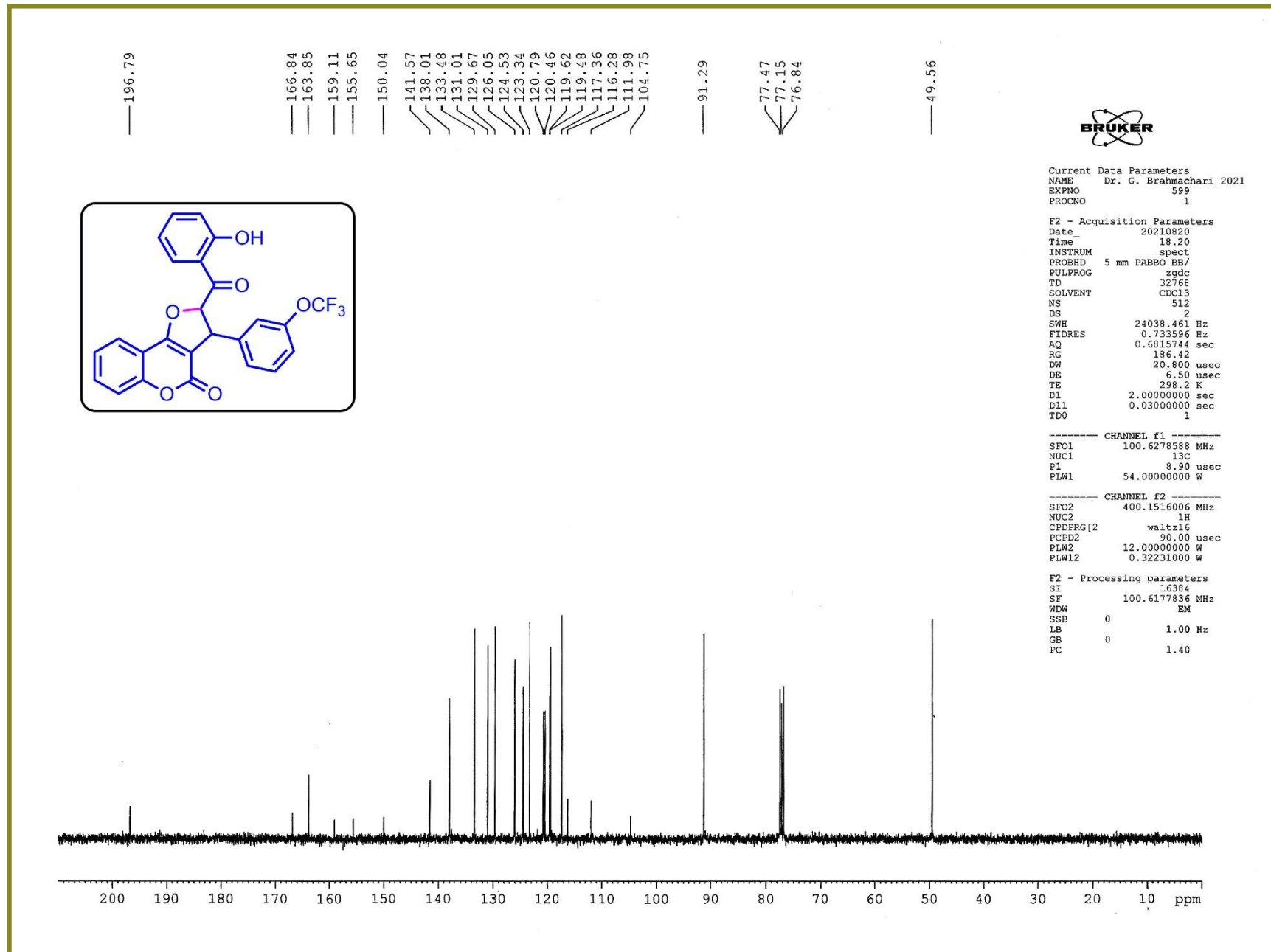


Figure S45. ^{13}C -NMR spectrum of 2-(2-hydroxybenzoyl)-3-(3-(trifluoromethoxy)phenyl)-2,3-dihydro-4*H*-furo[3,2-*c*]chromen-4-one (**2-10**)

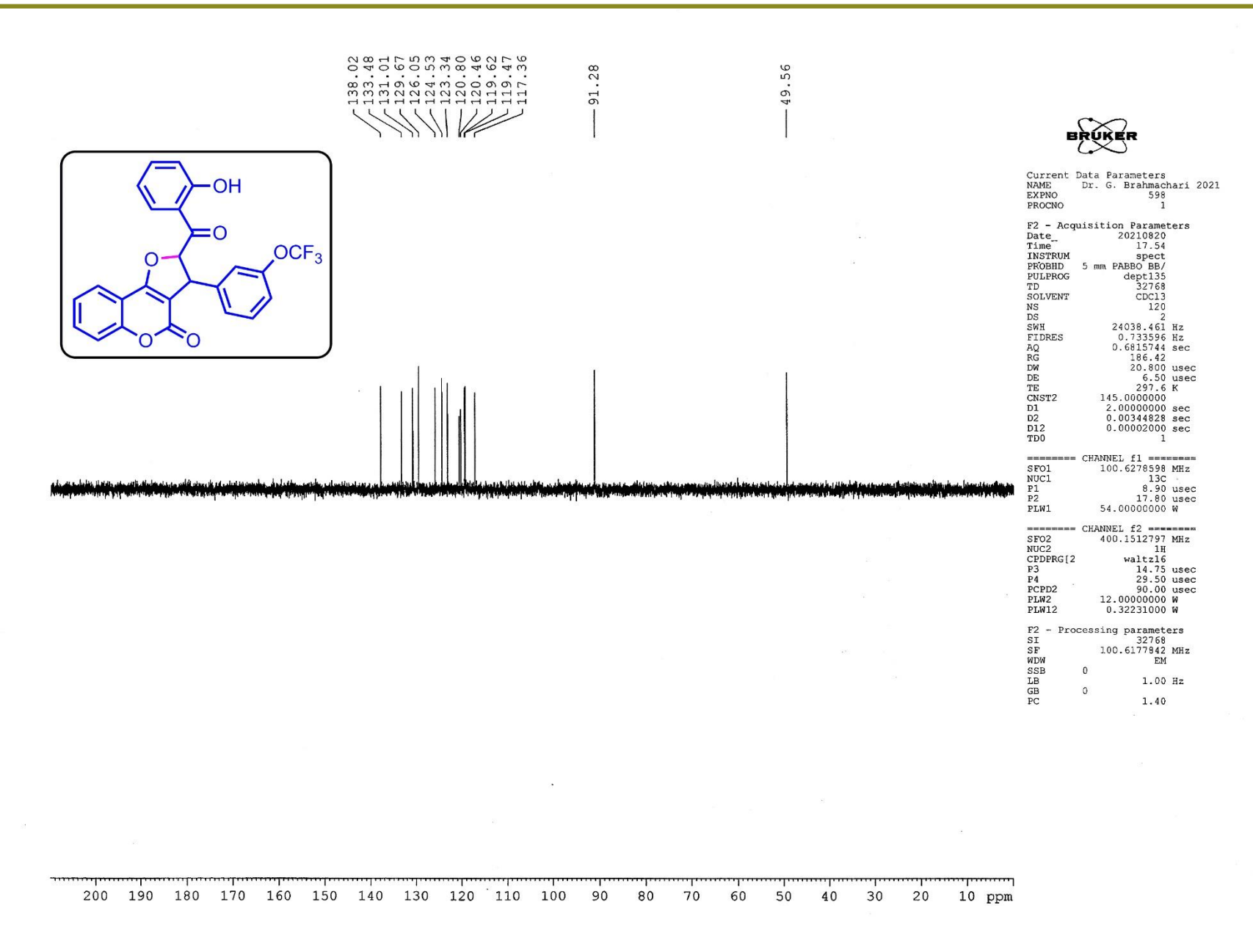


Figure S46. DEPT-135 NMR spectrum of 2-(2-hydroxybenzoyl)-3-(3-(trifluoromethoxy)phenyl)-2,3-dihydro-4*H*-furo[3,2-*c*]chromen-4-one (**2-10**)

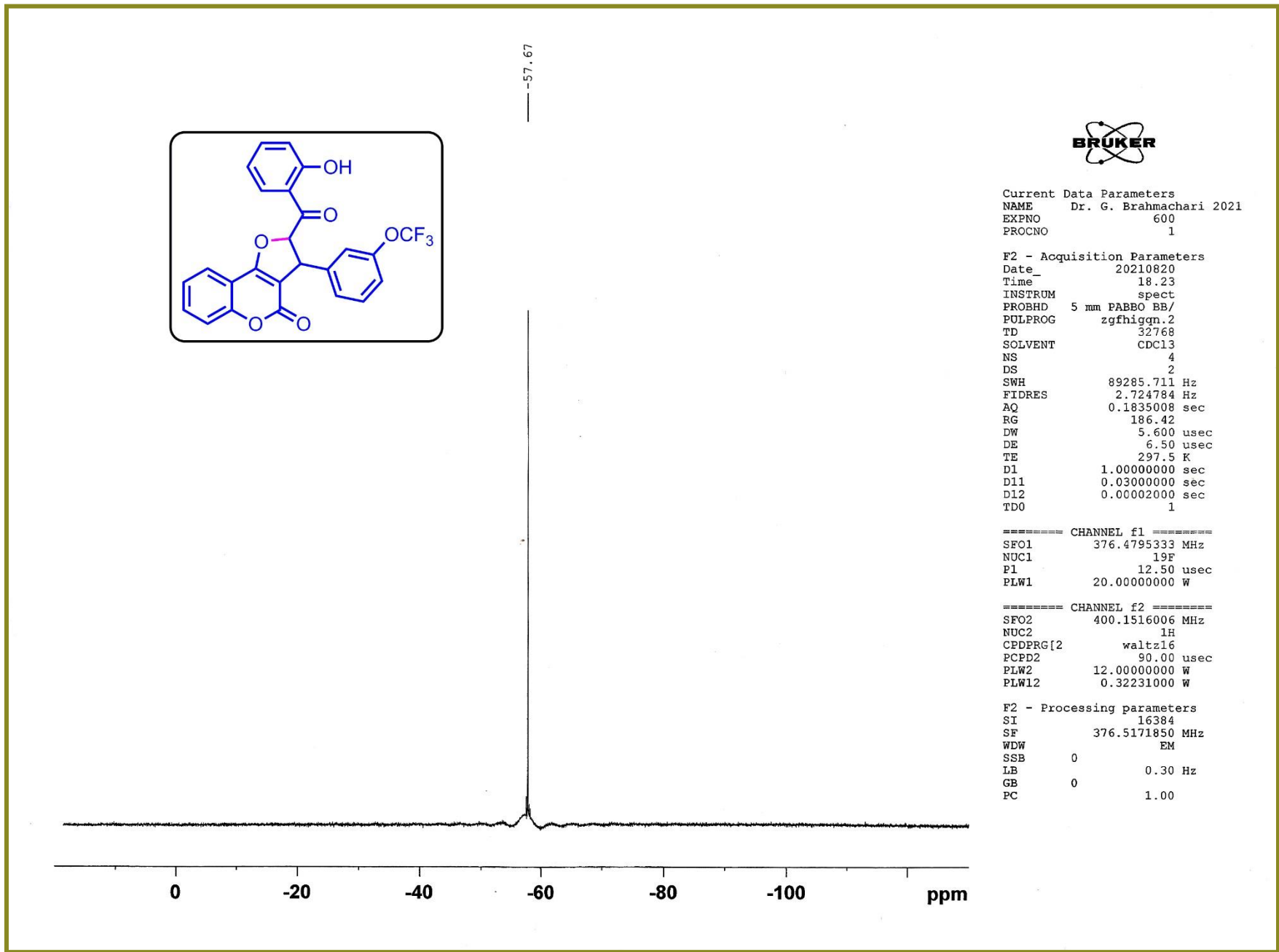


Figure S47. ¹⁹F NMR spectrum of 2-(2-hydroxybenzoyl)-3-(3-(trifluoromethoxy)phenyl)-2,3-dihydro-4H-furo[3,2-c]chromen-4-one (**2-10**)
S56

Acquisition Parameter

Source Type	ESI	Ion Polarity	Positive	Set Nebulizer	0.4 Bar
Focus	Active	Set Capillary	3400 V	Set Dry Heater	200 °C
Scan Begin	50 m/z	Set End Plate Offset	-500 V	Set Dry Gas	4.0 l/min
Scan End	3000 m/z	Set Charging Voltage	2000 V	Set Divert Valve	Source
		Set Corona	0 nA	Set APCI Heater	0 °C

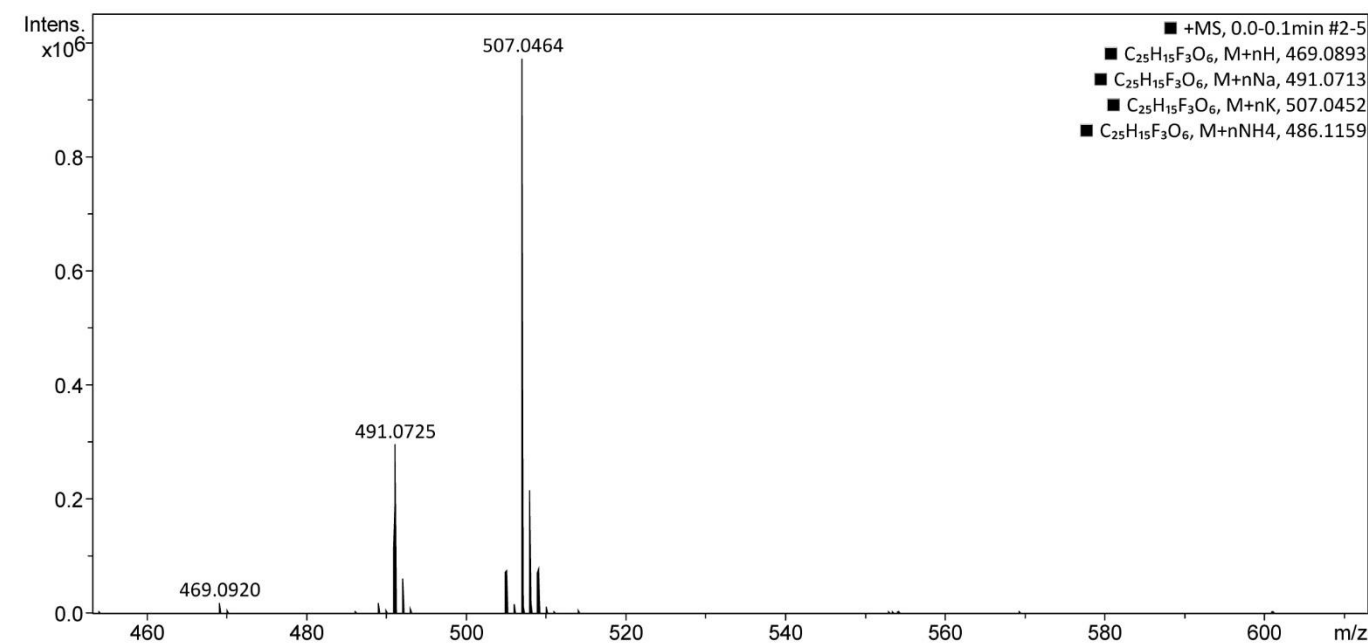
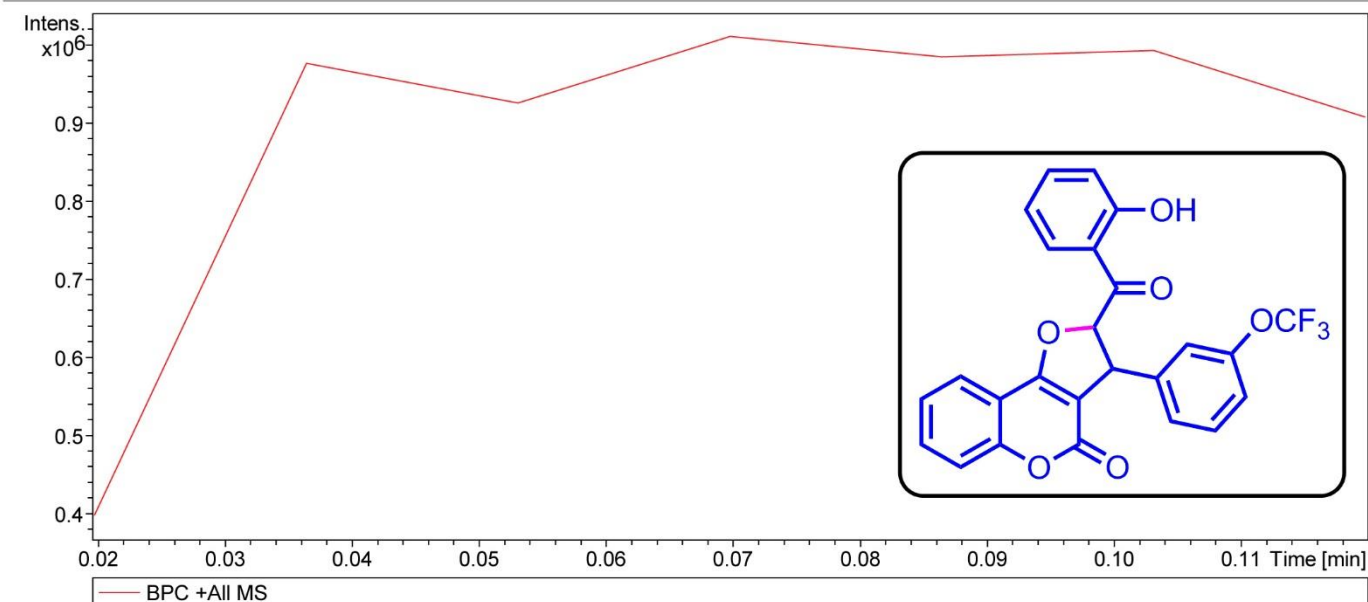


Figure S48. High-resolution Mass spectra of 2-(2-hydroxybenzoyl)-3-(3-(trifluoromethoxy)phenyl)-2,3-dihydro-4*H*-furo[3,2-*c*]chromen-4-one (**2-10**)

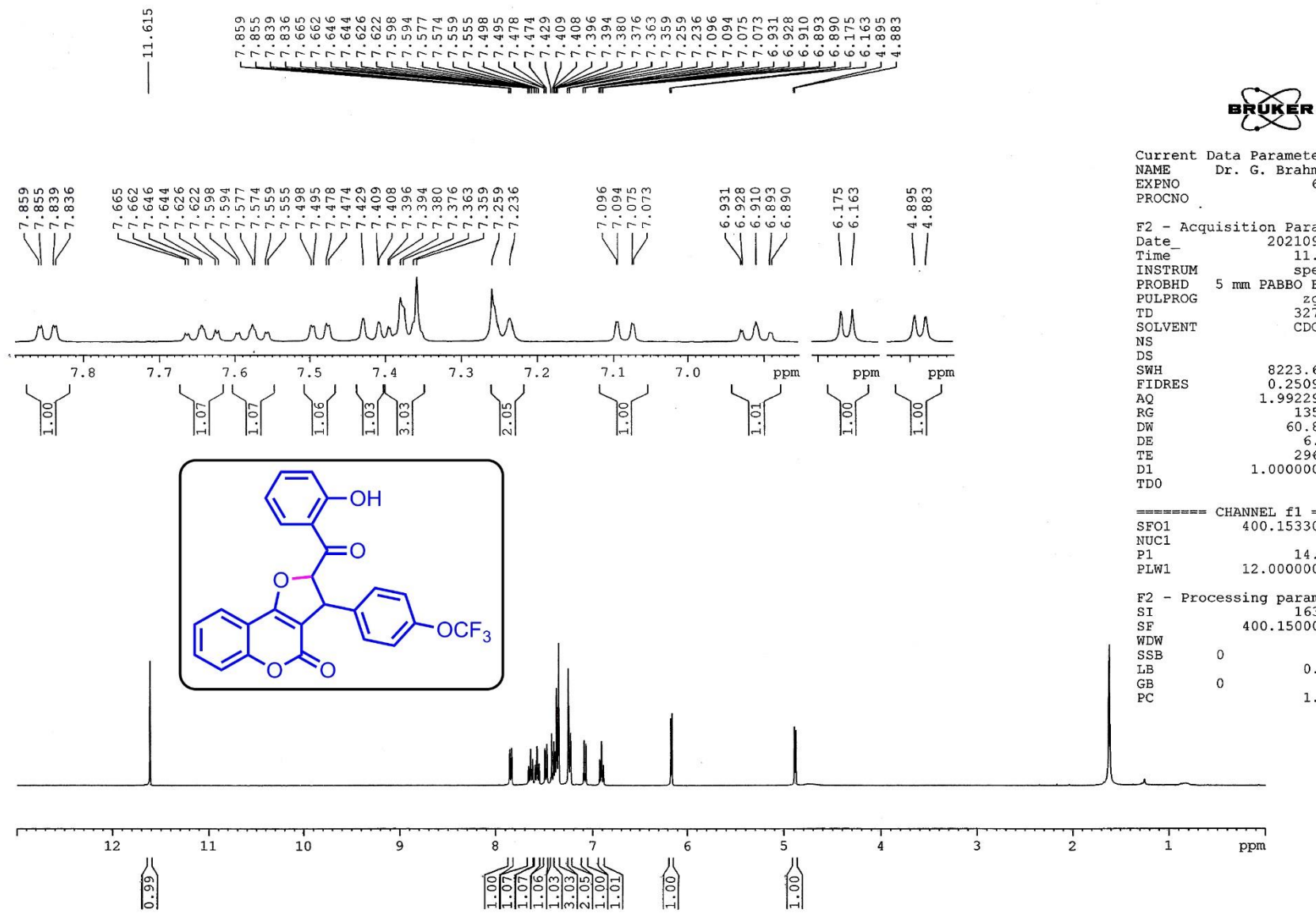


Figure S49. ¹H-NMR spectrum of 2-(2-hydroxybenzoyl)-3-(4-(trifluoromethoxy)phenyl)-2,3-dihydro-4H-furo[3,2-c]chromen-4-one (**2-11**)

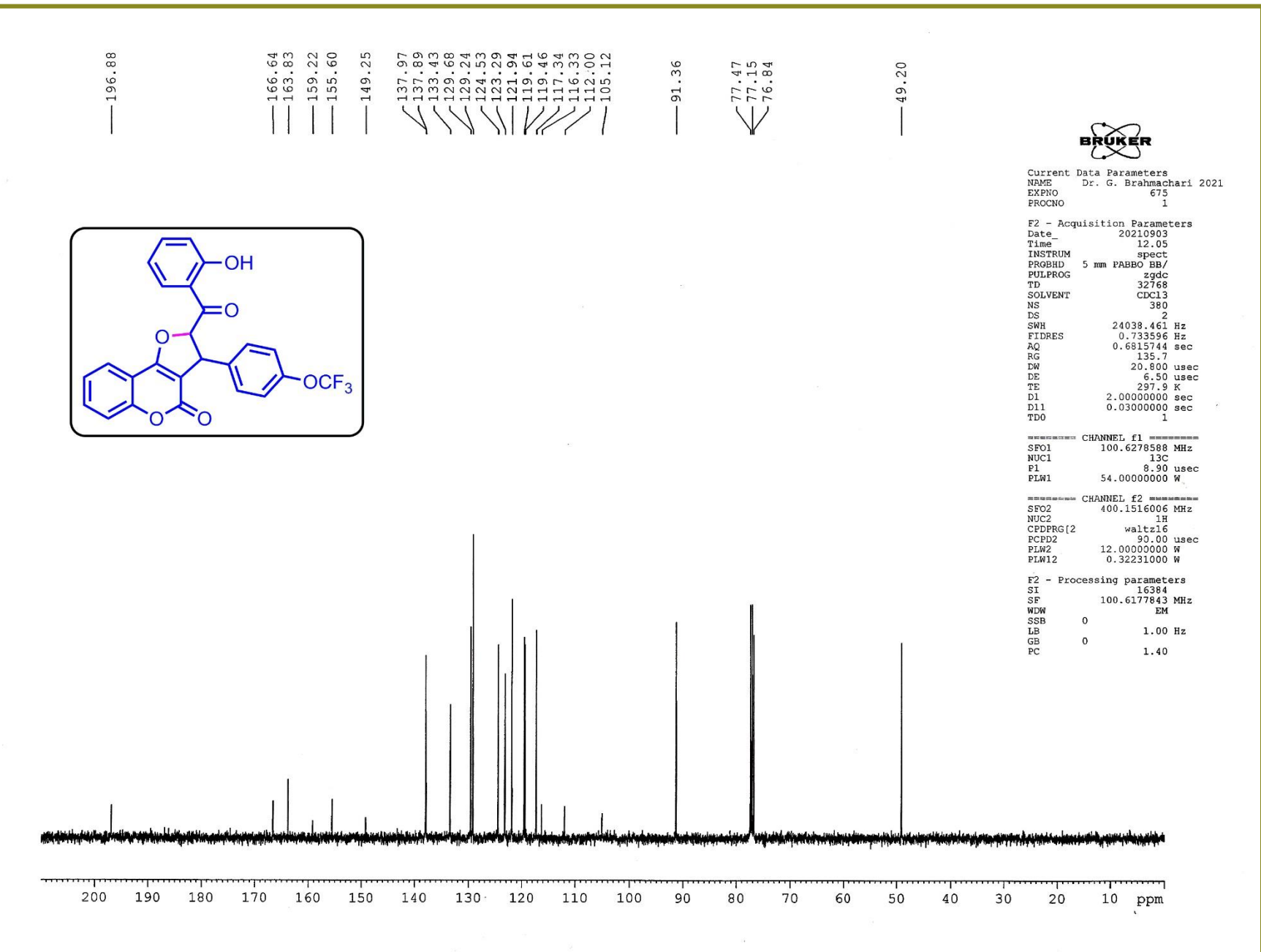


Figure S50. ^{13}C -NMR spectrum of 2-(2-hydroxybenzoyl)-3-(4-(trifluoromethoxy)phenyl)-2,3-dihydro-4*H*-furo[3,2-*c*]chromen-4-one (**2-11**)

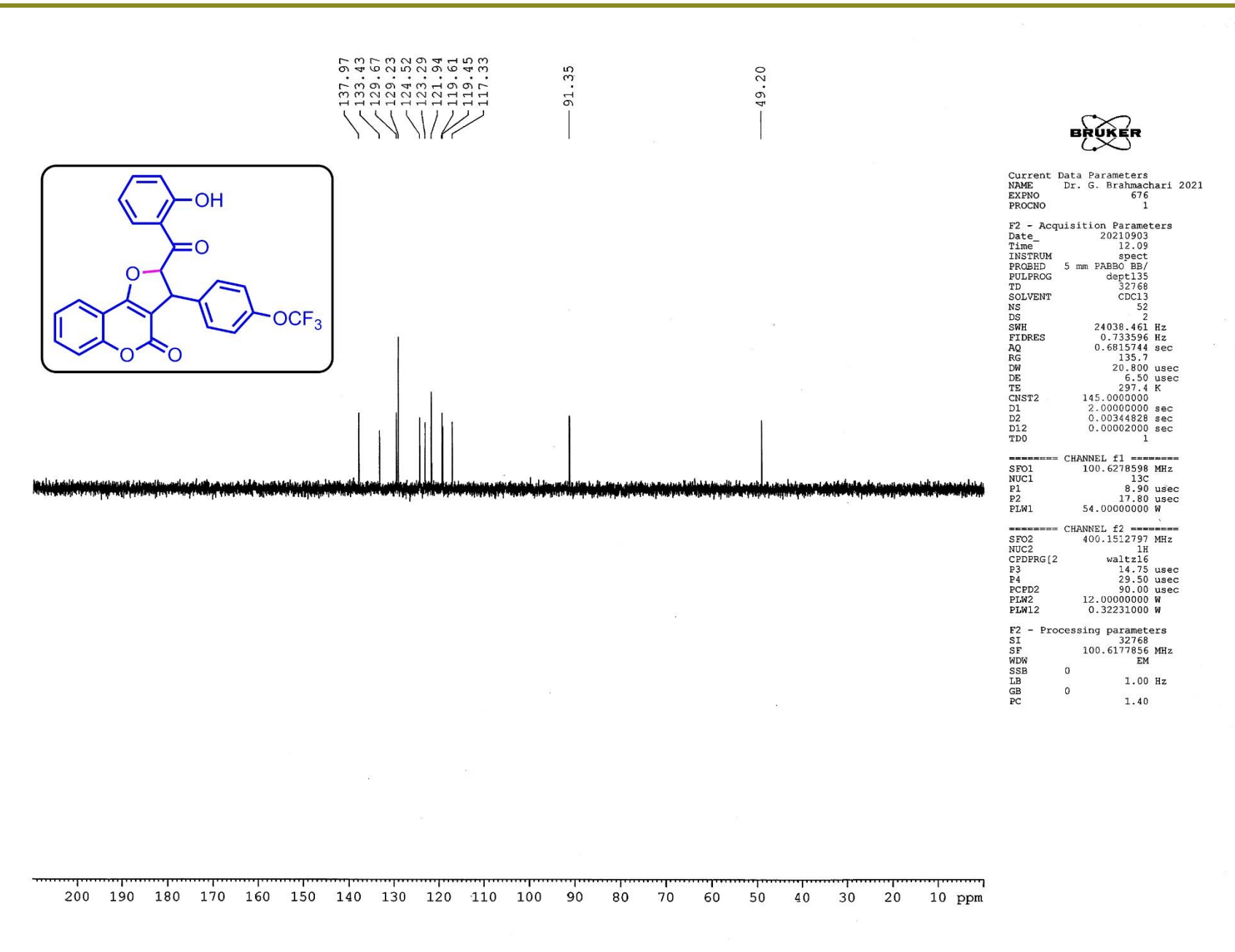


Figure S51. DEPT-135 NMR spectrum of 2-(2-hydroxybenzoyl)-3-(4-(trifluoromethoxy)phenyl)-2,3-dihydro-4*H*-furo[3,2-*c*]chromen-4-one (**2-11**)
S60

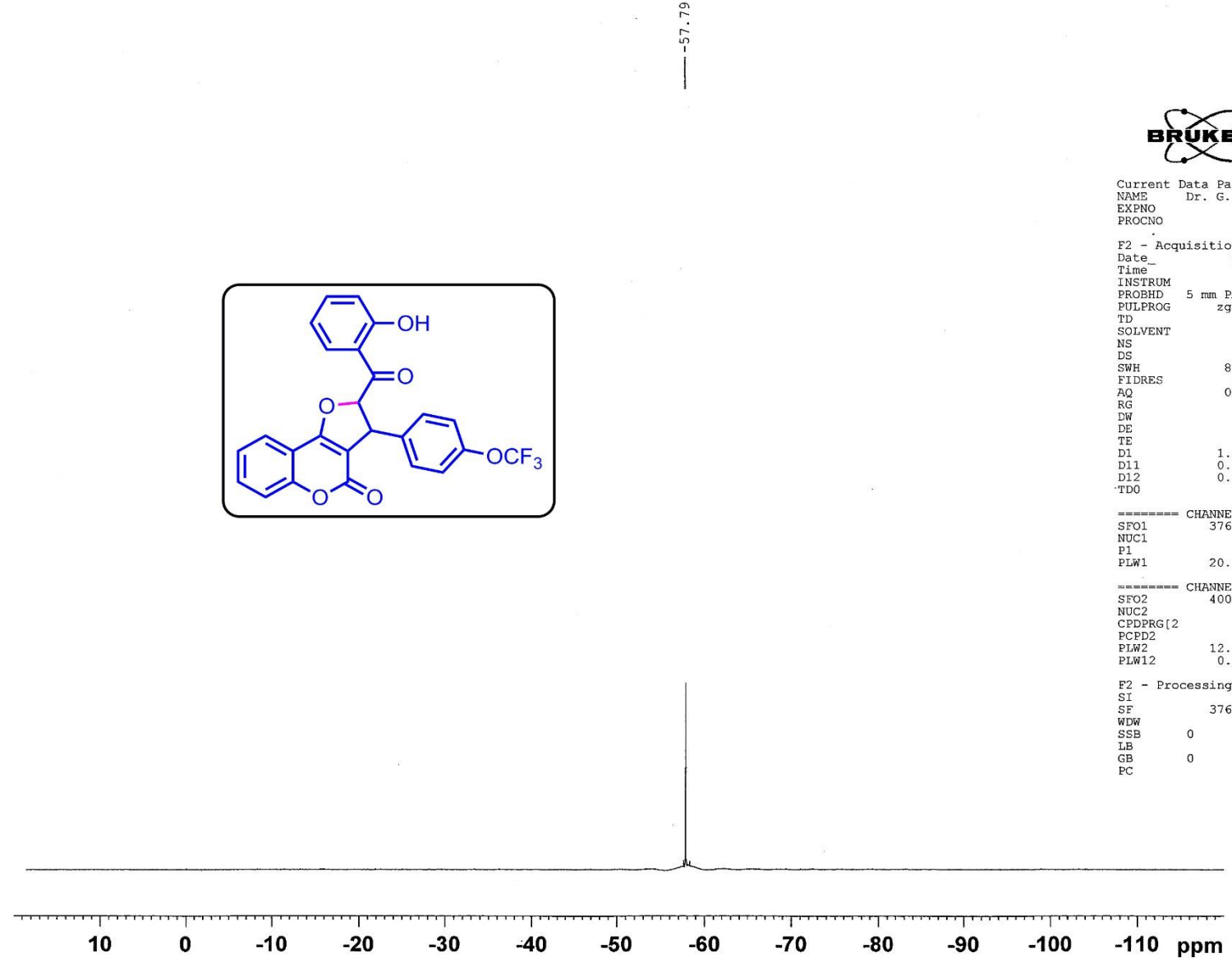


Figure S52. ^{19}F NMR spectrum of 2-(2-hydroxybenzoyl)-3-(4-(trifluoromethoxy)phenyl)-2,3-dihydro-4*H*-furo[3,2-*c*]chromen-4-one (**2-11**)

Acquisition Parameter

Source Type	ESI	Ion Polarity	Positive	Set Nebulizer	0.4 Bar
Focus	Active	Set Capillary	3400 V	Set Dry Heater	200 °C
Scan Begin	50 m/z	Set End Plate Offset	-500 V	Set Dry Gas	4.0 l/min
Scan End	3000 m/z	Set Charging Voltage	2000 V	Set Divert Valve	Source
		Set Corona	0 nA	Set APCI Heater	0 °C

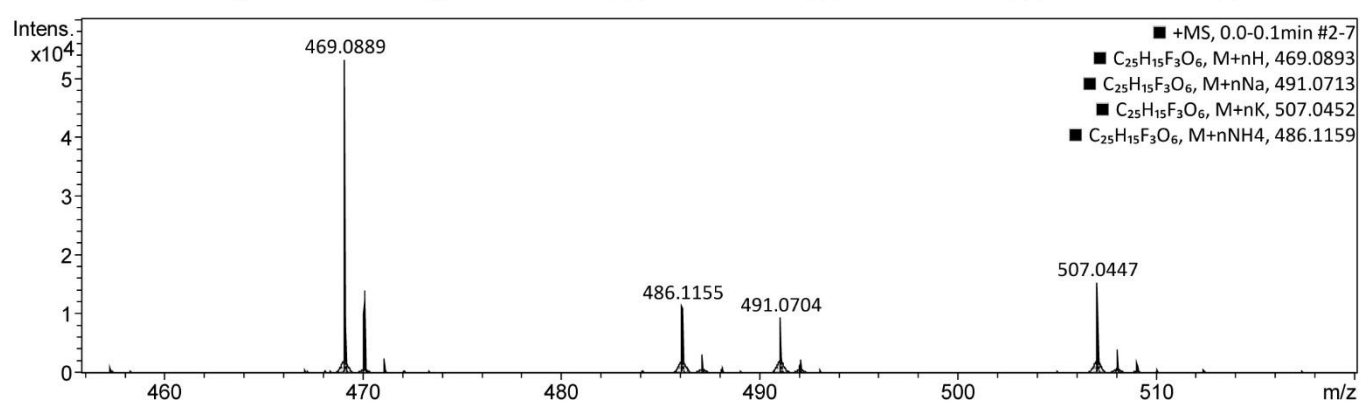
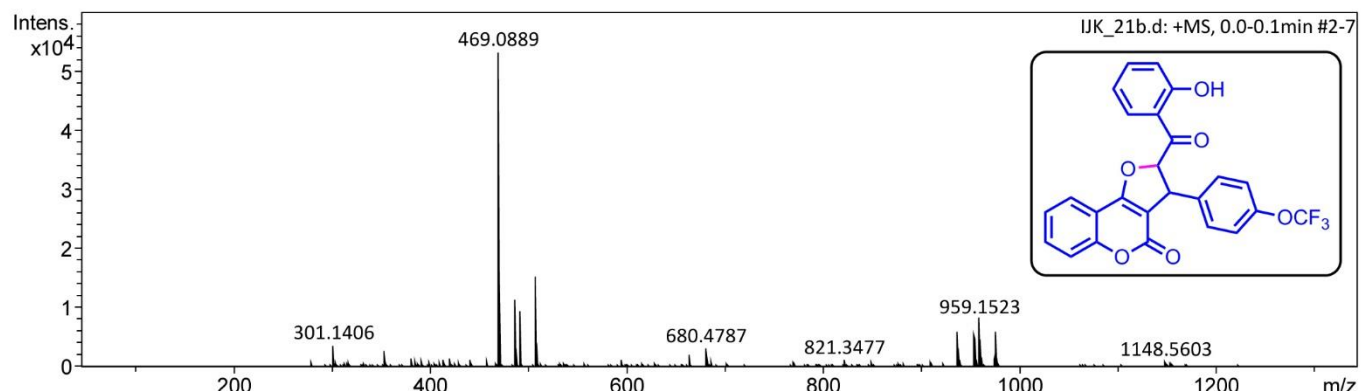
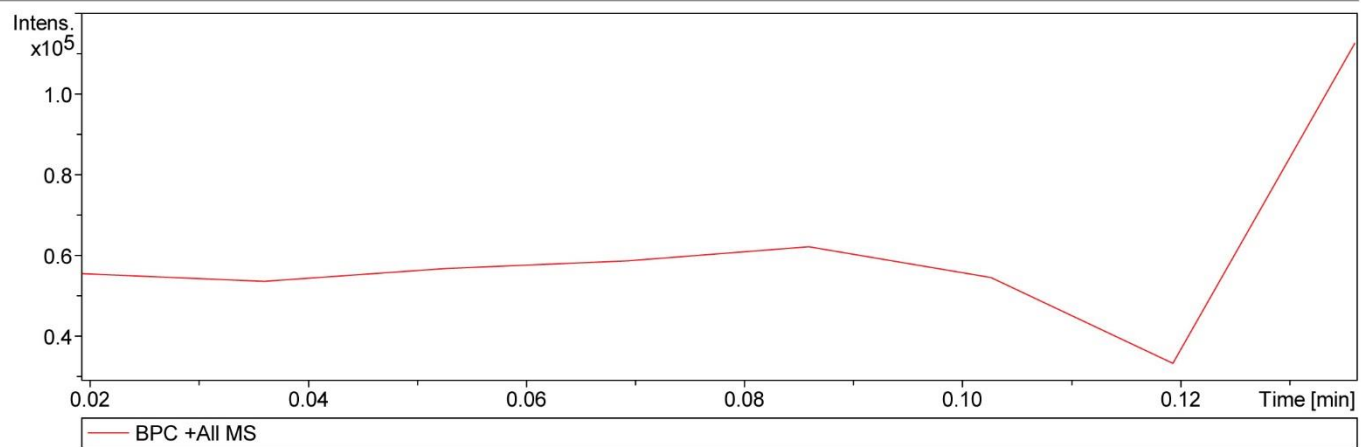


Figure S53. High-resolution Mass spectra of 2-(2-hydroxybenzoyl)-3-(4-(trifluoromethoxy)phenyl)-2,3-dihydro-4H-furo[3,2-c]chromen-4-one (**2-11**)

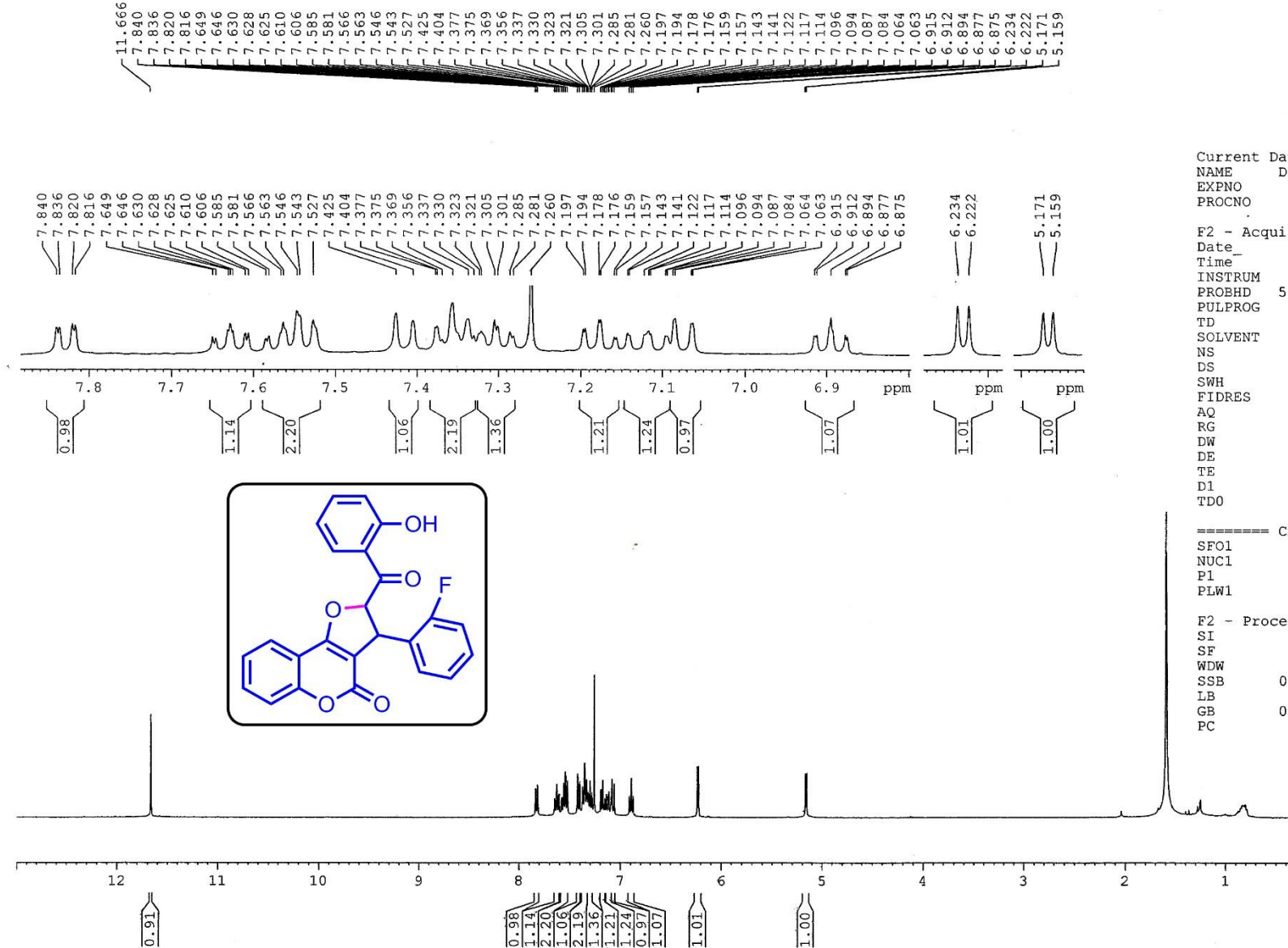


Figure S54. ¹H-NMR spectrum of 3-(2-fluorophenyl)-2-(2-hydroxybenzoyl)-2,3-dihydro-4*H*-furo[3,2-*c*]chromen-4-one (**2-12**)

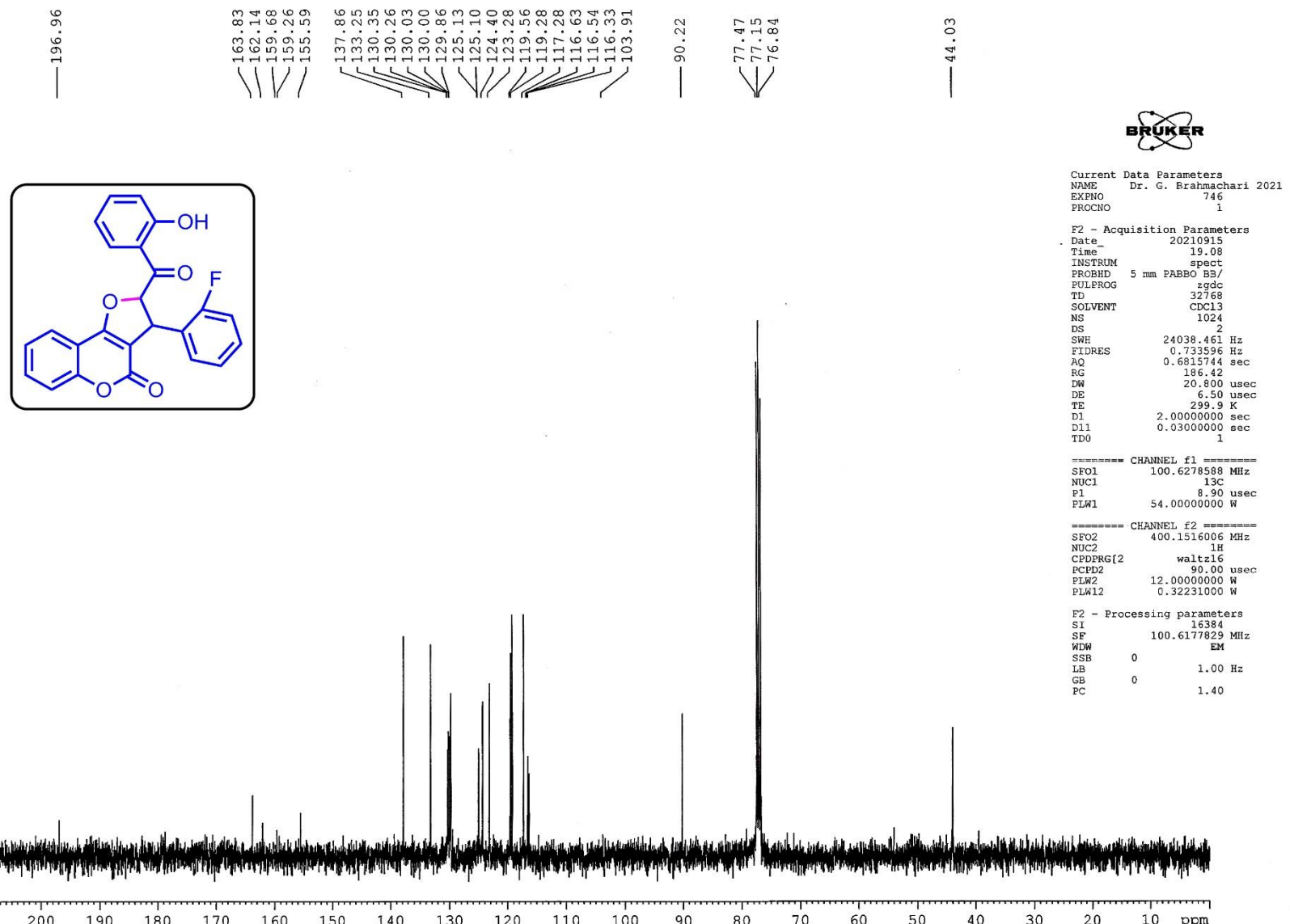


Figure S55. ^{13}C -NMR spectrum of 3-(2-fluorophenyl)-2-(2-hydroxybenzoyl)-2,3-dihydro-4*H*-furo[3,2-*c*]chromen-4-one (**2-12**)

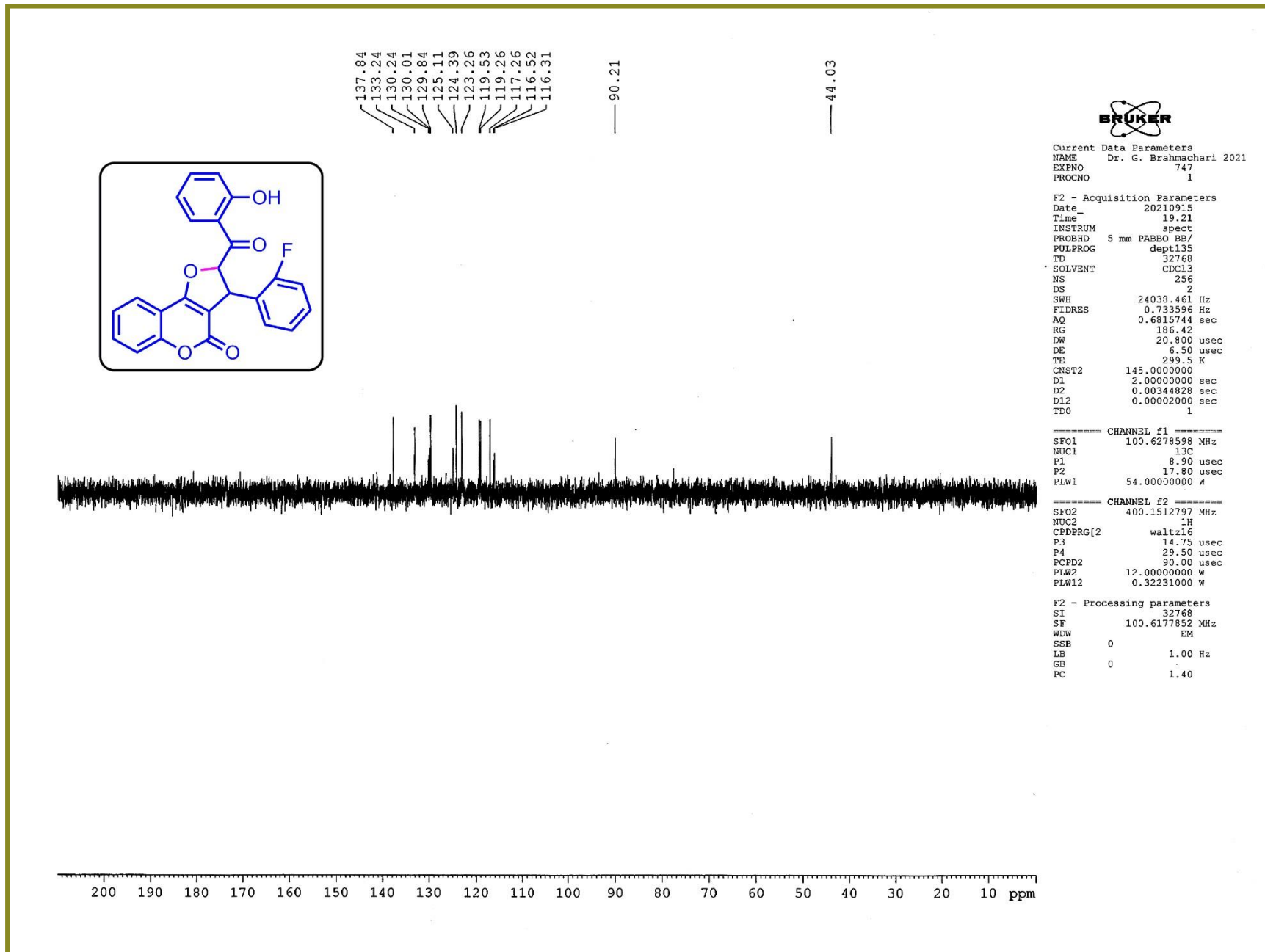


Figure S56. DEPT-135 NMR spectrum of 3-(2-fluorophenyl)-2-(2-hydroxybenzoyl)-2,3-dihydro-4*H*-furo[3,2-*c*]chromen-4-one (**2-12**)

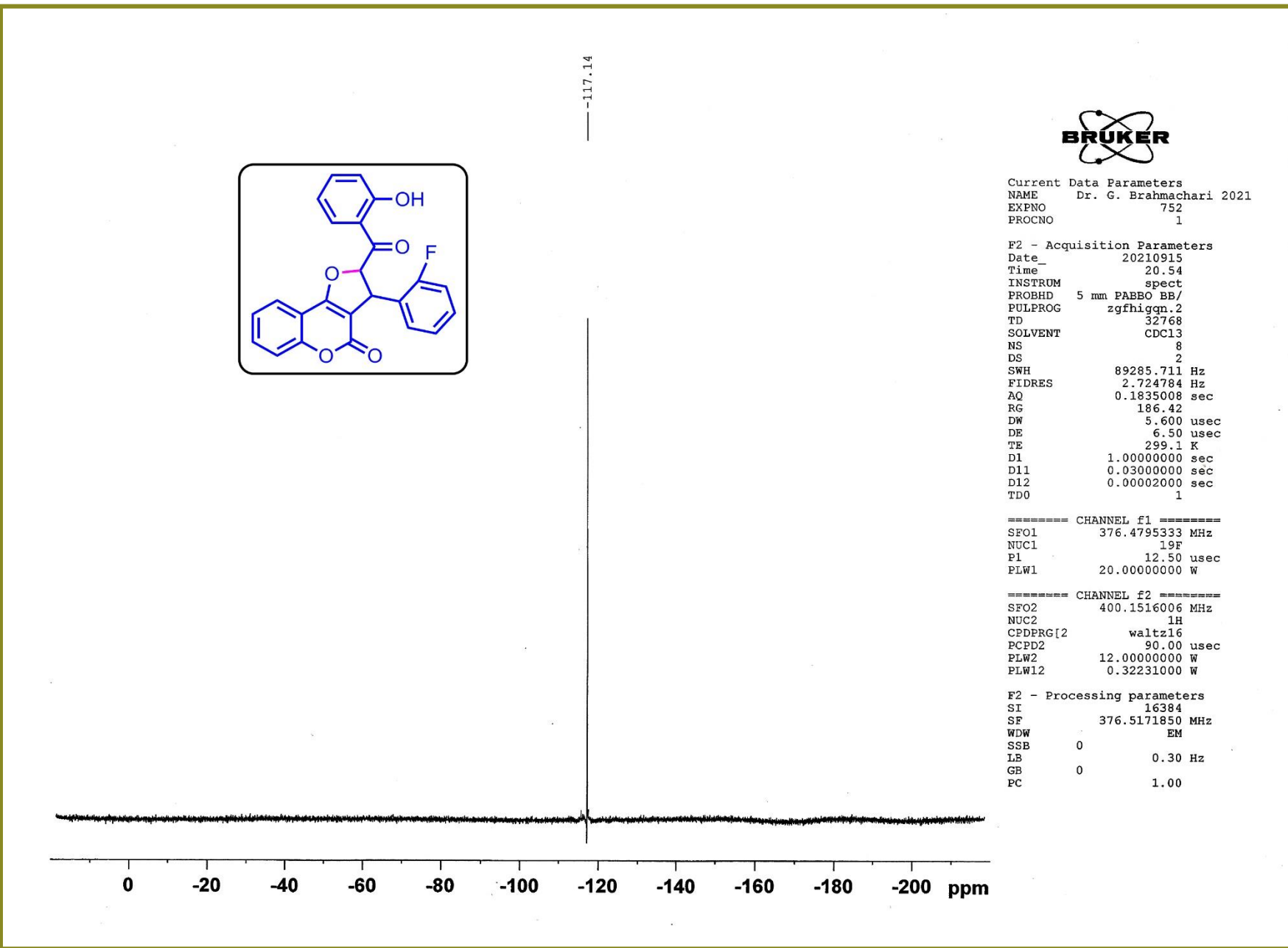


Figure S57. ^{19}F NMR spectrum of 3-(2-fluorophenyl)-2-(2-hydroxybenzoyl)-2,3-dihydro-4*H*-furo[3,2-*c*]chromen-4-one (**2-12**)

Acquisition Parameter

Source Type	ESI	Ion Polarity	Positive	Set Nebulizer	0.4 Bar
Focus	Active	Set Capillary	3400 V	Set Dry Heater	200 °C
Scan Begin	50 m/z	Set End Plate Offset	-500 V	Set Dry Gas	4.0 l/min
Scan End	3000 m/z	Set Charging Voltage	2000 V	Set Divert Valve	Source
		Set Corona	0 nA	Set APCI Heater	0 °C

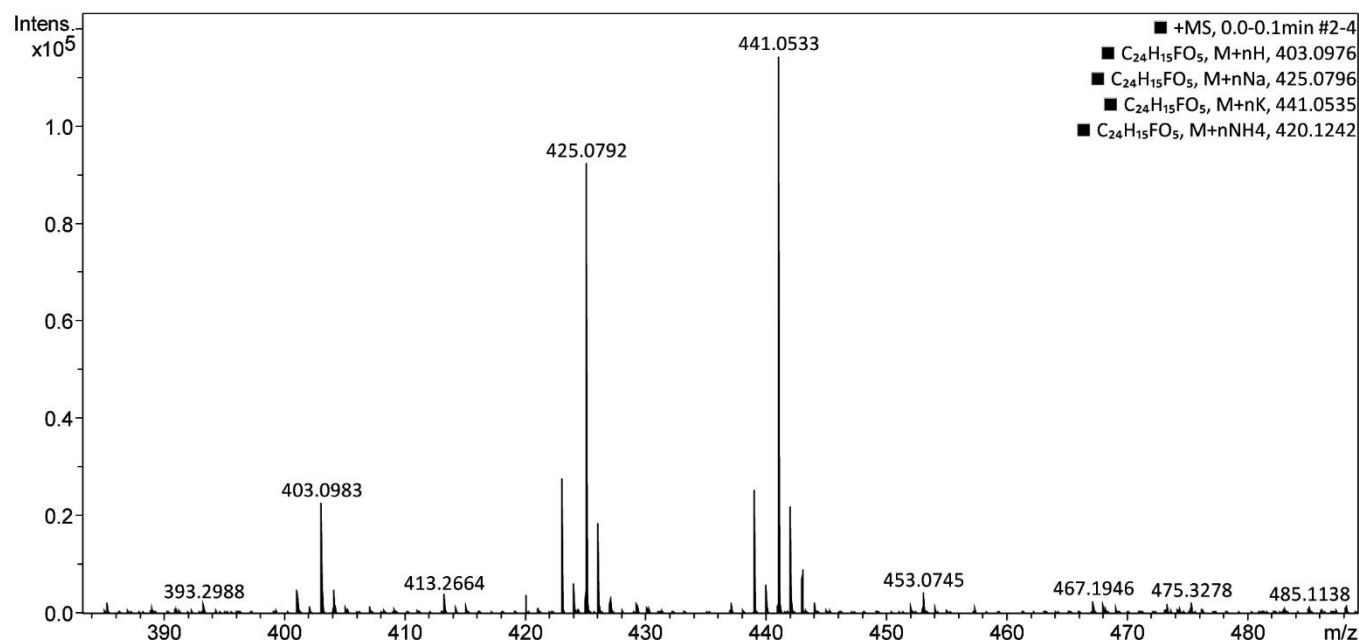
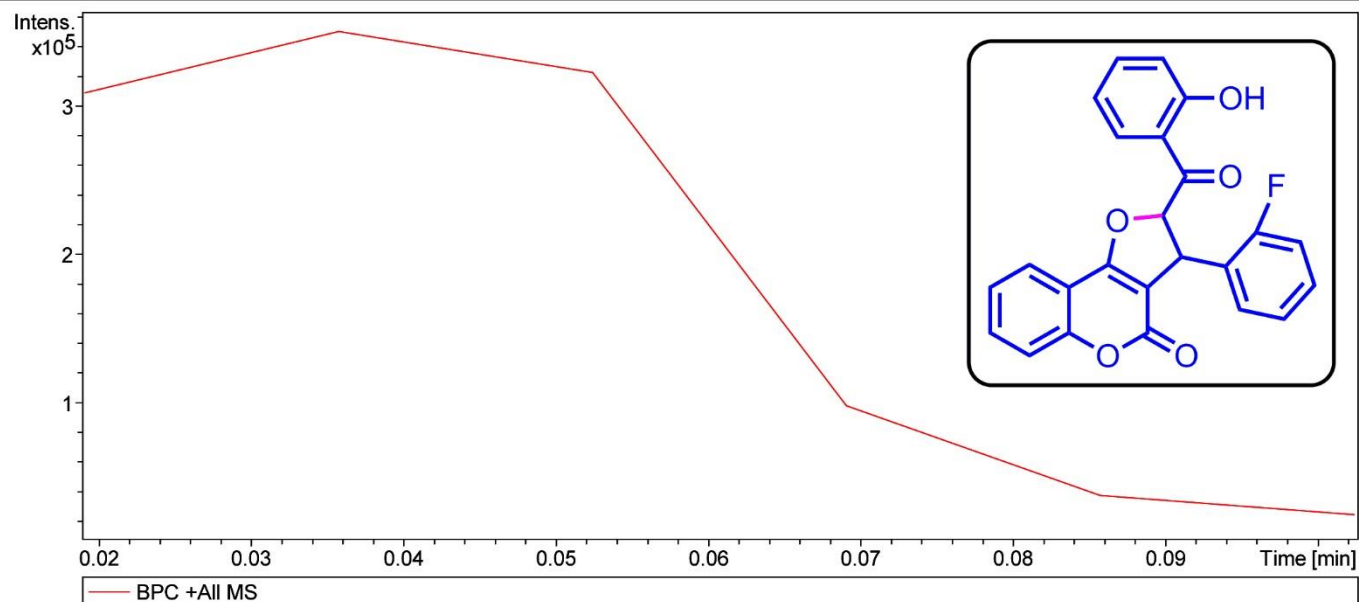


Figure S58. High-resolution Mass spectra of 3-(2-fluorophenyl)-2-(2-hydroxybenzoyl)-2,3-dihydro-4H-furo[3,2-c]chromen-4-one (**2-12**)

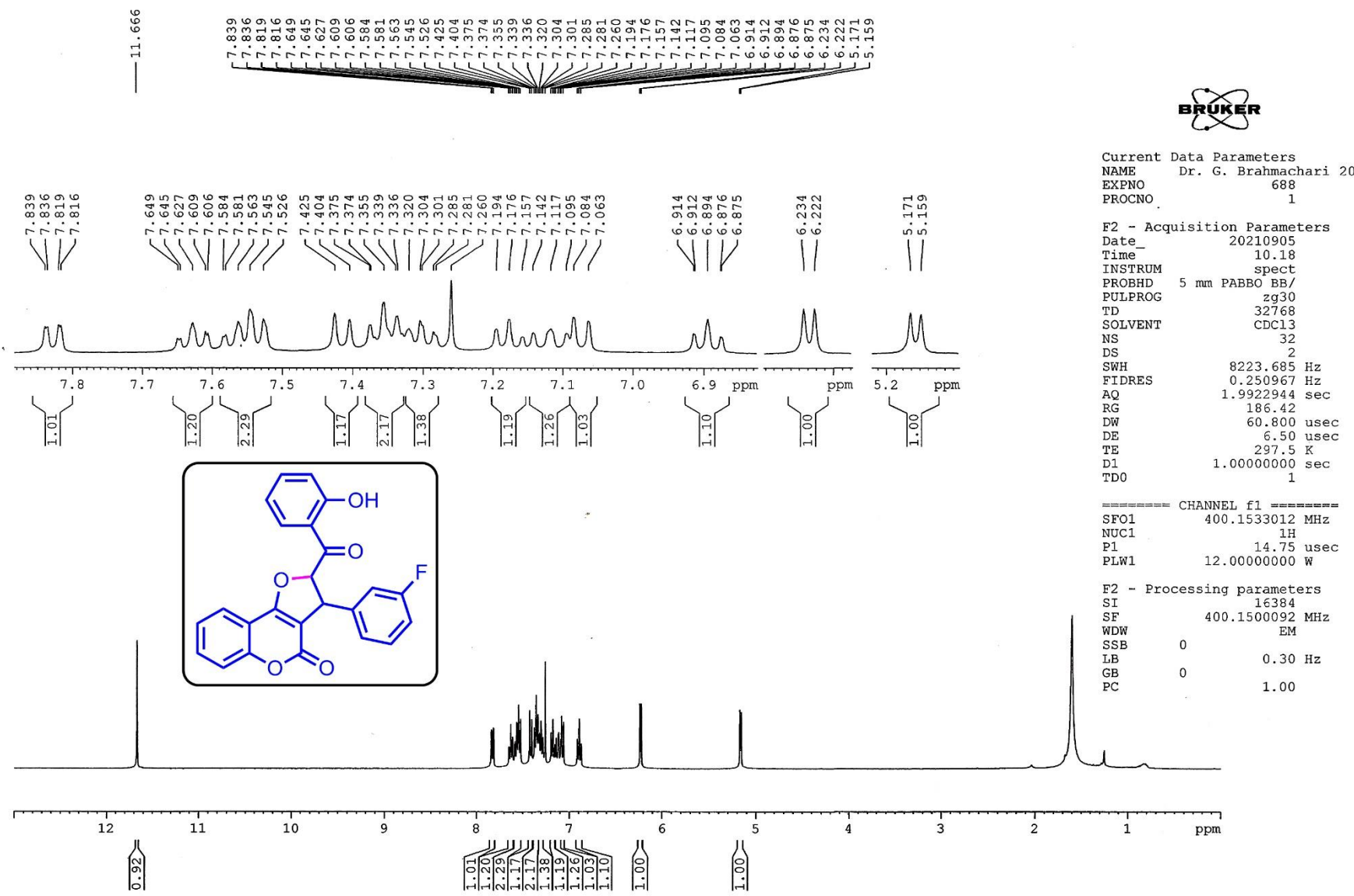


Figure S59. ^1H -NMR spectrum of 3-(3-fluorophenyl)-2-(2-hydroxybenzoyl)-2,3-dihydro-4*H*-furo[3,2-*c*]chromen-4-one (**2-13**)

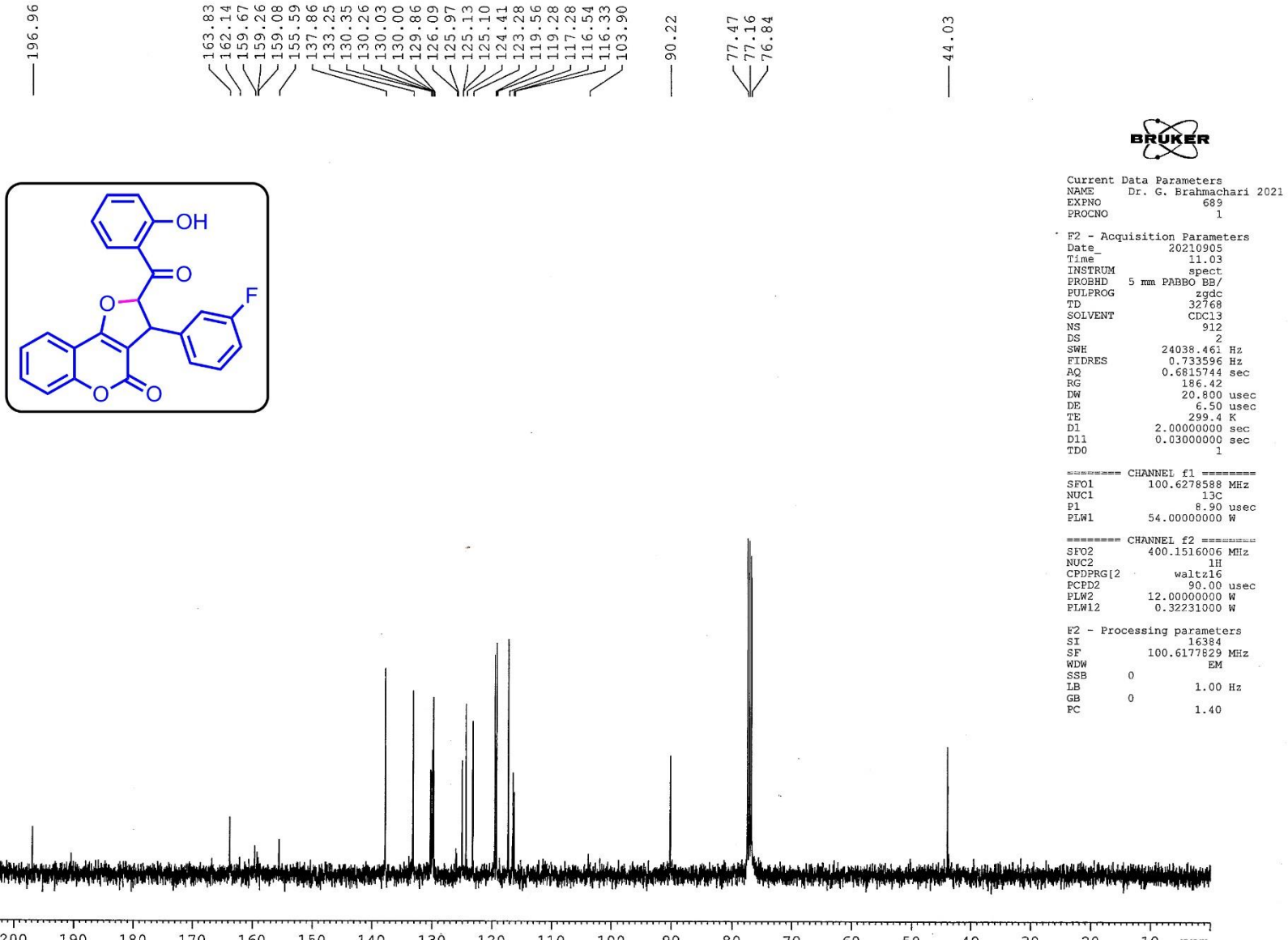


Figure S60. ^{13}C -NMR spectrum of 3-(3-fluorophenyl)-2-(2-hydroxybenzoyl)-2,3-dihydro-4*H*-furo[3,2-*c*]chromen-4-one (**2-13**)
S69

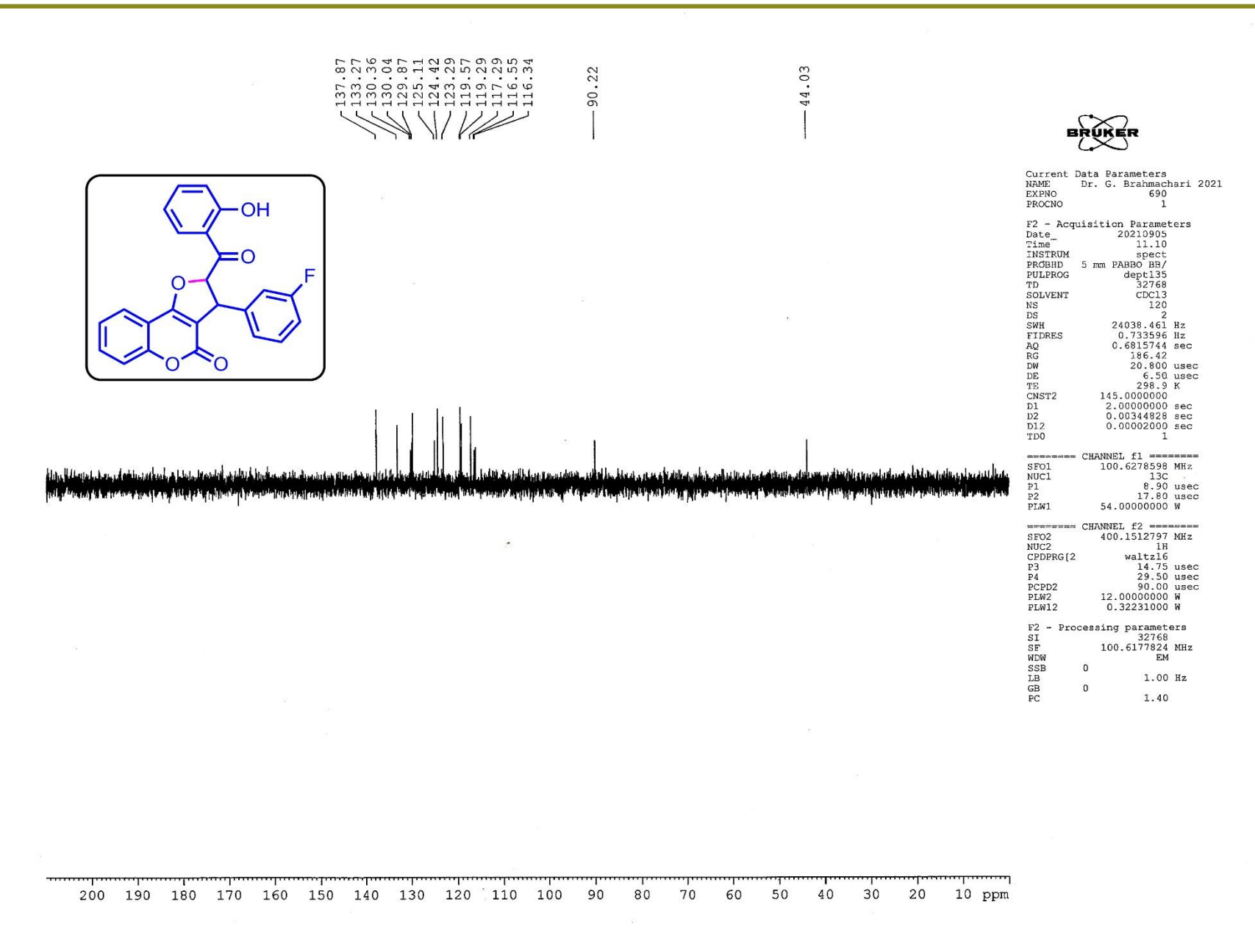
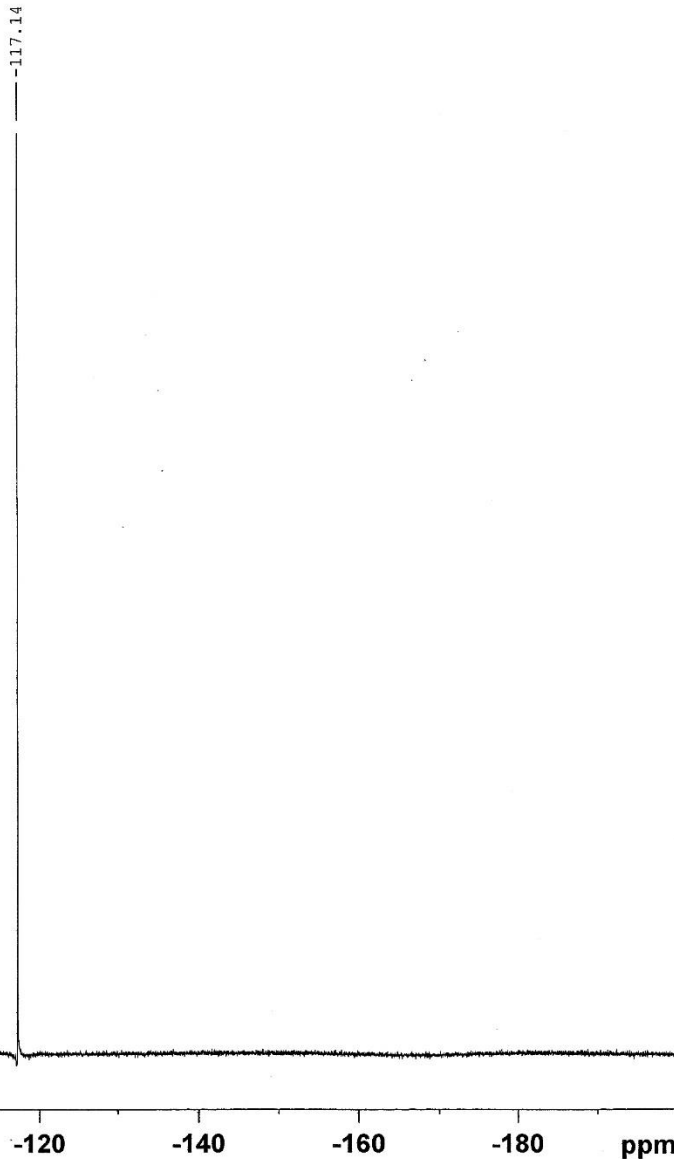
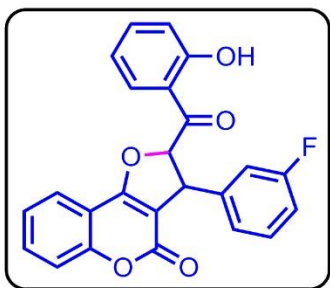


Figure S61. DEPT-135 NMR spectrum of 3-(3-fluorophenyl)-2-(2-hydroxybenzoyl)-2,3-dihydro-4*H*-furo[3,2-*c*]chromen-4-one (**2-13**)



Current Data Parameters
NAME Dr. G. Brahmachari 2021
EXPNO 691
PROCNO 1

F2 - Acquisition Parameters
Date 20210905
Time 11.12
INSTRUM spect
PROBHD 5 mm PABBO BB/
PULPROG zgfhigg.n.2
TD 32768
SOLVENT CDCl3
NS 8
DS 2
SWH 89285.711 Hz
FIDRES 2.724784 Hz
AQ 0.1835008 sec
RG 186.42
DW 5.600 usec
DE 6.50 usec
TE 298.7 K
D1 1.0000000 sec
D11 0.03000000 sec
D12 0.00002000 sec
TDO 1

===== CHANNEL f1 =====
SFO1 376.4795333 MHz
NUC1 19F
P1 12.50 usec
PLW1 20.0000000 W

===== CHANNEL f2 =====
SFO2 400.1516006 MHz
NUC2 1H
CPDPRG[2 waltz16
PCPD2 90.00 usec
PLW2 12.0000000 W
PLW12 0.32231000 W

F2 - Processing parameters
SI 16384
SF 376.5171850 MHz
WDW EM
SSB 0
LB 0.30 Hz
GB 0
PC 1.00

Figure S62. ¹⁹F NMR spectrum of 3-(3-fluorophenyl)-2-(2-hydroxybenzoyl)-2,3-dihydro-4H-furo[3,2-c]chromen-4-one (**2-13**)

Acquisition Parameter

Source Type	ESI	Ion Polarity	Positive	Set Nebulizer	0.4 Bar
Focus	Active	Set Capillary	3400 V	Set Dry Heater	200 °C
Scan Begin	50 m/z	Set End Plate Offset	-500 V	Set Dry Gas	4.0 l/min
Scan End	3000 m/z	Set Charging Voltage	2000 V	Set Divert Valve	Source
		Set Corona	0 nA	Set APCI Heater	0 °C

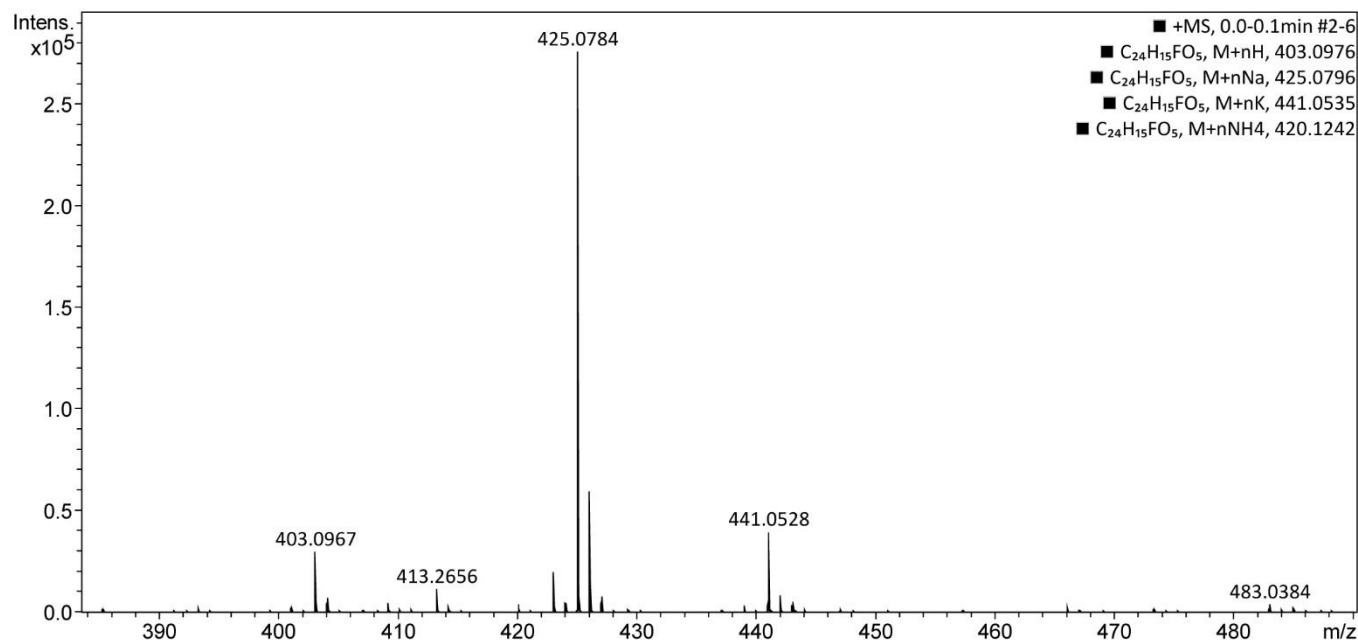
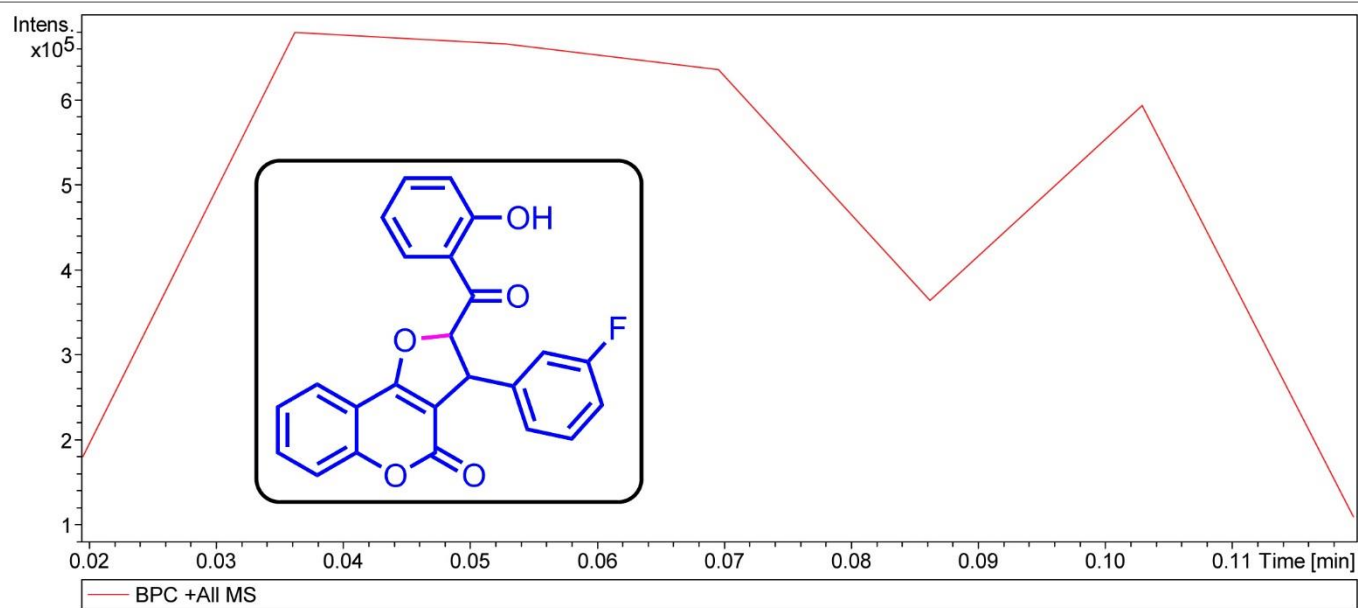


Figure S63. High-resolution Mass spectra of 3-(3-fluorophenyl)-2-(2-hydroxybenzoyl)-2,3-dihydro-4H-furo[3,2-c]chromen-4-one (**2-13**)

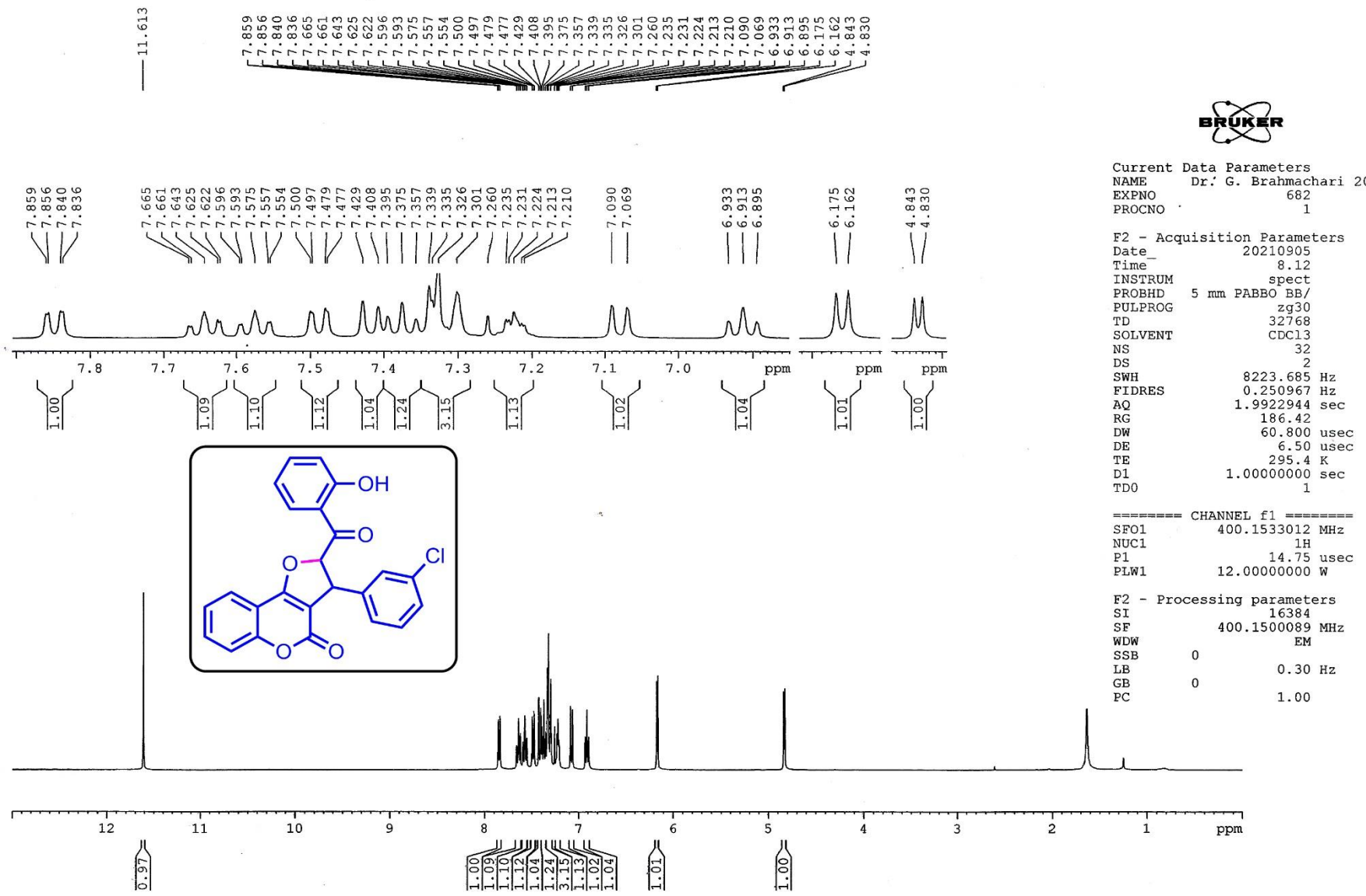


Figure S64. ^1H -NMR spectrum of 3-(3-chlorophenyl)-2-(2-hydroxybenzoyl)-2,3-dihydro-4*H*-furo[3,2-*c*]chromen-4-one (**2-14**)

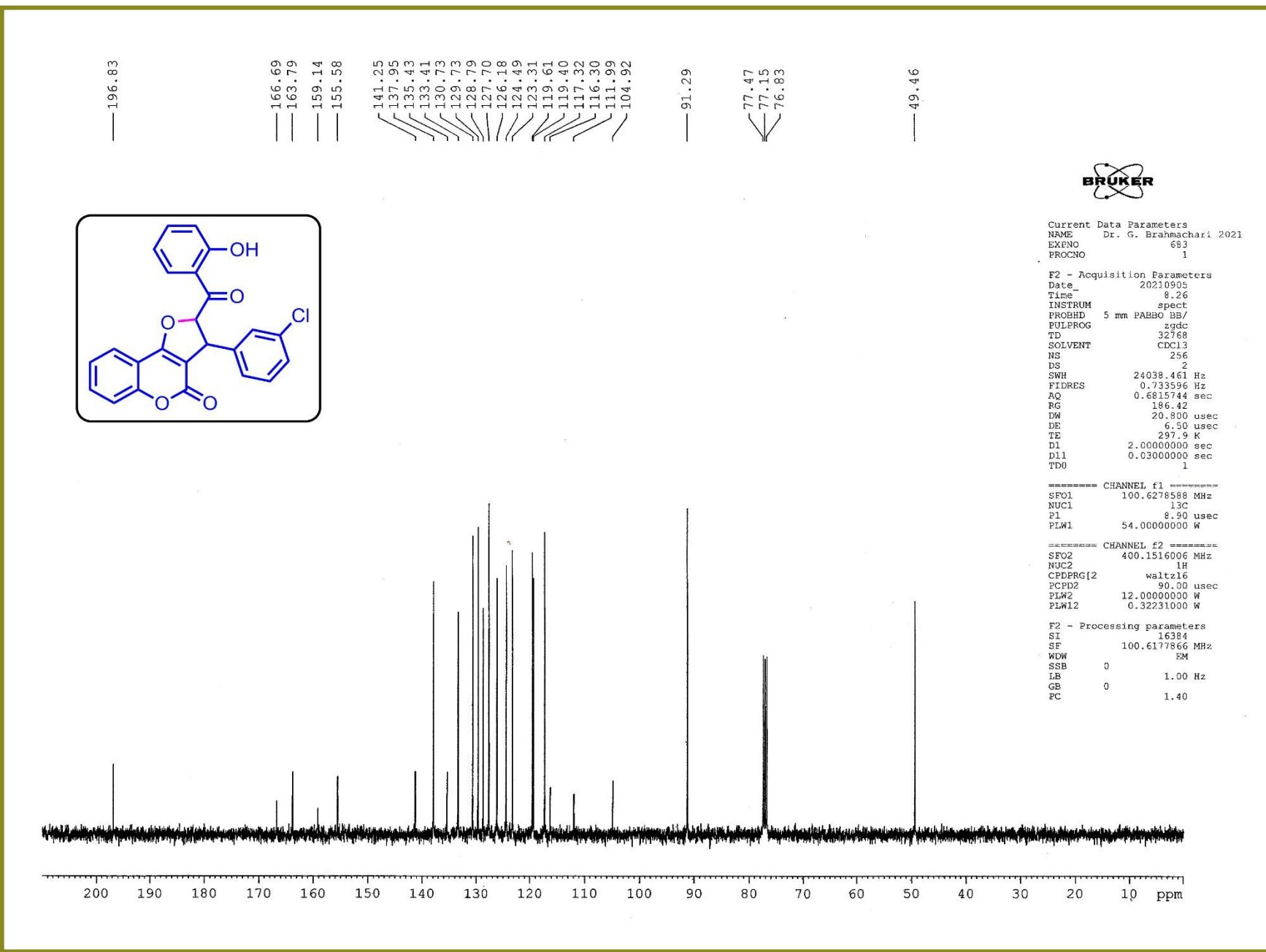


Figure S65. ^{13}C -NMR spectrum of 3-(3-chlorophenyl)-2-(2-hydroxybenzoyl)-2,3-dihydro-4*H*-furo[3,2-*c*]chromen-4-one (**2-14**)

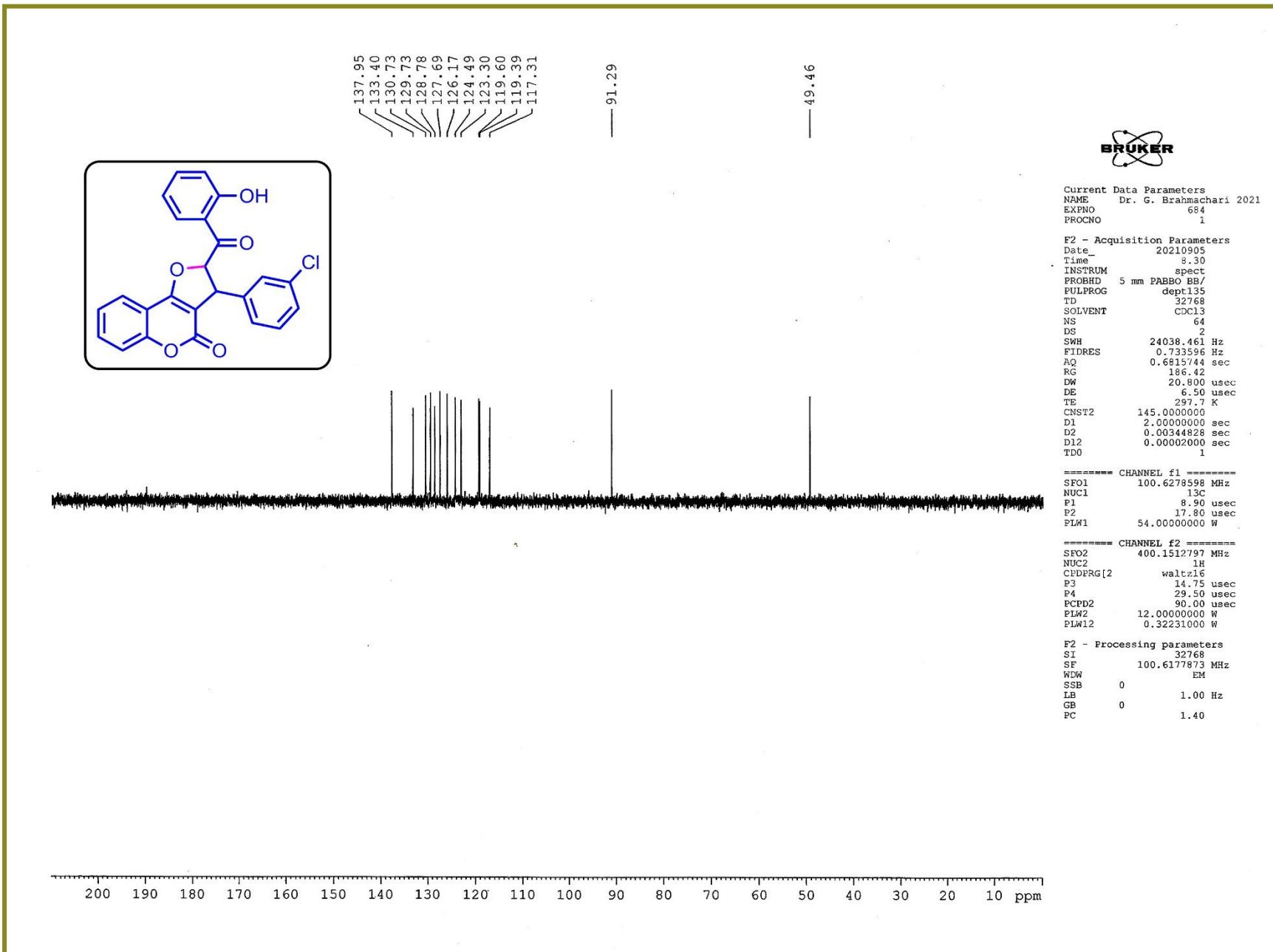


Figure S66. DEPT-135 NMR spectrum of 3-(3-chlorophenyl)-2-(2-hydroxybenzoyl)-2,3-dihydro-4H-furo[3,2-c]chromen-4-one (**2-14**)

Acquisition Parameter

Source Type	ESI	Ion Polarity	Positive	Set Nebulizer	0.4 Bar
Focus	Active	Set Capillary	3400 V	Set Dry Heater	200 °C
Scan Begin	50 m/z	Set End Plate Offset	-500 V	Set Dry Gas	4.0 l/min
Scan End	3000 m/z	Set Charging Voltage	2000 V	Set Divert Valve	Source
		Set Corona	0 nA	Set APCI Heater	0 °C

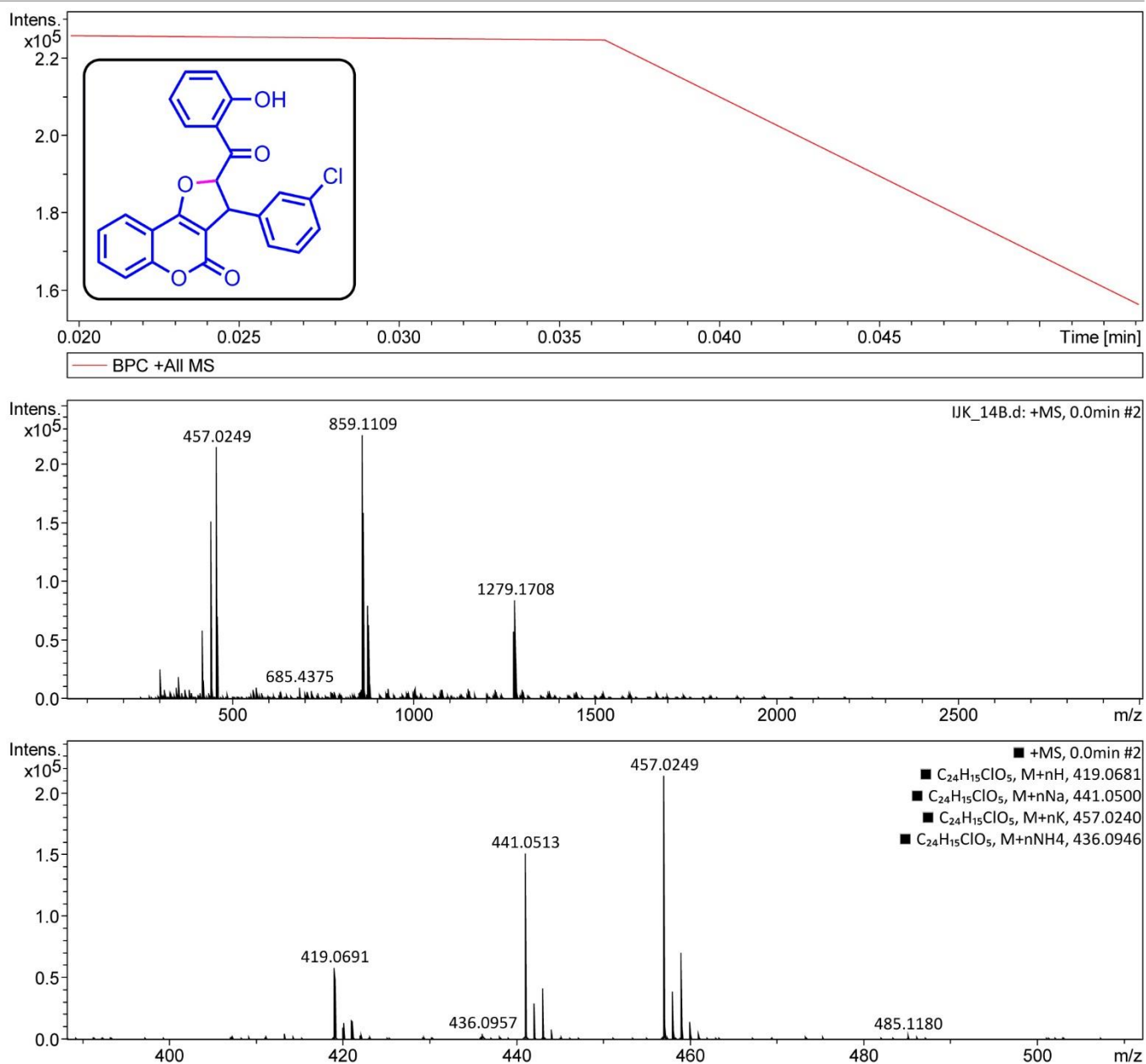


Figure S67. High-resolution Mass spectra of 3-(3-chlorophenyl)-2-(2-hydroxybenzoyl)-2,3-dihydro-4H-furo[3,2-c]chromen-4-one (**2-14**)

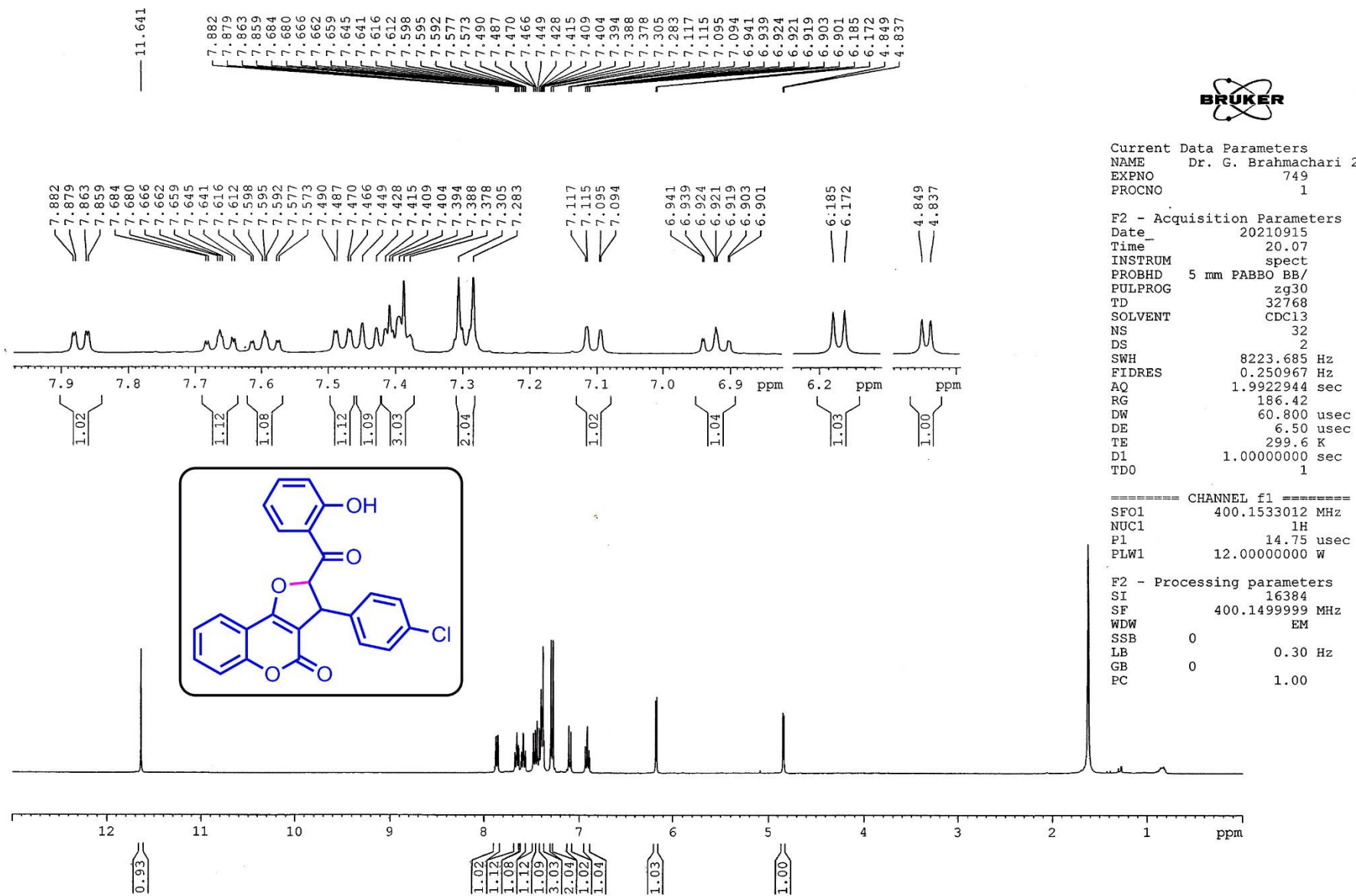


Figure S68. ¹H-NMR spectrum of 3-(4-chlorophenyl)-2-(2-hydroxybenzoyl)-2,3-dihydro-4*H*-furo[3,2-*c*]chromen-4-one (**2-15**)

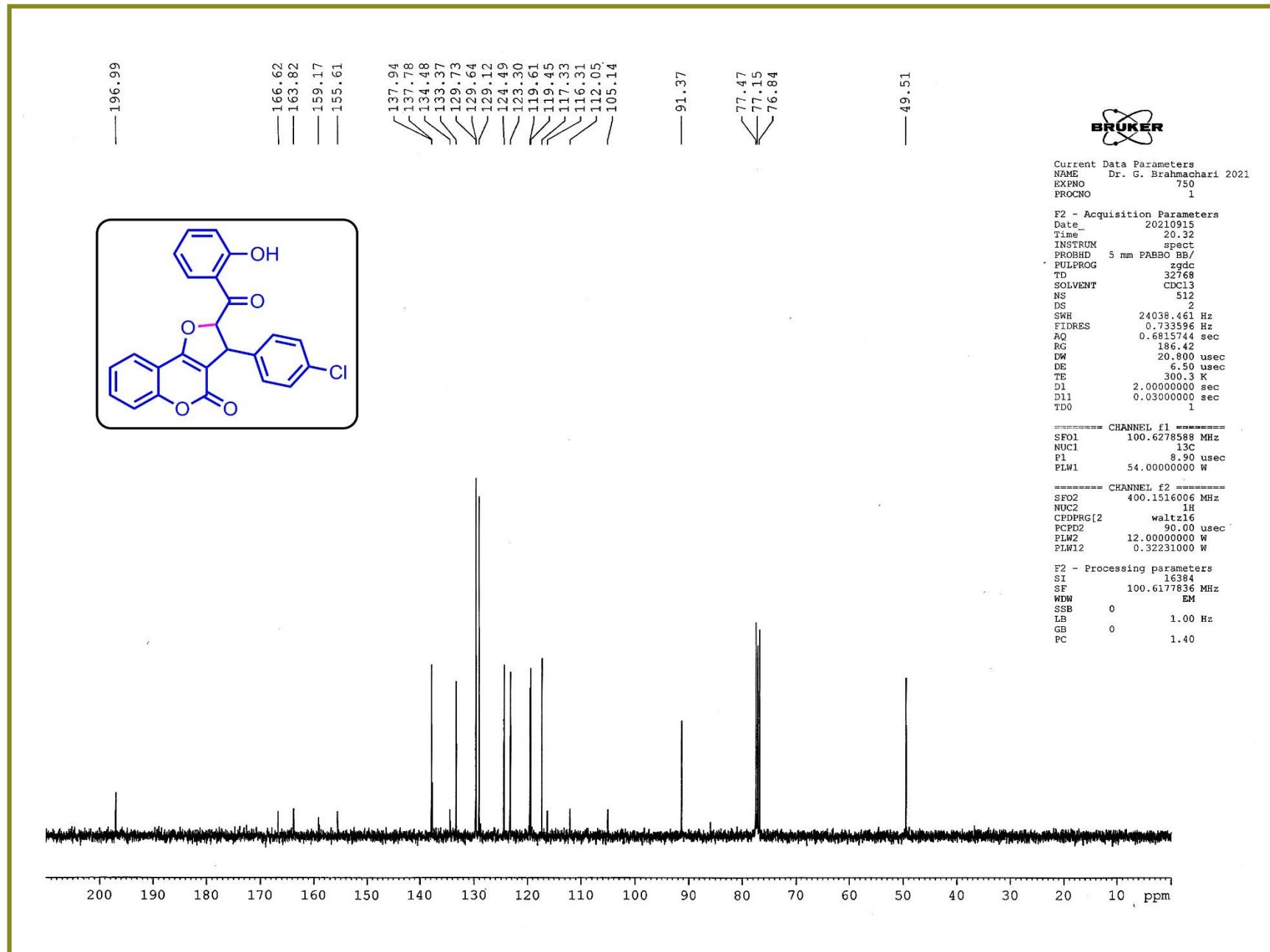


Figure S69. ¹³C-NMR spectrum of 3-(4-chlorophenyl)-2-(2-hydroxybenzoyl)-2,3-dihydro-4H-furo[3,2-c]chromen-4-one (**2-15**)

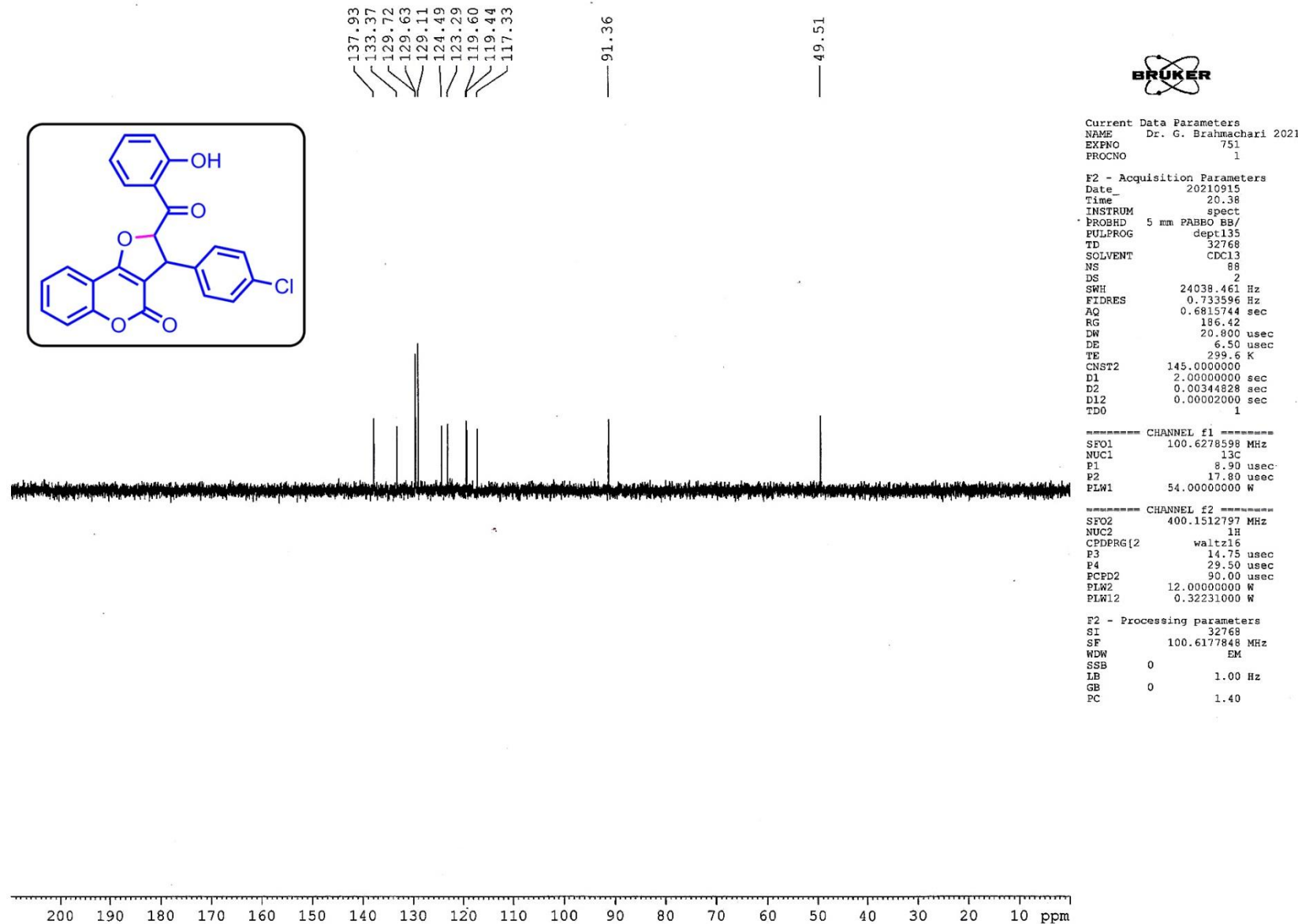


Figure S70. DEPT-135 NMR spectrum of 3-(4-chlorophenyl)-2-(2-hydroxybenzoyl)-2,3-dihydro-4*H*-furo[3,2-*c*]chromen-4-one (**2-15**)

Acquisition Parameter

Source Type	ESI	Ion Polarity	Positive	Set Nebulizer	0.4 Bar
Focus	Active	Set Capillary	3400 V	Set Dry Heater	200 °C
Scan Begin	50 m/z	Set End Plate Offset	-500 V	Set Dry Gas	4.0 l/min
Scan End	3000 m/z	Set Charging Voltage	2000 V	Set Divert Valve	Source
		Set Corona	0 nA	Set APCI Heater	0 °C

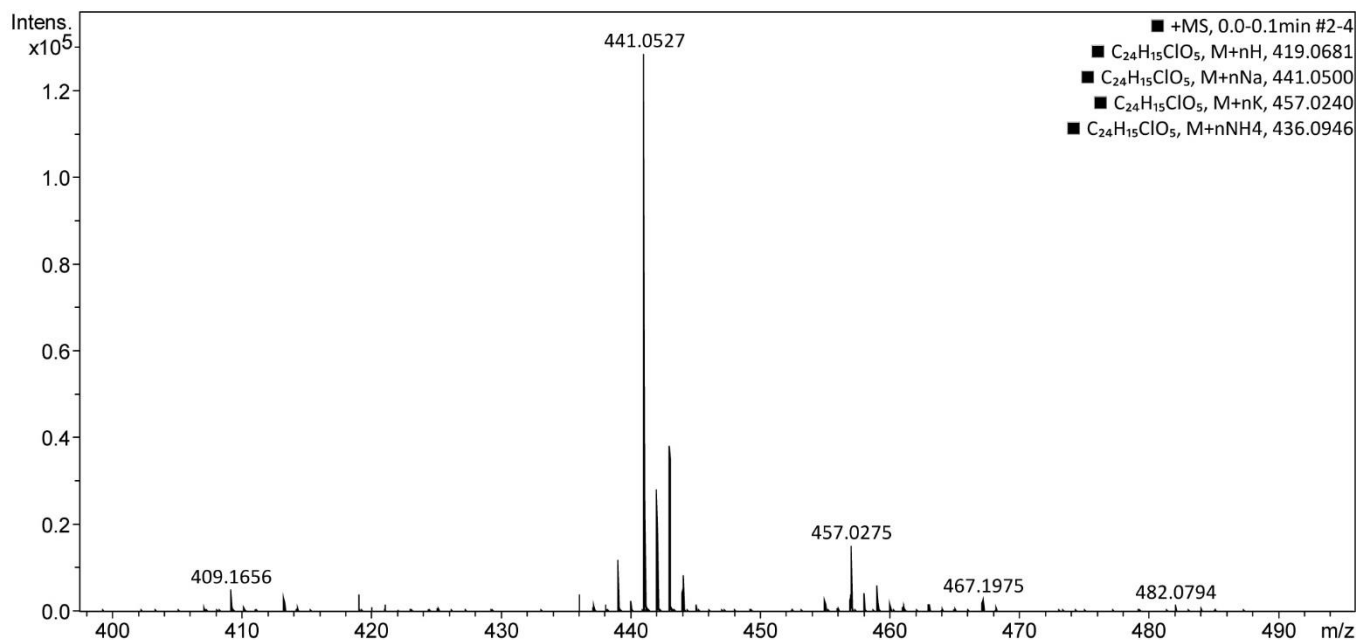
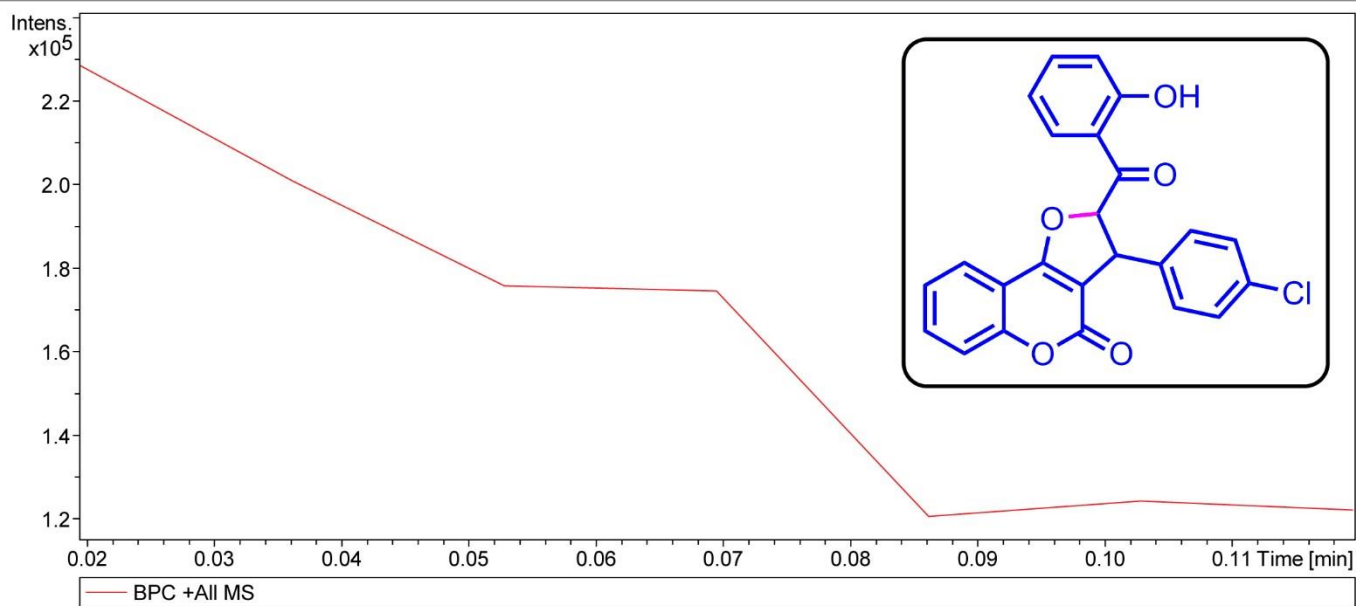


Figure S71. High-resolution Mass spectra of 3-(4-chlorophenyl)-2-(2-hydroxybenzoyl)-2,3-dihydro-4H-furo[3,2-c]chromen-4-one (**2-15**)

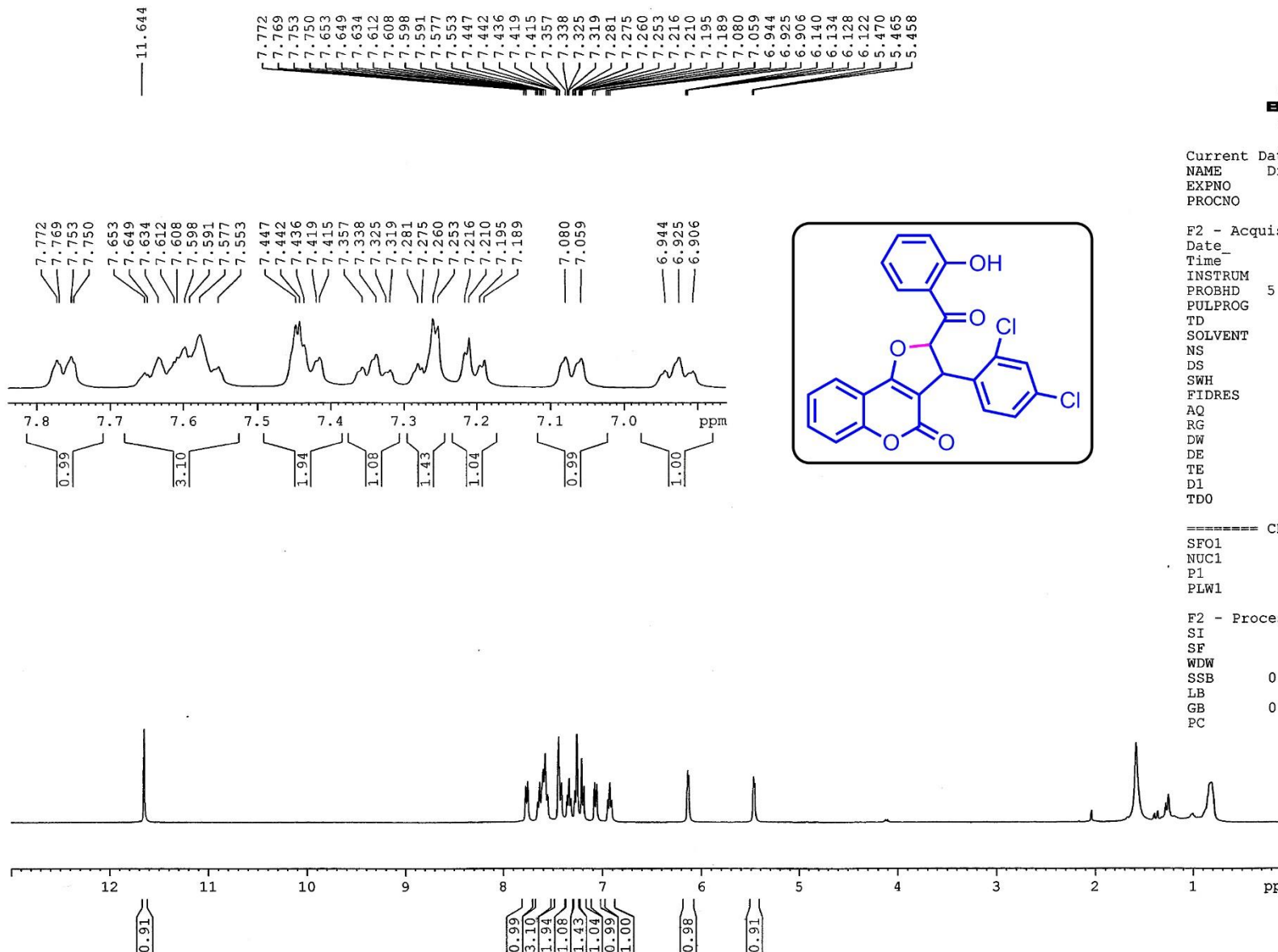


Figure S72. $^1\text{H-NMR}$ spectrum of 3-(2,4-dichlorophenyl)-2-(2-hydroxybenzoyl)-2,3-dihydro-4*H*-furo[3,2-*c*]chromen-4-one (**2-16**)

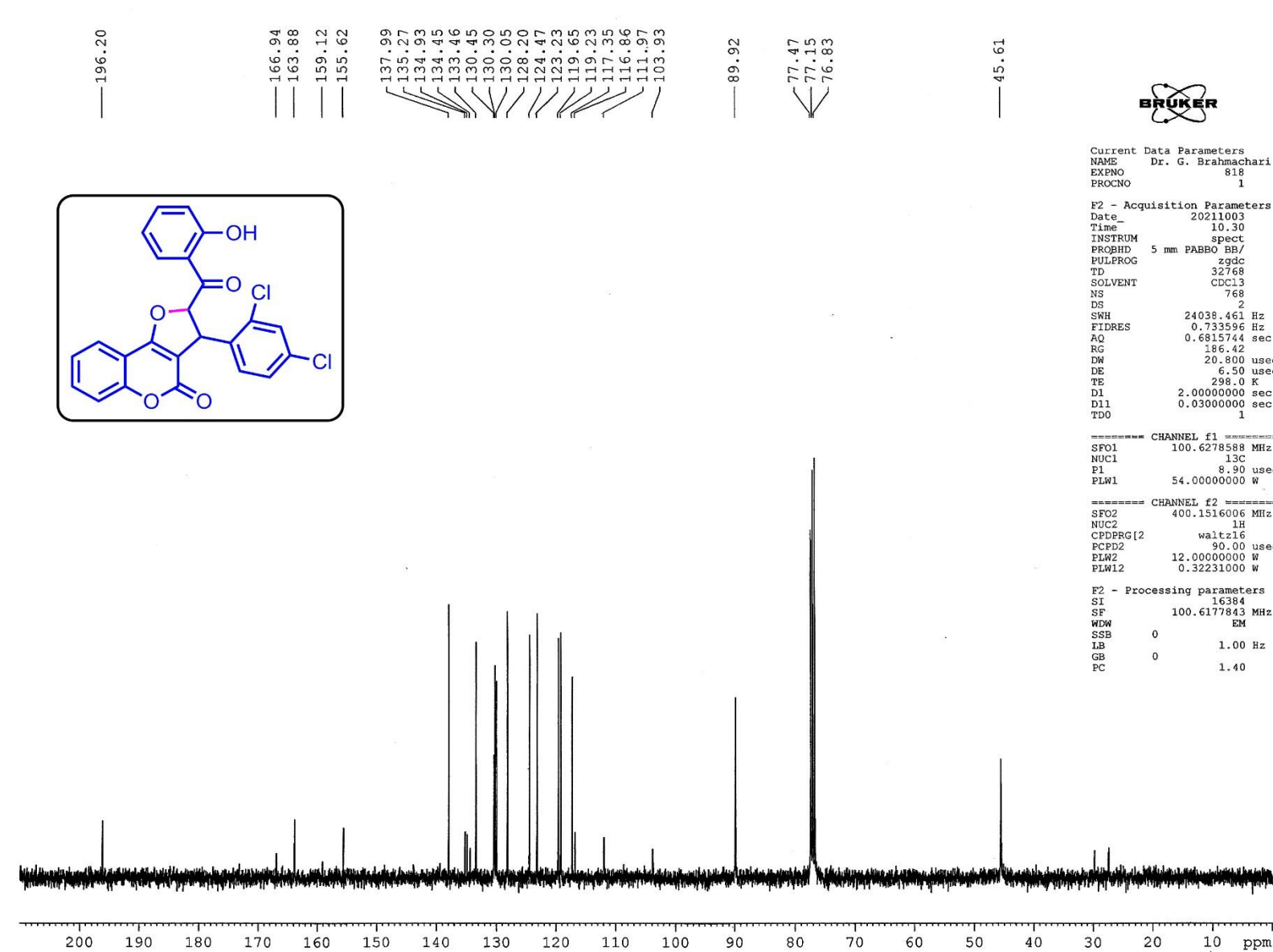


Figure S73. ^{13}C -NMR spectrum of 3-(2,4-dichlorophenyl)-2-(2-hydroxybenzoyl)-2,3-dihydro-4*H*-furo[3,2-*c*]chromen-4-one (**2-16**)

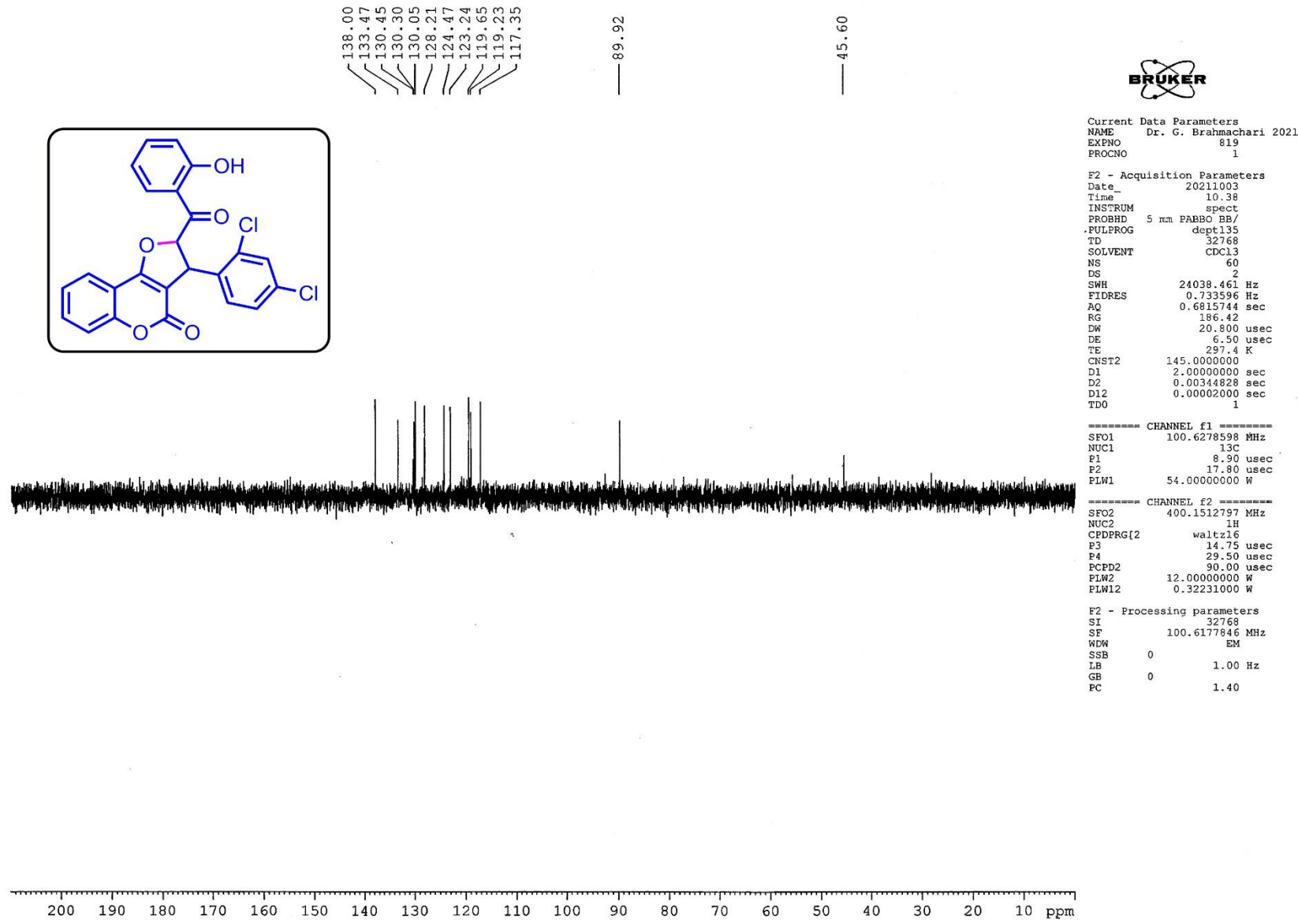


Figure S74. DEPT-135 NMR spectrum of 3-(2,4-dichlorophenyl)-2-(2-hydroxybenzoyl)-2,3-dihydro-4*H*-furo[3,2-*c*]chromen-4-one (**2-16**)

Acquisition Parameter

Source Type	ESI	Ion Polarity	Positive	Set Nebulizer	0.4 Bar
Focus	Active	Set Capillary	3400 V	Set Dry Heater	200 °C
Scan Begin	50 m/z	Set End Plate Offset	-500 V	Set Dry Gas	4.0 l/min
Scan End	3000 m/z	Set Charging Voltage	2000 V	Set Divert Valve	Source
		Set Corona	0 nA	Set APCI Heater	0 °C

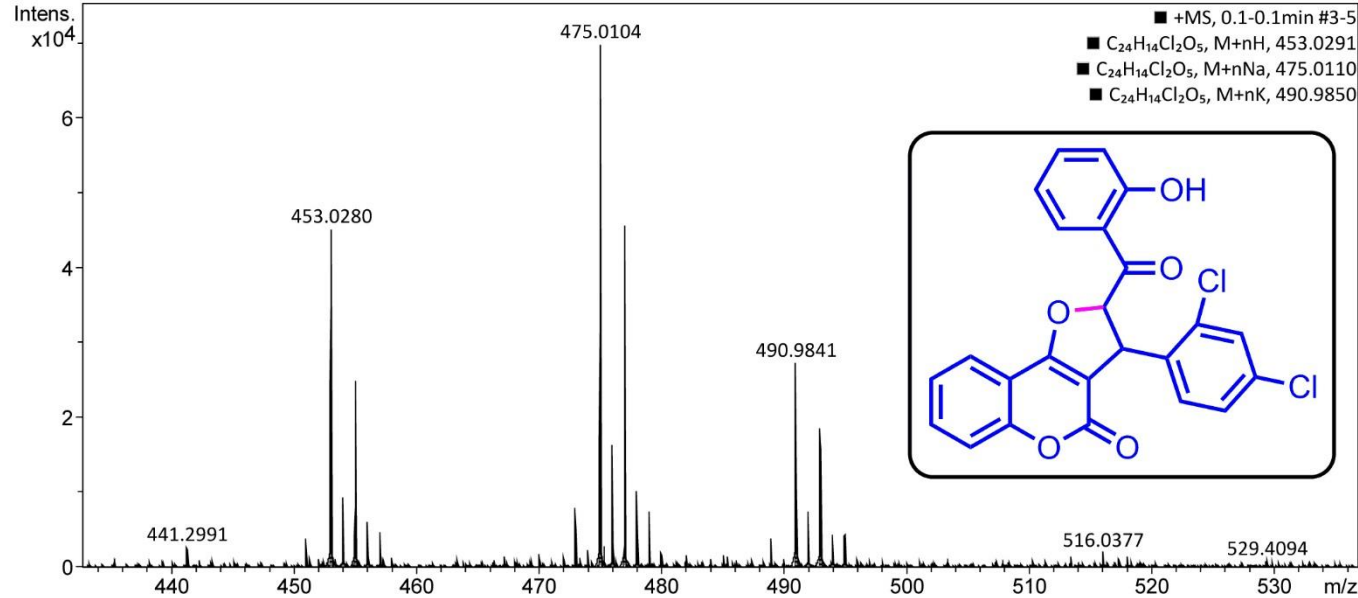
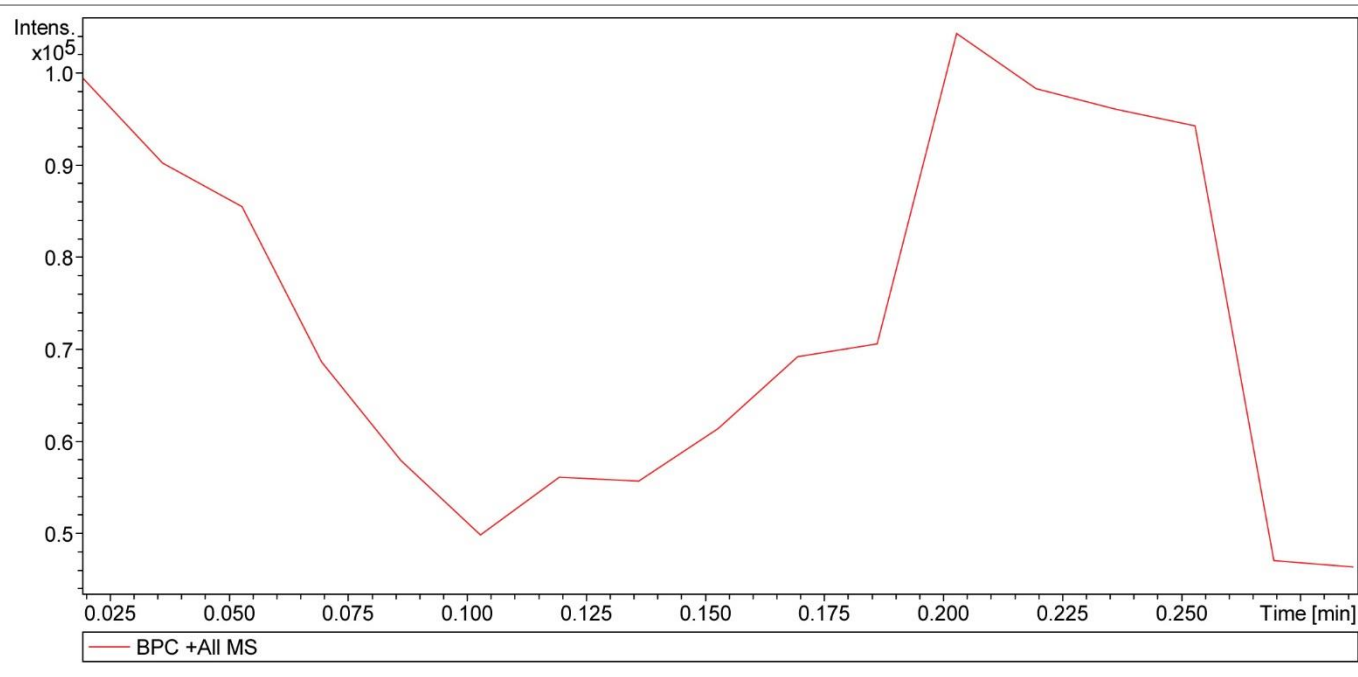


Figure S75. High-resolution Mass spectra of 3-(2,4-dichlorophenyl)-2-(2-hydroxybenzoyl)-2,3-dihydro-4*H*-furo[3,2-*c*]chromen-4-one (**2-16**)

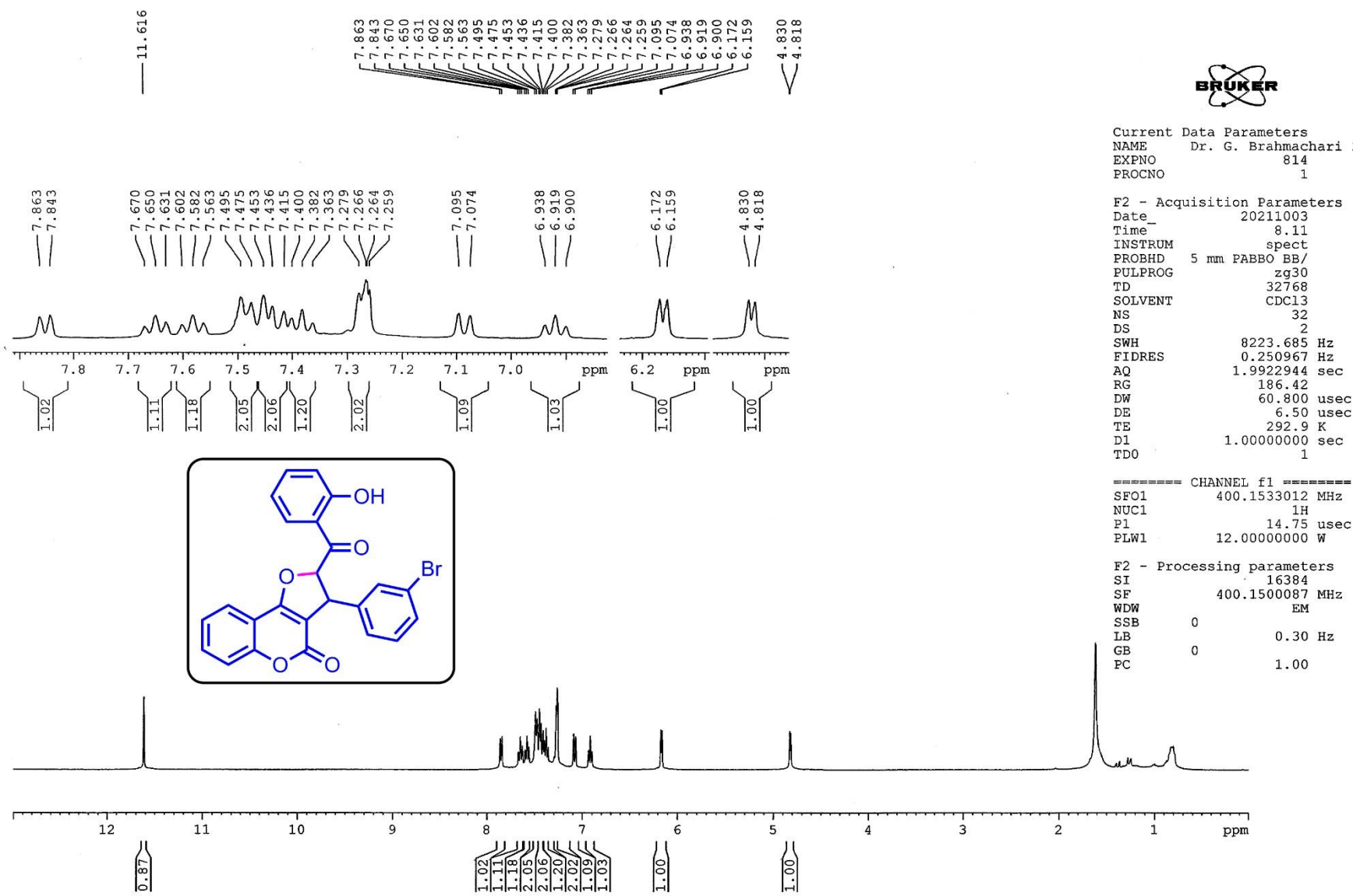


Figure S76. ^1H -NMR spectrum of 3-(3-bromophenyl)-2-(2-hydroxybenzoyl)-2,3-dihydro-4*H*-furo[3,2-*c*]chromen-4-one (**2-17**)

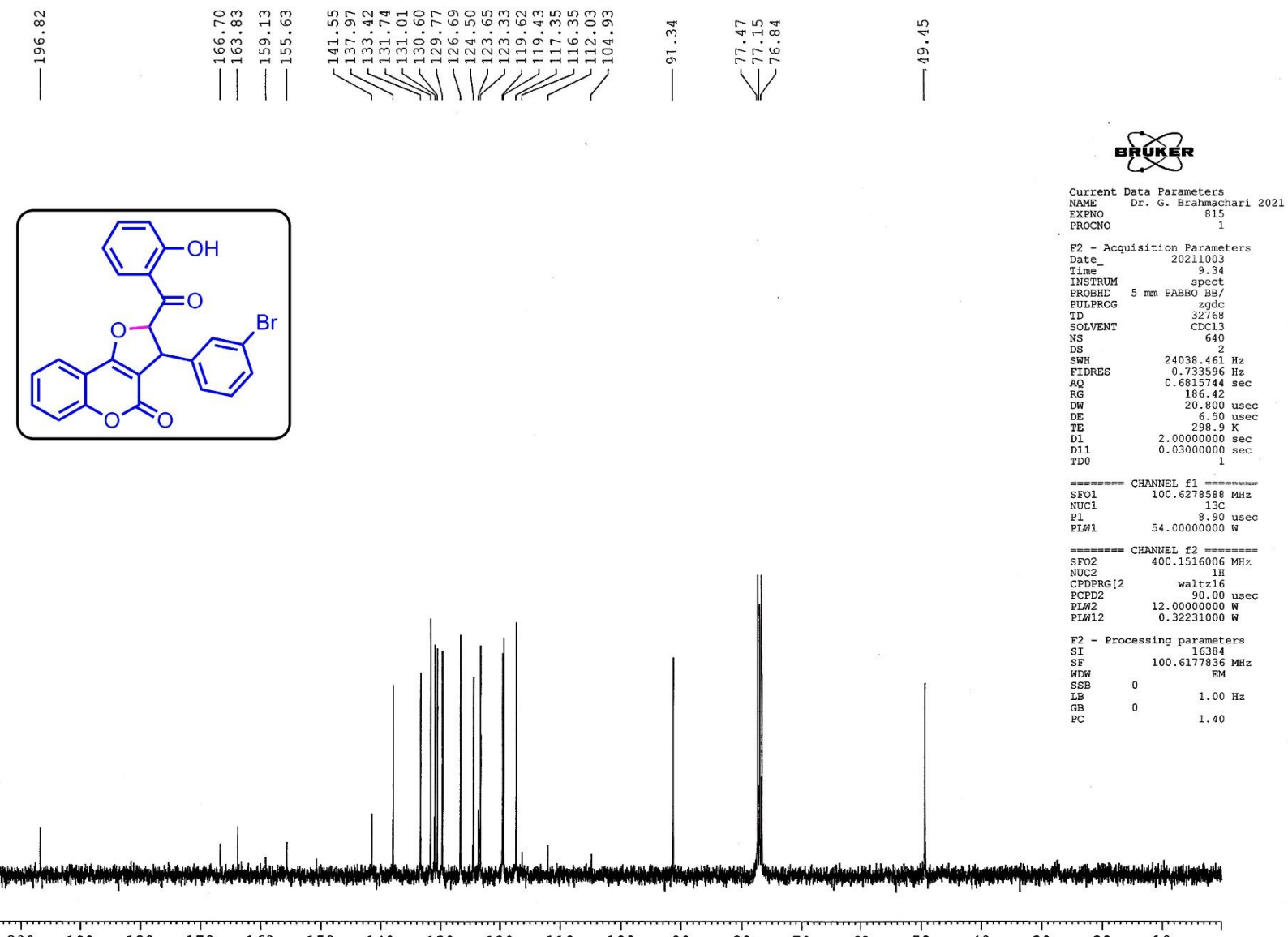


Figure S77. ¹³C-NMR spectrum of 3-(3-bromophenyl)-2-(2-hydroxybenzoyl)-2,3-dihydro-4H-furo[3,2-c]chromen-4-one (**2-17**)

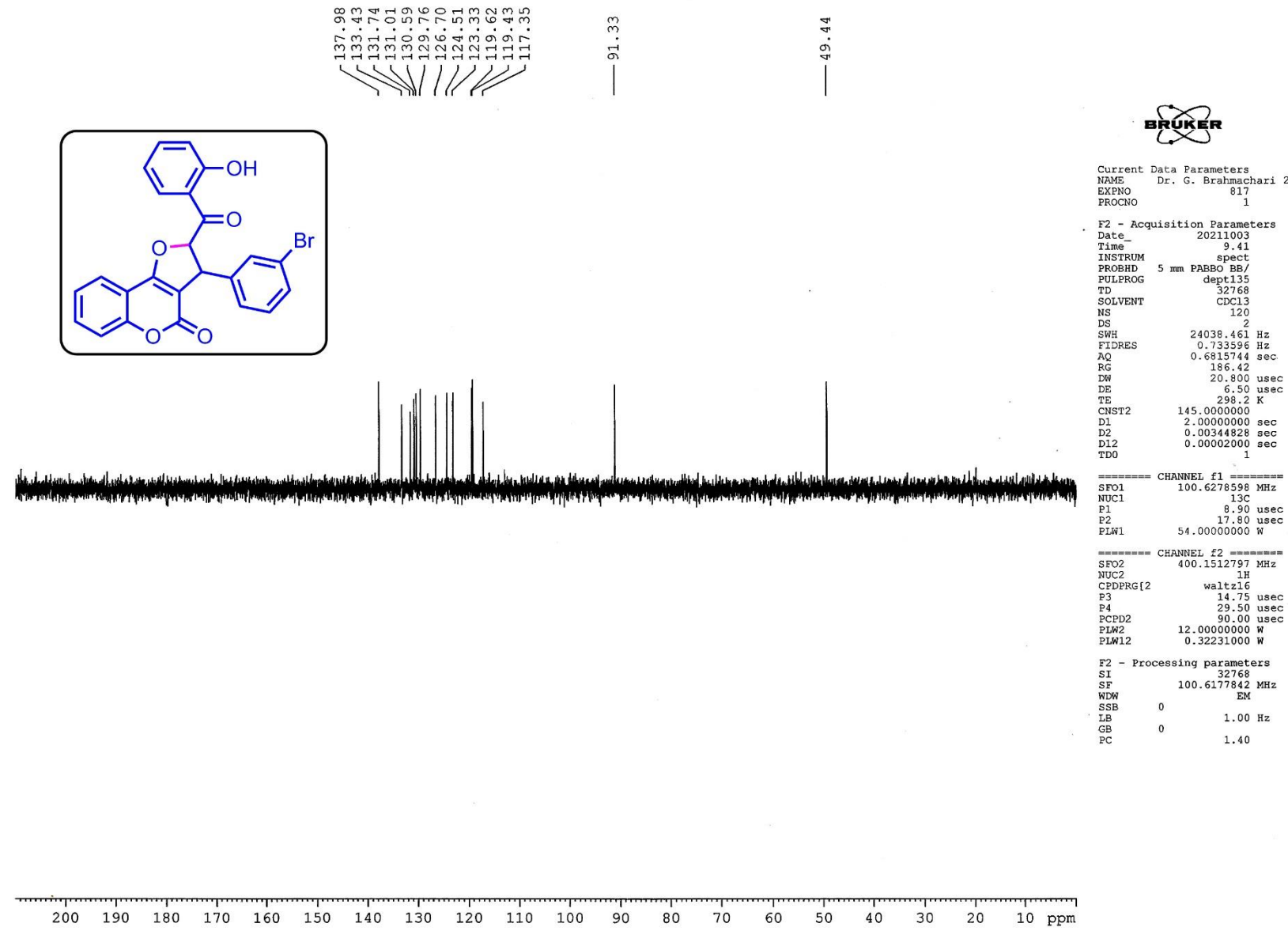


Figure S78. DEPT-135 NMR spectrum of 3-(3-bromophenyl)-2-(2-hydroxybenzoyl)-2,3-dihydro-4*H*-furo[3,2-*c*]chromen-4-one (**2-17**)

Acquisition Parameter

Source Type	ESI	Ion Polarity	Positive	Set Nebulizer	0.4 Bar
Focus	Active	Set Capillary	3400 V	Set Dry Heater	200 °C
Scan Begin	50 m/z	Set End Plate Offset	-500 V	Set Dry Gas	4.0 l/min
Scan End	3000 m/z	Set Charging Voltage	2000 V	Set Divert Valve	Source
		Set Corona	0 nA	Set APCI Heater	0 °C

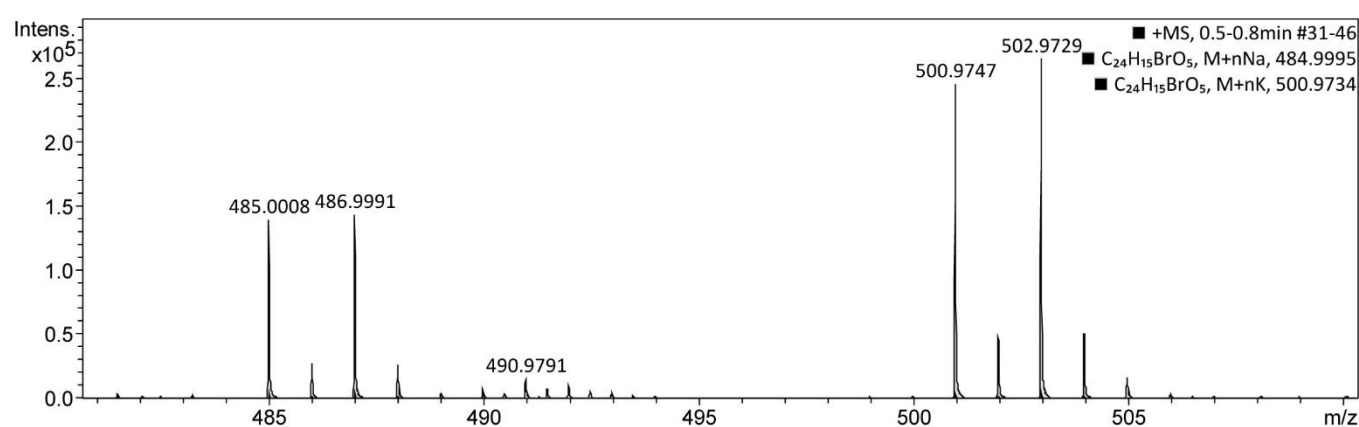
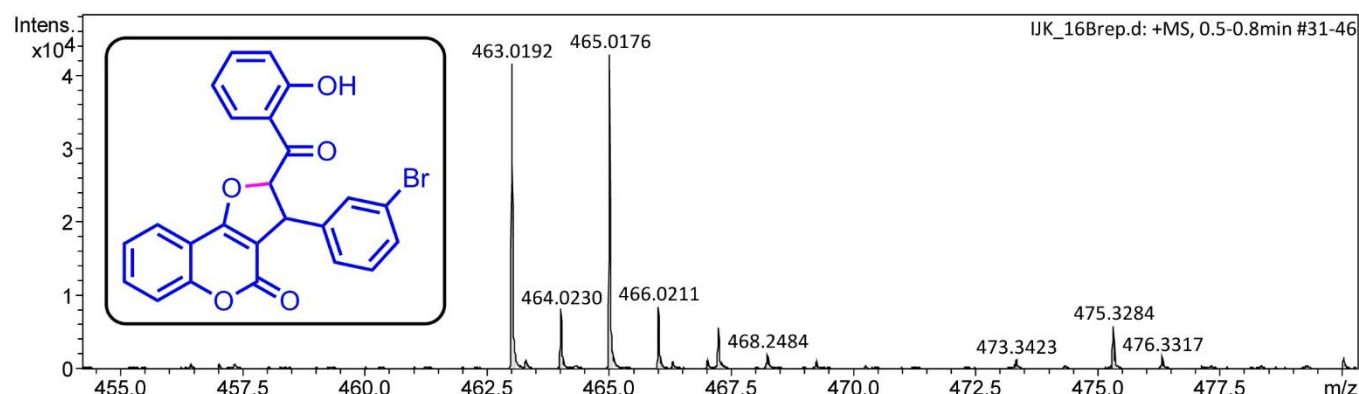
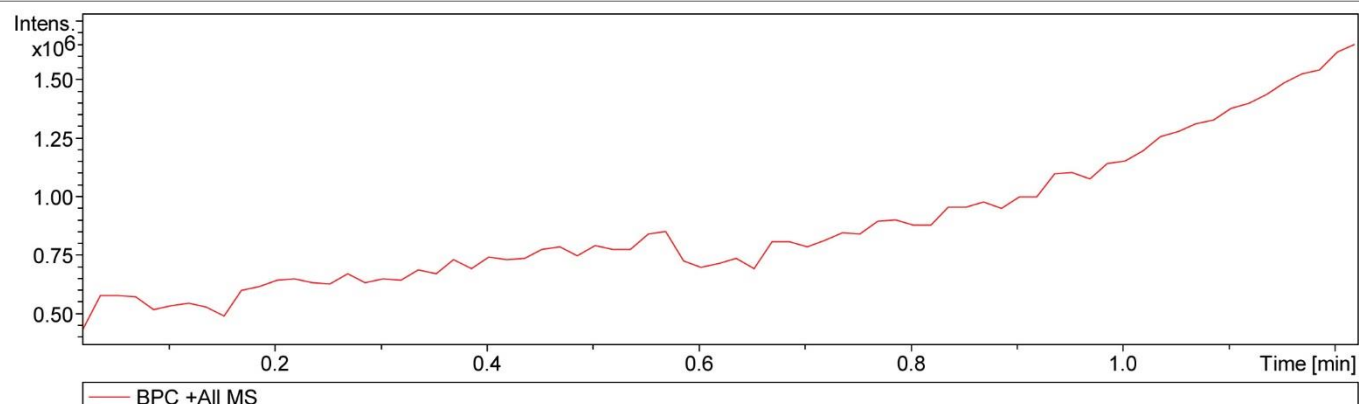


Figure S79. High-resolution Mass spectra of 3-(3-bromophenyl)-2-(2-hydroxybenzoyl)-2,3-dihydro-4*H*-furo[3,2-*c*]chromen-4-one (**2-17**)

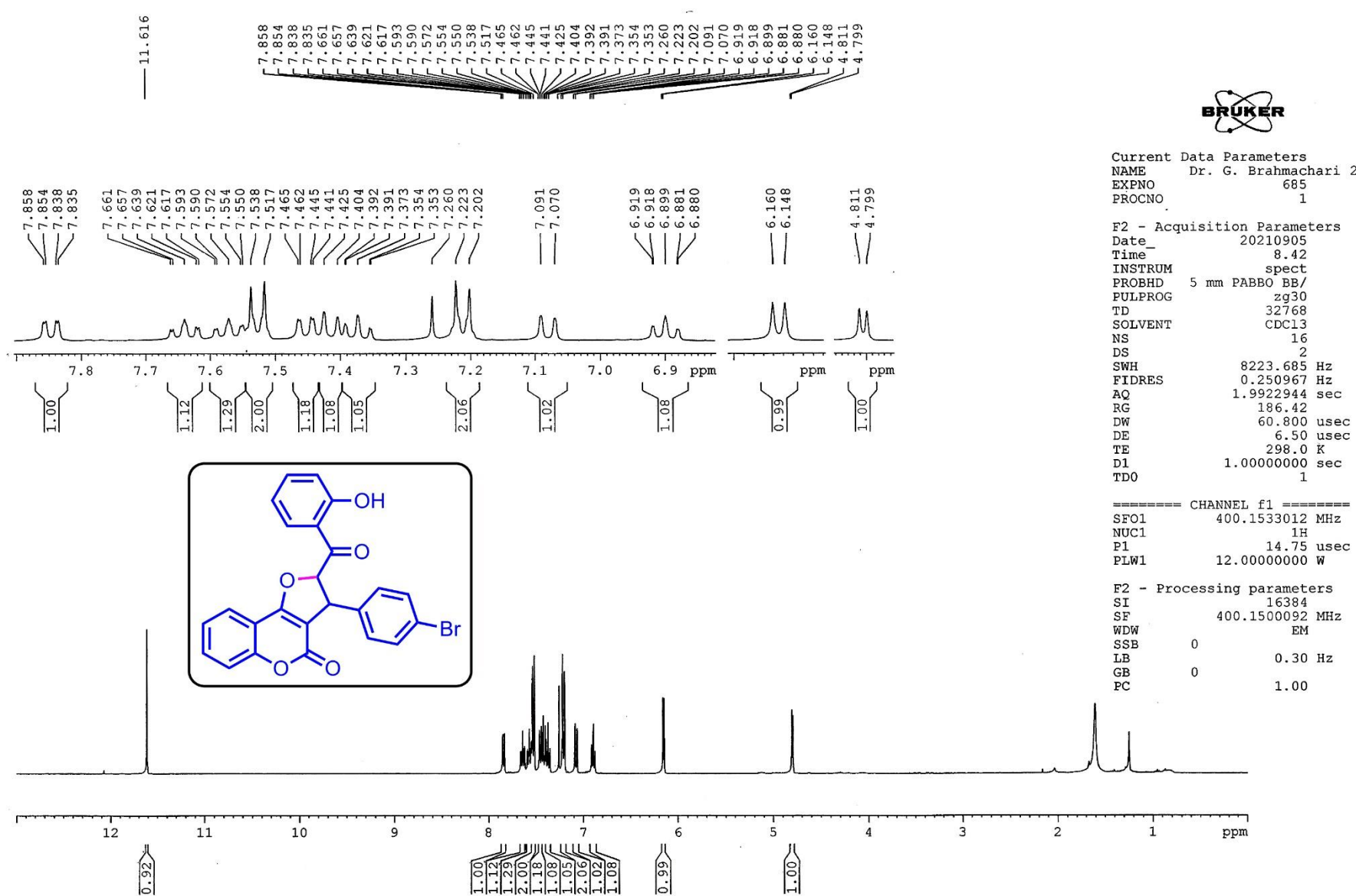


Figure S80. ¹H-NMR spectrum of 3-(4-bromophenyl)-2-(2-hydroxybenzoyl)-2,3-dihydro-4H-furo[3,2-c]chromen-4-one (**2-18**)

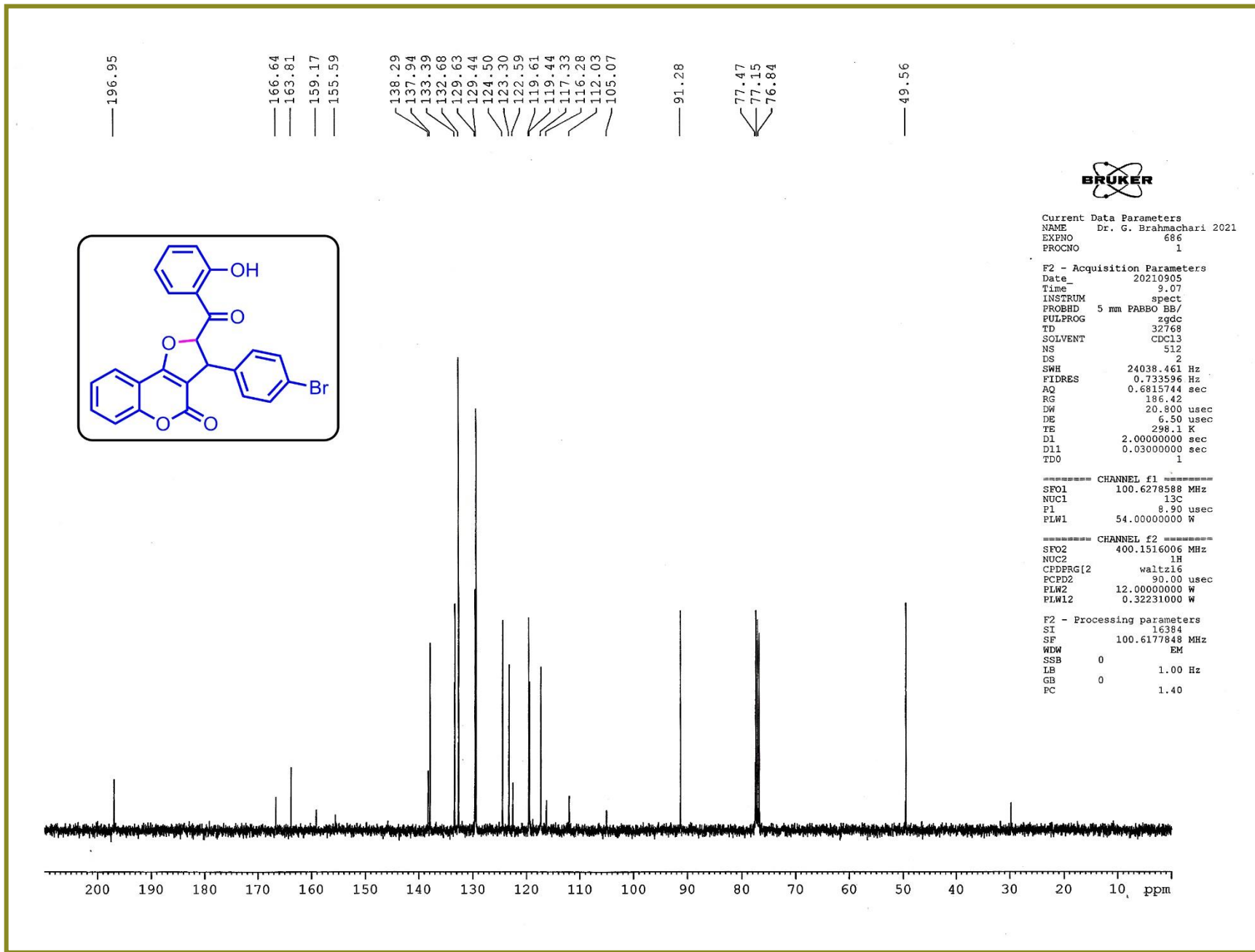


Figure S81. ^{13}C -NMR spectrum of 3-(4-bromophenyl)-2-(2-hydroxybenzoyl)-2,3-dihydro-4*H*-furo[3,2-*c*]chromen-4-one (**2-18**)

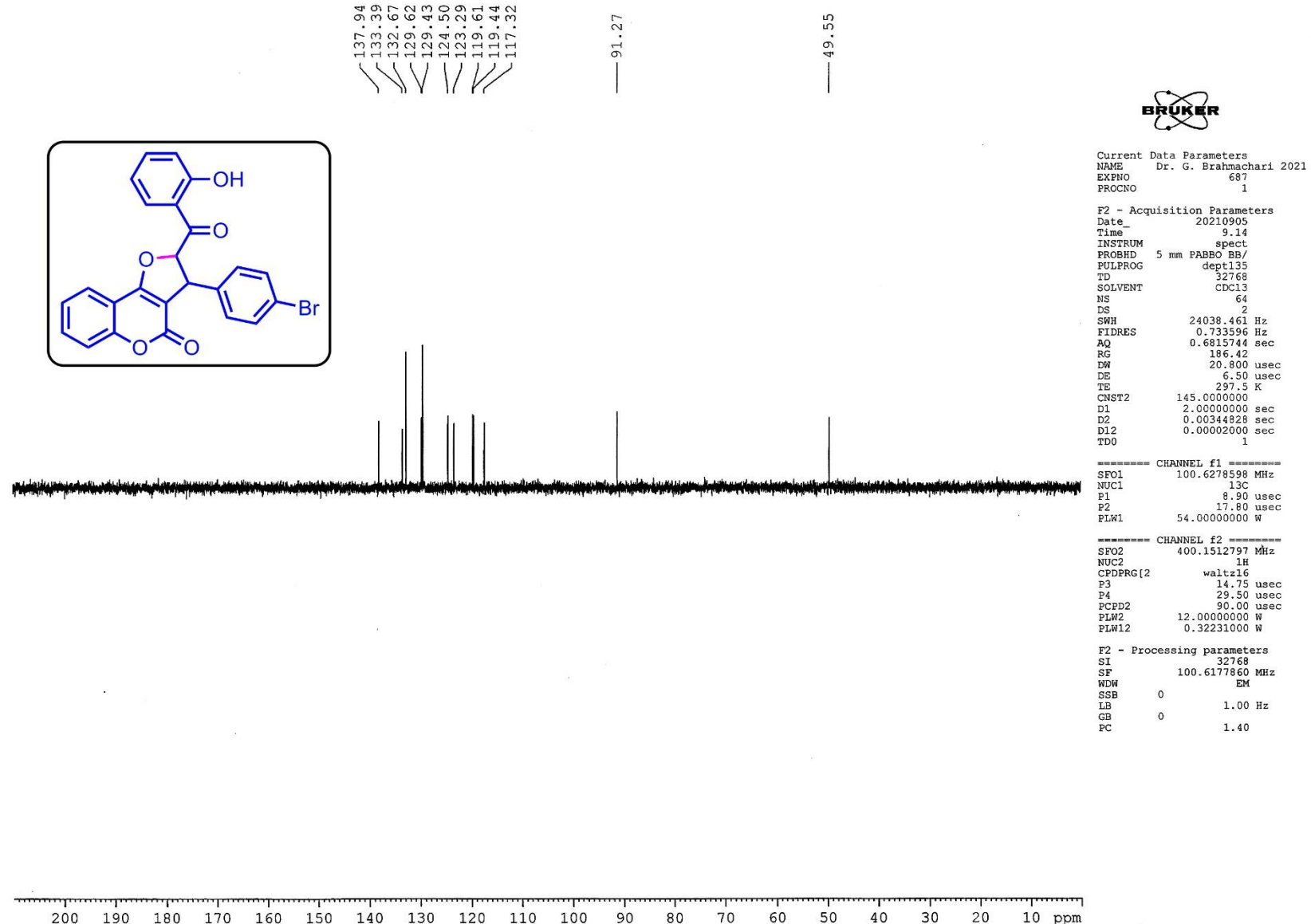


Figure S82. DEPT-135 NMR spectrum of 3-(4-bromophenyl)-2-(2-hydroxybenzoyl)-2,3-dihydro-4*H*-furo[3,2-*c*]chromen-4-one (**2-18**)

Acquisition Parameter

Source Type	ESI	Ion Polarity	Positive	Set Nebulizer	0.4 Bar
Focus	Active	Set Capillary	3400 V	Set Dry Heater	200 °C
Scan Begin	50 m/z	Set End Plate Offset	-500 V	Set Dry Gas	4.0 l/min
Scan End	3000 m/z	Set Charging Voltage	2000 V	Set Divert Valve	Source
		Set Corona	0 nA	Set APCI Heater	0 °C

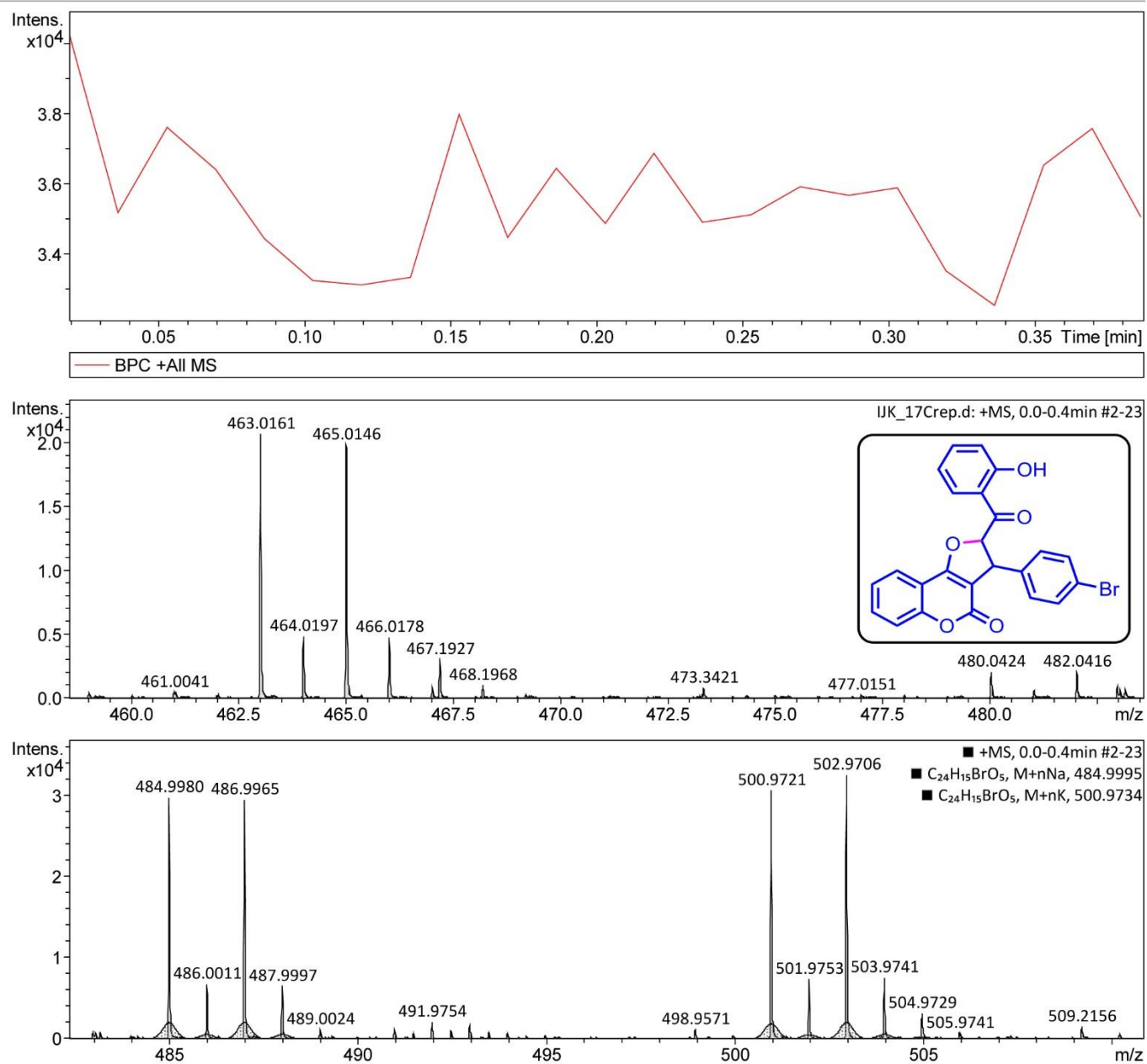


Figure S83. High-resolution Mass spectra of 3-(4-bromophenyl)-2-(2-hydroxybenzoyl)-2,3-dihydro-4H-furo[3,2-c]chromen-4-one (**2-18**)

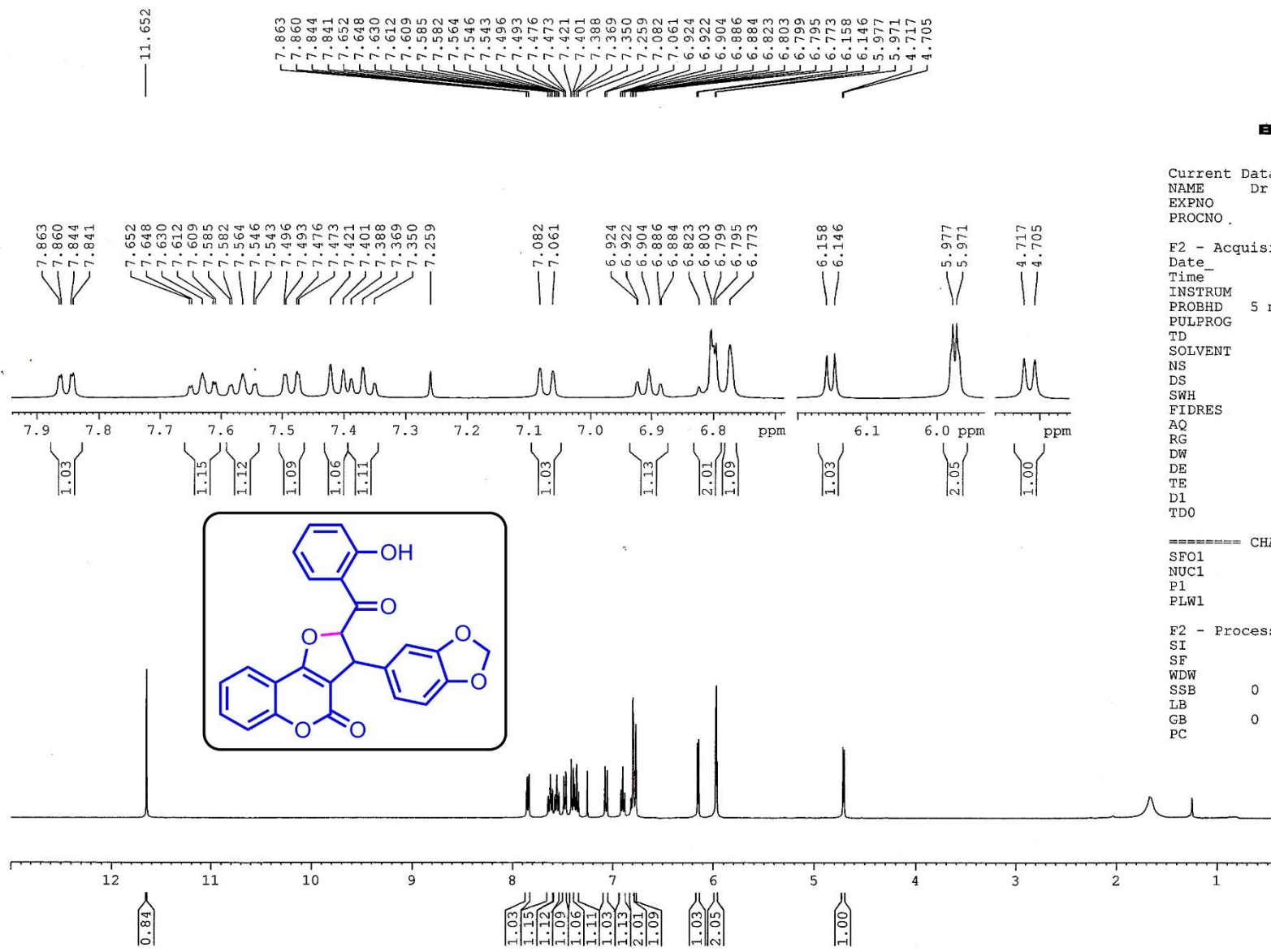


Figure S84. ^1H -NMR spectrum of 3-(benzo[d][1,3]dioxol-5-yl)-2-(2-hydroxybenzoyl)-2,3-dihydro-4*H*-furo[3,2-*c*]chromen-4-one (**2-19**)

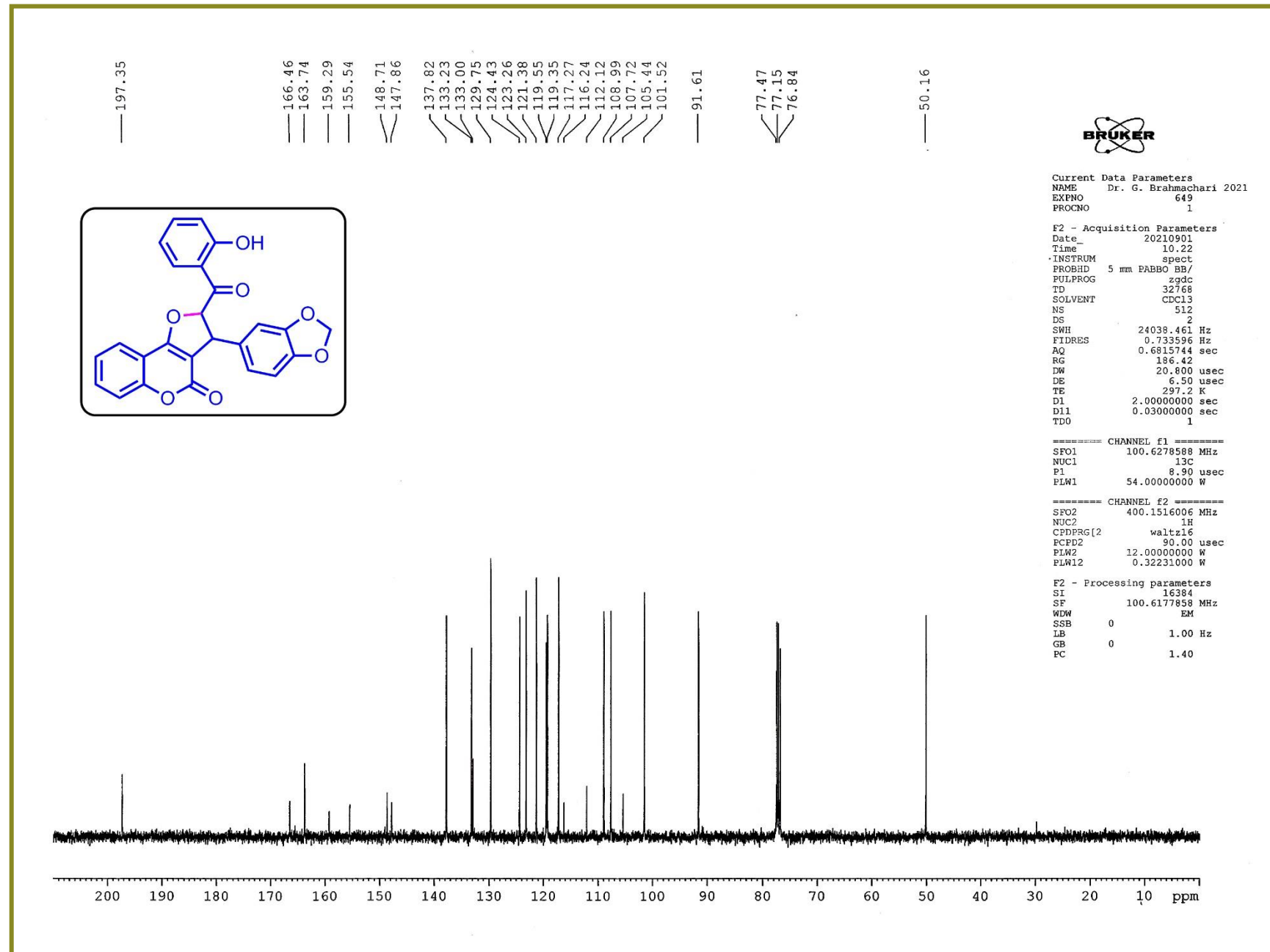


Figure S85. ^{13}C -NMR spectrum of 3-(benzo[d][1,3]dioxol-5-yl)-2-(2-hydroxybenzoyl)-2,3-dihydro-4*H*-furo[3,2-*c*]chromen-4-one (**2-19**)

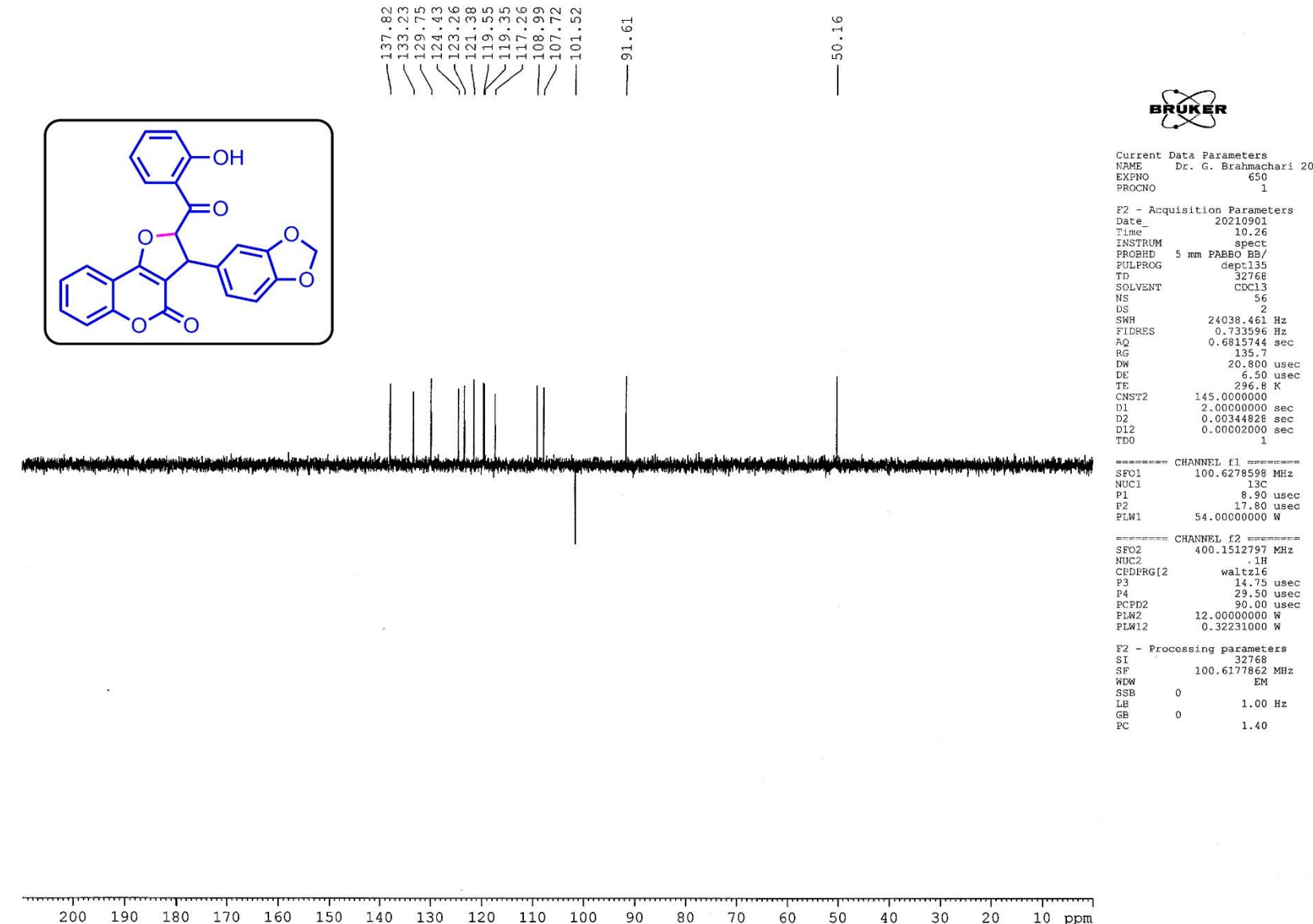


Figure S86. DEPT-135 NMR spectrum of 3-(benzo[d][1,3]dioxol-5-yl)-2-(2-hydroxybenzoyl)-2,3-dihydro-4*H*-furo[3,2-*c*]chromen-4-one (**2-19**)

Acquisition Parameter

Source Type	ESI	Ion Polarity	Positive	Set Nebulizer	0.4 Bar
Focus	Active	Set Capillary	3400 V	Set Dry Heater	200 °C
Scan Begin	50 m/z	Set End Plate Offset	-500 V	Set Dry Gas	4.0 l/min
Scan End	3000 m/z	Set Charging Voltage	2000 V	Set Divert Valve	Source
		Set Corona	0 nA	Set APCI Heater	0 °C

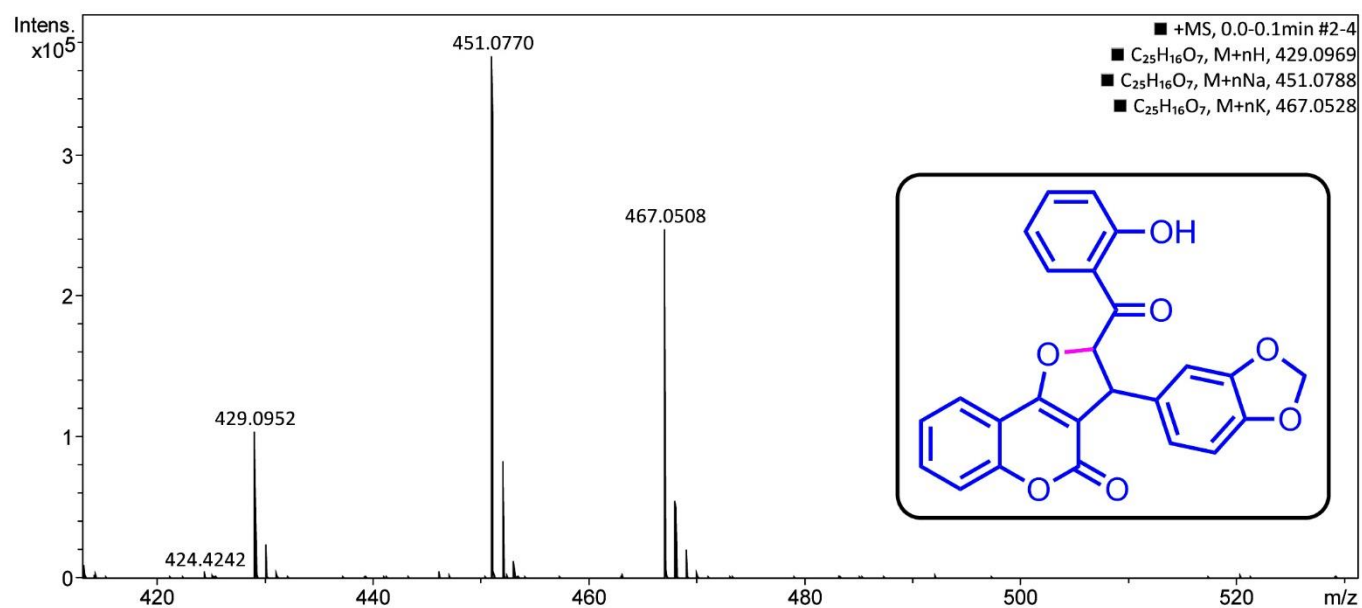
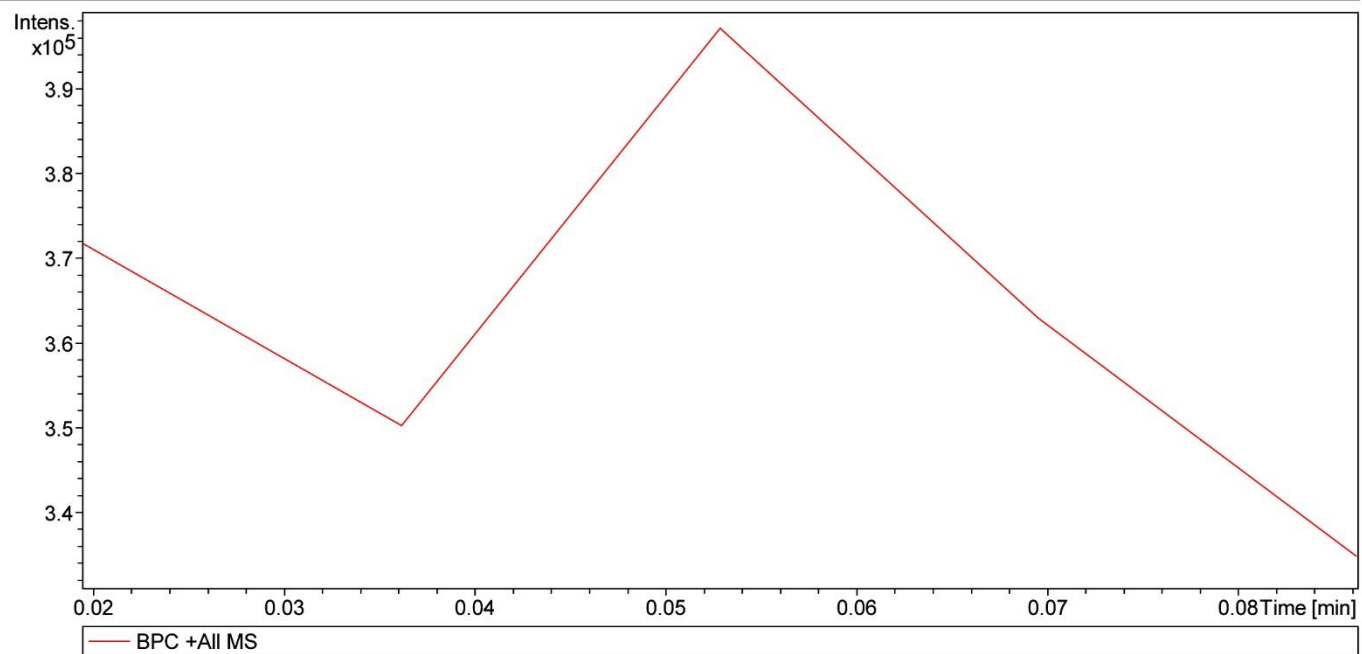


Figure S87. High-resolution Mass spectra of 3-(benzo[d][1,3]dioxol-5-yl)-2-(2-hydroxybenzoyl)-2,3-dihydro-4H-furo[3,2-c]chromen-4-one (**2-19**)

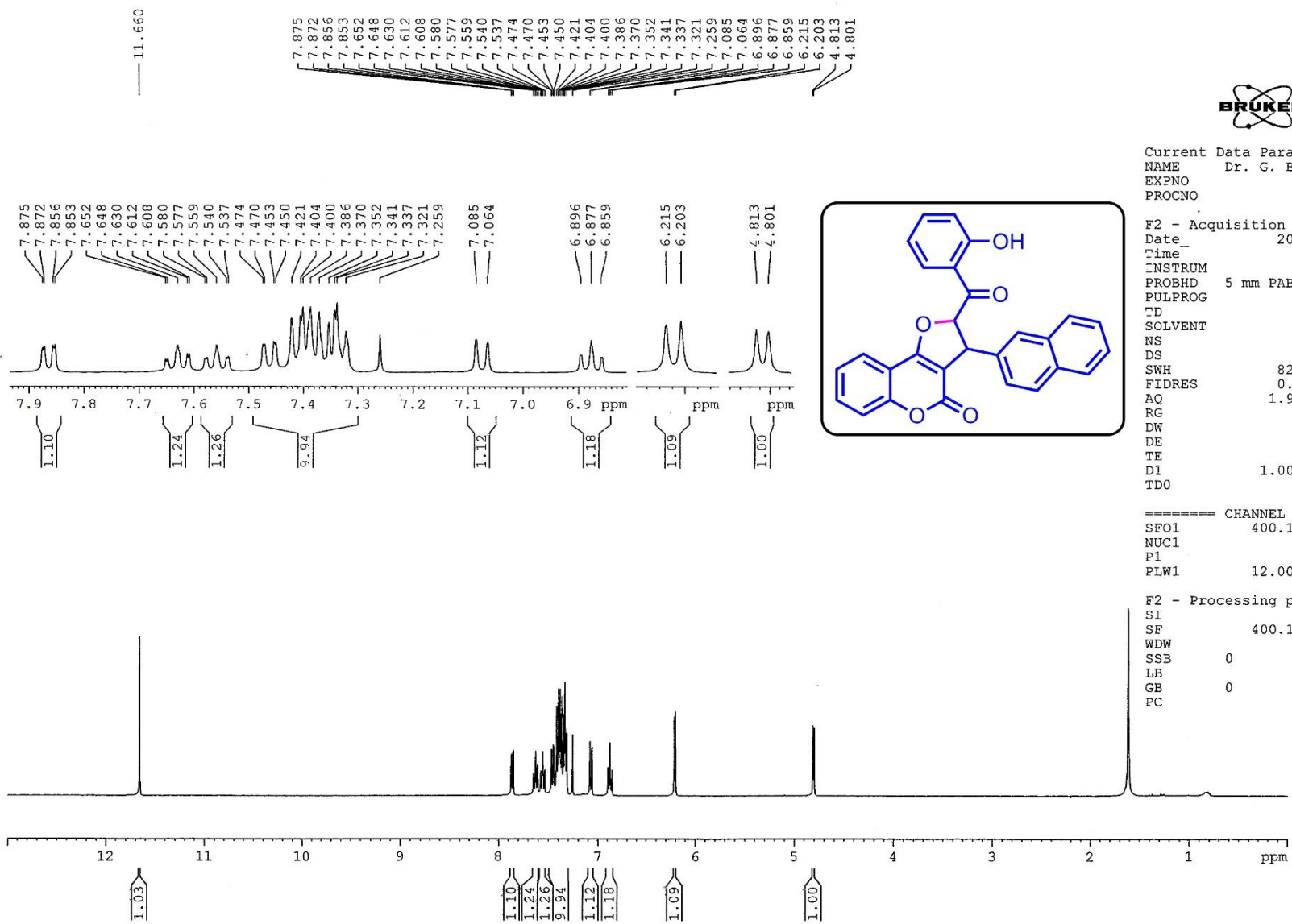


Figure S88. ¹H-NMR spectrum of 2-(2-hydroxybenzoyl)-3-(naphthalen-2-yl)-2,3-dihydro-4*H*-furo[3,2-*c*]chromen-4-one (**2-20**)

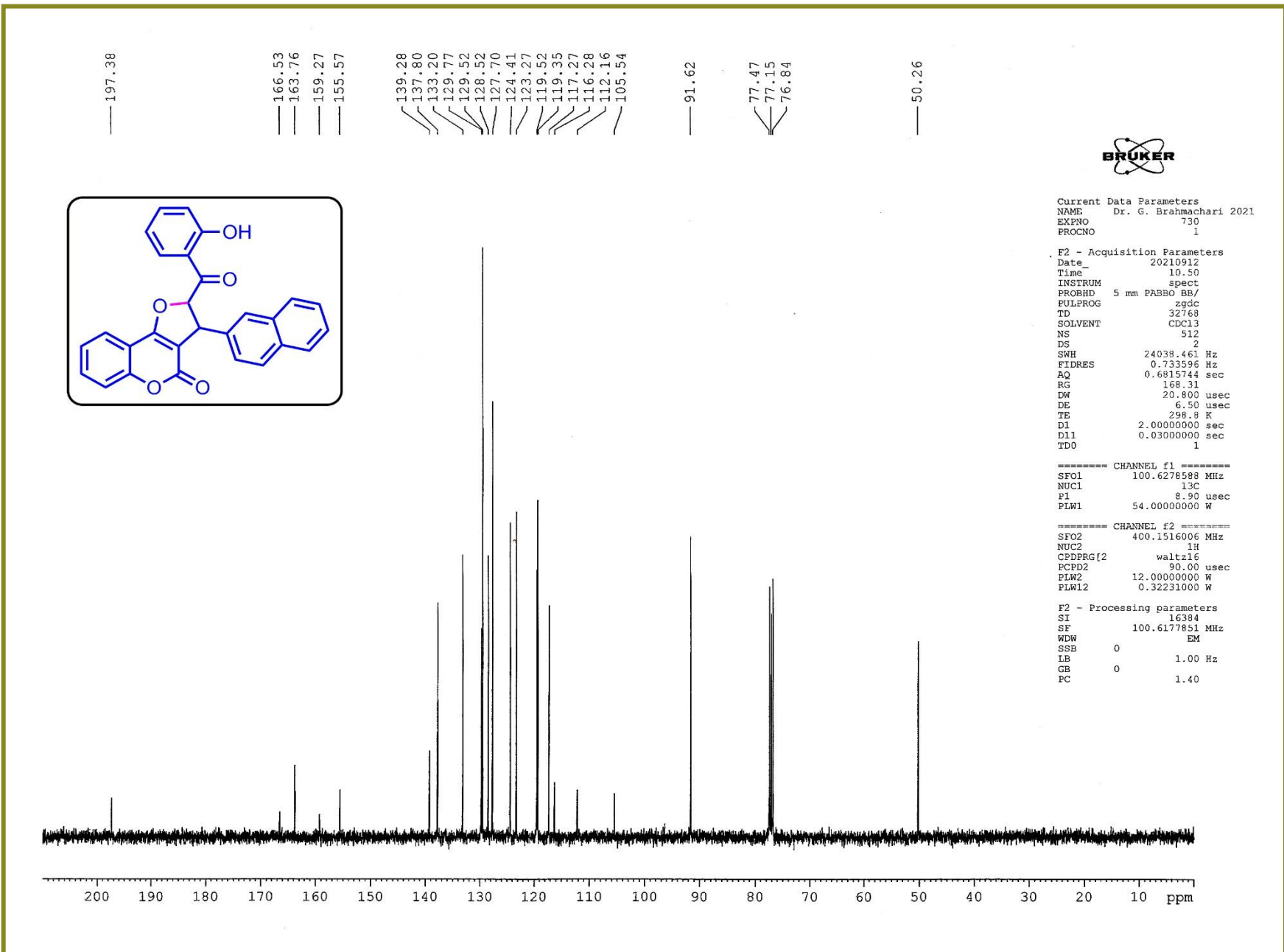


Figure S89. ¹³C-NMR spectrum of 2-(2-hydroxybenzoyl)-3-(naphthalen-2-yl)-2,3-dihydro-4H-furo[3,2-c]chromen-4-one (**2-20**)

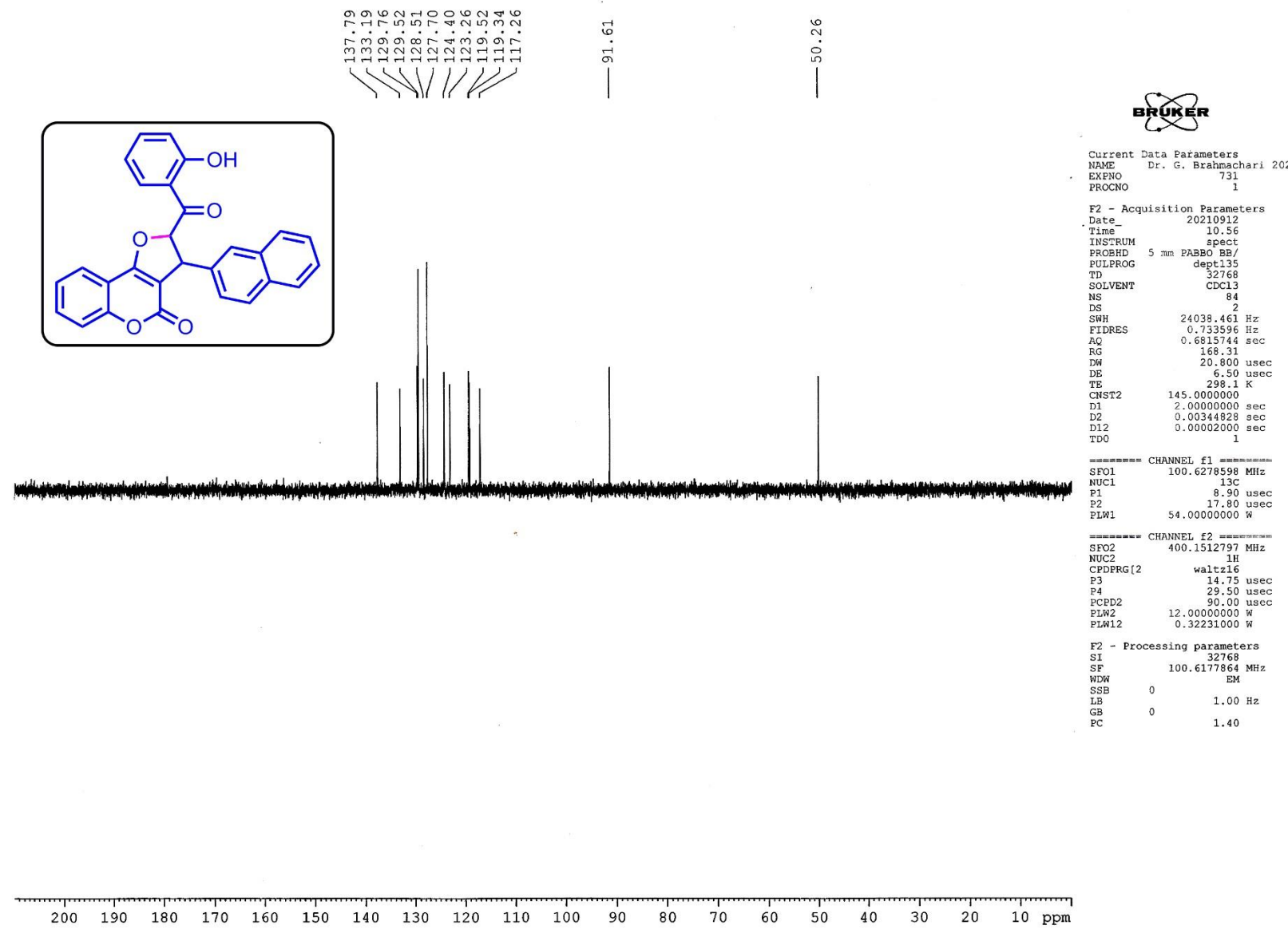


Figure S90. DEPT-135 NMR spectrum of 2-(2-hydroxybenzoyl)-3-(naphthalen-2-yl)-2,3-dihydro-4*H*-furo[3,2-*c*]chromen-4-one (**2-20**)

Acquisition Parameter

Source Type	ESI	Ion Polarity	Positive	Set Nebulizer	0.4 Bar
Focus	Active	Set Capillary	3400 V	Set Dry Heater	200 °C
Scan Begin	50 m/z	Set End Plate Offset	-500 V	Set Dry Gas	4.0 l/min
Scan End	3000 m/z	Set Charging Voltage	2000 V	Set Divert Valve	Source
		Set Corona	0 nA	Set APCI Heater	0 °C

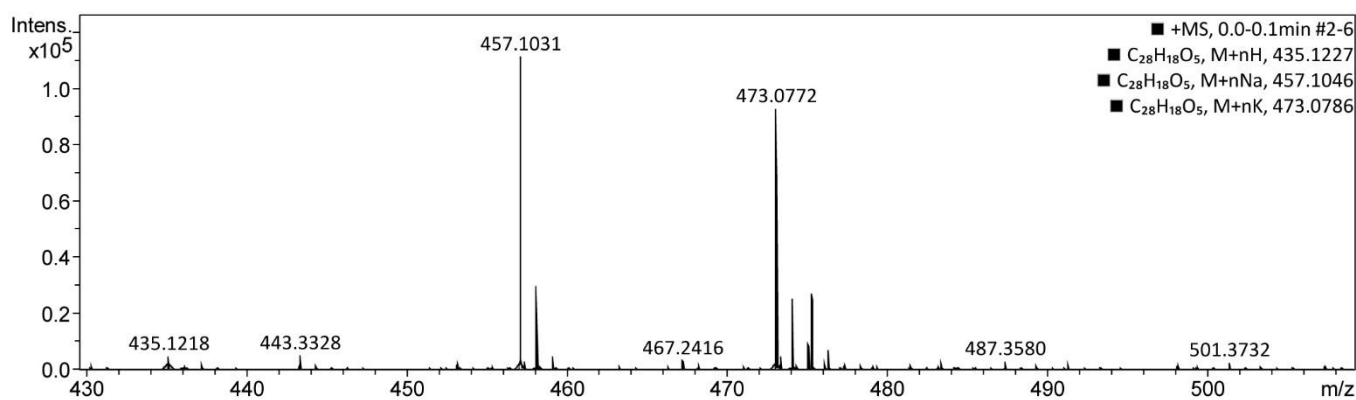
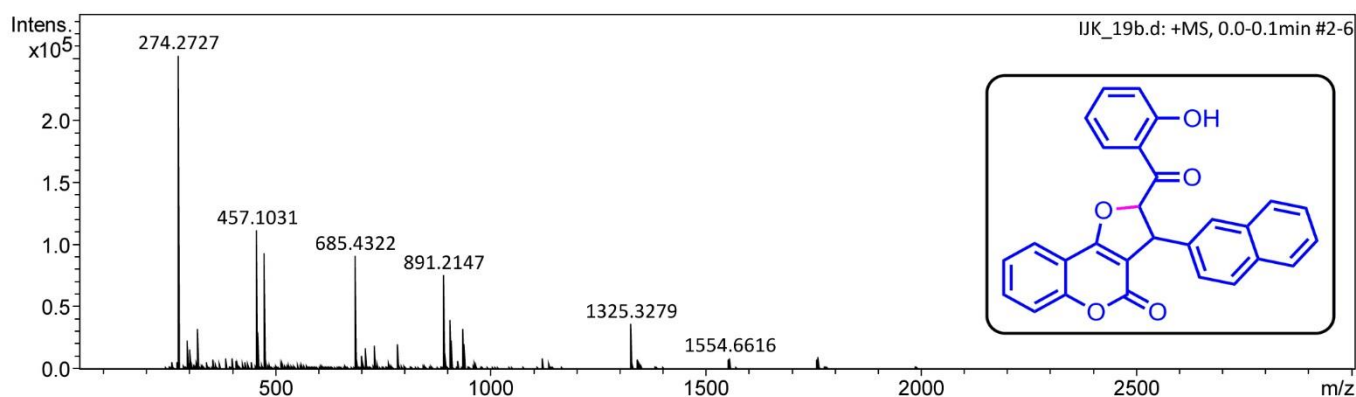
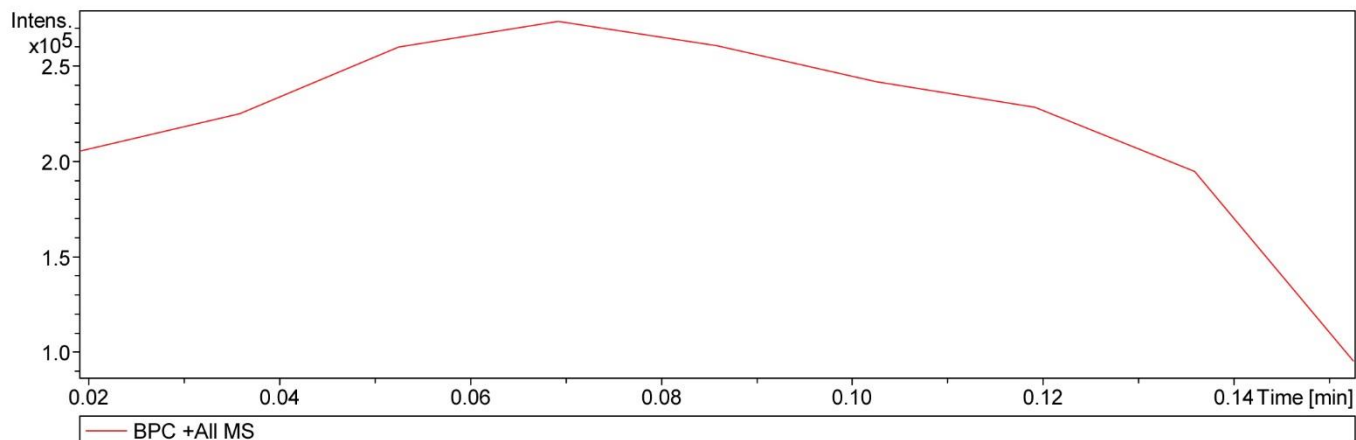


Figure S91. High-resolution Mass spectra of 2-(2-hydroxybenzoyl)-3-(naphthalen-2-yl)-2,3-dihydro-4H-furo[3,2-c]chromen-4-one (**2-20**)

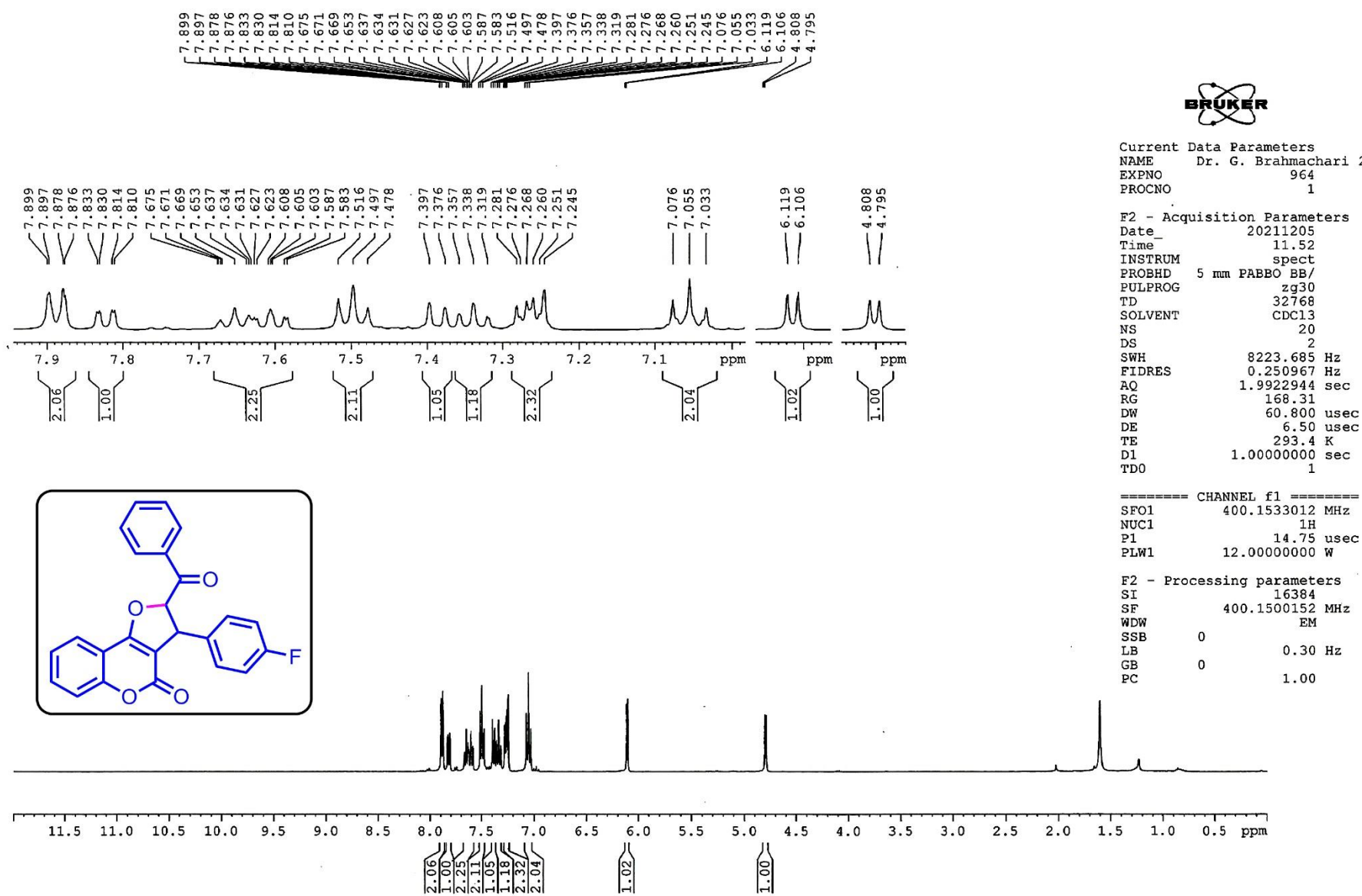


Figure S92. ¹H-NMR spectrum of 2-benzoyl-3-(4-fluorophenyl)-2,3-dihydro-4H-furo[3,2-c]chromen-4-one (**2-21**)

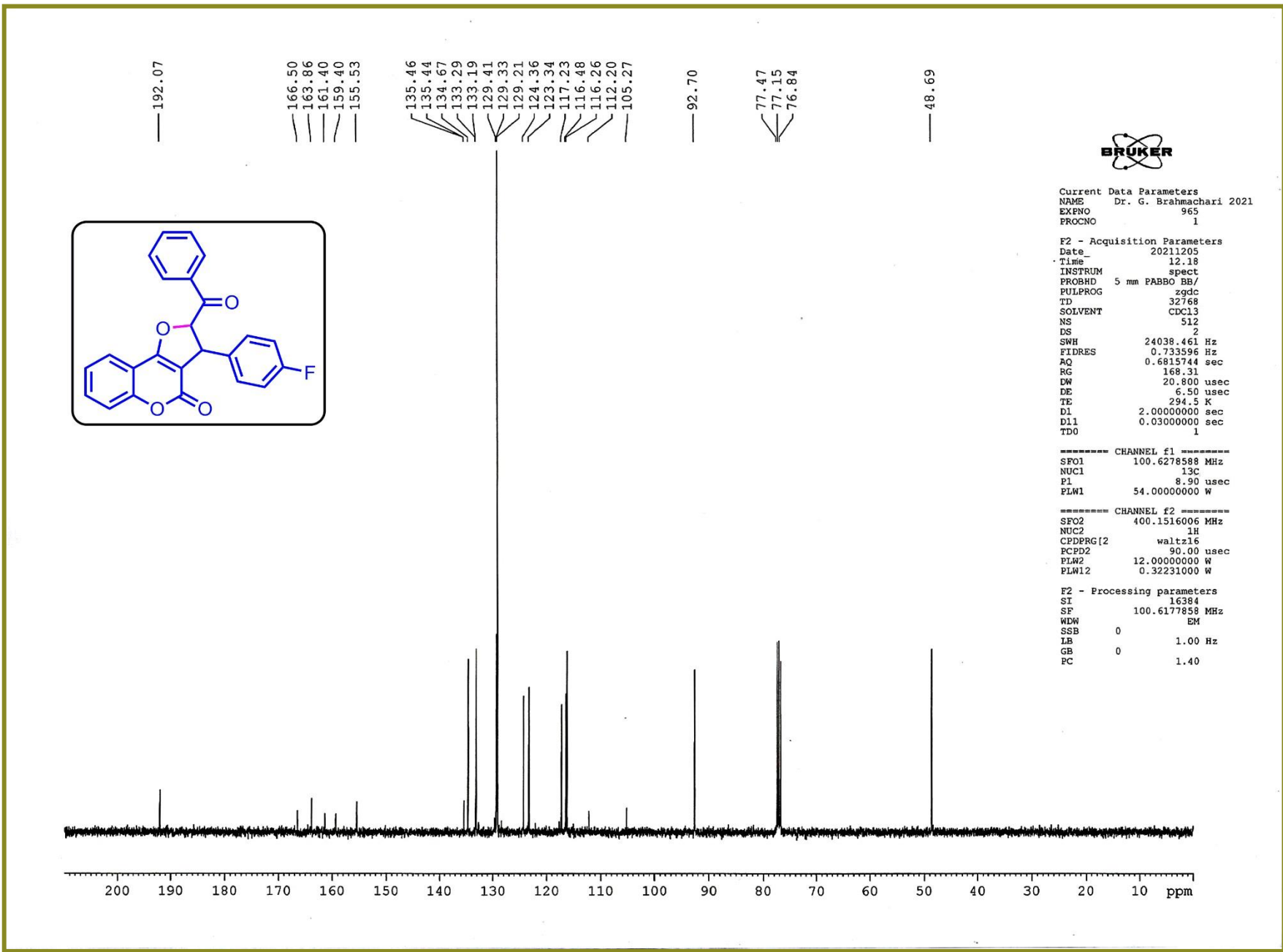


Figure S93. ¹³C-NMR spectrum of 2-benzoyl-3-(4-fluorophenyl)-2,3-dihydro-4H-furo[3,2-c]chromen-4-one (**2-21**)

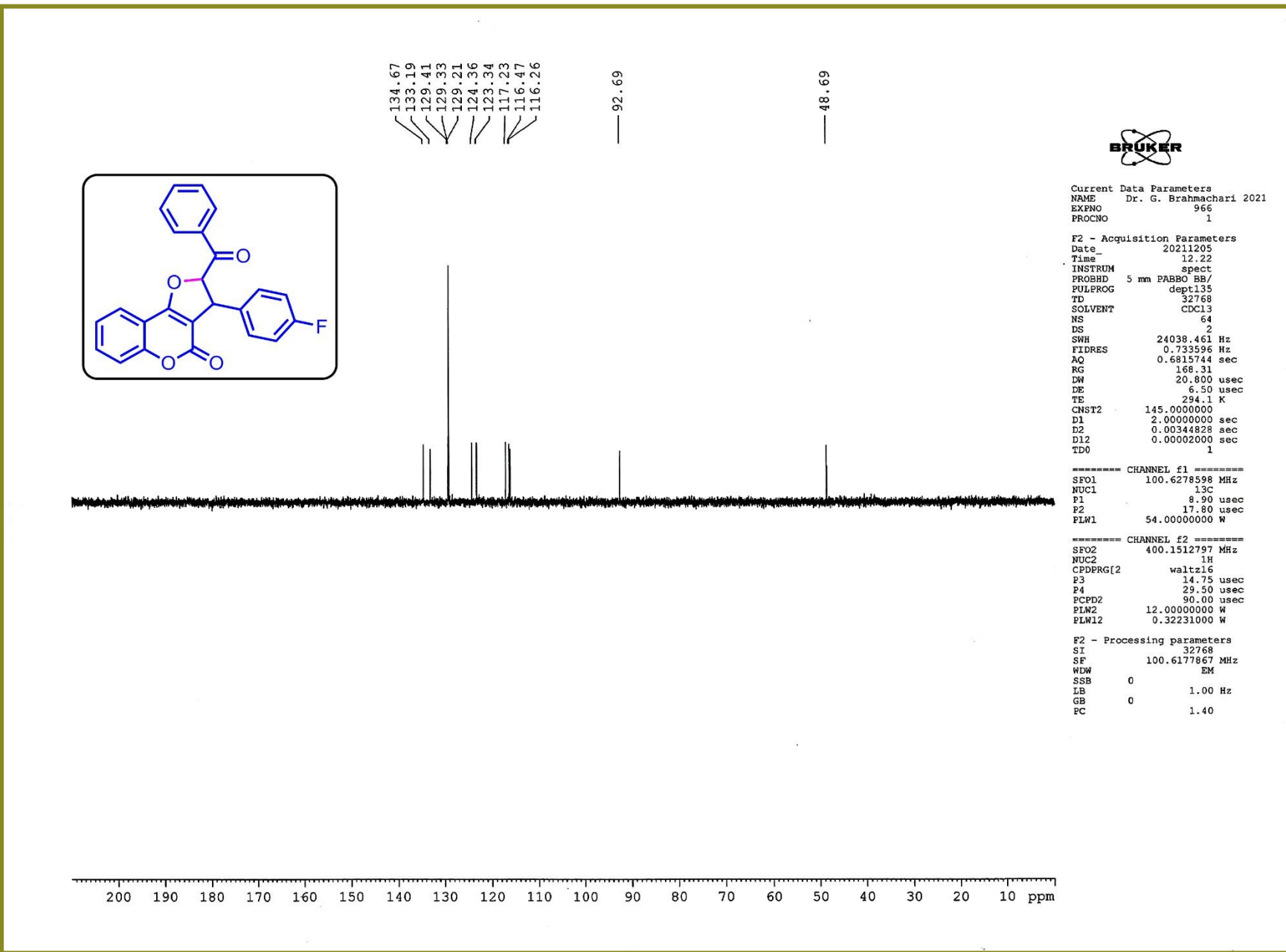


Figure S94. DEPT-135 NMR spectrum of 2-benzoyl-3-(4-fluorophenyl)-2,3-dihydro-4H-furo[3,2-c]chromen-4-one (**2-21**)

Acquisition Parameter

Source Type	ESI	Ion Polarity	Positive	Set Nebulizer	0.4 Bar
Focus	Active	Set Capillary	3400 V	Set Dry Heater	200 °C
Scan Begin	50 m/z	Set End Plate Offset	-500 V	Set Dry Gas	4.0 l/min
Scan End	3000 m/z	Set Charging Voltage	2000 V	Set Divert Valve	Source
		Set Corona	0 nA	Set APCI Heater	0 °C

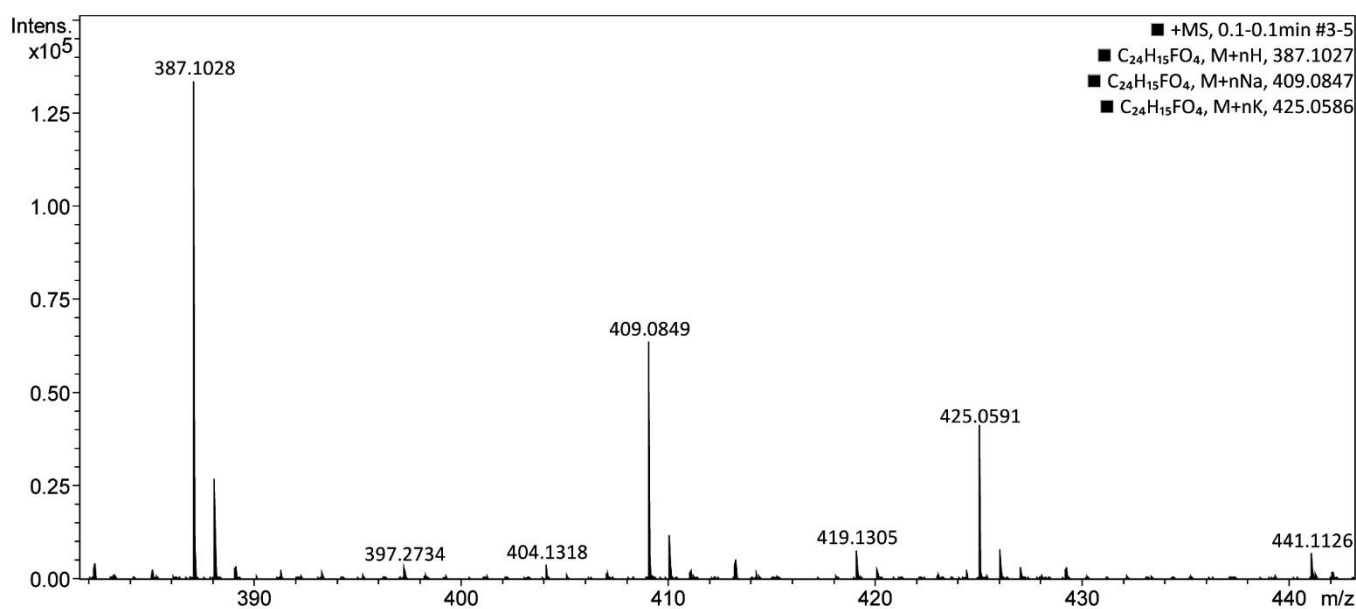
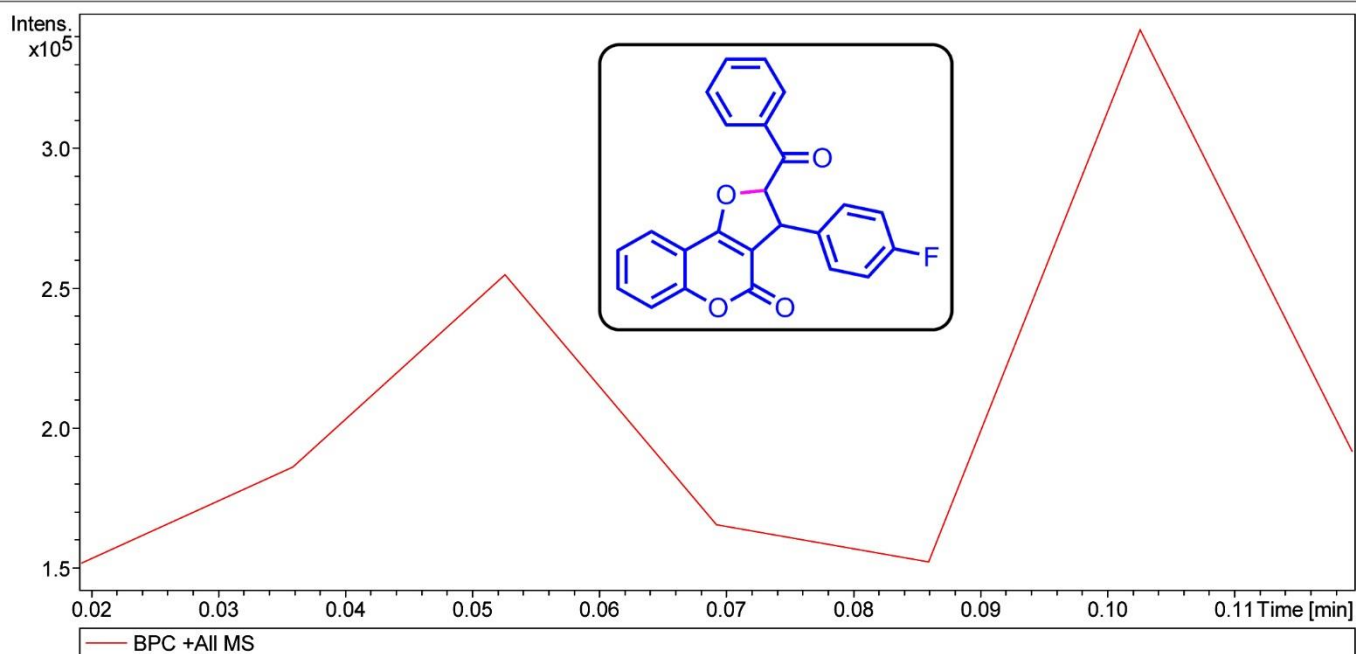


Figure S95. High-resolution Mass spectra of 2-benzoyl-3-(4-fluorophenyl)-2,3-dihydro-4H-furo[3,2-c]chromen-4-one (**2-21**)

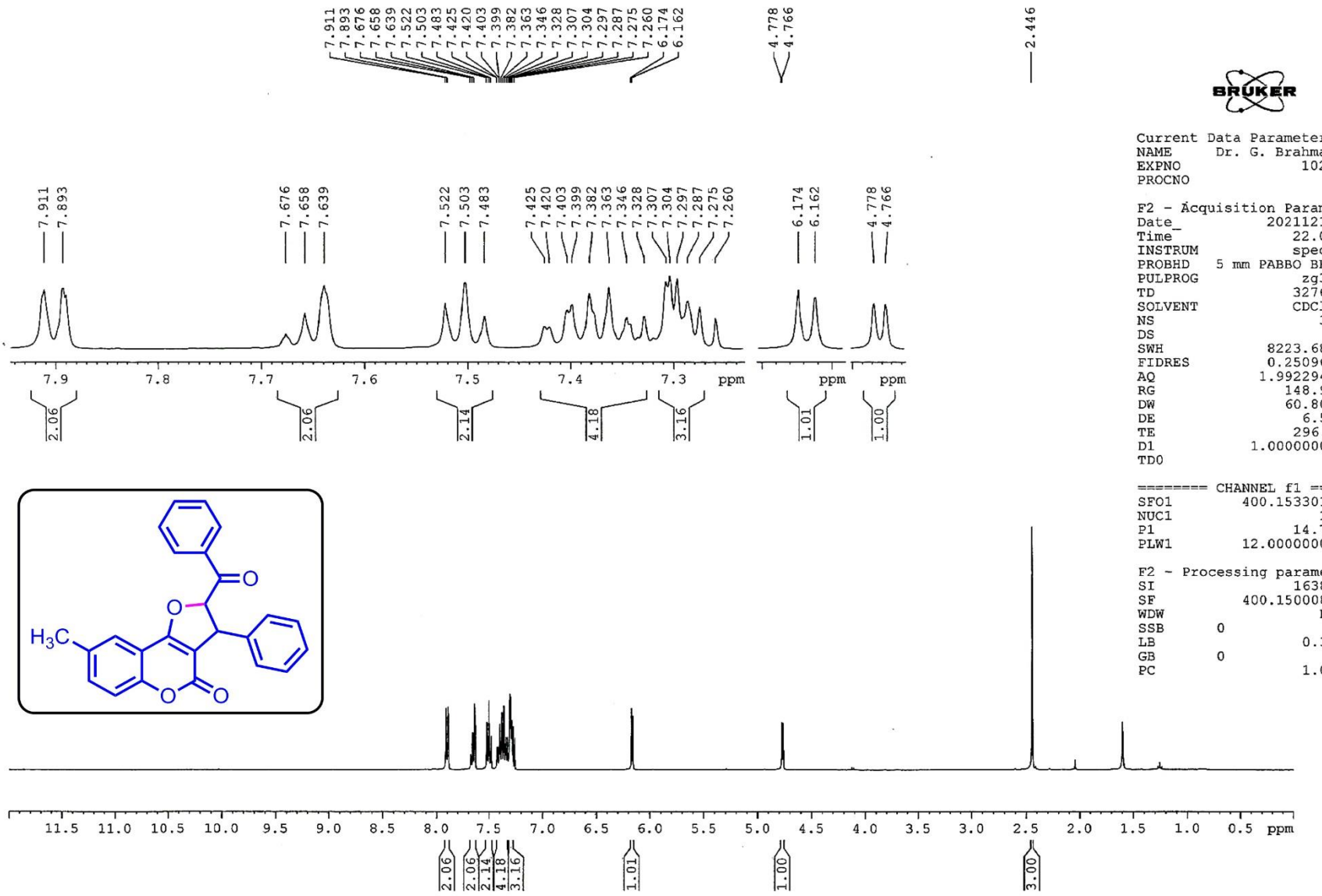


Figure S96. ^1H -NMR spectrum of 2-benzoyl-8-methyl-3-phenyl-2,3-dihydro-4*H*-furo[3,2-*c*]chromen-4-one (2-22)

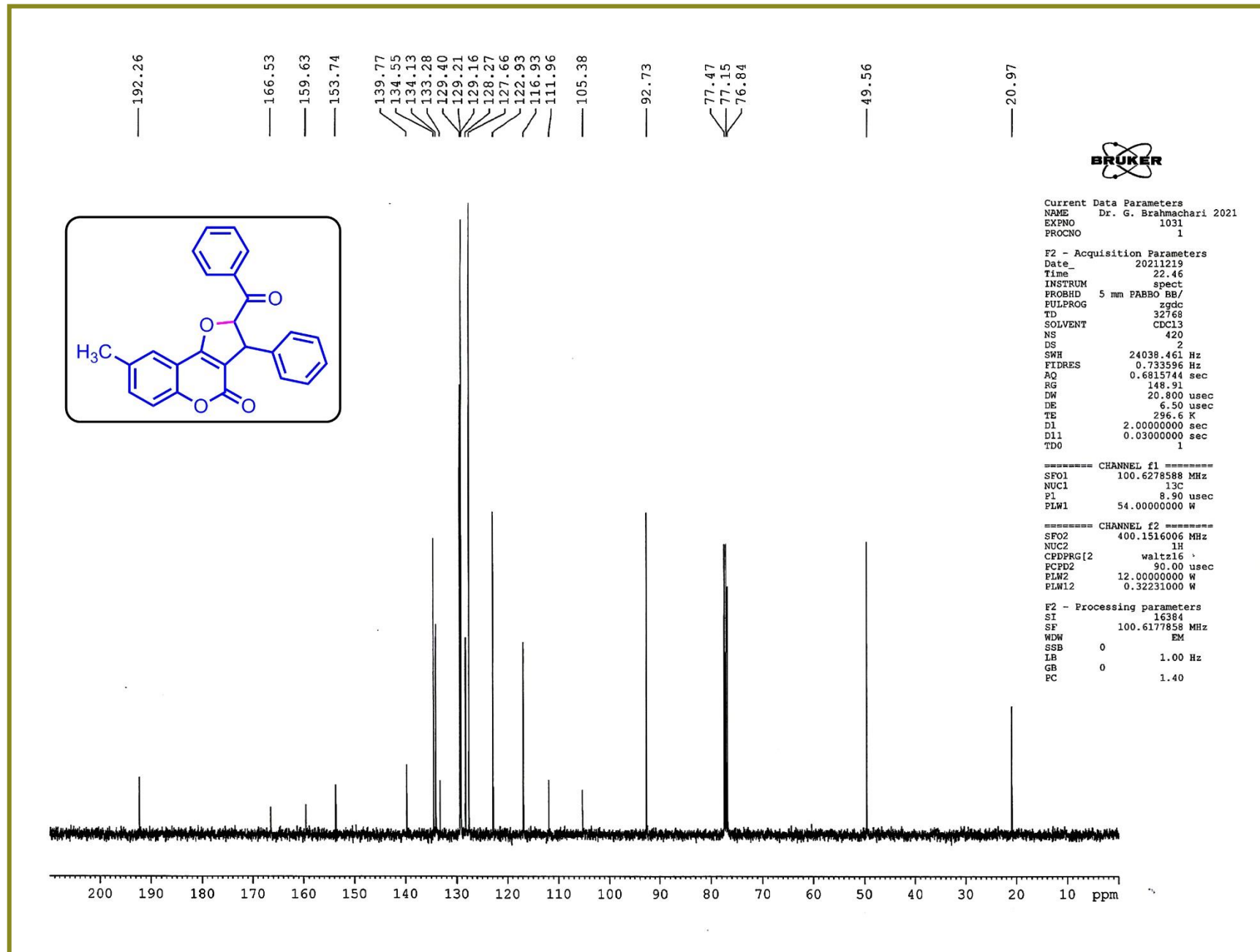


Figure S97. ¹³C-NMR spectrum of 2-benzoyl-8-methyl-3-phenyl-2,3-dihydro-4H-furo[3,2-c]chromen-4-one (**2-22**)

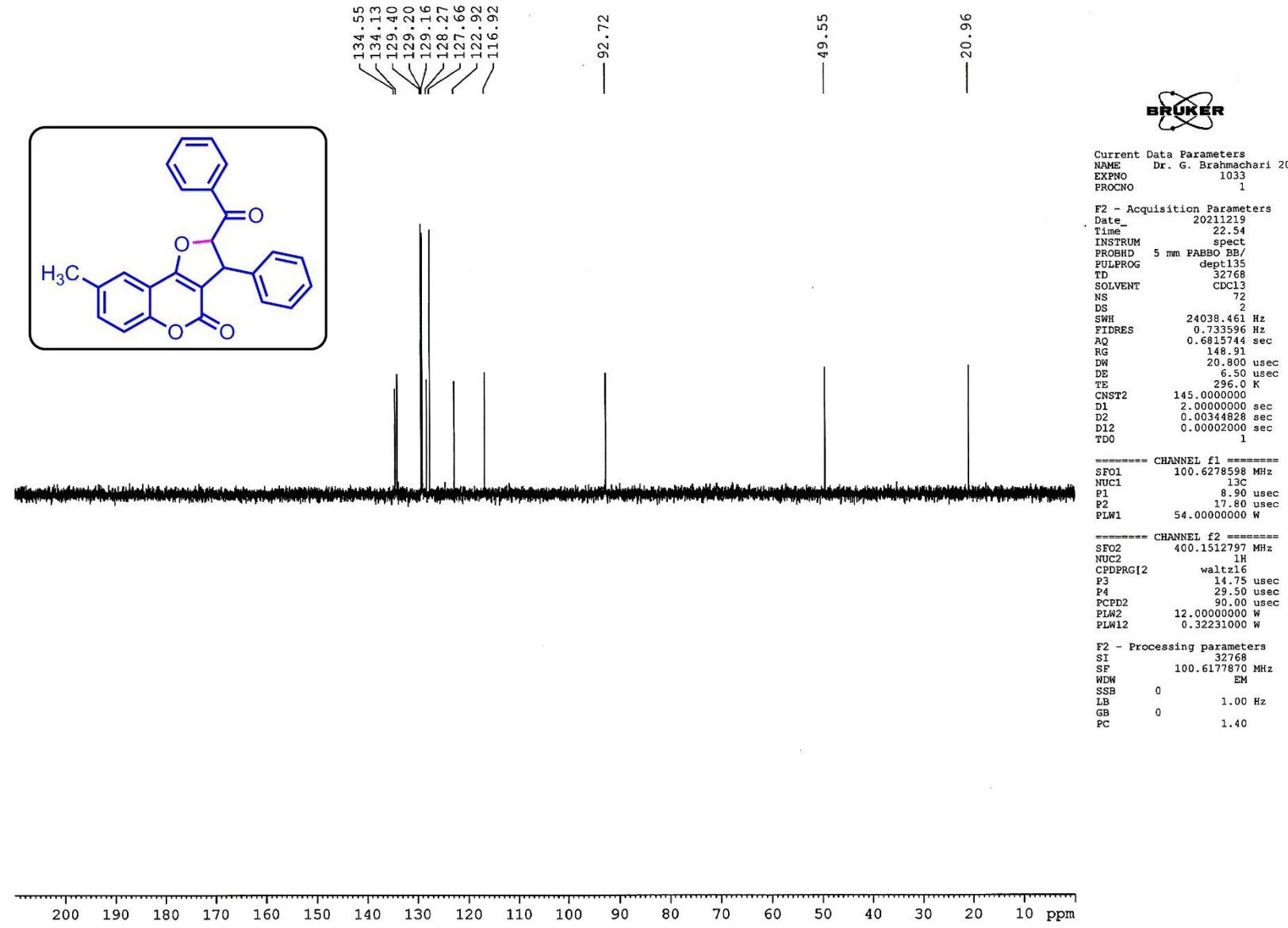


Figure S98. DEPT-135 NMR spectrum of 2-benzoyl-8-methyl-3-phenyl-2,3-dihydro-4H-furo[3,2-c]chromen-4-one (**2-22**)

Acquisition Parameter

Source Type	ESI	Ion Polarity	Positive	Set Nebulizer	0.4 Bar
Focus	Active	Set Capillary	3400 V	Set Dry Heater	200 °C
Scan Begin	50 m/z	Set End Plate Offset	-500 V	Set Dry Gas	4.0 l/min
Scan End	3000 m/z	Set Charging Voltage	2000 V	Set Divert Valve	Source
		Set Corona	0 nA	Set APCI Heater	0 °C

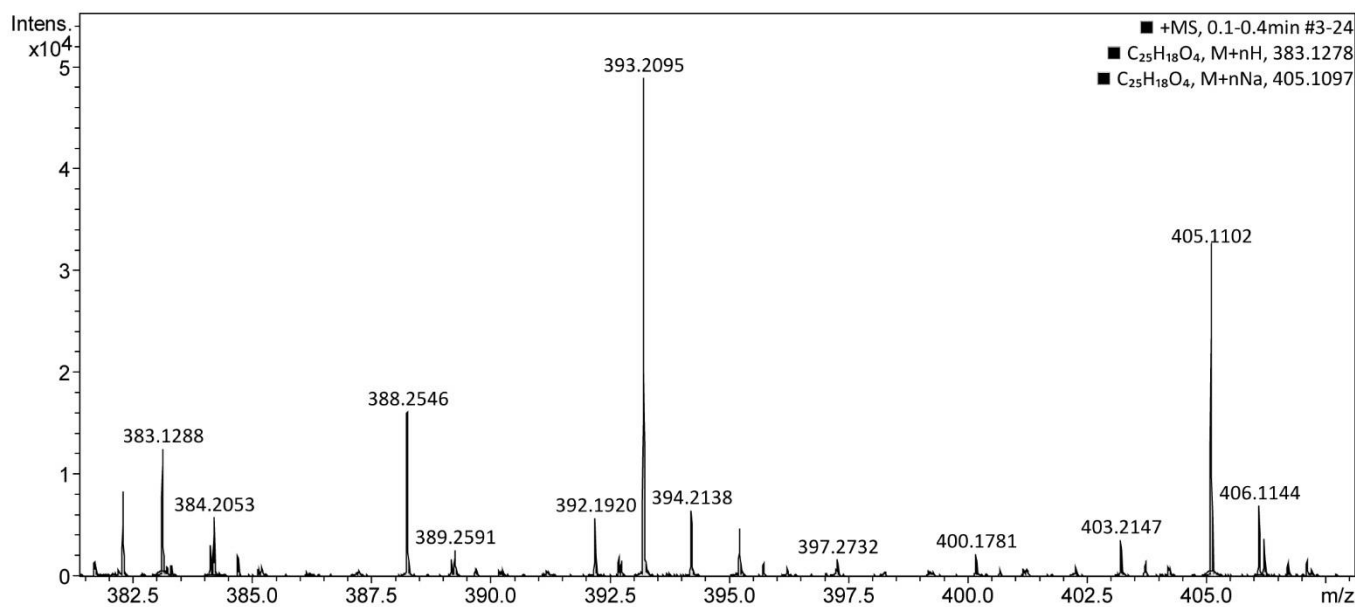
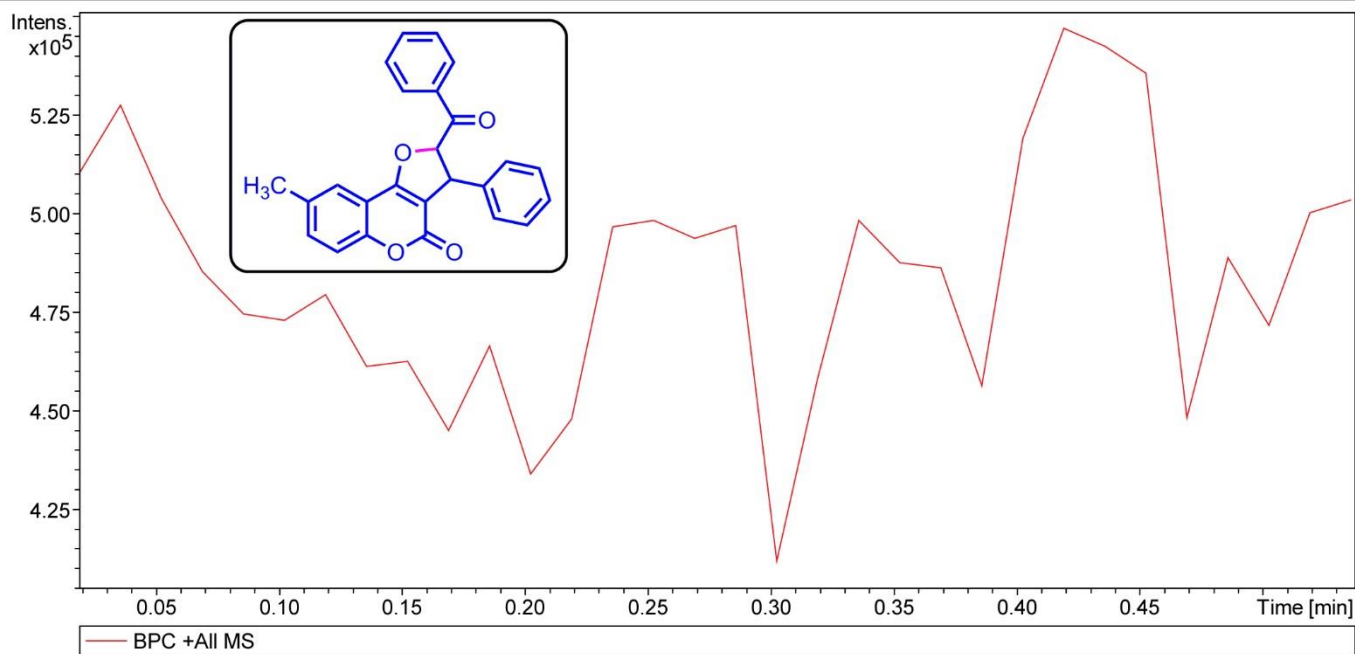


Figure S99. High-resolution Mass spectra of 2-benzoyl-8-methyl-3-phenyl-2,3-dihydro-4H-furo[3,2-c]chromen-4-one (2-22)

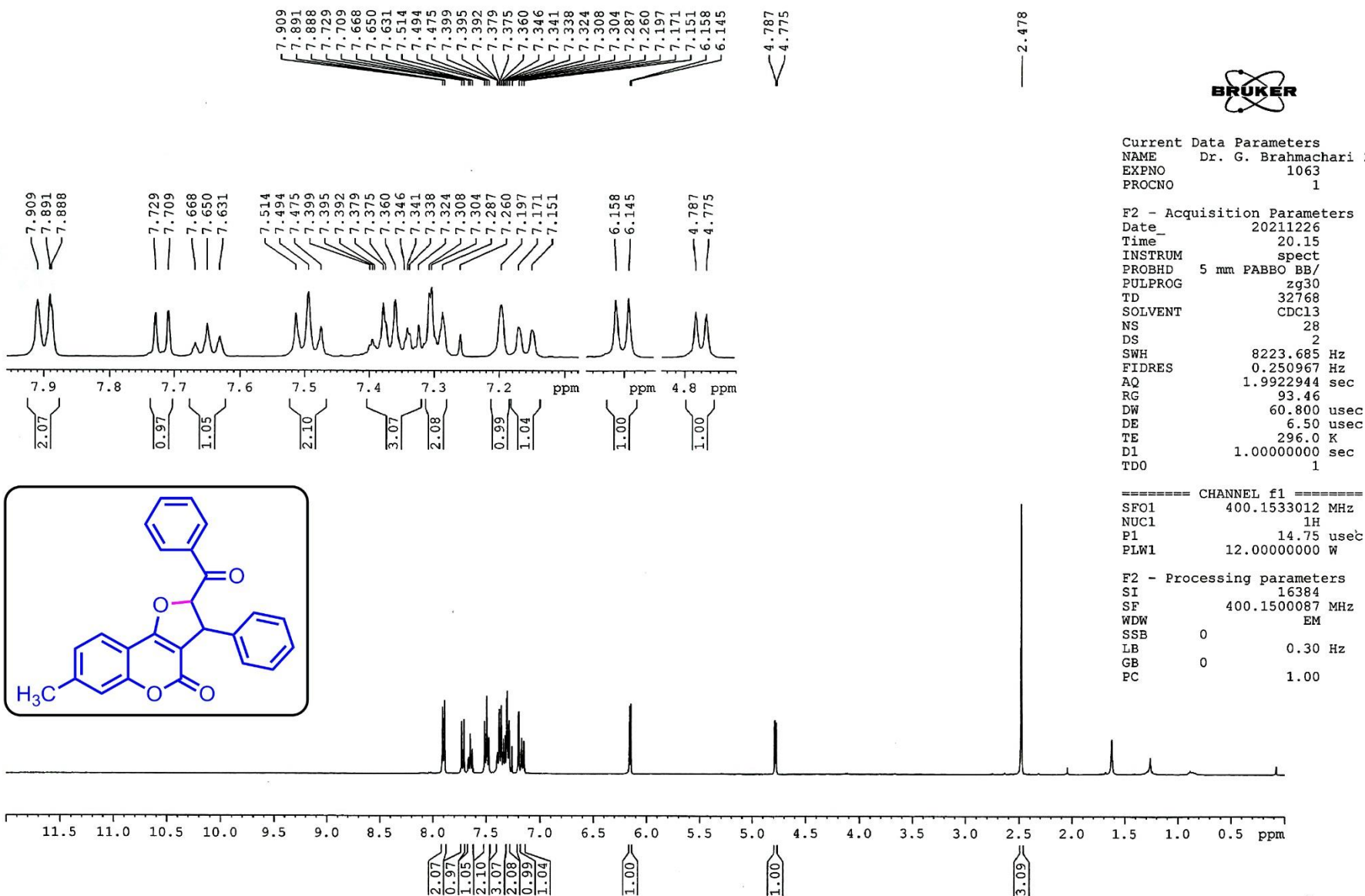


Figure S100. ¹H-NMR spectrum of 2-benzoyl-7-methyl-3-phenyl-2,3-dihydro-4*H*-furo[3,2-*c*]chromen-4-one (2-23)

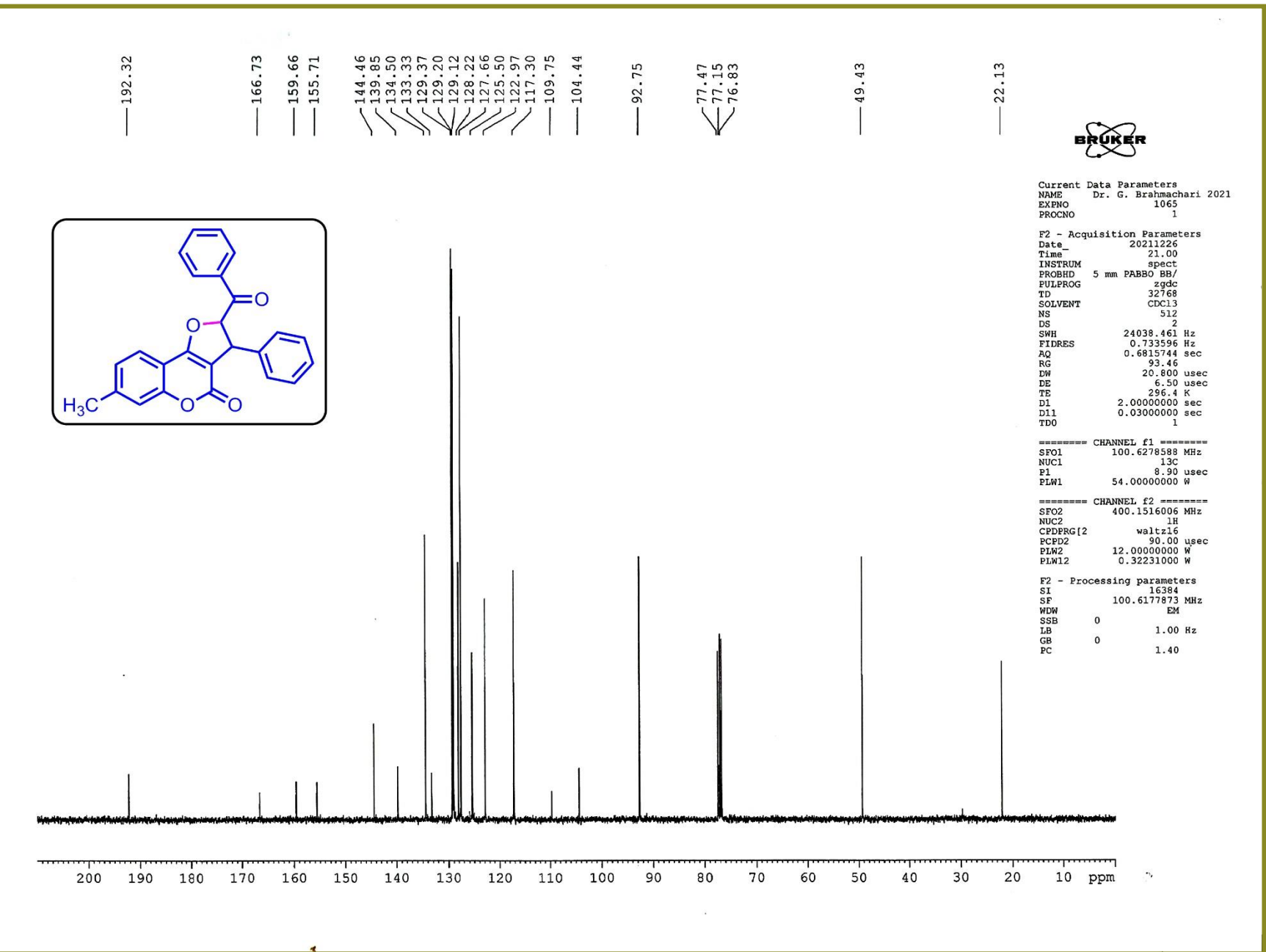


Figure S101. ¹³C-NMR spectrum of 2-benzoyl-7-methyl-3-phenyl-2,3-dihydro-4H-furo[3,2-c]chromen-4-one (**2-23**)

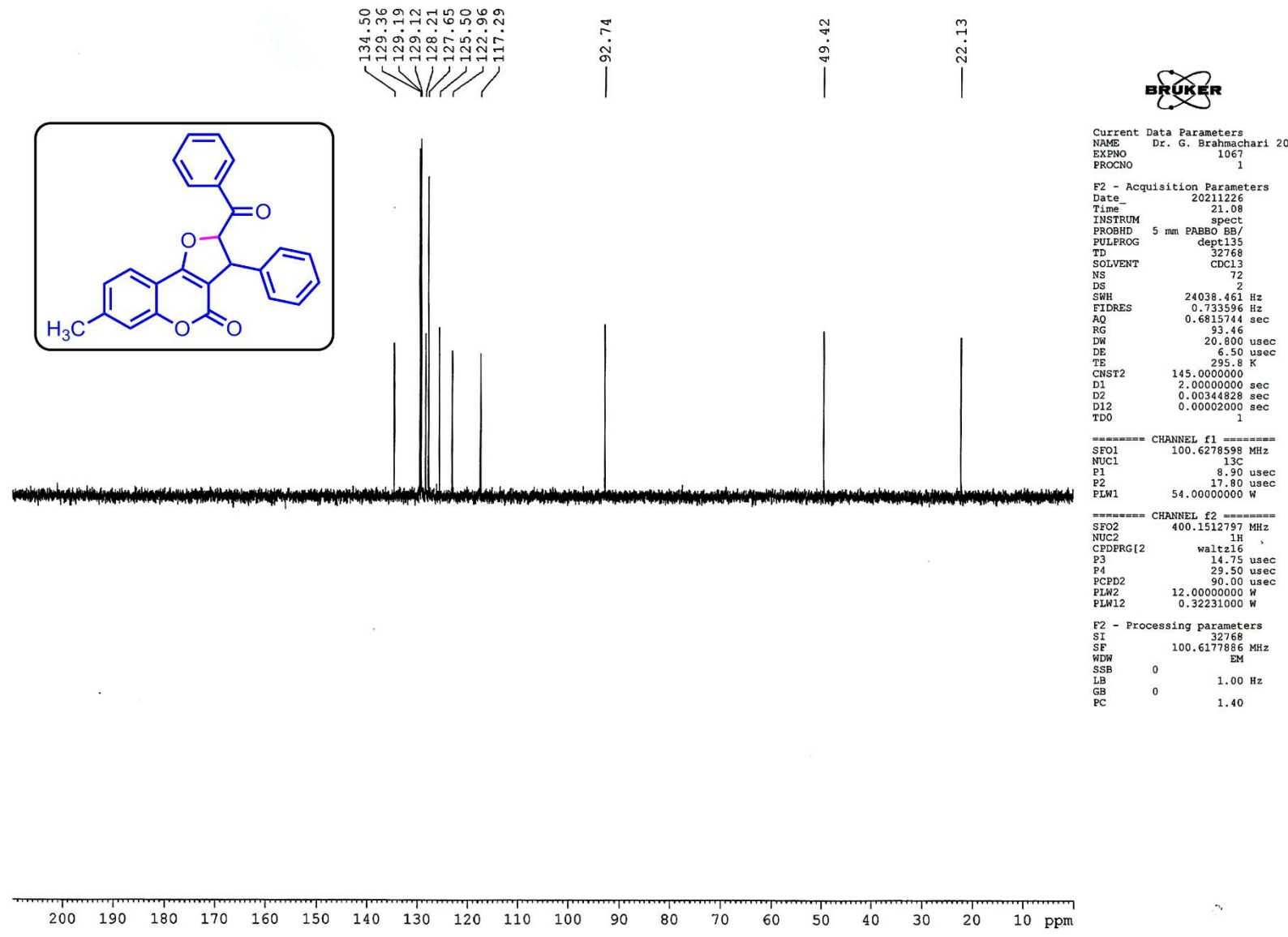


Figure S102. DEPT-135 NMR spectrum of 2-benzoyl-7-methyl-3-phenyl-2,3-dihydro-4*H*-furo[3,2-*c*]chromen-4-one (**2-23**)

Acquisition Parameter

Source Type	ESI	Ion Polarity	Positive	Set Nebulizer	0.4 Bar
Focus	Active	Set Capillary	3400 V	Set Dry Heater	200 °C
Scan Begin	50 m/z	Set End Plate Offset	-500 V	Set Dry Gas	4.0 l/min
Scan End	3000 m/z	Set Charging Voltage	2000 V	Set Divert Valve	Source
		Set Corona	0 nA	Set APCI Heater	0 °C

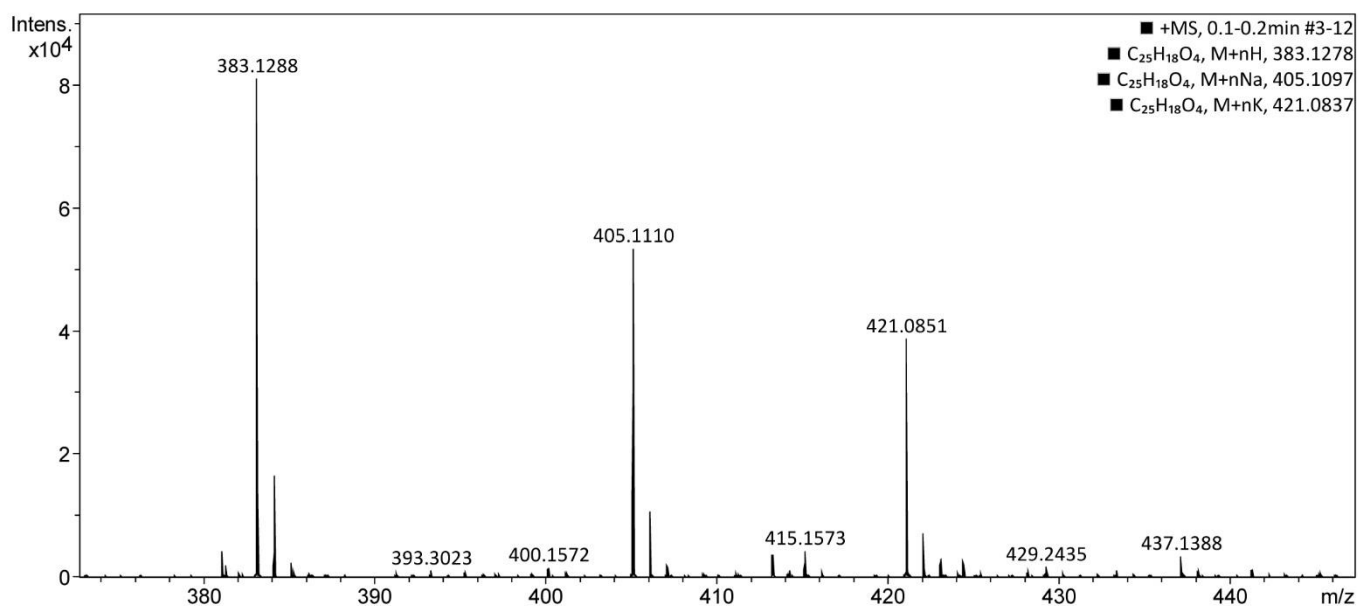
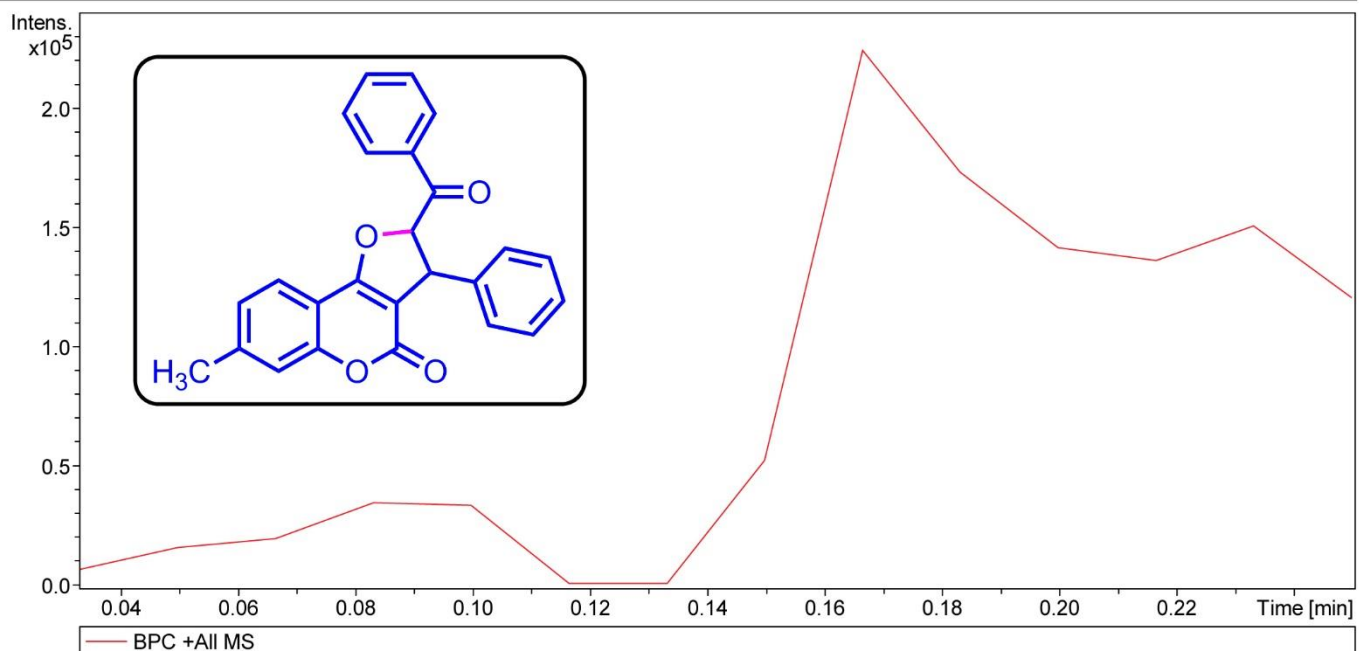


Figure S103. High-resolution Mass spectra of 2-benzoyl-7-methyl-3-phenyl-2,3-dihydro-4H-furo[3,2-c]chromen-4-one (2-23)

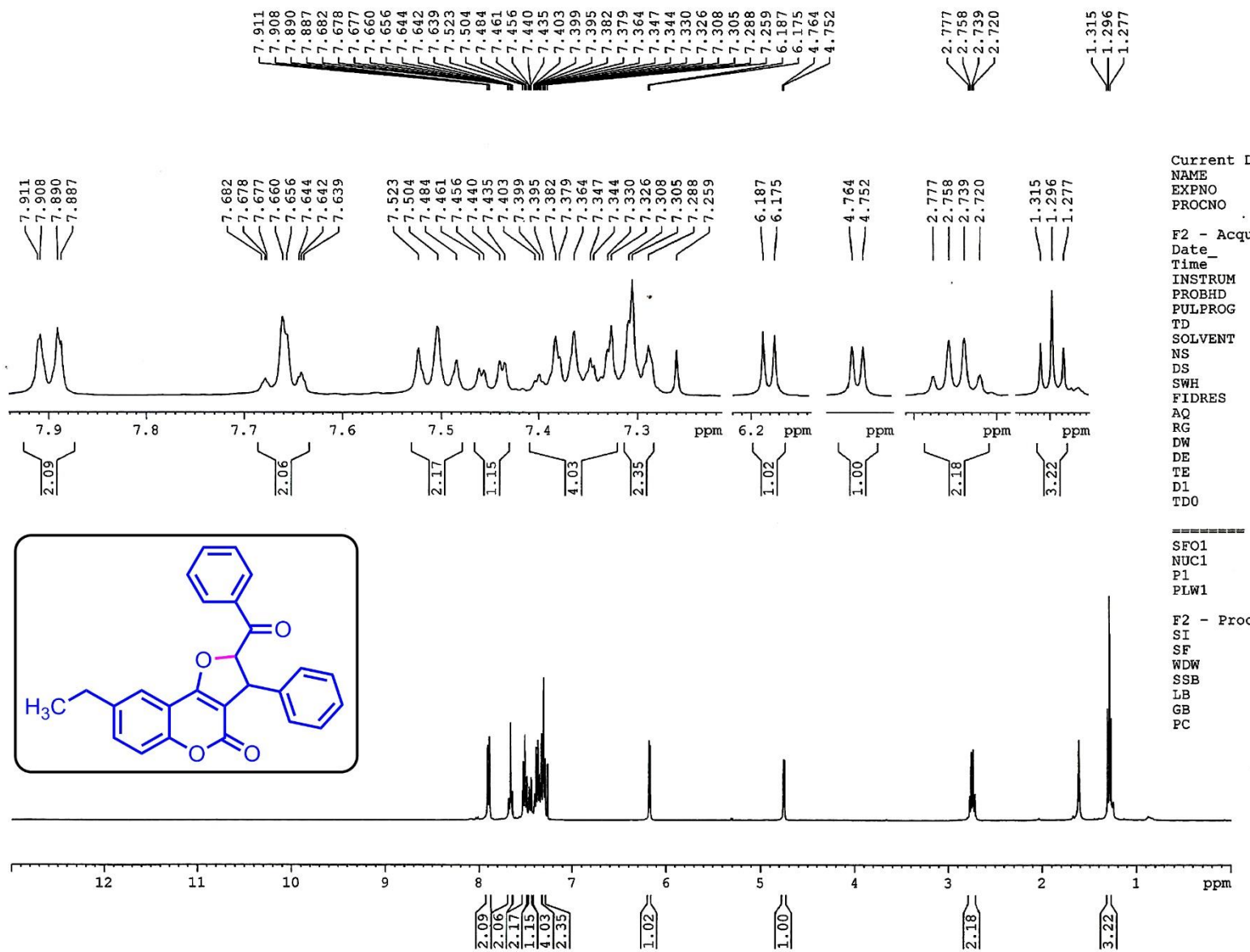


Figure S104. ^1H -NMR spectrum of 2-benzoyl-8-ethyl-3-phenyl-2,3-dihydro-4*H*-furo[3,2-*c*]chromen-4-one (**2-24**)

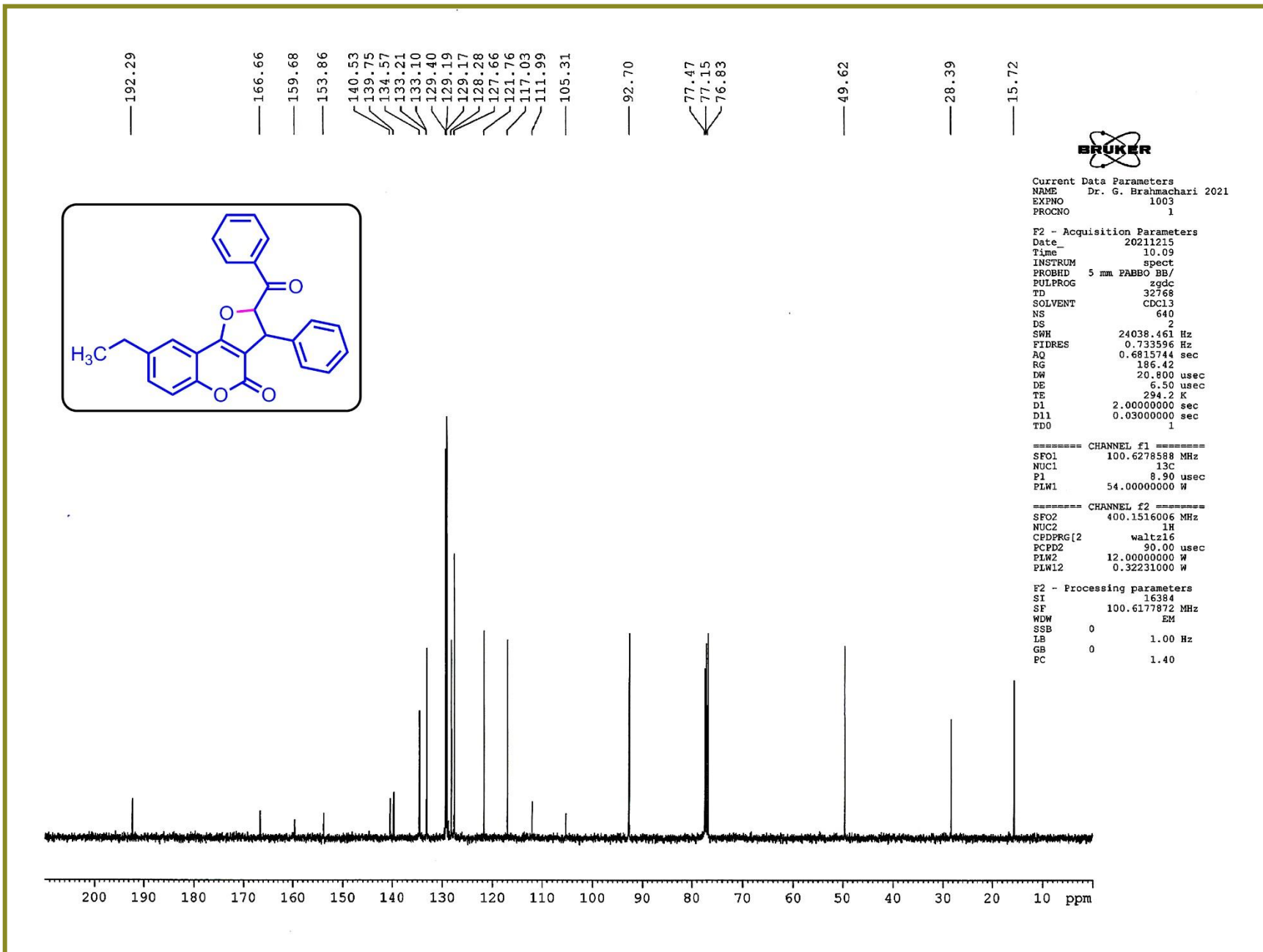


Figure S105. ¹³C-NMR spectrum of 2-benzoyl-8-ethyl-3-phenyl-2,3-dihydro-4H-furo[3,2-c]chromen-4-one (**2-24**)

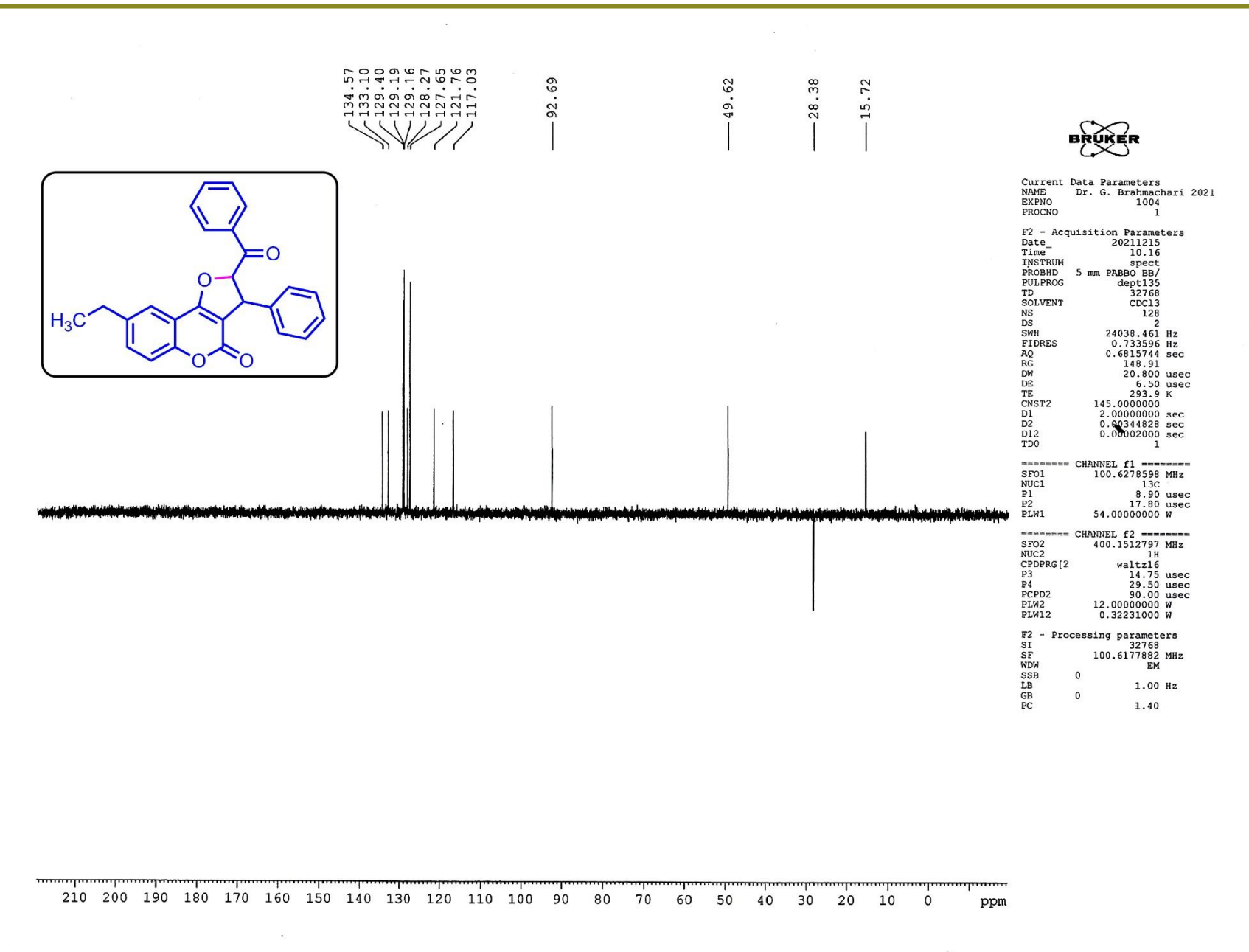


Figure S106. DEPT-135 NMR spectrum of 2-benzoyl-8-ethyl-3-phenyl-2,3-dihydro-4H-furo[3,2-*c*]chromen-4-one (**2-24**)

Acquisition Parameter

Source Type	ESI	Ion Polarity	Positive	Set Nebulizer	0.4 Bar
Focus	Active	Set Capillary	3400 V	Set Dry Heater	200 °C
Scan Begin	50 m/z	Set End Plate Offset	-500 V	Set Dry Gas	4.0 l/min
Scan End	3000 m/z	Set Charging Voltage	2000 V	Set Divert Valve	Source
		Set Corona	0 nA	Set APCI Heater	0 °C

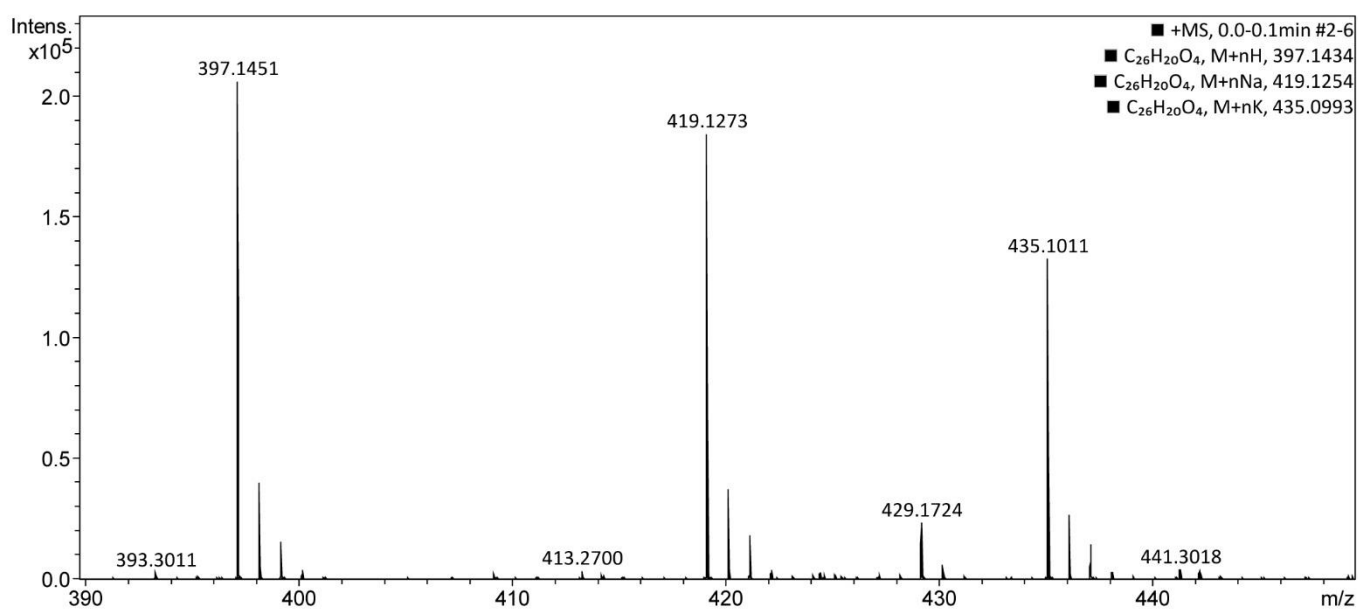
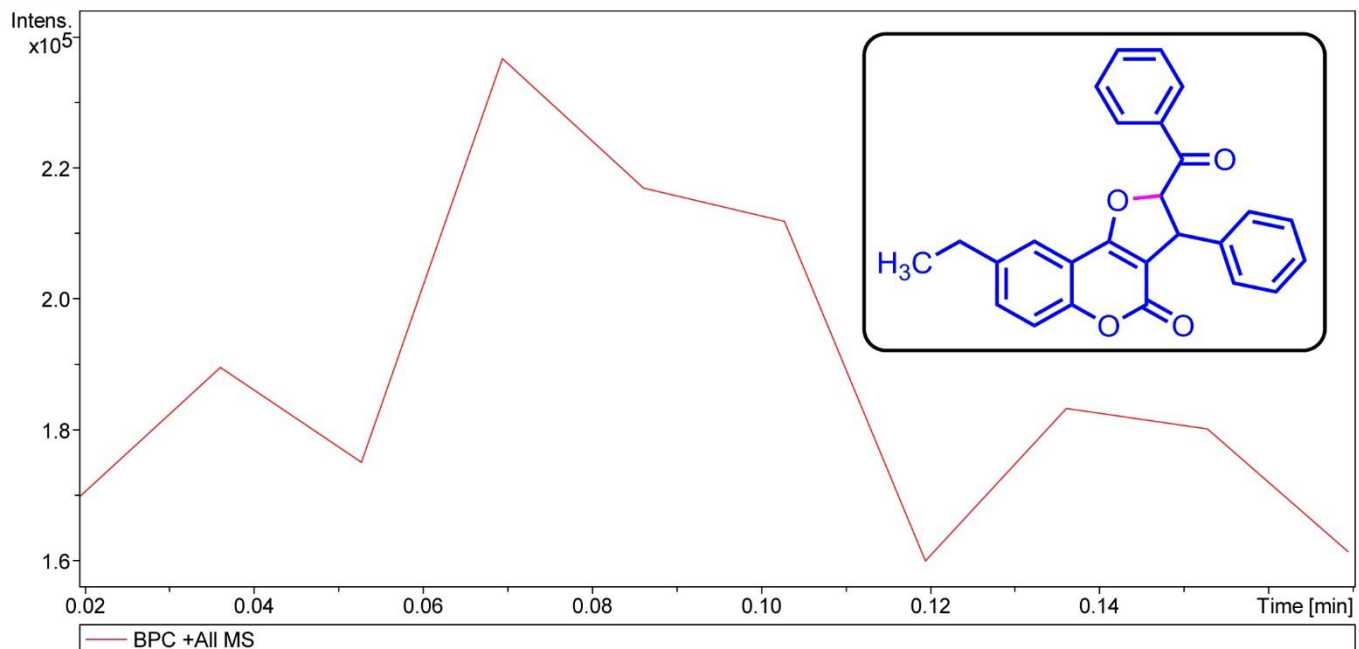


Figure S107. High-resolution Mass spectra of 2-benzoyl-8-ethyl-3-phenyl-2,3-dihydro-4H-furo[3,2-c]chromen-4-one (2-24)

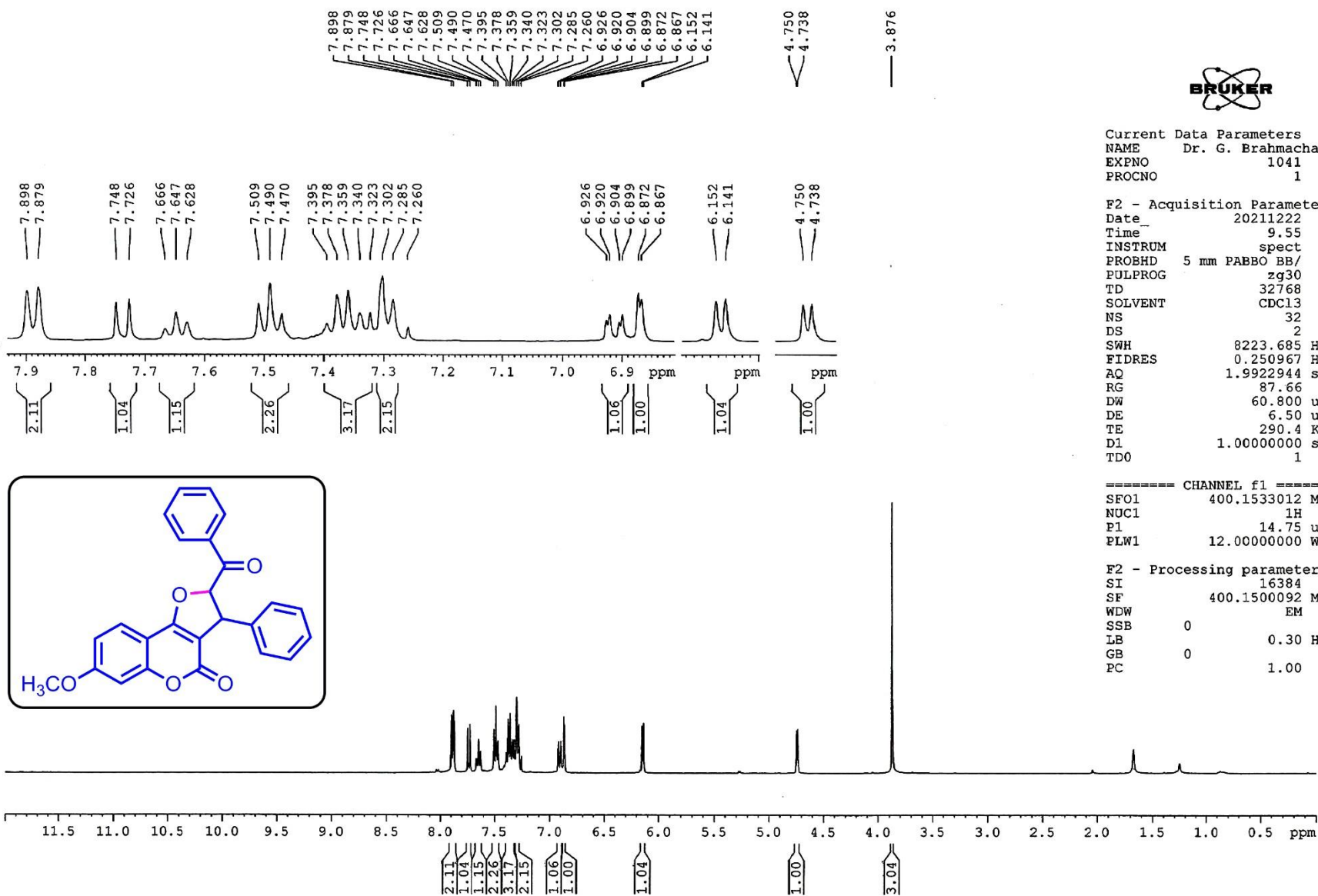


Figure S108. ¹H-NMR spectrum of 2-benzoyl-7-methoxy-3-phenyl-2,3-dihydro-4H-furo[3,2-c]chromen-4-one (**2-25**)

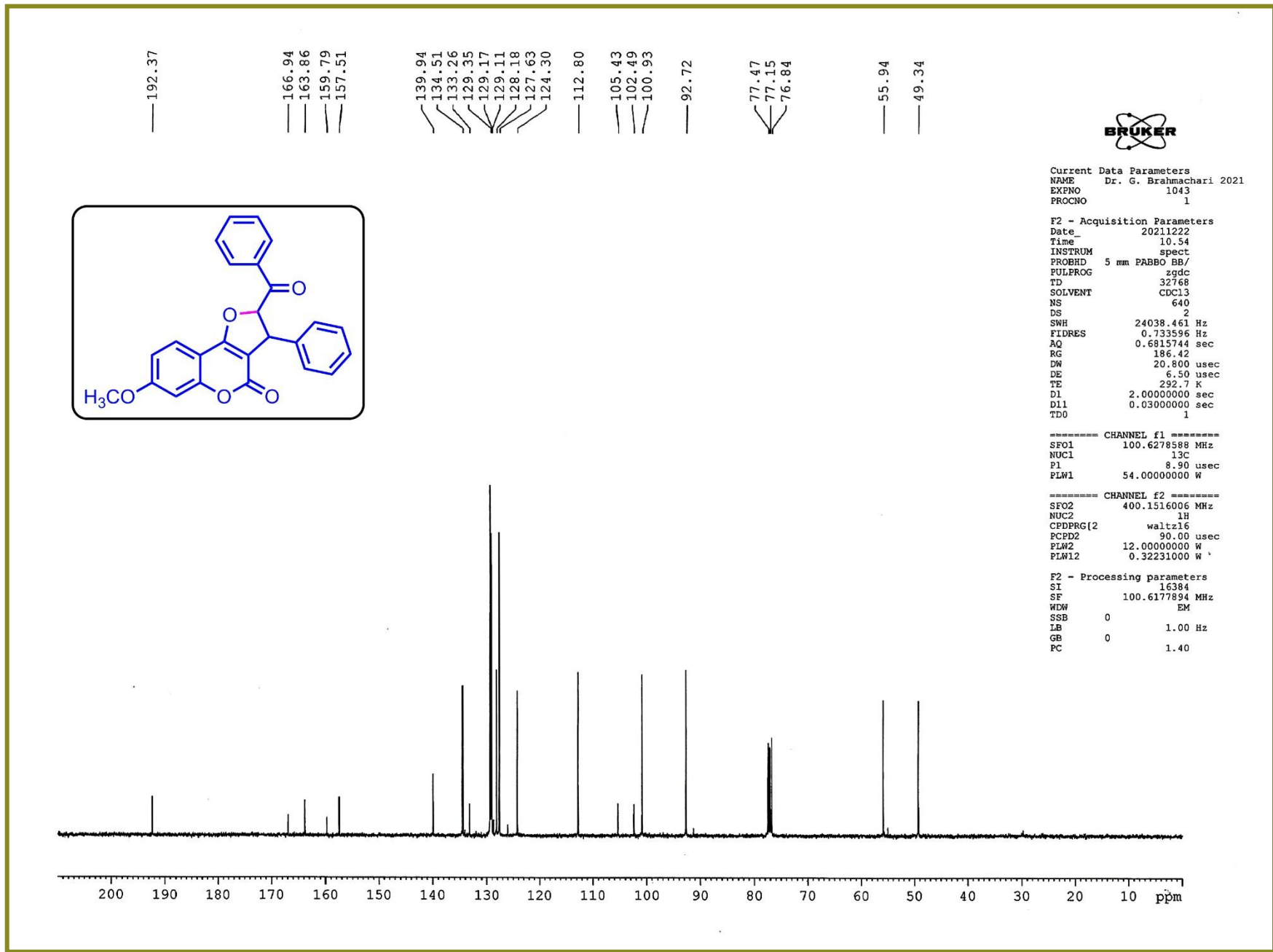


Figure S109. ¹³C-NMR spectrum of 2-benzoyl-7-methoxy-3-phenyl-2,3-dihydro-4H-furo[3,2-c]chromen-4-one (2-25)

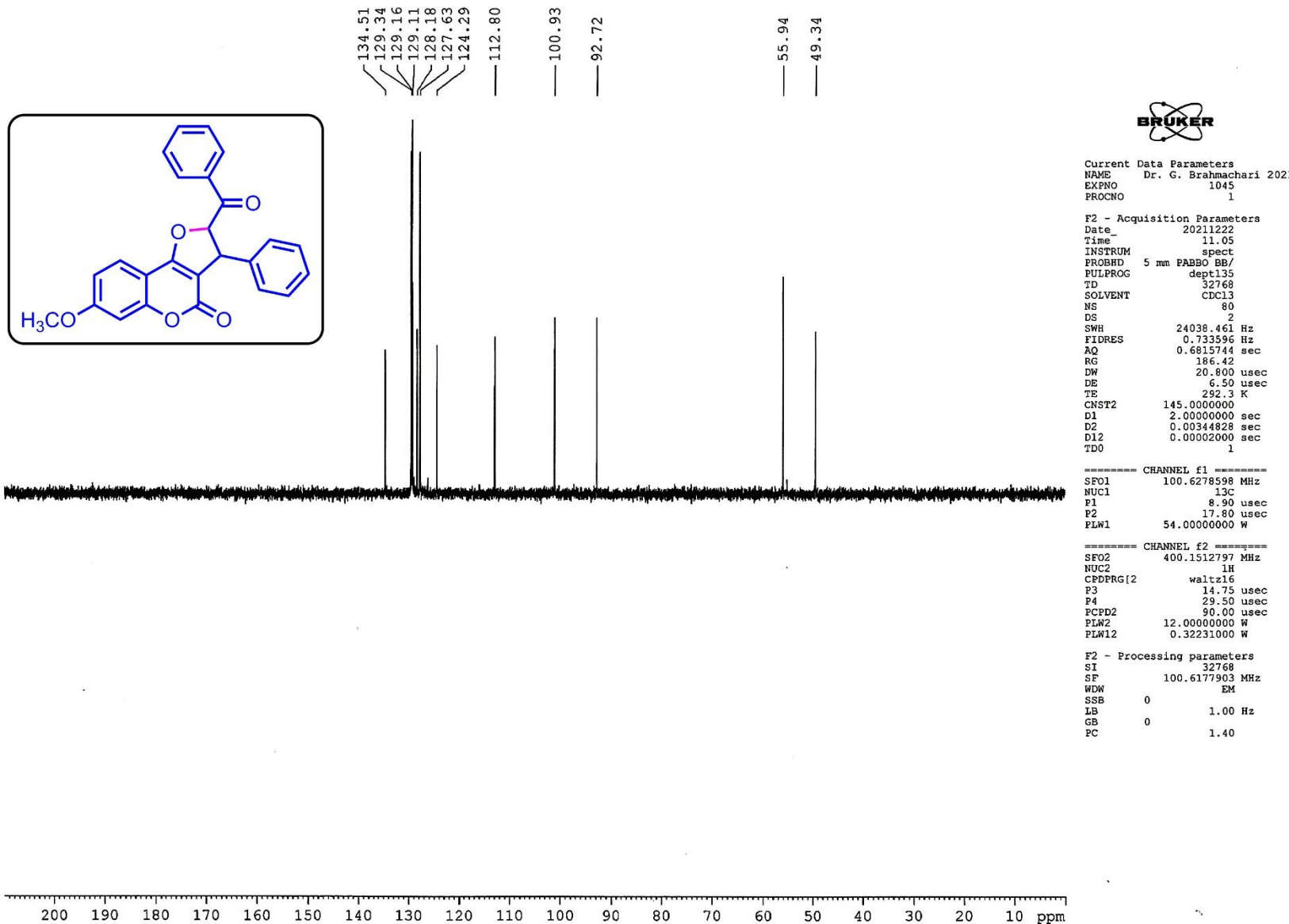


Figure S110. DEPT-135 NMR spectrum of 2-benzoyl-7-methoxy-3-phenyl-2,3-dihydro-4H-furo[3,2-c]chromen-4-one (**2-25**)

Acquisition Parameter

Source Type	ESI	Ion Polarity	Positive	Set Nebulizer	0.4 Bar
Focus	Active	Set Capillary	3400 V	Set Dry Heater	200 °C
Scan Begin	50 m/z	Set End Plate Offset	-500 V	Set Dry Gas	4.0 l/min
Scan End	3000 m/z	Set Charging Voltage	2000 V	Set Divert Valve	Source
		Set Corona	0 nA	Set APCI Heater	0 °C

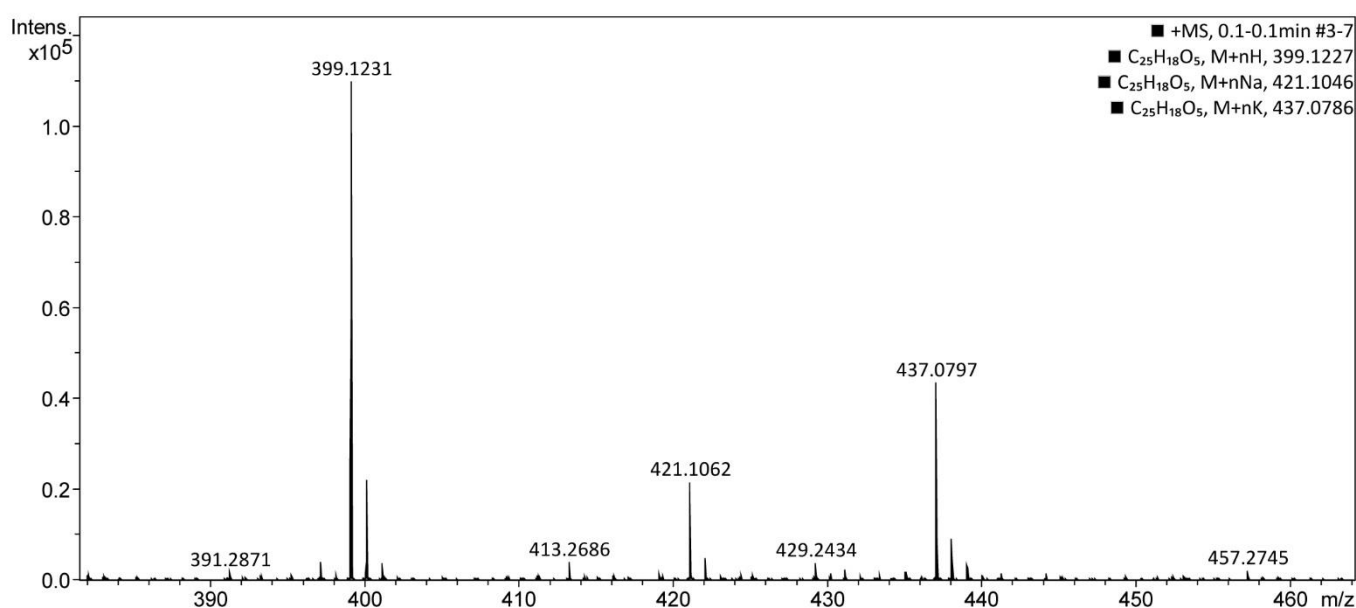
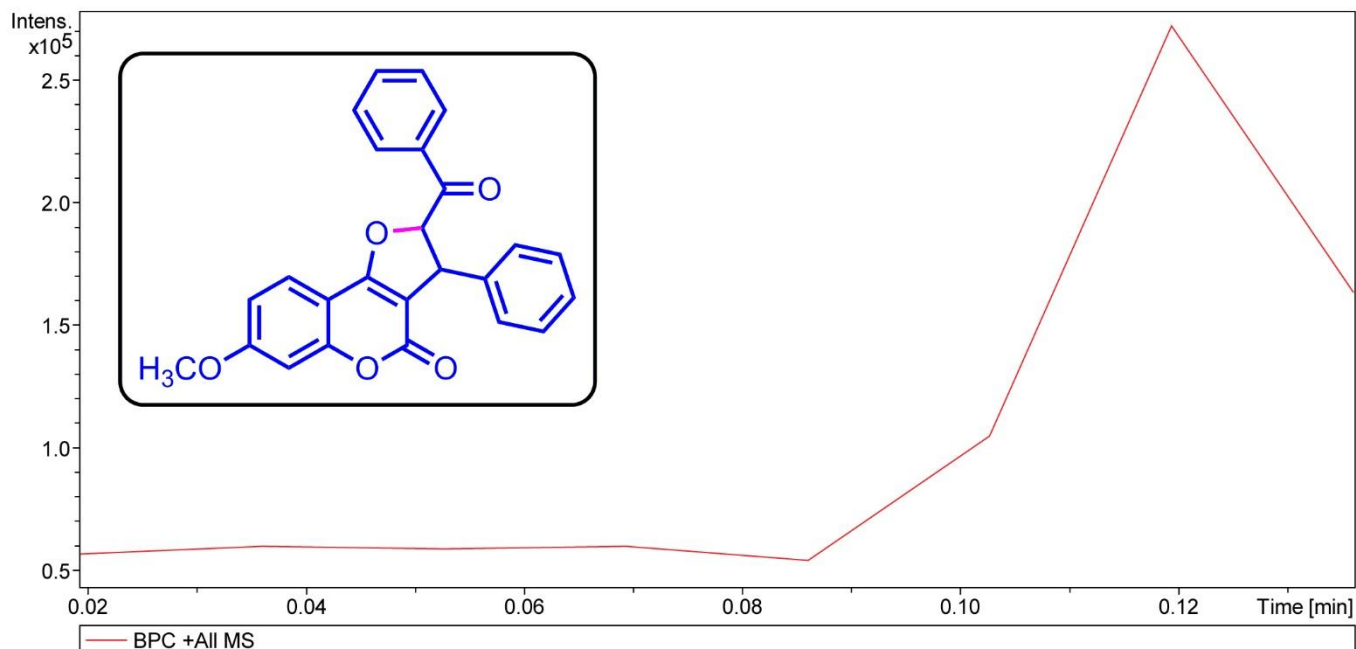


Figure S111. High-resolution Mass spectra of 2-benzoyl-7-methoxy-3-phenyl-2,3-dihydro-4*H*-furo[3,2-*c*]chromen-4-one (**2-25**)

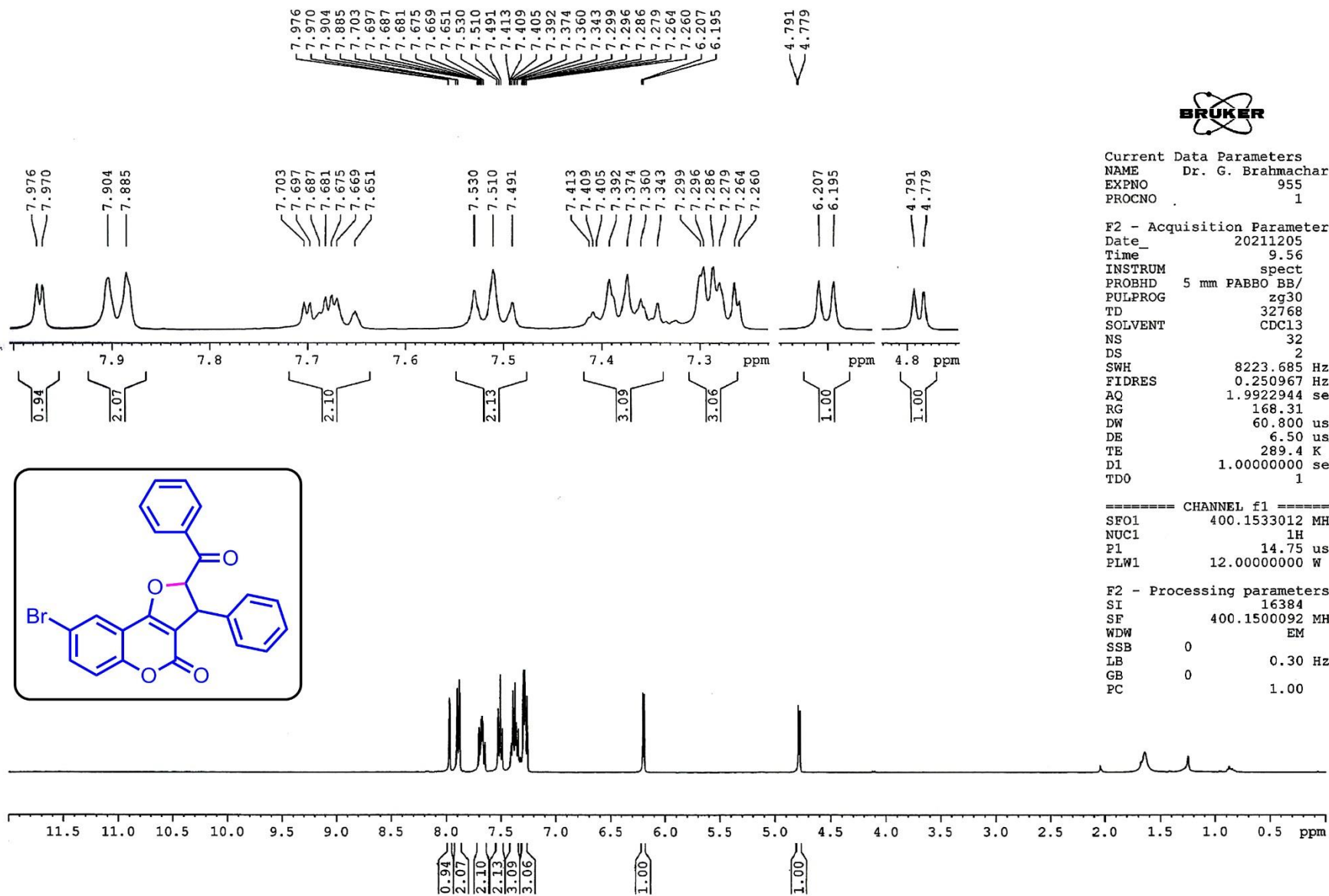


Figure S112. $^1\text{H-NMR}$ spectrum of 2-benzoyl-8-bromo-3-phenyl-2,3-dihydro-4*H*-furo[3,2-*c*]chromen-4-one (**2-26**)

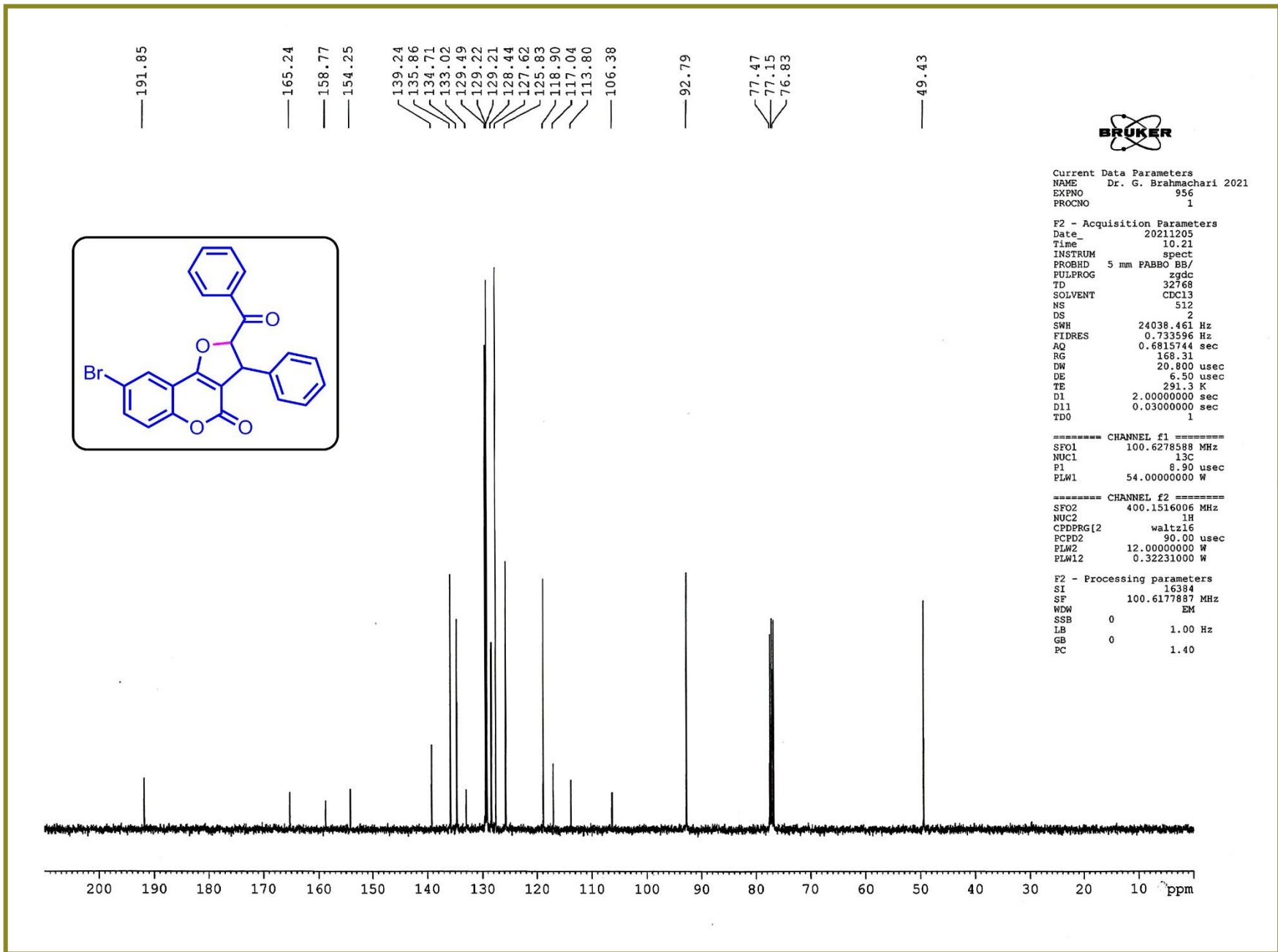


Figure S113. ^{13}C -NMR spectrum of 2-benzoyl-8-bromo-3-phenyl-2,3-dihydro-4*H*-furo[3,2-*c*]chromen-4-one (**2-26**)

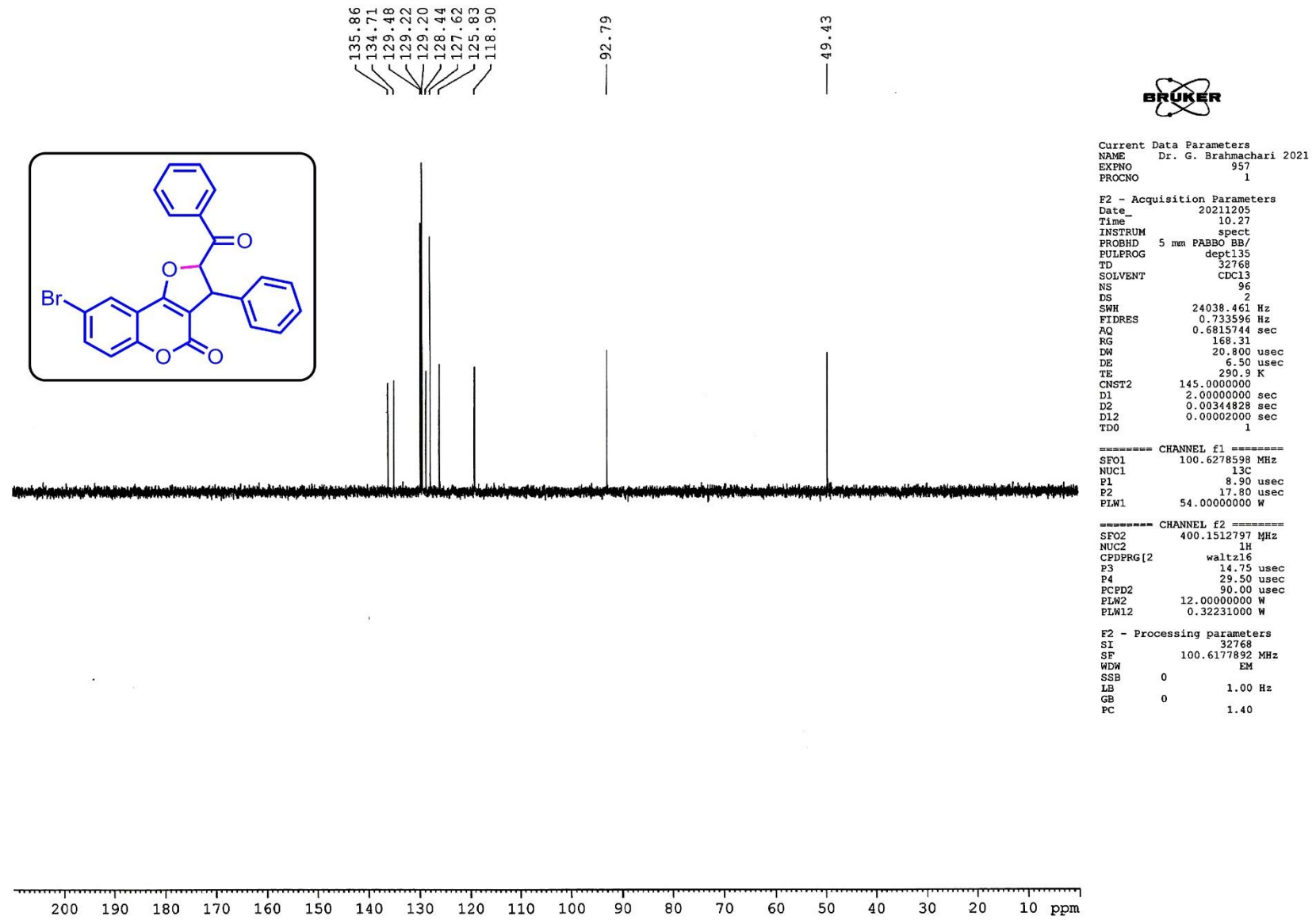


Figure S114. DEPT-135 NMR spectrum of 2-benzoyl-8-bromo-3-phenyl-2,3-dihydro-4H-furo[3,2-c]chromen-4-one (**2-26**)

Acquisition Parameter

Source Type	ESI	Ion Polarity	Positive	Set Nebulizer	0.4 Bar
Focus	Active	Set Capillary	3400 V	Set Dry Heater	200 °C
Scan Begin	50 m/z	Set End Plate Offset	-500 V	Set Dry Gas	4.0 l/min
Scan End	3000 m/z	Set Charging Voltage	2000 V	Set Divert Valve	Source
		Set Corona	0 nA	Set APCI Heater	0 °C

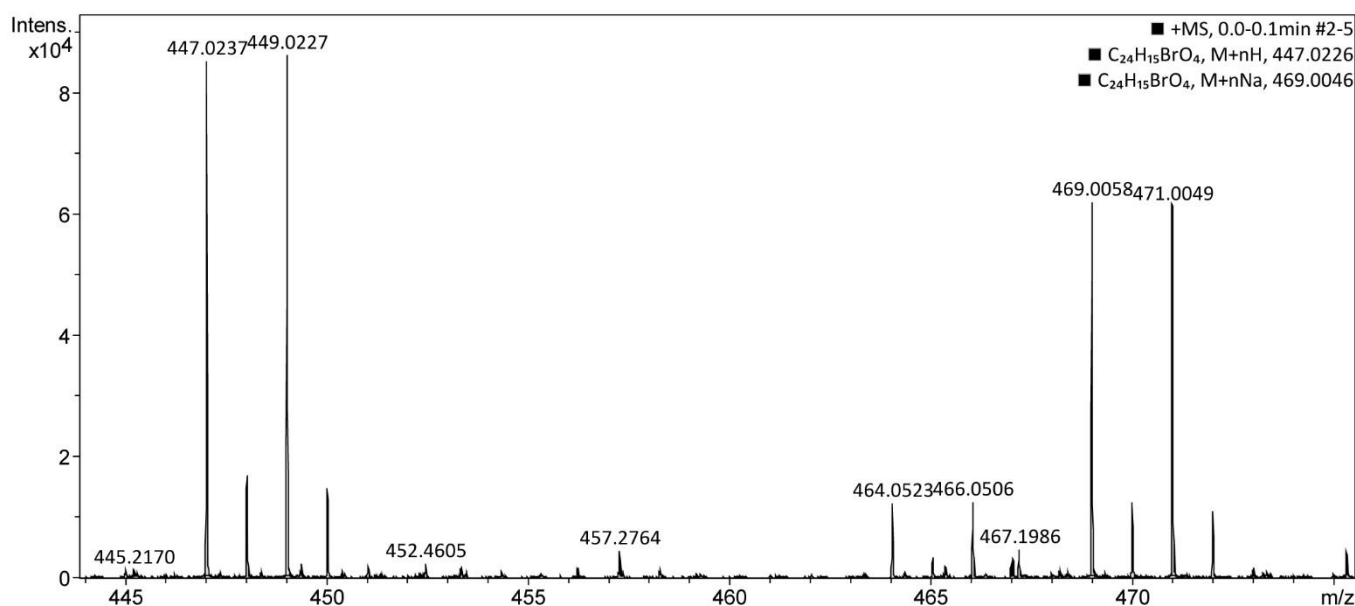
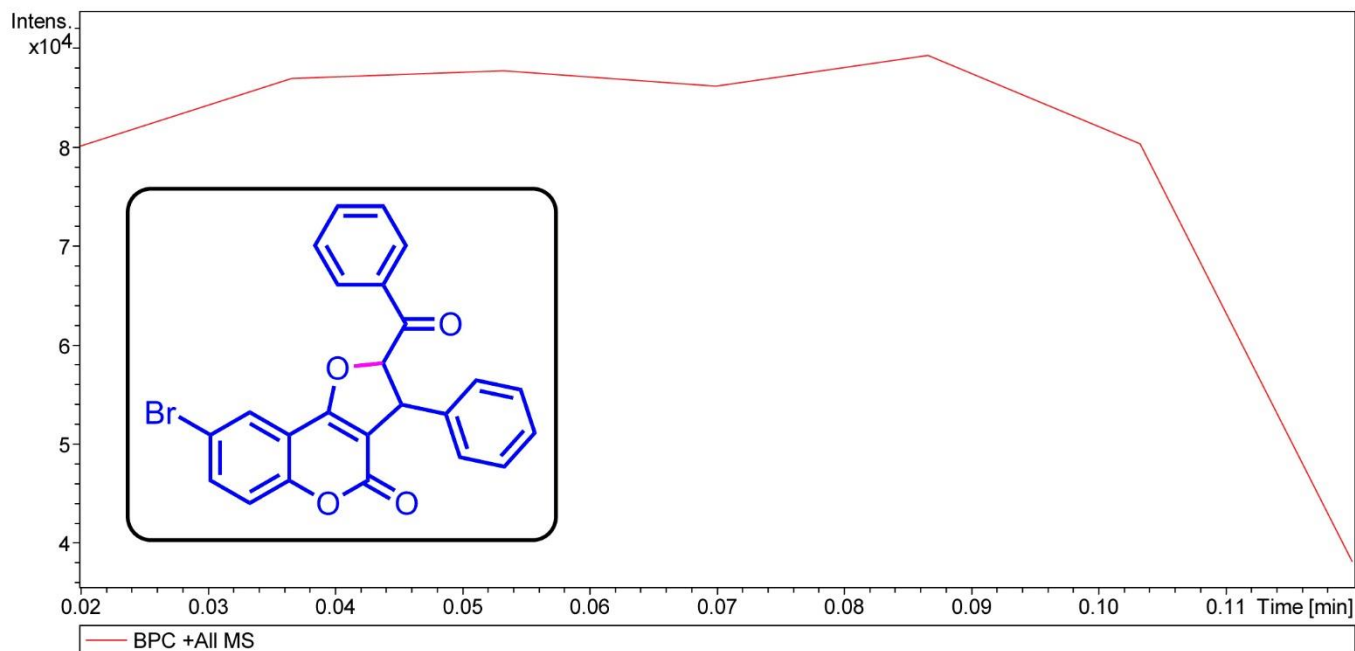


Figure S115. High-resolution Mass spectra of 2-benzoyl-8-bromo-3-phenyl-2,3-dihydro-4H-furo[3,2-c]chromen-4-one (2-26)

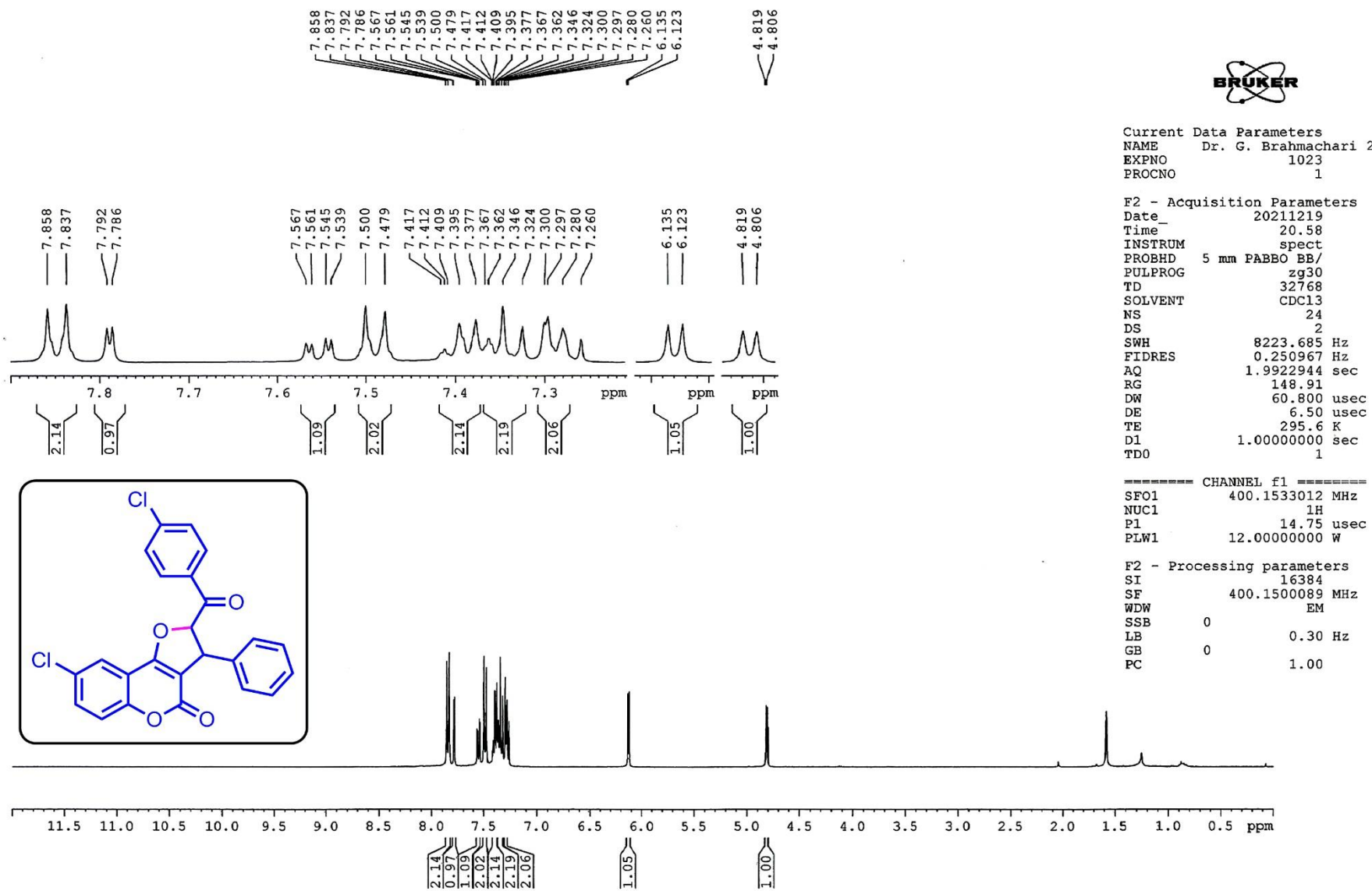


Figure S116. $^1\text{H-NMR}$ spectrum of 8-chloro-2-(4-chlorobenzoyl)-3-phenyl-2,3-dihydro-4*H*-furo[3,2-*c*]chromen-4-one (**2-27**)

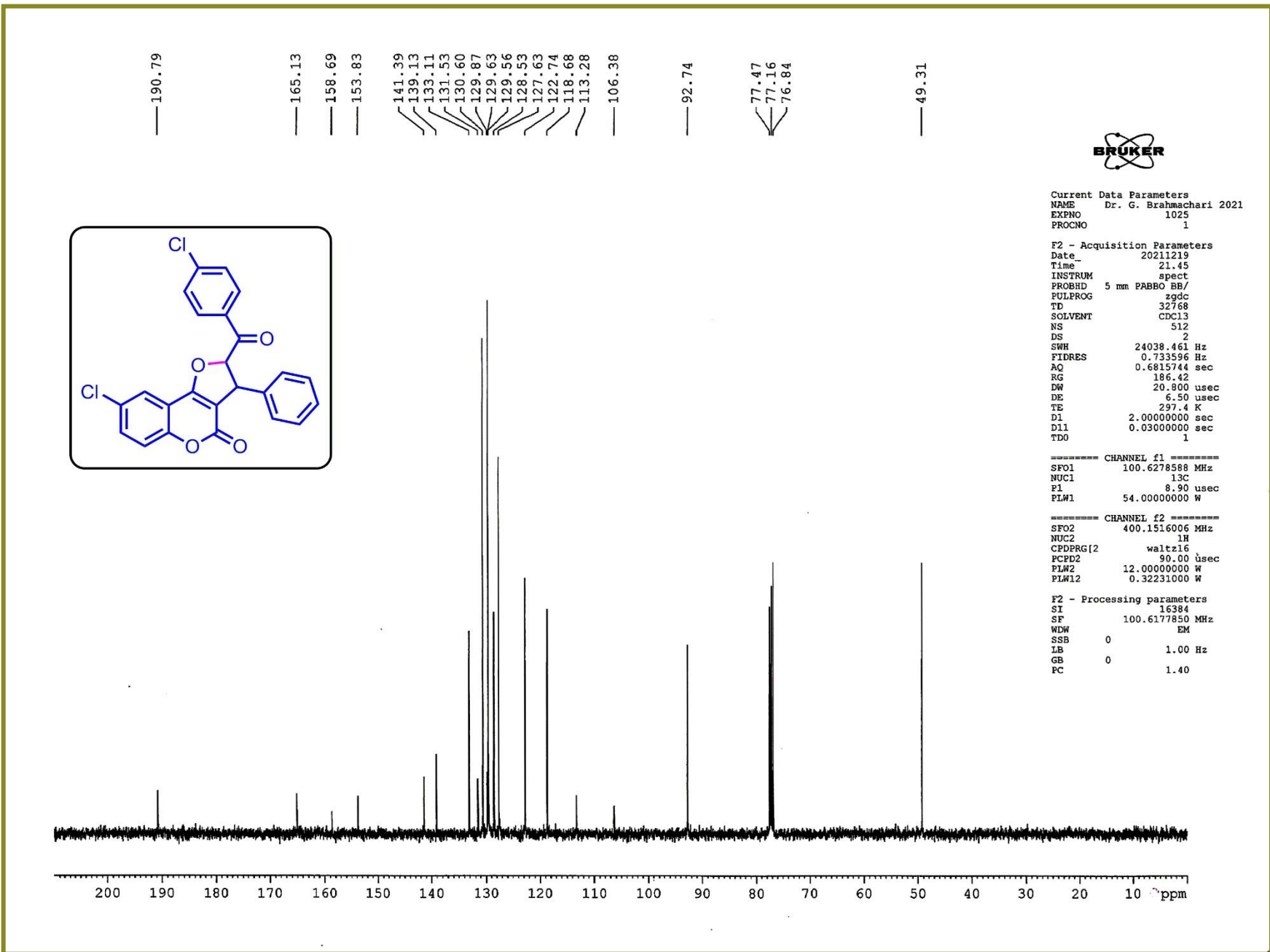


Figure S117. ¹³C-NMR spectrum of 8-chloro-2-(4-chlorobenzoyl)-3-phenyl-2,3-dihydro-4H-furo[3,2-c]chromen-4-one (**2-27**)

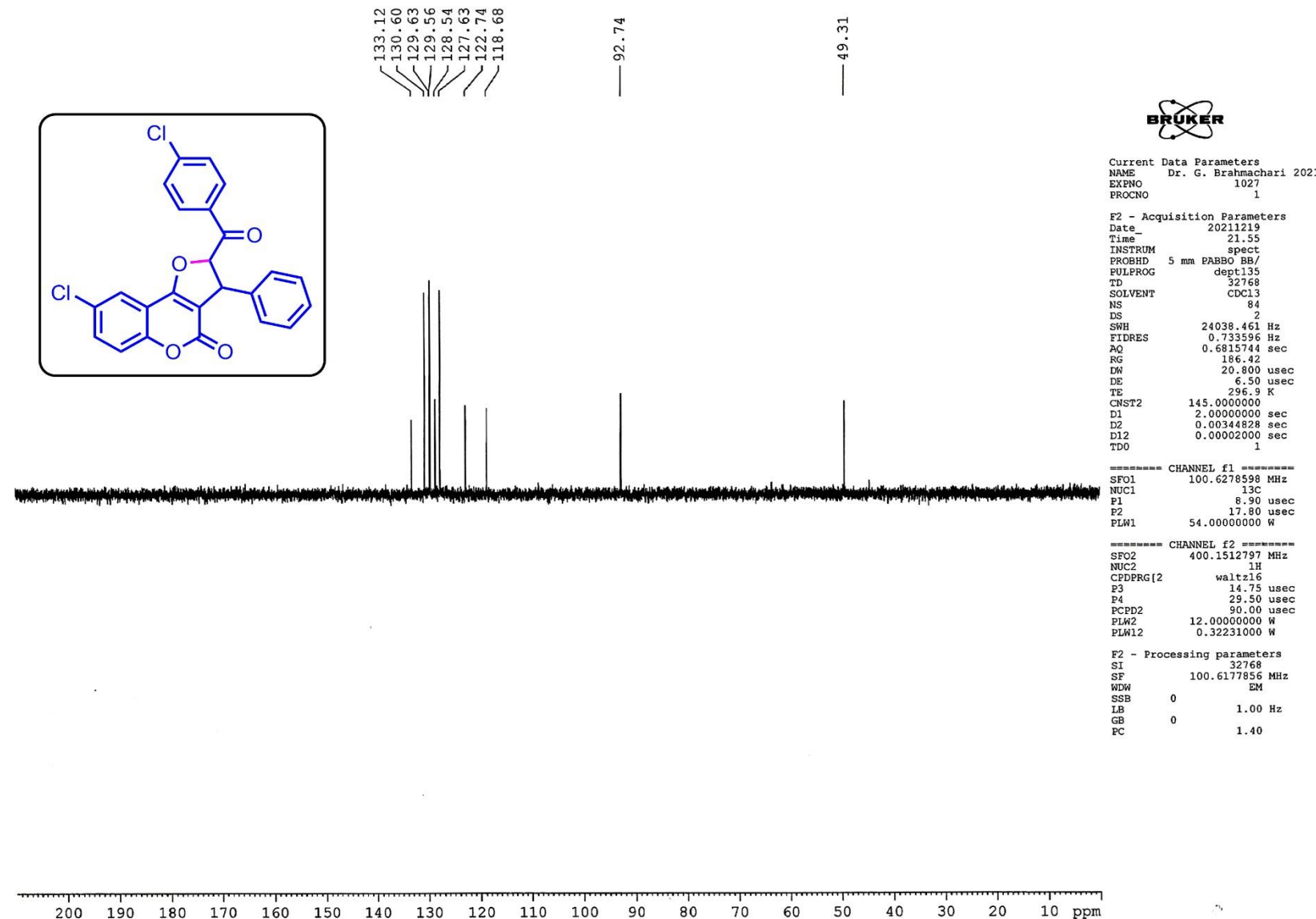


Figure S118. DEPT-135 NMR spectrum of 8-chloro-2-(4-chlorobenzoyl)-3-phenyl-2,3-dihydro-4*H*-furo[3,2-*c*]chromen-4-one (**2-27**)

Acquisition Parameter

Source Type	ESI	Ion Polarity	Positive	Set Nebulizer	0.4 Bar
Focus	Active	Set Capillary	3400 V	Set Dry Heater	200 °C
Scan Begin	50 m/z	Set End Plate Offset	-500 V	Set Dry Gas	4.0 l/min
Scan End	3000 m/z	Set Charging Voltage	2000 V	Set Divert Valve	Source
		Set Corona	0 nA	Set APCI Heater	0 °C

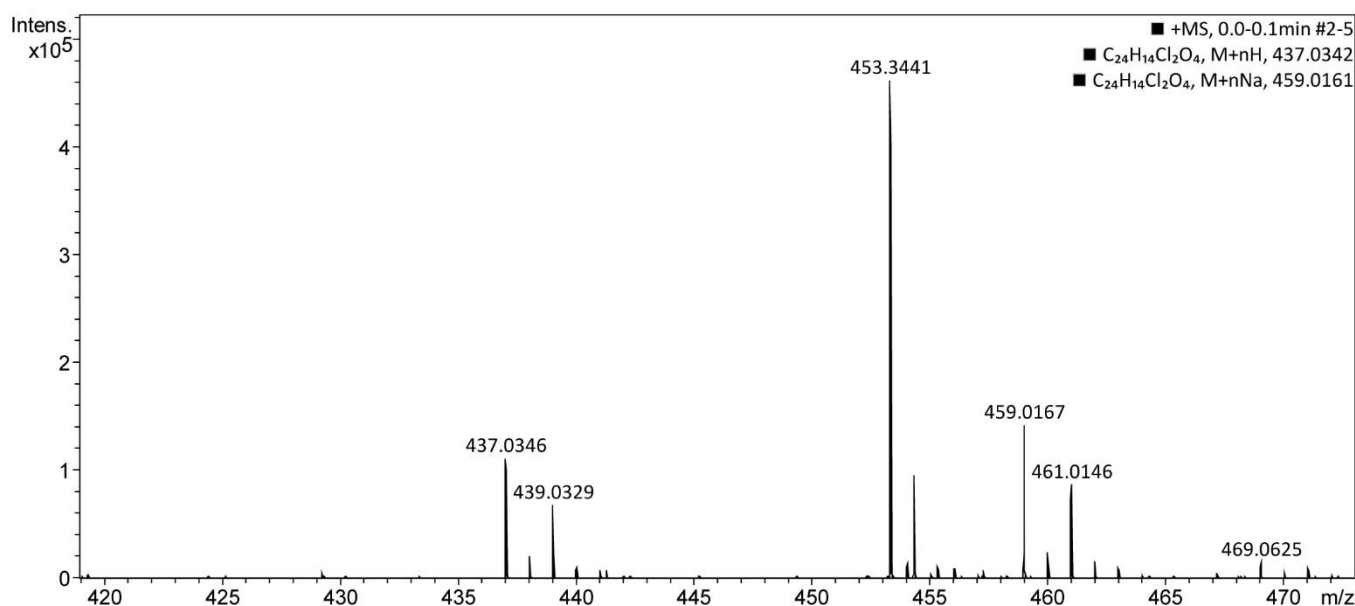
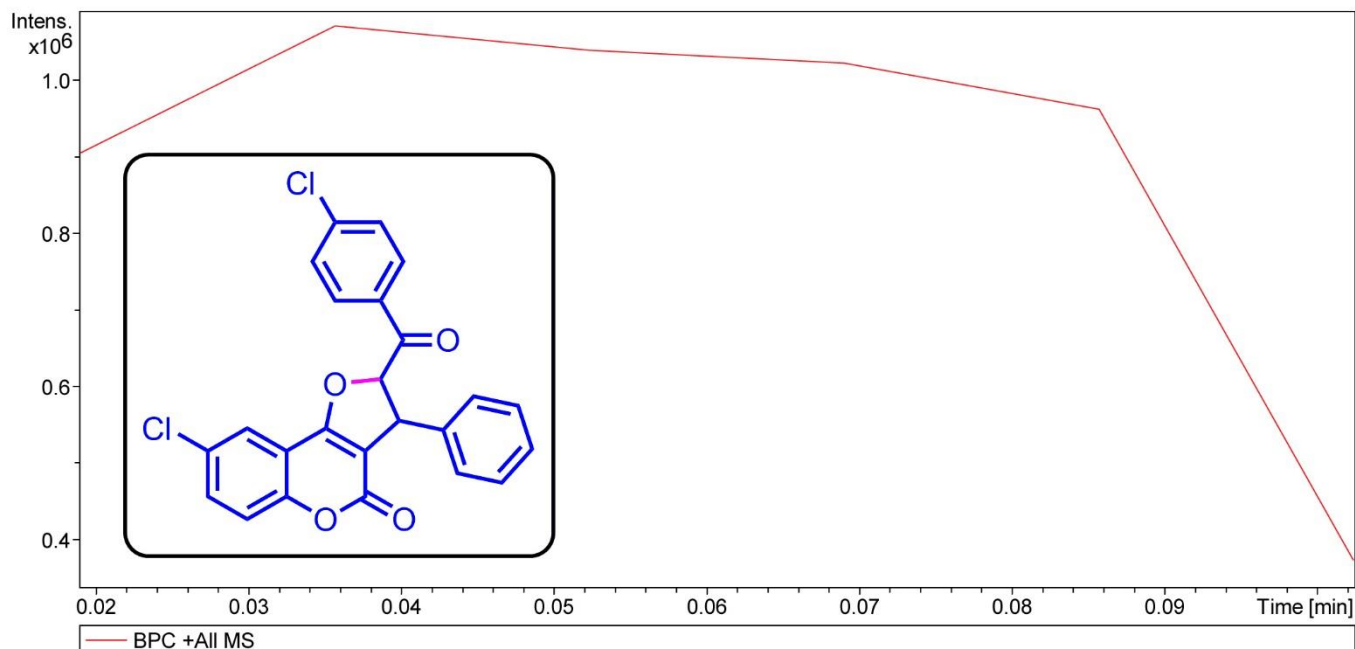


Figure S119. High-resolution Mass spectra of 8-chloro-2-(4-chlorobenzoyl)-3-phenyl-2,3-dihydro-4*H*-furo[3,2-*c*]chromen-4-one (**2-27**)

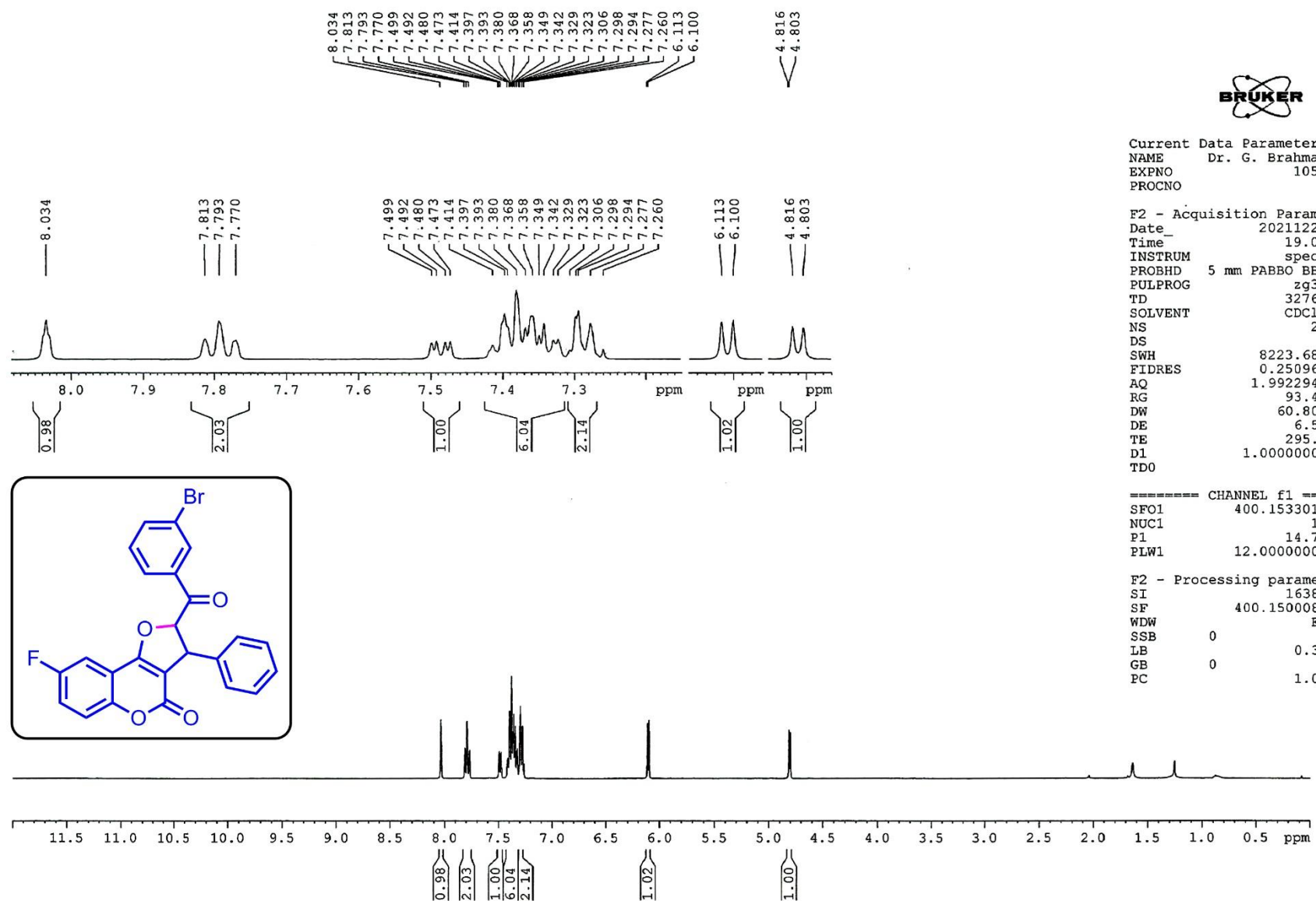


Figure S120. ¹H-NMR spectrum of 2-(3-bromobenzoyl)-8-fluoro-3-phenyl-2,3-dihydro-4*H*-furo[3,2-*c*]chromen-4-one (**2-28**)

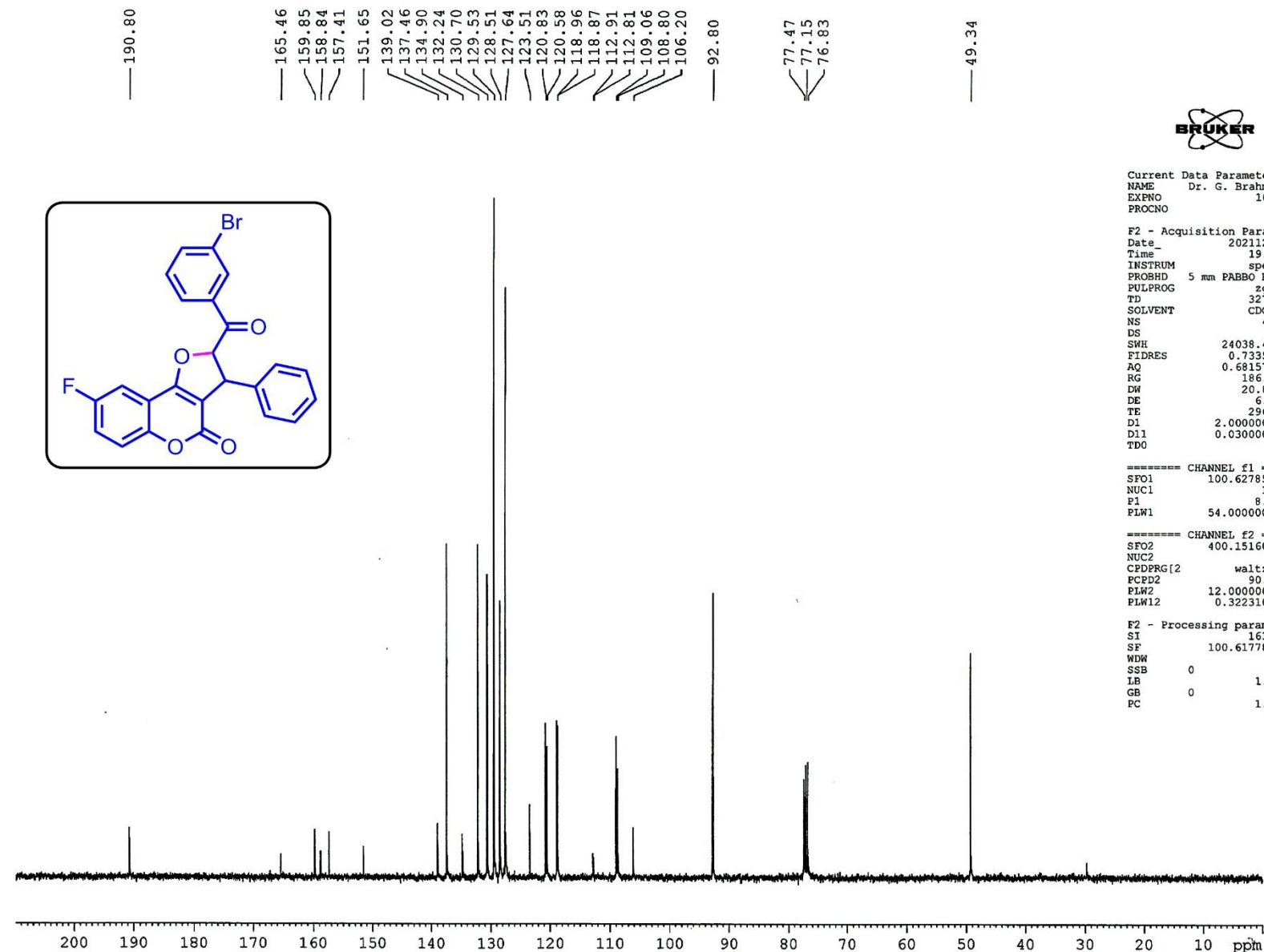


Figure S121. ¹³C-NMR spectrum of 2-(3-bromobenzoyl)-8-fluoro-3-phenyl-2,3-dihydro-4H-furo[3,2-c]chromen-4-one (**2-28**)
S130

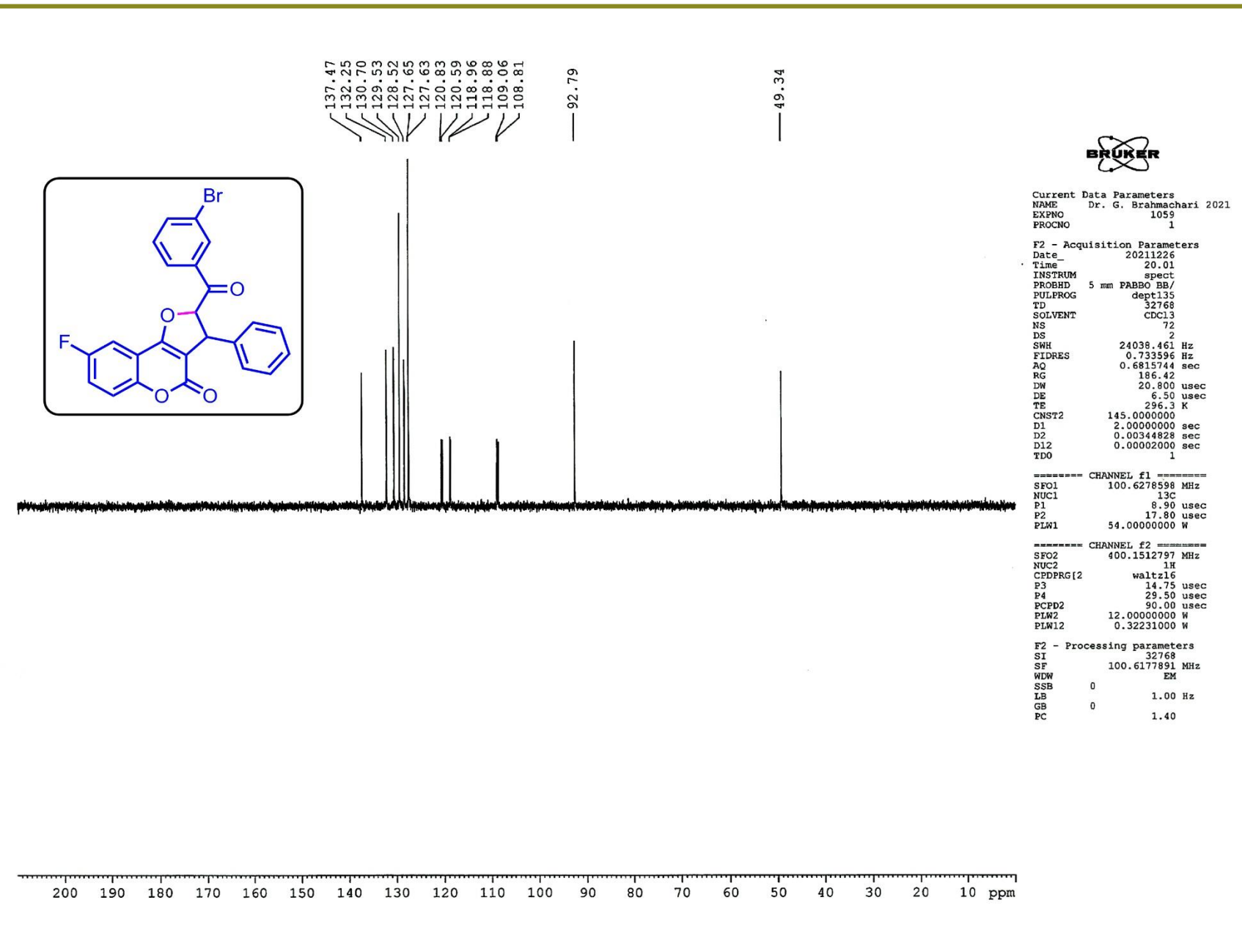


Figure S122. DEPT-135 NMR spectrum of 2-(3-bromobenzoyl)-8-fluoro-3-phenyl-2,3-dihydro-4*H*-furo[3,2-*c*]chromen-4-one (**2-28**)

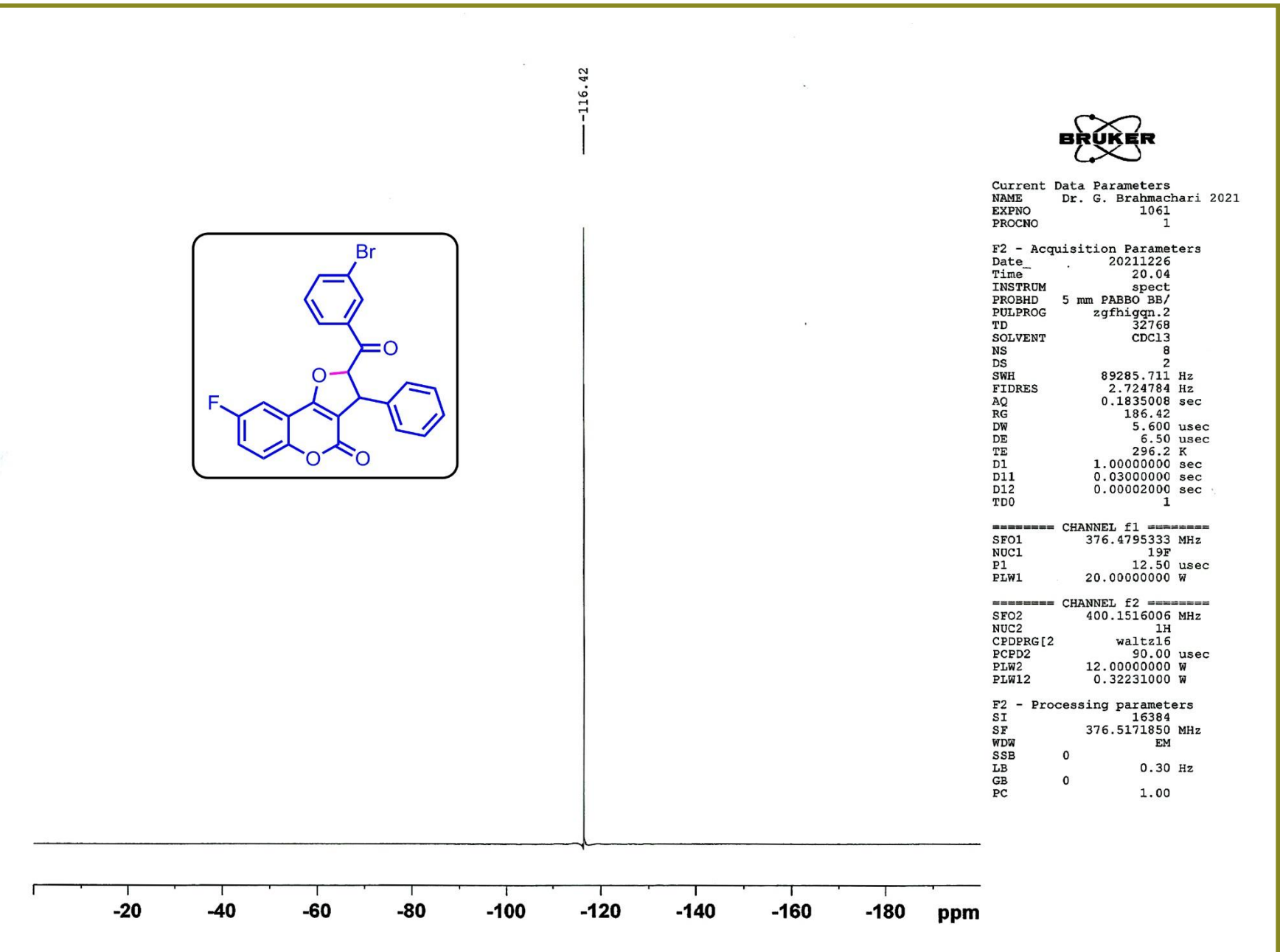


Figure S123. ¹⁹F NMR spectrum of 2-(3-bromobenzoyl)-8-fluoro-3-phenyl-2,3-dihydro-4*H*-furo[3,2-*c*]chromen-4-one (**2-28**)

Acquisition Parameter

Source Type	ESI	Ion Polarity	Positive	Set Nebulizer	0.4 Bar
Focus	Active	Set Capillary	3400 V	Set Dry Heater	200 °C
Scan Begin	50 m/z	Set End Plate Offset	-500 V	Set Dry Gas	4.0 l/min
Scan End	3000 m/z	Set Charging Voltage	2000 V	Set Divert Valve	Source
		Set Corona	0 nA	Set APCI Heater	0 °C

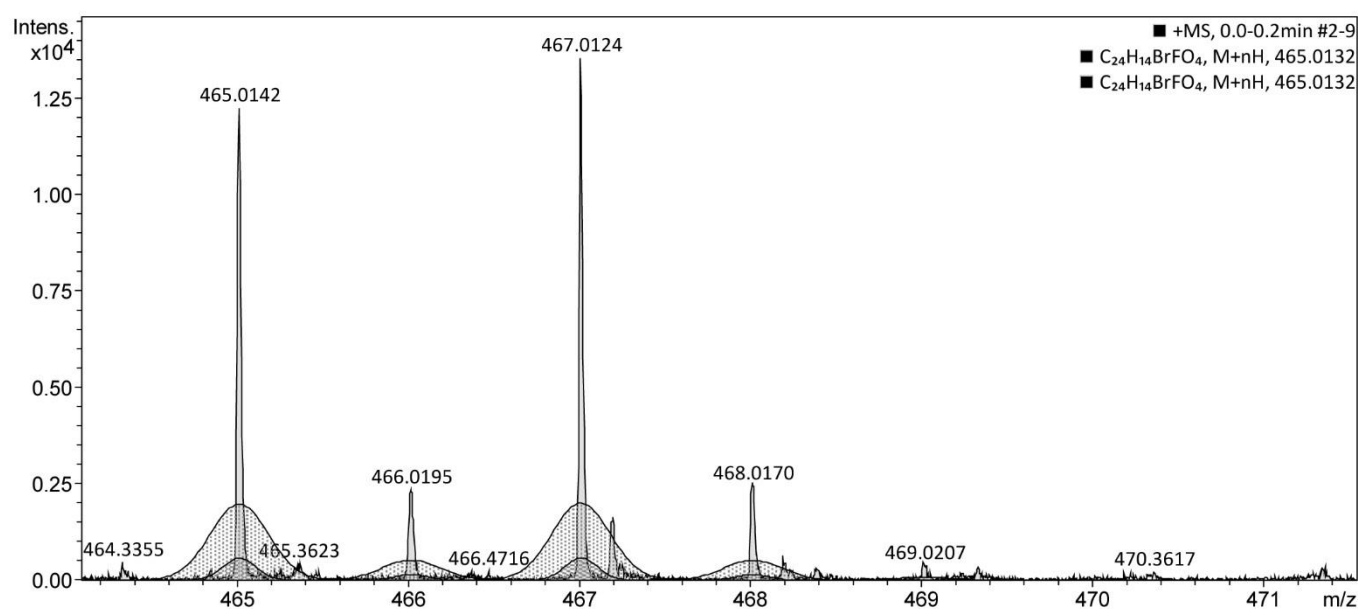
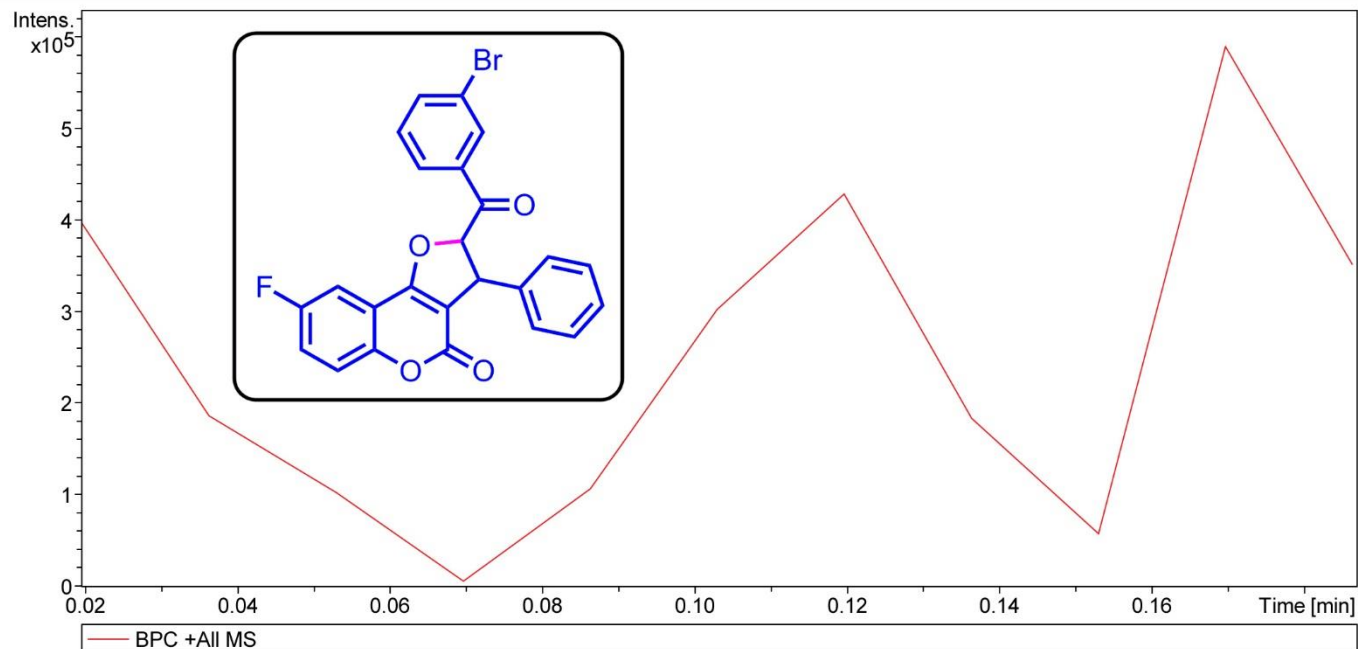


Figure S124. High-resolution Mass spectra of 2-(3-bromobenzoyl)-8-fluoro-3-phenyl-2,3-dihydro-4H-furo[3,2-c]chromen-4-one (**2-28**)

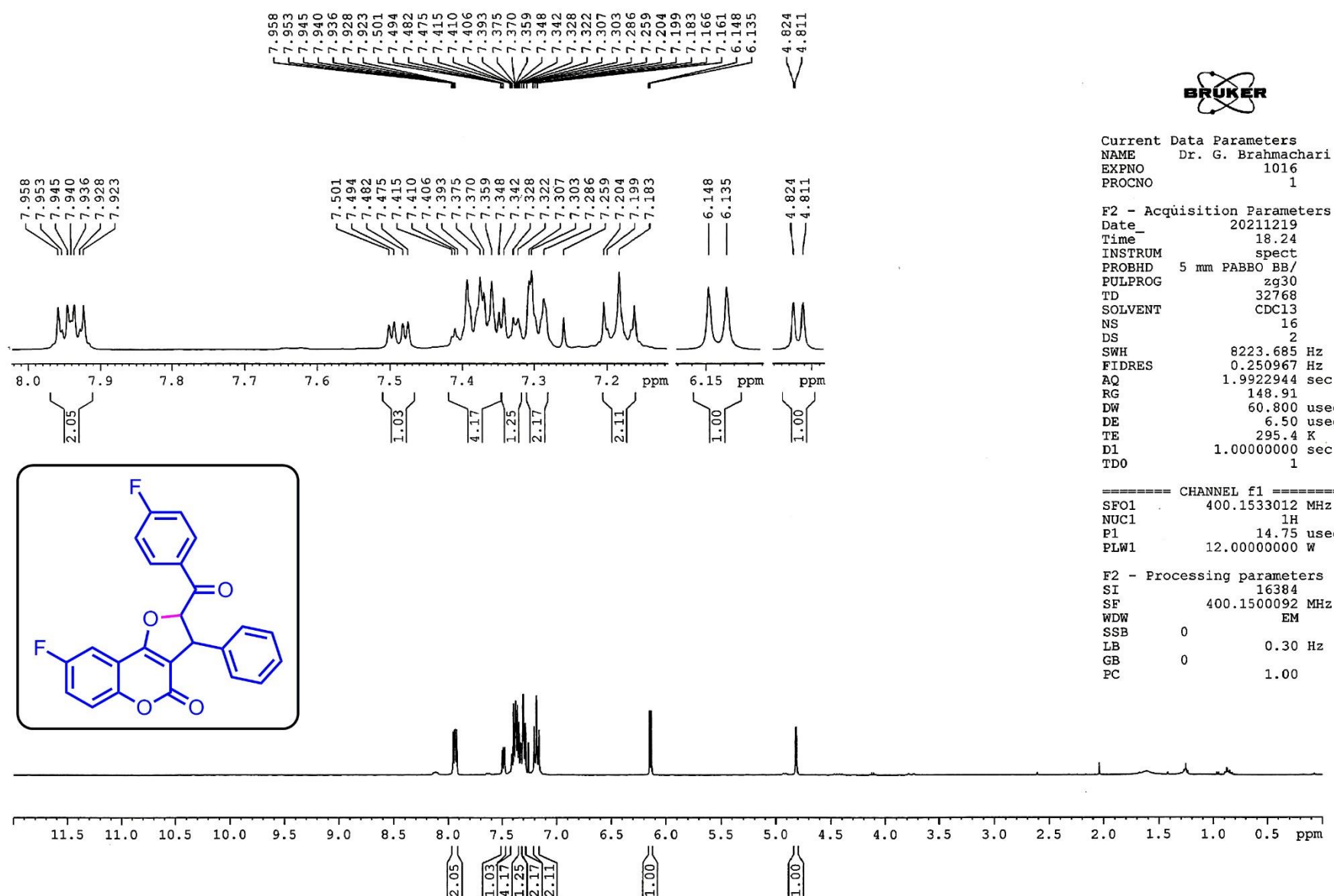


Figure S125. $^1\text{H-NMR}$ spectrum of 8-fluoro-2-(4-fluorobenzoyl)-3-phenyl-2,3-dihydro-4*H*-furo[3,2-*c*]chromen-4-one (**2-29**)

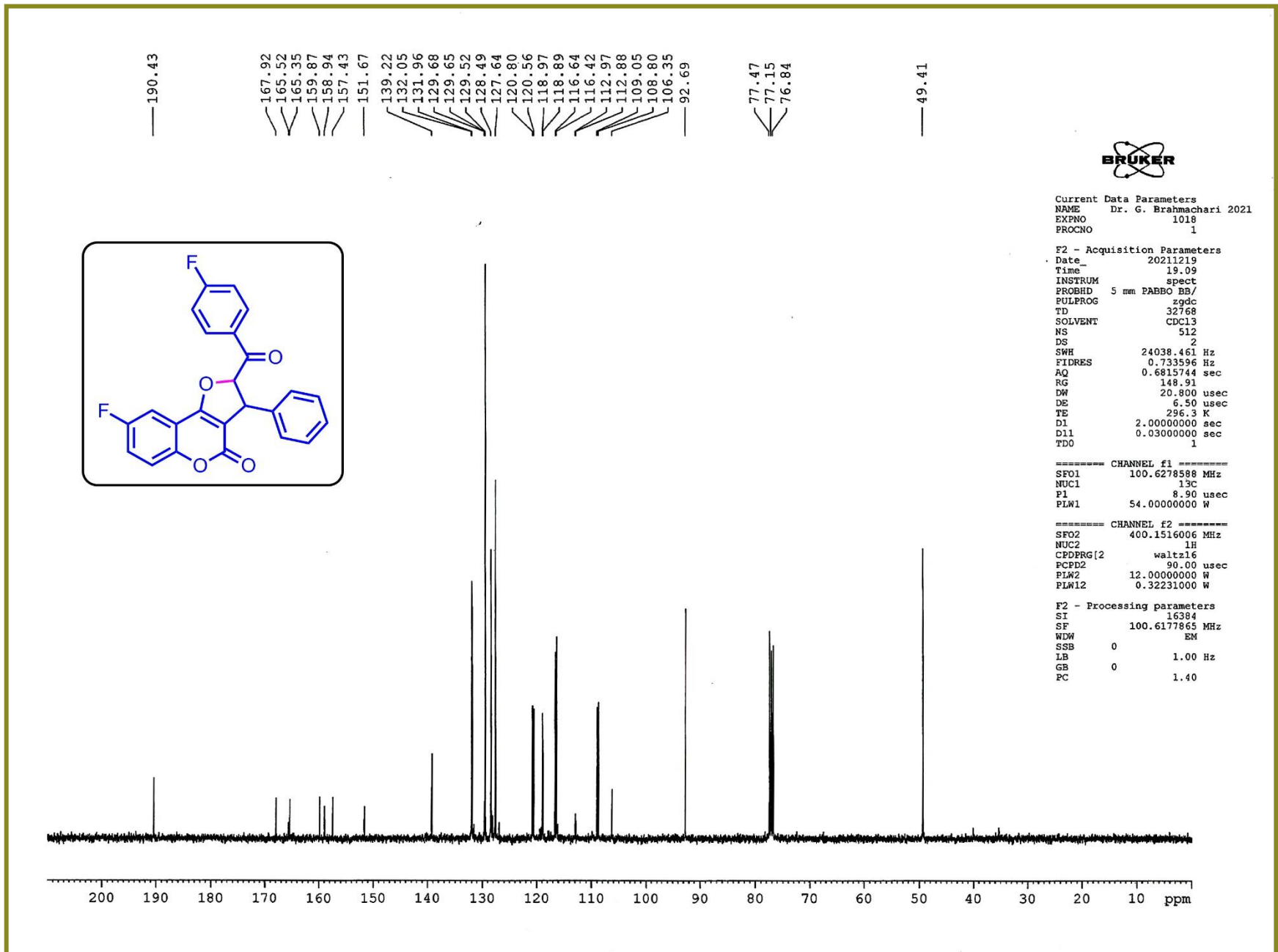


Figure S126. ¹³C-NMR spectrum of 8-fluoro-2-(4-fluorobenzoyl)-3-phenyl-2,3-dihydro-4H-furo[3,2-c]chromen-4-one (**2-29**)

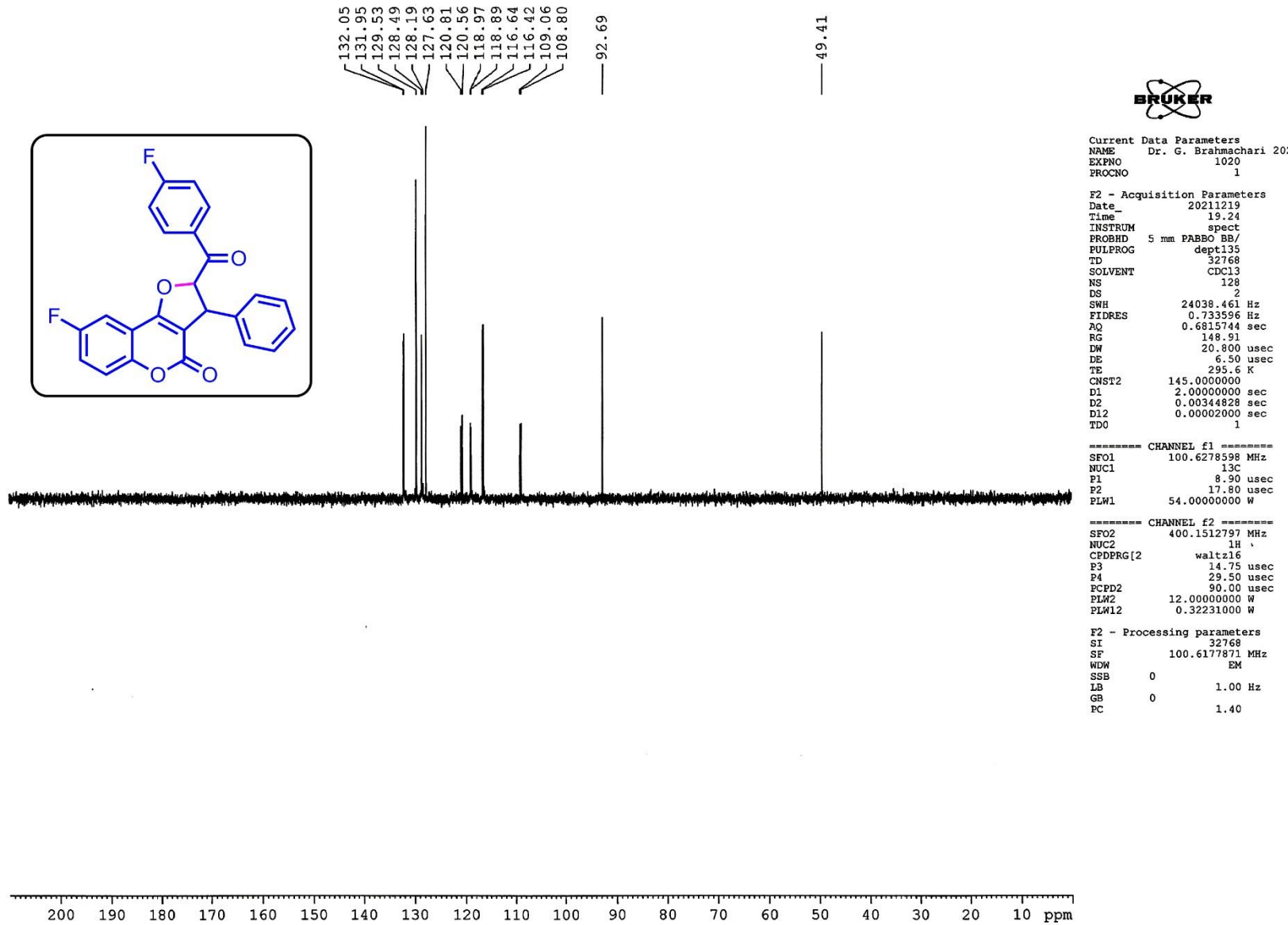


Figure S127. DEPT-135 NMR spectrum of 8-fluoro-2-(4-fluorobenzoyl)-3-phenyl-2,3-dihydro-4H-furo[3,2-c]chromen-4-one (**2-29**)

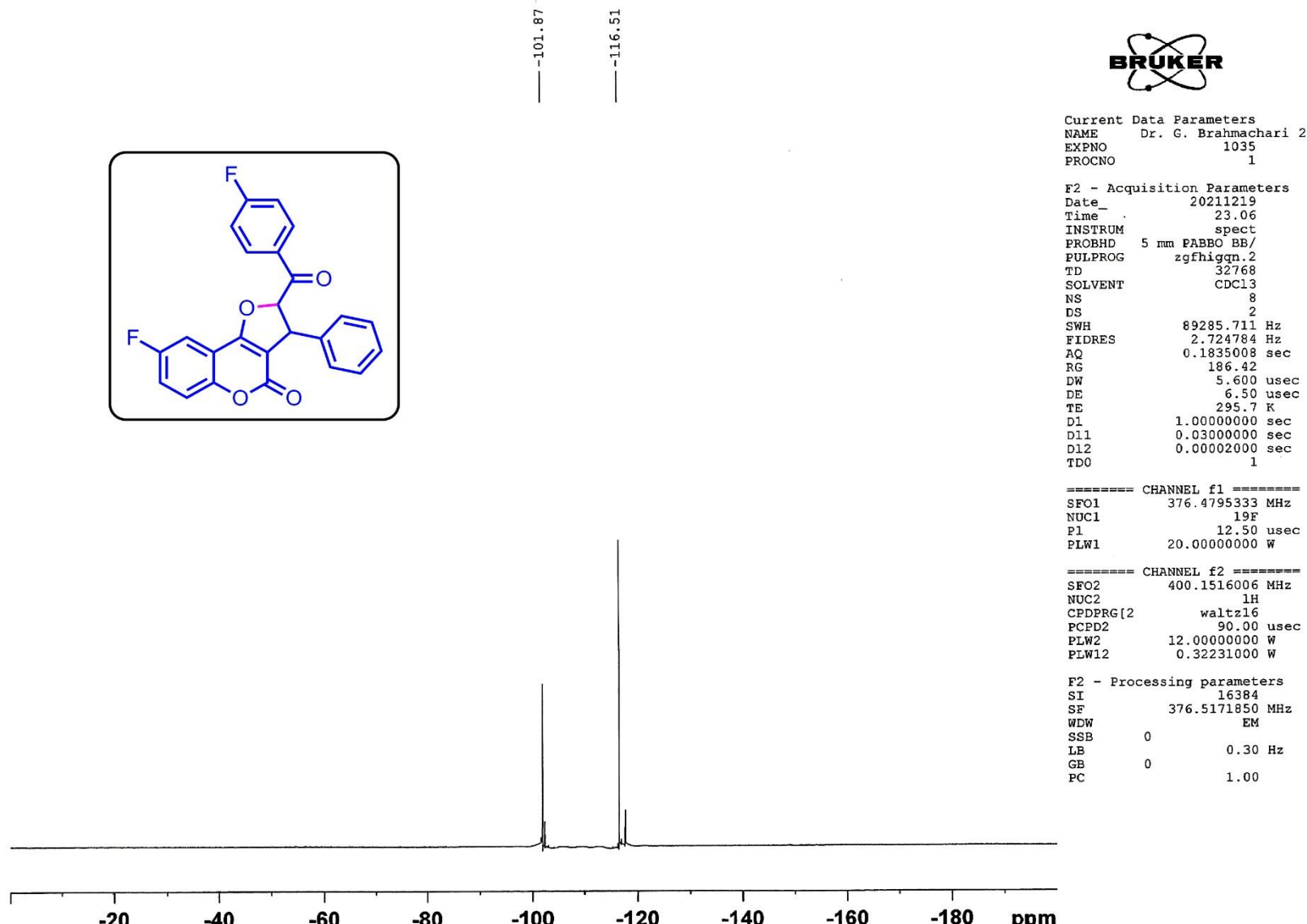
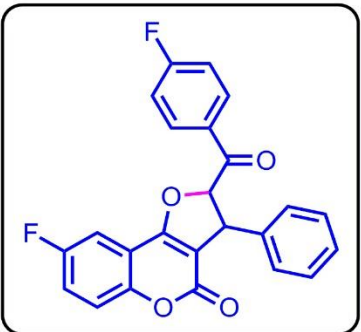


Figure S128. ¹⁹F NMR spectrum of 8-fluoro-2-(4-fluorobenzoyl)-3-phenyl-2,3-dihydro-4H-furo[3,2-c]chromen-4-one (**2-29**)

Acquisition Parameter

Source Type	ESI	Ion Polarity	Positive	Set Nebulizer	0.4 Bar
Focus	Active	Set Capillary	3400 V	Set Dry Heater	200 °C
Scan Begin	50 m/z	Set End Plate Offset	-500 V	Set Dry Gas	4.0 l/min
Scan End	3000 m/z	Set Charging Voltage	2000 V	Set Divert Valve	Source
		Set Corona	0 nA	Set APCI Heater	0 °C

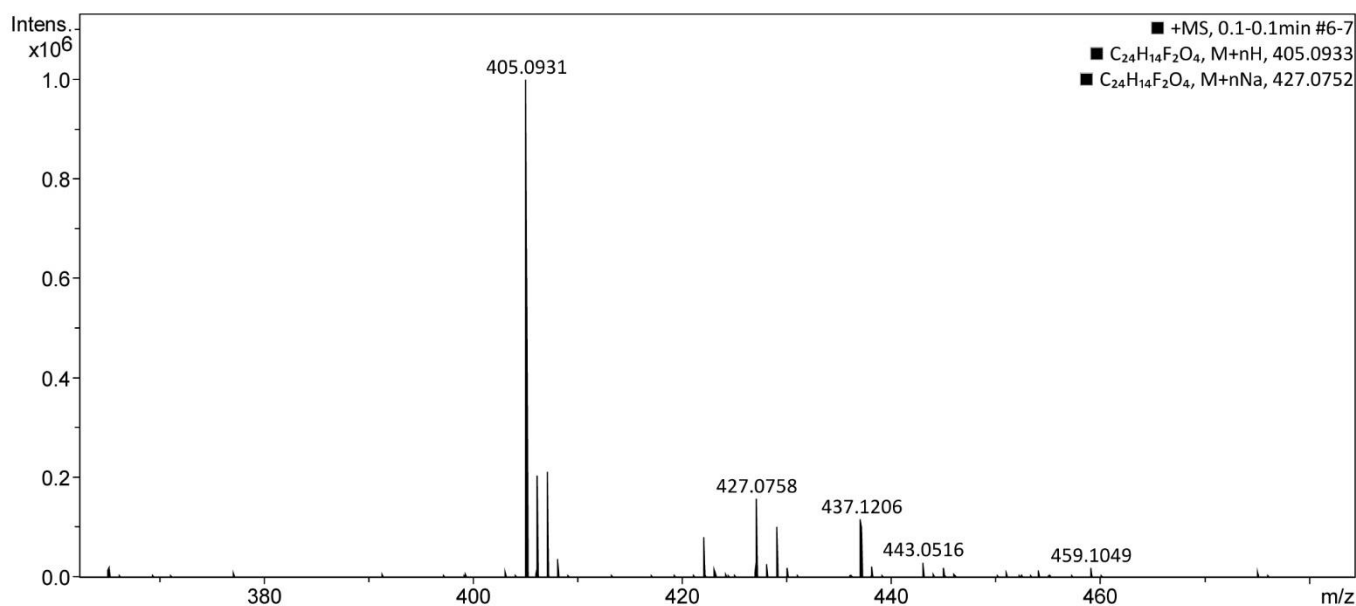
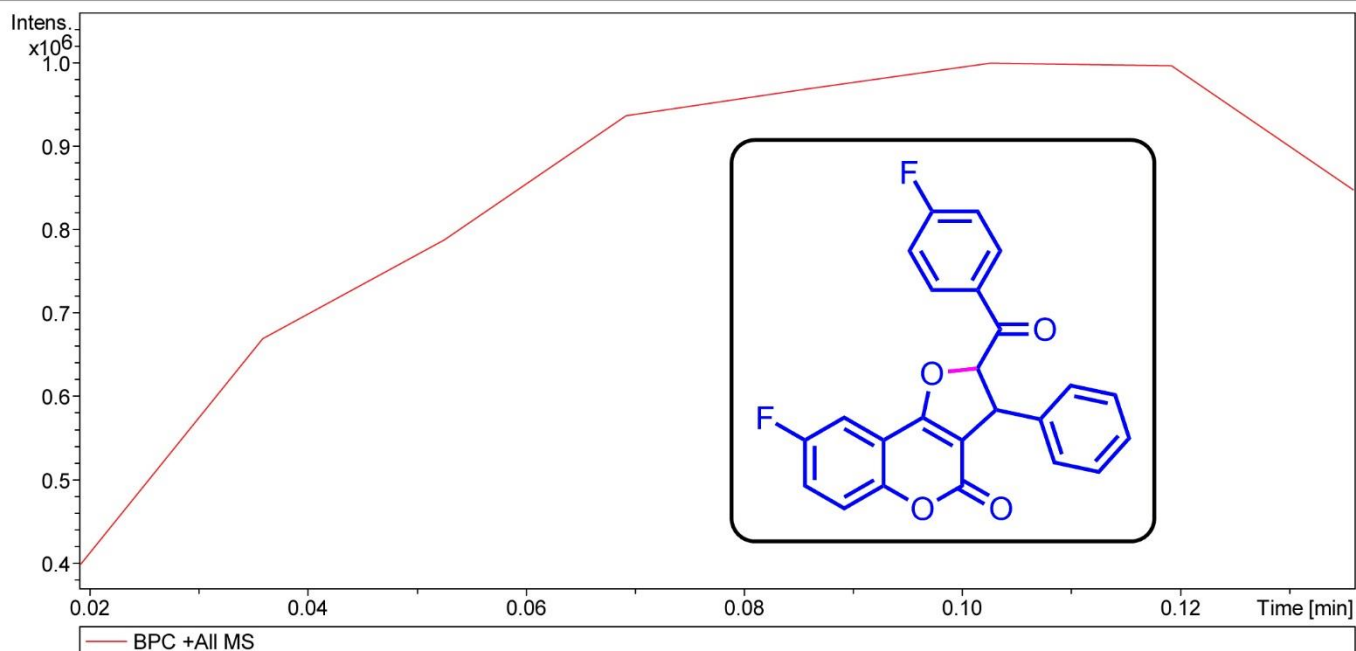


Figure S129. High-resolution Mass spectra of 8-fluoro-2-(4-fluorobenzoyl)-3-phenyl-2,3-dihydro-4*H*-furo[3,2-*c*]chromen-4-one (**2-29**)

4. Single X-ray crystal structure analysis of 2-(2-hydroxybenzoyl)-3-phenyl-2,3-dihydro-4H-furo[3,2-c]chromen-4-one (2-1)

4.1 Preparation of single crystals of compound 2-1

For preparing single crystals of compound **2-1**, 30 mg of the sample was dissolved in 5 mL of chloroform, and the solution was left for 3 days for slow evaporation at ambient temperature to yield colourless block-shaped crystals.

CCDC 2115681 (Compound **2-1**) contains the supplementary crystallographic data for this paper. These data can be obtained free of charge from *The Cambridge Crystallographic Data Centre* via www.ccdc.cam.ac.uk/data_request/cif

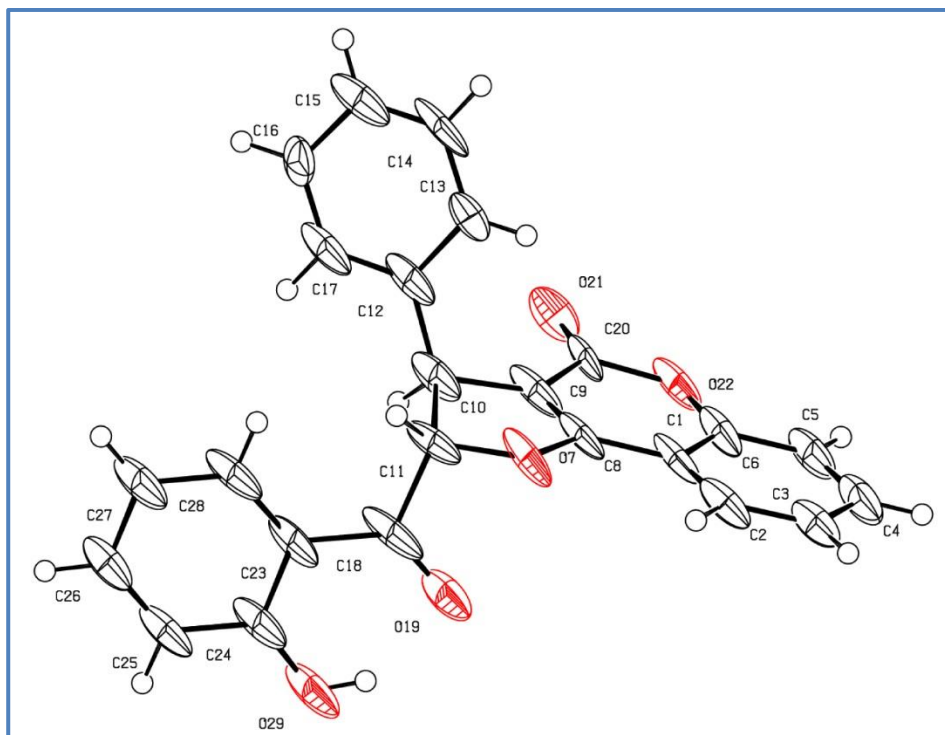


Fig. 130a ORTEP view of the molecule, showing the atom-labelling scheme
Displacement ellipsoids are drawn at the 50% probability level and H atoms are shown as small spheres of arbitrary radii.

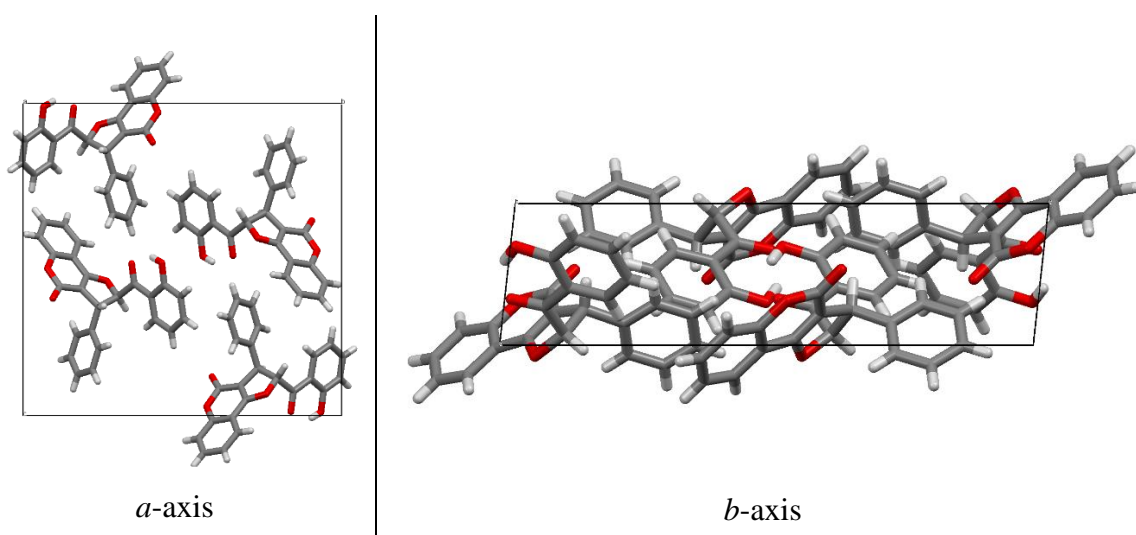


Fig. 130b. The packing arrangement of molecules viewed down the *a*-axis and *b*-axis.

Table S2. Crystal data and structure refinement for 2-(2-hydroxybenzoyl)-3-phenyl-2,3-dihydro-4*H*-furo[3,2-*c*]chromen-4-one (**2-1**)

CCDC Number	2115681	
Empirical formula	$C_{24}H_{16}O_5$	
Formula weight	384.37	
Temperature	150.00(7) K	
Wavelength	0.71073 Å	
Crystal system	Monoclinic	
Space group	$P\bar{2}_1/c$	
Unit cell dimensions	$a = 4.9980(5)$ Å	$\alpha = 90^\circ$
	$b = 19.0007(14)$ Å	$\beta = 96.275(11)^\circ$
	$c = 18.7257(19)$ Å	$\gamma = 90^\circ$
Volume	$1767.6(3)$ Å ³	
Z	4	
Density (calculated)	1.444 g/cm ³	
Absorption coefficient	0.101 mm ⁻¹	
F(000)	800.0	
Crystal size	$0.314 \times 0.254 \times 0.156$ mm ³	
Crystal shape (colour)	Block (colourless)	
Theta range for data collection	4.38 to 57.04°	
Index ranges	-6≤h≤6, -24≤k≤19, -13≤l≤24	
Reflections collected	5401	
Independent reflections	3658 [R _{int} = 0.1695, R _{sigma} = 0.1841]	
Completeness to theta = 28.640°	71.9 %	
Refinement method	Full-matrix least-squares on F ²	
Data / restraints / parameters	3658 / 0 / 263	
Goodness-of-fit on F ²	0.934	
Final R indices [I≥ 2σ(I)]	R ₁ = 0.0982, wR ₂ = 0.2102	
R indices (all data)	R ₁ = 0.1489, wR ₂ = 0.2541	
Largest diff. peak and hole	0.38 and -0.46 e.Å ⁻³	
Scan mode	ω scan	
Reflections observed (I > 2σ(I))	1585	
Structure determination	Direct methods	
No. of parameters refined	263	
Final residual electron density	0.38 and -0.46 e.Å ⁻³	
Software for geometry calculation	WinGX [2]	
Software for geometrical calculation	PARST [3]	
Software for molecular plotting	PLATON [4], Ortep3 [5]	
Software for structure solution	SHELXS-97 [6]	
Software for refinement	SHELXL-97 [7]	

5. References

1. (a) G. Brahmachari, M. Mandal and I. Karmakar, *Synthesis*, 2022, **54**, 451-464; (b) O. Talhi, J. A. Fernandes, D. C. G. A. Pinto, F. A. A. Paz, A. M. S. Silva, *J. Mol. Struct.*, 2015, **1094**, 13-21.
 2. L. J. Farrugia, *J. Appl. Crystallogr.*, 1999, **32**, 837.
 3. M. Nardelli, *J. Appl. Crystallogr.*, 1995, **28**, 659.
 4. A. L. Spek, *Acta Crystallogr. D.*, 2009, **65**, 148.
 5. L. J. Farrugia, *J Appl Crystallogr.*, 1997, **30**, 565.
 6. G. M. Sheldrick, SHELXS97, Program for the solution of the crystal structure, University of Gottingen, Germany, 1997.
 7. G. M. Sheldrick, SHELXL97, University of Göttingen, Germany, 1997.
-